Disrupting BMP/Noggin Balance Perturbs Myofiber Integrity Leading to Mammalian Muscle Plasticity

Inaugural-Dissertation

to obtain the academic degree

Doctor rerum naturalium (Dr. rer. nat.)

to the Department of Biology, Chemistry and Pharmacy

of the

Freie Universität Berlin

by

Arunima Murgai

2020

An ode to Berlin, the city where BMPs are ubiquitous.

This thesis was carried out during the period of November 2013 and January 2020 at **Freie Universität Berlin** and **Max-Planck-Institute for Molecular Genetics** under the supervision of Prof. Dr. Sigmar Stricker.

First Reviewer: Prof. Dr. Sigmar Stricker

Institute for Biochemistry

Freie Universität Berlin

Thielallee 63, 14195 Berlin

Tel.: +49 30 838 75799

E-Mail: sigmar.stricker@fu-berlin.de

Second Reviewer: Prof. Dr. Petra Knaus

Institute for Biochemistry

Freie Universität Berlin

Thielallee 63, 14195 Berlin

Tel.: +49 30 838 52935

E-Mail: knaus@chemie.fu-berlin.de

Date of defense: 12.02.2020

I declare that this thesis entitled "Disrupting BMP/Noggin Balance Perturbs Myofiber Integrity Leading to Mammalian Muscle Plasticity" has been composed solely by myself and that it has not been submitted, in whole or in part, in any previous application for a degree. Except where stated otherwise by reference or acknowledgment, the work presented is entirely my own.

Berlin, January 2020

_____

Arunima Murgai

TABLE OF CONTENTS

GRAPHICAL SUMMARY

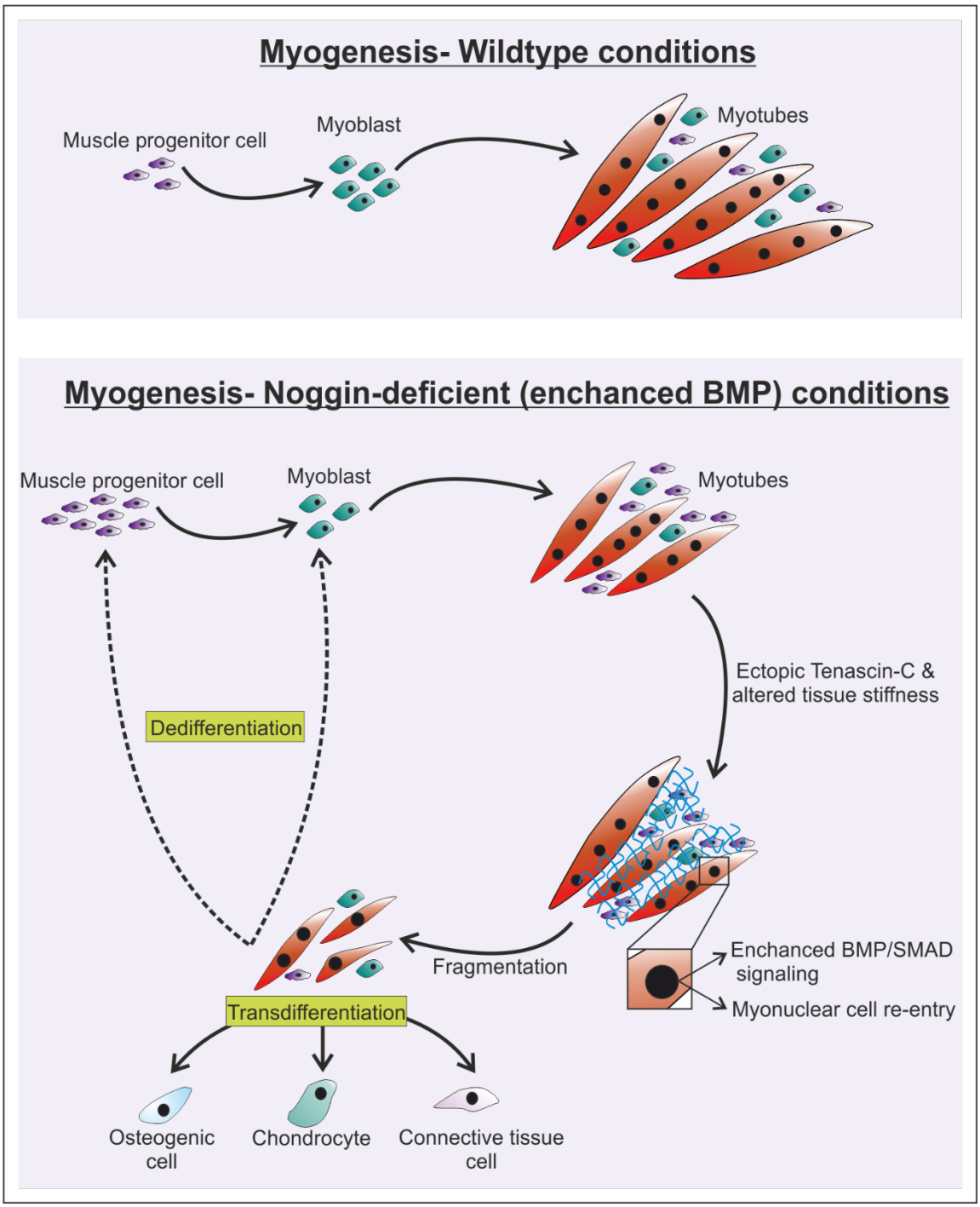

Key findings:

- Noggin-deficiency in developing mouse fetuses induces proliferation, differentiation and fusion defects in myogenic cells
- Ectopic expression of Tenascin-C in the muscle alters the biomechanical niche
- Myotubes show increased BMP/SMAD signalling and myonuclear cell cycle re-entry which leads to myotube fragmentation
- Muscle progenitors and myotube-derived cells undergo cell-fate change and transdifferentiate to other tissues lineages

SUMMARY

Myogenesis is a highly co-ordinated process driven by paracrine signalling in conjunction with an intricate biomechanical niche. Bone morphogenetic proteins (BMPs) and the antagonist Noggin balance proliferation and differentiation of muscle progenitors and adult muscle stem cells. However, there is a lack of systematic understanding of how BMP/Noggin signalling co-ordinates with the microenvironment during fetal myogenesis in mammals. Understanding the mechanisms that drive the myogenic program is essential to determine the molecular basis of muscle disease and regeneration.

This study investigated the role of BMP/Noggin signalling during limb myogenesis. A comprehensive phenotypic analysis of a Noggin knockout mouse model (Nog KO) showed altered proliferation, differentiation and fusion of myogenic progenitor cells altogether decreasing myofiber formation. This was re-capitulated by a CRISPR-Cas9 generated Noggin-deficient C2C12 myoblast cell line. Furthermore, a striking disappearance of myofibers was observed in fetal stages which was accompanied by loss of the basal lamina and ectopic expression of the extracellular matrix component Tenascin-C (TnC). This altered the biomechanical niche by reducing the stiffness of the muscle tissue. Myotubes in these muscles were characterized by exacerbated BMP/SMAD signalling and displayed hallmarks of de-differentiation including cell cycle re-entry in otherwise post-mitotic myonuclei. Furthermore, *in vivo* genetic lineage tracing analysis in the Nog KO fetuses revealed trans-differentiation of the myogenic cells into chondrogenic, osteogenic and connective tissue cells. Analysis of mouse myotubes *in vitro* demonstrated that myonuclear cell cycle re-entry can be initiated by BMPs with superb potency, such as generated upon protease cleavage, in combination with TnC and substrate stiffness below the endogenous range for muscle.

This study reveals a previously unseen capacity of muscle fragmentation and cell-fate switch in a mammalian organism. It was demonstrated that a combination of exacerbated BMP signalling and the biomechanical niche influences muscle-cell plasticity. This work highlights the importance of maintaining the intricate balance between BMP and Noggin during developmental myogenesis. This knowledge can be extrapolated to gain a novel perspective on muscle diseases like muscular atrophy and to develop new tools to foster muscle regeneration.

ZUSAMMENFASSUNG

Der Skelettmuskel ist eines der größten Gewebe des Körpers und für seine Bewegung und Unterstützung unerlässlich. Die Myogenese ist ein koordinierter Prozess, der durch parakrine Signale in Verbindung mit einer komplexen biomechanischen Nische gesteuert wird. Bone Morphogenetic Proteins (BMPs) und deren Antagonist Noggin koordinieren die Proliferation und Differenzierung von fetalen Muskelvorläufern und adulten Muskelstammzellen. Es fehlt jedoch ein systematisches Verständnis der Koordination der BMP / Noggin-Signalübertragung mit der Mikroumgebung während der fetalen Myogenese bei Säugetieren. Das Verständnis der Mechanismen, die das myogene Programm steuern, ist für die Bestimmung der molekularen Grundlagen von Muskelerkrankungen und Regeneration von entscheidender Bedeutung.

Diese Studie untersuchte die Rolle des BMP / Noggin-Signalwegs während der Extremitätenmyogenese. Eine umfassende phänotypische Analyse eines Noggin-Knockout-Mausmodells (Nog KO) zeigte eine veränderte Proliferation, Differenzierung und Fusion von myogenen Vorläuferzellen, die die Muskelfaserbildung insgesamt verringerte. Dies wurde durch eine CRISPR-Cas9-generierte Noggin-defiziente C2C12-Myoblasten-Zelllinie in vitro bestätigt. Darüber hinaus wurde in fetalen Stadien ein bemerkenswertes Verschwinden von Muskelfasern beobachtet, das von einem Verlust der Basallamina und einer ektopischen Expression der extrazellulären Matrixkomponente Tenascin-C (TnC) begleitet war. Dies veränderte die biomechanische Nische, indem die Steifheit des Muskelgewebes verringert wurde. Die Muskelfasern in diesen Muskeln waren durch verstärkte BMP / SMAD-Signale gekennzeichnet und zeigten Merkmale der Dedifferenzierung, einschließlich des Wiedereintritts von normalerweise postmitotischen Myonuklei in den Zellzyklus. Darüber hinaus ergab eine genetische Zelllinien-Analyse in vivo in den Nog KO-Feten eine Transdifferenzierung der myogenen Zellen in chondrogene, osteogene und Bindegewebszellen. Die Analyse von Maus-Muskelfasern in vitro zeigte, dass der Wiedereintritt in den Zellzyklus von Myonuklei durch exogene BMPs (in einer durch Serumprotease gespaltenen Form) in Kombination mit TnC und einem weichen Substrat synergistisch gesteigert werden kann.

ZUSAMENFASSUNG

Diese Studie zeigt eine bisher nicht gekannte Fähigkeit der Muskelfragmentierung und des Zellschicksalswechsels in einem Säugetierorganismus. Es wurde gezeigt, dass eine Kombination aus verstärktem BMP-Signal und der biomechanischen Nische die Plastizität der Muskelzellen beeinflusst. Diese Arbeit unterstreicht die Bedeutung der Aufrechterhaltung des komplexen Gleichgewichts zwischen BMP und Noggin während der pränatalen Myogenese. Dieses Wissen kann extrapoliert werden, um eine neue Perspektive auf Muskelerkrankungen zu erhalten und neue Instrumente zur Förderung der Muskelregeneration zu entwickeln.

ACKNOWLEDGEMENTS

“The most exciting phrase to hear in science, the one that heralds new discoveries, is not 'Eureka!' but 'That's funny'….” - Isaac Asimov

These last years have been a rollercoaster ride filled with exhilaration, bursts of adrenaline, anticipation of the unknown and one big **Eureka** moment! The past six years embody the most challenging, yet most rewarding years of my life with marked personal and scientific development and growth. This journey would be incomplete without the mention of mentors, colleagues, friends and family who showered me with constant support and constitute a valuable part of my scientific adventures.

First of all, I would like thank my PhD supervisor or ‘Doktorvater’, **Prof. Dr. Sigmar Stricker** for supporting me through this whirlwind of a journey. You introduced me to the exciting world of muscles and embryogenesis and helped me shape a beautiful story along the way. Thank you for the countless discussions and brain-storming sessions during the lab seminars and for the open-door policy whereby I could come into your office anytime to discuss scientific and technical challenges. You have inspired me to develop into a good scientist and most importantly, taught me the virtue of patience. One of my most special memories is of the email I wrote to you with the subject ‘Eureka moment’. This was truly a turning point in my research and the start of an exciting new scientific path. I sincerely appreciate all the support and encouragement you have given me over the last years. I especially treasure the nod of reinforcement you give me from the crowd every time I stand up on stage to present my work. I would like to thank you for six years of constant motivation and trust, and for being an incredible support system.

Secondly, I would like to thank **Prof. Dr. Petra Knaus** who co-supervised this thesis. Thank you for introducing me to the fine world of BMPs, and for numerous invaluable suggestions for my research. Every lab seminar and meeting where I presented my latest work to you, I came out beaming with new ideas and a zeal to take my research to the next level. Petra, you have been one of my biggest sources of scientific and personal inspiration along this journey. Thank you for your words of support and encouragement starting six years ago at the BSRT assessment centre and continuing all the way through today. Lastly, I would like to express my

gratitude to you for including me as an ‘adopted’ member of the Knaus lab and for providing me with numerous possibilities to collaborate with your group.

I would like to give a special thanks to **Hans-Georg Simon**, for being a consistent scientific advisor and mentor to me through the last years. I am still flabbergasted by how our paths crossed at the right point in time. The research you undertook in Amphibians has proved invaluable for my PhD thesis. Thank you for your support, honesty and for all the ‘good vibes’.

I would like to thank the Berlin-Brandenburg School of Regenerative Therapies (BSRT) for providing me with a doctoral scholarship and innumerable soft skill resources to develop into a well-rounded scientist. I would also like to thank **Dr. Sabine Bartosch** for her support over these last years.

I would sincerely like to thank everyone at the Max Planck of Molecular Genetics whose support made it possible for me to successfully conduct my research there. Firstly, I would like to thank **Prof. Stefan Mundlos** for making his laboratory and resources available for use. Secondly, I would like to thank **Ludgar Hartmann** and **Katja Zill** from the animal facility. Thirdly, I would like to thank **Thorsten Mielke**, **Beatrix Fauler** and **Uta Marchfelder** from the Microscopy facility.

Stricktastics- the dream team! I cannot even begin to write how fortunate I feel to be a part of this amazing group. From the Eifel tower to Parthenon, we have extended our adventures far and beyond. Being with you in the lab, turned every day into a pandemonium full of music and dances. **Sophie**, thank you for being Queen-bee! You have been one of my strongest advocates, and have always been there to offer a listening ear. I am proud to say that we have finally mastered the art of rowing a boat together. Thank you for being my partner in crime, and the perfect fit for my glitter madness. **George**, you brought light and life into the lab. I love our funny conversations, and all the ‘extra’ wisdom I have acquired through our google and youtube searches. Thank you for taking us to Greece, and filling our bellies with so much Greek-love. **Xiao**, thank you for being so authentic and brutally honest, I love your wit and humor. Thank you being such a big support in the last years, I especially enjoyed our late evening talks at the computer. **Pedro**, thank you for being helpful in the lab and for your amazing guacamole.

I would like to thank all the students who contributed to various projects I undertook- **Akin**, **Caspar**, **Chuck**, **Franzi**, **Manuel**, **Mareike**, **Miriam**, **Markus**, and **Kira**. Akin, you are a mix of love, smiles and sparkle packaged together in the form of a unicorn. Thank you for always showing me the brighter side of life and for all our fun evenings together. Miriam, thank you for being a super student and a great friend. From 7am FACS runs to hair dresser visits, we have done it all.

I am especially thankful to all the members of the **Knaus lab** that made me feel so at home on the second floor. **Chris**, you have been a box full of surprises. Thank you for our 'spontaneous' adventures all the way from Munich to Tokyo. One day, we ought to re-create our Japanese karaoke madness by singing '99 luftballoons' in Berlin. **Jerome**, thank you for being a great travel companion and the best cuddle buddy. **Susanne**, I loved our time in Tokyo and I really appreciate your openness and honesty. The only Russian-born German scientist I know, **Vladimir**, thank you for being the one to make me laugh and give me endless words of support. **Nadine**, **Carolina** and **Nurcan** thank you the nice talks during lunch and the encouraging words every time I passed by the kitchen. I would also like to thank **Katharina Hoffmann**, for providing administrative support and always greeting me with a huge smile. A big thank you to all of you for making me an extended member of this group.

I would like to thank current members and alumni from the **Mundlos group** who have become great friends along the way. **Sinje**, I happy to see how our friendship has blossomed over the years. Exploring India, Netherlands and Germany with you has a very special place in my heart. Thank you for introducing me to the magical world of Christmas and our adventures in Bergisch Gladbach. **Ivana**, **Iza** and **Georgie** as you all have said before "whatever cosmic event put us at the same time in the same place; it had a great plan". Thank you for being my BoBs, and for putting an extra spin to my time in Berlin. **Guilia**, thank you your warm Italian hugs and wonderful conversations. I would like to thank **Norbert** for all the technical support, and for eagerly sharing giant portions of his home-made goodies. Thank you for entertaining me with your impressive Photoshop skills and most importantly for finding me my bike, which has shared many-a-adventures with me over the last years. Lastly, I would like to thank **Asita** for technical support and for all the early morning words of encouragement.

ACKNOWLEDGEMENTS

Lastly, I would like to say a huge thank you to my **family** who made the 5763km between New Delhi and Berlin disappear! My mom, who constantly kept me in the loop by flooding my phone with pictures, and subtly letting me know every single day that she is there for me. My dad, for humouring me by saying “you can lose everything in life, but the one thing that will forever stay with you is your education”. Thank you for always believing in me and cheering me up with our crazy phone conversations. My brother, for just being his fun self. A special mention to my grandmother, who never fails to assert how incredibly proud she is of me; dadi this one is for YOU!

Special mention to all the unicorns, shooting stars and rainbows I met along the way that brought magic and love into my life…..

1. INTRODUCTION

1.1. From limb development to regeneration

Vertebrates lack the ability to regenerate limbs whereas amphibians have a remarkable capacity to regenerate a fully functional limb after amputation at any point along the limb axis. Although limb development in amphibians is largely parallel to avian or mammalian development, one key difference lies in the plasticity of differentiated cells. At the site of amputation, amphibian limbs cells display reversibility of cell commitment which confers them this high regenerative ability. These blastemal cells can re-enter the cell cycle and lose their differentiated character and express a new genetic program that is distinct to that to mesenchymal cells of the limb or to that of the limb bud (Kintner and Brockes, 1985). It is likely that plasticity of each of the tissues types present in the limb is regulated differently. A key question to address is whether molecular mechanisms underlining limb regeneration are reminiscent of signalling processes that occur during limb development. Furthermore, it is yet to be determined whether to what extent the de-differentiated cells maintain memory of the process of embryonic development. Development differs from regeneration in the complexity of the tissue landscape. During embryonic development the limb bud consists of undifferentiated cells that gradually undergo commitment and differentiation to different cell types. In contrast, limb regeneration presents a complex starting point consisting of epidermis, muscle, done, blood vessels and nerves which leads to formation to the blastema that initiates developmental programs. Despite the differences in complexities between development and regeneration, it is likely that the molecular mechanics converge at one point. A recent study has implicated bone morphogenetic proteins (BMPs) in muscle cell de-differentiation (Wagner et al., 2017). BMPs are known to be key in developmental patterning of the early embryo, specification, commitment and differentiation of various cell types. This presents BMPs as a potential target for induction or manipulation of cell plasticity during regeneration. With the advent of new genomic tools like single-cell RNA sequencing and sophisticated genetic fate tracing a deep understanding of molecular mechanism that regulate cell plasticity can be explored.

1.2. Introduction into myogenesis

The skeletal muscle is one of the largest tissues of the body as is essential for movement in support. Myogenesis refers to the process of building muscle and represents a paradigm for studying stem cell identity, cell specification and commitment, and cellular differentiation. Understanding the molecular mechanism that drives the process of muscle development is essential to gain a new perspective on muscular diseases and develop new tools to support muscle regeneration The cellular and molecular processes that drive myogenesis will be described in this section.

1.2.1. Origin and specification of the skeletal muscle

Skeletal muscle originates from the paraxial mesoderm which constitutes the presomitic mesoderm at the posterior tip of the embryo. Soon after somite formation, compartmentalization along the dorsal ventral axis results in formation of the dorsal epithelial dermomyotome and the ventral mesenchymal sclerotome. The dermomyotome gives rise to the skeletal muscles whereas the sclerotome gives rise to the skeleton and tendons. (Aulehla and Pourquié 2006). The cells of the newly formed somites are not yet committed to any specific lineage however induction of BMP, WNT and SHH signaling pathways leads to specification of cells into different somitic fates (Yusuf and Brand-Saberi, 2006). BMP signaling inhibition dorsally is essential for dermomyotome specification whereas WNT signals from the dorsal neural tube and ectoderm are crucial to maintain the fate of dermomyotomal cells (Hirsinger et al., 2000).

The first sign of myogenesis is the activation of Myf5, a myogenic factor, in the dorsomedial region of the newly formed somite while Pax3 is expressed in the dorsal epithelial dermomyotome (Ott et al., 1991; Gros et al., 2004). Formation of the dermomyotome leads to downregulation of Pax3 while Myf5 expression is upregulated (Ott et al., 1991). At this stage the myotome appears between the dermomyotome on the dorsal side and sclerotome on the ventral side (Ordahl et al., 1993). The initial appearance of mononucleated myocytes is observed in the myotome and these cells express cytoskeletal proteins like myosins, actin and desmin (Babai et al., 1990; Furst et al., 1989; Sassoon et al., 1988). The myocytes span the entire length of the somite and addition of more cells from the

dermomyotomal lips leads to fusion and formation of multinucleate myofibers (Gros et al., 2004). After formation of the myotome, the Pax3 expressing cells from the dermomyotome are incorporated into the myotome thereby providing myogenic precursors for further stages of myogenesis (Relaix et al., 2005). Cells migrate from the lateral dermomyotome into the limb bud thereby creating the founding population of the limb muscles (Jacob et al., 1979). Somitic myogenesis is depicted in Figure 1.1.

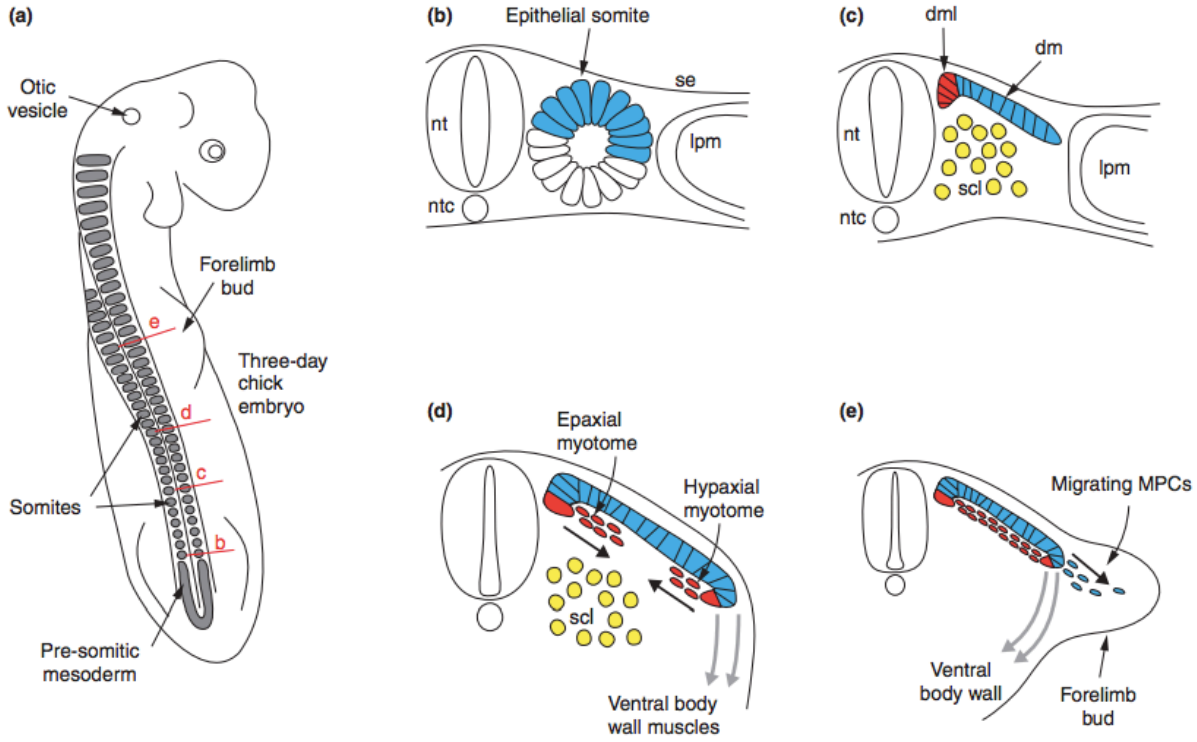

Figure 1.1: Somitic myogenesis in early chick embryo
Schematic view of three-day old chick embryo (a), and cross sections of somites (b-e) showing early somatic myogenesis. Epithelial somite receives signals from notochord (nt) and neural tube (nt) to form the dermomyotome (dm) (blue) and sclerotome (scl) (yellow). The dorsomedial lip (dml) cells (red) form the epaxial and hypaxial myotome. Muscle progenitor cells (MPCs) migrate from the dml into the limb bud. From Bailey et al., 2001

1.2.2. Embryonic and fetal myogenesis

During development myogenesis can be separated into two distinct phases- embryonic/primary and fetal/ secondary myogenesis. In mice, primary myogenesis occurs from E10.5-E13.5 and results in the formation of primary myofibers from Pax3 expression dermomyotome-derived cells. These fibers expression slow myosin heavy chain and myosin light chain I (Hutcheson et al., 2005).. The primary myofibers form the template for secondary and adult myogenesis. During

secondary myogenesis myogenic progenitor cells downregulate expression of Pax3 and start expressing Pax7, fusion of these cells leads to formation of secondary fibers (Kelly et al., 1997). The secondary fibers express β-endolase, Nfix and myosin light chain III (Kelly et al., 1997; Messina et al., 2010). Addition of Pax7 expressing cells and fusion events lead to muscle growth during secondary myogenesis (White et al., 2010). Muscle progenitor cell fusion events lead to formation of multinucleate myotubes which further mature to give rise of myofibers. Subset of Pax7 cells from the pool of adult muscle satellite cells and are enclosed under the basal lamina (Relaix et al., 2005). Fusion competent myoblasts produce actin-based podosomal structures that invade the muscle founder cell thereby allowing transfer of nucleus and cytoplasm from the myoblast into the fusing cell (Kim et al., 2015). During maturation each myofiber is surrounded by a basal lamina and harbours a special plasma membrane called the sarcolemma which provides structural stability. The sarcolemma and the basal lamina associate through the transmembrane dystrophin-associated glycoprotein complex which connects the myofiber to the extraceullar matrix (Sanes 2003).

1.2.3. Genetic network controlling developmental myogenesis

Myogenic regulatory factors (MRFs) refer to highly conserved basis-helix-loop-helix factors that regulate myogenesis. These include MyoD, Myf5, myogenin and MRF4. DNA binding is mediated via the basic domain of the MRFs whereas the helix-loop-helix motif is required for heterodimerization with E-proteins which allows recognition of E-box sequences which are rich in the promoters of muscle-specific genes (Massari and Murre 2000). The earliest MRF that is expressed is Myf5 which is seen in the paraxial mesoderm and later together with other MRFs in the myotome (Buckingham 1992). Lack of Myf5 in mice leads to delayed embryonic myogenesis until the point where MyoD is expressed (Braun et al., 1992). On contrary, deletion of MyoD leads to prolonged and compensatory expression of Myf5 (Rudnicki et al., 1992). Genetic ablation of Myf5 using diphtheria toxin showed that not all myoblasts express Myf5 and that MyoD – lineage cells can fully restore myogenesis (Haldar et al., 2008). The redundancy of Myf5 and MyoD became evident using double knockout of MyoD and Myf5 wherein no skeletal muscle formation was observed (Rudnicki et al., 1993).

Paired homeobox transcription factors- Pax3 and Pax7 are key regulators of the myogenic process and are expressed in the early dermomyotome cells (Kassar-Duchossoy et al., 2005). Although in cells that delaminate from the dermomyotome and migrate into the limb bud, only Pax3 but not Pax7 is expressed. Loss of Pax3 in mice leads to lack in formation of hypaxial muscles including those of the limb and the diaphragm whereas epaxial muscles are less affected (Tremblay et al., 1998). Triple mutants of Pax3, Myf5 and MRF4 are devoid of all body muscles and lack expression of downstream myogenic factors like MyoD (Tajbaksh et al., 1997). This indicates that Pax3 acts upstream of the myogenic regulatory signalling. Pax3/Pax7 double mutants show muscle formation defects, in contrast to Pax3 null mutants where only the early myotome develops (Relaix et al., 2005). Moreover, knock-in of Pax7 into the Pax3 locus restores mygenic function in these mutants (Relaix et al., 2004). For specific ablation of cell populations, Pax3 and Pax7 Cre drivers were used to show that loss off Pax3 lineage leads to embryonic lethality whereas loss of Pax7 cells leads to smaller and fewer muscle fibers (Hutcheson et al., 2009).

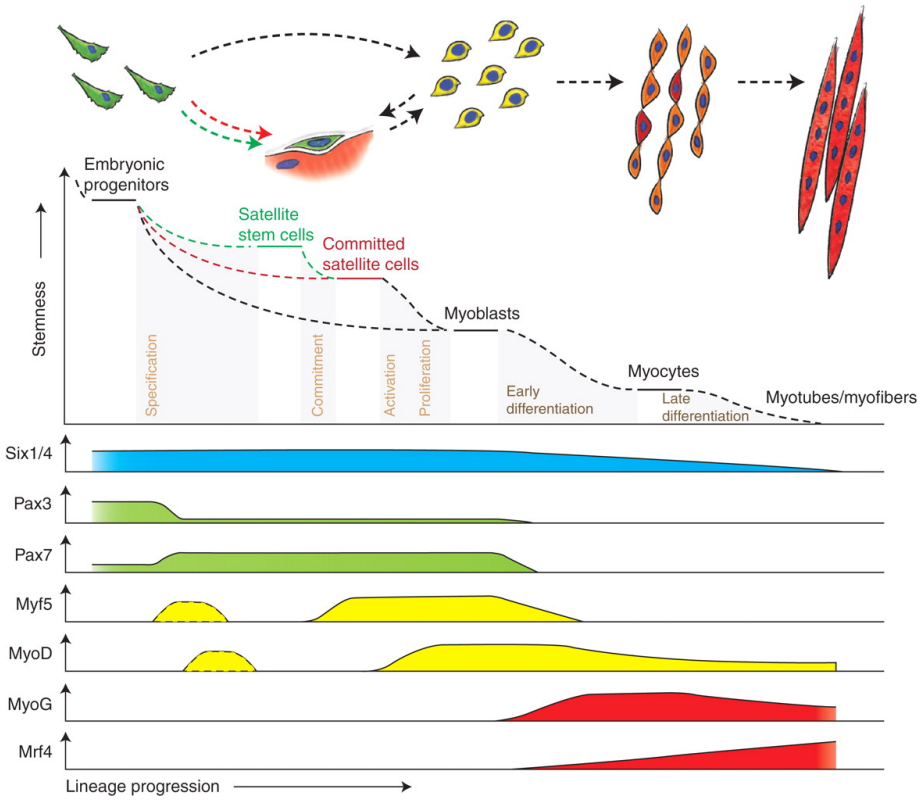

Figure 1.2: Transcription factors regulating progression of myogenesis
Embryonic progenitors differentiate into myoblasts and myocytes and fusion events lead to myotube formation. Six1/4 and Pax3/7 are master regulators of myogenic lineage specification Myf5 and MyoD commit cells to a myogenic lineage. MyoG and Mrf4 play a key role in terminal differentiation of myoblasts and myocytes. From Bentzinger et al., 2012.

Six (sine occulis related homebox) family of proteins including Six 1 and Six 4 are characterized by a six-type homeodomain that binds DNA and an amino-terminal six domain that interacts with co-activators or co-repressors to mediate transcription (Zu et al., 2002). Six proteins can bind to Eya1 and Eya2 and translocate them to the nucleus thereby regulation Six-target genes like Pax3, MyoD, myogenin and MRF4 (Grifone et al., 2005). Double mutants of Six1 and Six4 do not show expression of Pax3 in the dermomyotome and no limb or trunk muscles are formed. Myf5 expression, which is independent of Pax3, is also affected in these mutants (Grifone et al., 2007).

1.2.4. Postnatal myogenesis

In mammals, postnatal skeletal muscle rapidly continues to grow until adulthood. Muscle growth is a result of fusion of adult muscle stem cells, called satellite cells (SCs), with myofibers and through increase in protein synthesis which leads to hypertrophy and hyperplasty. Satellite cells are regulated by the same instrinsic regulators that are involved during embryonic myogenesis (Rudnicki et al., 2008). SCs give rise to new progeny via asymmetric divisions for self-maintenance and to generate progenitors committed for myogenesis (Shinin et al., 2006). The SC cell population is highly heterogeneous and the cells have the ability to differentiate towards other mesodermal lineages such as muscle, bone and brown fat (Asakura et al., 2001). In comparison with embryonic progenitors which are at the early stage of commitment and rely on intrinsic programming, the SCs are dependent on extrinsic regulatory factors (Bentzinger et al., 2010).

The SCs reside close to the myofibers under the extracellular matrix of the basement membrane (Mauro 1961). The SC niche allows the cells to remain in a quiescent, non-proliferative state (Shea et al., 2010), unless activated upon injury. Several studies have demonstrated that SCs originate from multipotent cells of the somites. Diptheria-toxin mediated ablation of Pax3/Pax7 expressing cells results in the absence of muscle progenitor cells in the limb (Hutcheson et al., 2009). Lineage tracing experiments using chick/quail grafting indicated dermomyotomal origin of SCs (Gros et al., 2005; Relaix et al., 2005; Lepper and Fan 2010). SCs express markers that keep them in a quiescent state such as Pax7, α7-integrin and CD34 (Kuang et al., 2007; Lepper et al., 2009; Sacco et al., 2008; Beauchamp et

al., 2000). In adult muscle, the SC niche is essentially static and homeostasis is maintained by the extrinsic environment. Upon injury, the SC niche undergoes dramatic compositional changes which activates the SCs inducing proliferation, differentiation and fusion to repair or build new myofibers (Murphy et al., 2011). SCs represent the major population of myogenic cells in adult muscles and are indispensable for muscle regeneration.

SCs are tightly regulated by cell-cell or cell-matrix interactions and this dynamic microenvironment influences autocrine and paracrine signalling in the SC niche. Several signalling pathways regulate SC maintenance, activation and proliferation. Wnt/β-catenin pathway regulates a variety of cellular processes including self-renewal by inhibiting differentiation (Perez-Ruiz et al., 2008) and regulation of proliferation (Otto et al., 2008). Wnts have also been shown to promote myogenic commitment and differentiation of SCs (Brack et al., 2008). Notch signalling is essential for maintaining SC quiescence (Mourikis et al., 2012), while it also regulates activation and proliferation of SCs (Conboy and Rando, 2002). Following muscle injury, expression of delta ligand is upregulated in both SCs and myofibers leading to NCID expression in SCs which in turn allows activation and proliferation of SCs (Conboy and Rando, 2002). However, inhibition of Notch signalling, mediated by the inhibitor numb is required for terminal differentiation and fusion of myoblasts. Concomitantly, Notch signalling is antagonized by Wnts in differentiating myoblasts (Brack et al., 2008). Other signalling pathways like fibroblast growth factor (FGF) and Hepatocyte growth factor (HGF) are activated upon injury to promote proliferation and inhibit differentiation of myogenic cells (Floss et al., 1997; Miller et al., 2000). Another important regulator of myogenesis are bone morphogenetic proteins (BMPs), the role of which is described in the following sections.

1.3. BMP signal transduction

The term bone mophogenetic proteins (BMPs) was coined in 1965 by Marshall Urist. He discovered that implantation of decalcified bone matrix in muscles of mouse, rat, rabbit, guinea pig, dog and human resulted in ectopic bone formation (Urist, 1965). The following decade identified BMPs as regulators of chemotaxis, callus and endochondral and intramembranous bone formation. These advances allowed the sequencing and cloning of BMPs in 1988 (Wozney et al., 1988). In 1988, the first clinical application of BMPs was undertaken to support non-unions and segmental bone defects (Johnson et al., 1988). In the past two decades, research in the field of BMPs has expanded extensively and BMPs have been shown to be involved in embryonic development, as well as organogenesis and tissue homeostasis in adults thereby it has been proposed to revise the terminology to body morphogenetic proteins (Reddi, 2005; Wagner et al., 2010).

1.3.1. BMP ligands

BMPs are members of the TGFβ super family of extracellular secreted signalling molecules which includes 33 members in mammals. These include TGFβs, activins and inhibins, myostatin and Müllerian-inhibiting substance (MIS) and nodal. The BMPs comprise of the biggest subfamily and are further divided into 4 sub-groups 1) BMP2 and BMP4; 2) BMP5 and BMP6; 3) BMP9, BMP19 and 4) GDF5 (BMP14), GDF6 (BMP13) and GDF7 (BMP12) (Bragdon et al., 2011; Miyazono et al., 2010).

BMPs are synthesized as large precursors of about 400-500 amino acids consisting of a N-terminal signal peptide for secretion, a pro-domain for folding and a C-terminal mature peptide. Upon dimerization the mature proteins are cleaved from the pro-domain an Arg-X-X-Arg sequence by serine endoproteases like Furin, PC6 and PC7 to generate N- and C-terminal fragments (Nelsen and Christian, 2009; Sieber et al., 2009; Xiao et al., 2007). Active BMPs are 50-100 amino acids with seven cysteines, of which six are involved in the formation of three intramolecular disulphide bonds called as cysteine knots and one intermolecular di-sulfide bond to form biologically active homo- or heterodimers (Bragdon et al., 2011). Recent studies have shown that BMP heterodimers are more potent than homodimers, as seen in BMP9/10 heterodimers which are responsible for most of the biological activity of blood plasma (Tillet et al., 2018). BMP ligands show a

characteristic butterfly-shaped arrangement with the c-terminal locked in between the dimer interface, and distinct wrist and knuckle epitopes that confer binding to Type-1 and Typ-2 receptors respectively. (Mueller and Nickel, 2012).

The pro-domain, after cleavage, remains associated with the mature active BMP dimer as seen in BMP4, 7, 9, 10, 11, and GDF5, 8. This association of the pro-domain does not affect the latency of the BMP molecules and rather this allows direct targeting of the extracellular matrix especially pro-domain mediated binding to the fibrillins (Brown et al., 2005; Sengle et al., 2008a; Sengle et al., 2008b). Thus, BMPs which are released as soluble proteins can diffuse away from the cell of origin to from gradients while those associated with their pro-domain can bind to ECM containing microfibrils (Bragdon et al., 2011). Additionally, certain BMPs like BMP2 contain a heparin-binding site that tethers then to the cell surface or to the ECM (Gandhi and Mancera, 2012), thereby controlling its bioavailabilty.

1.3.2. BMP antagonists

The BMP pathway can be regulated extracellularly by a family of secreted antagonists. These antagonists can bind to the BMP ligands thereby preventing their interaction with BMP receptors. The BMP antagonists in vertebrates include Noggin, Chordin, Gremlin, Follistatin, Twisted gastrulation, Sclerostin, Crossveinless 2 and USAG-1 (Balemas et al., 2002). BMP antagonists are typically 170-250 aa in length, with the exception of Chordin (948 aa) and Crossveinless 2 (CV2) (685 aa). A latency/propeptide domain of 20 aa rich in leucine and valine is present on the N-terminus of the secreted BMP antagonists. Upon cleavage, the N-terminus forms the clip or the finger domain which interacts with the BMP ligands (Groppe et al. 2002). The BMP antagonists are expressed in a tightly regulated temporo-spatial manner during embryonic development and deletion of one or more of the antagonists leads to lethal developmental defects. Early dorsal-ventral patterning in Drosophila is mediated by twisted gastrulation (Mason et al., 1994). Loss of Chordin in mice results in defects in the ear structure, pharyngeal and cardiovascular disorganization (Bachiller et al., 2000). Whereas Gremlin has shown to be essential for limb and digit formation and kidney development in mice (Kokha et al, 2003; Michos et al., 2004).

1.3.2.1 Noggin

Noggin, is a secreted protein encoded by the *Nog* gene and is a key regulator of the BMP/SMAD pathway. It is secreted as a homodimer of 64 kDa. It was identified in *Xenopus laevis* for its ability to rescue dorsal development, ventralized by UV irradiation (Smith and Harland 1992). Noggin binds and antagonizes BMP2, BMP4, BMP5, BMP7, BMP13 and BMP14 thereby preventing the ligands from binding to BMP receptors (Zimmerman et al., 1996; Song et al., 2010; Seemann et al., 2009). This leads to blockage of SMAD-dependent and non-SMAD signalling (Groppe et al., 2002). Noggin dimerizes via a core body through which 2 pairs of β-strands is preceded by the clip segment which is a 20 aa rich N-terminal segment. This clip segment wraps around the BMP dimers thereby preventing binding to the BMPRs (Groppe et al., 2002). Noggin-BMP7 complex is shown in Figure 1.3.

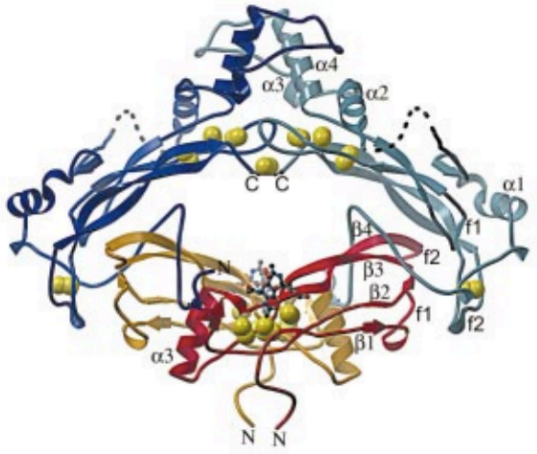

Figure 1.3: Structure of Noggin-BMP7 complex
Ribbon diagram of Noggin-BMP7 complex viewed with two-fold symmetry axis. Noggin subunits are shown in blue and light blue, BMP7 homodimer subunits are in red and gold while sulphur atoms of the di-sulphide linkages are shown as yellow spheres. From Groppe et al., 2002.

Noggin is a pleotropic factor expressed in the early stages of gastrulation in the Spemann organizer and creates BMP gradients to support dorsal-ventral patterning of the early embryo (Smith and Harland 1992; Zimmerman et al., 1996). Later in embryonic development noggin promotes development of the notochord, somites and limbs (McMahon et al., 1998). Noggin knockout mice are characterized by several defects including reduction in size of somites, failure in neural tube closure, skeletal malformations and cutaneous syndactyly (McMahon et al., 1998; Brunet et al., 1998; Tylzanowski et al., 2006; Murgai et al., 2018).

In humans, heterozygous missense mutations in Noggin leads to functional haploinsufficiency leading to skeletal dysplasias, proximal symphalangism (SYM1) and multiple synostoses syndrome (SYNS1) (Marcelino et al., 2001). Mutations in BMP14 at position N64, as seen in patients with SYM1, prevents Noggin antagonism (Seemann et al., 2009). Additionally, other mutations associated with SYM1 include BMP7 at position E60 which prevents BMPR 2 binding thereby resulting in strong osteogenic induction (Song et al., 2010). Genetically engineering BMPs that are insensitive to Noggin inhibition such as BMP14/N64 and BMP7/E60 could have potential clinical applications to support bone healing and regeneration.

1.3.3. BMP receptors

One released the BMP ligands bind to specific transmembrane receptors for signal transduction. These receptors can be divided into two categories- BMPR type I and type II based on differences in their cytoplasmic regions. The key differences lies in the presence of a membrane proximal serine-glycine rich sequence which is on the N-terminal to the intrinsic serine-threonine kinase domain. In mammals, seven Type I receptors have been identified and can be classified into various groups based on their structure and function. These are BMPR I group which includes BMPR-IA and BMPR-IB (ALK3 and ALK6), ALK1 group with ALK-1 and ALK-2, TβR-I group with ALK4, ALK5 and ALK7 (Kawabata et al., 1998). Three Type II receptors have been identified in mammals, BMPR-II, ActR-II and ActR-IIB. Here, BMPR-II is specific for BMPs, whereas ActR-II and ActR-IIB are are bound by activins, myostatin and BMPs (Yu et al., 2005).

BMP ligands bind to BMPR type I, which in turn recruits BMPR type II (Rosenzweig et al., 1995). The intracellular domain of BMPR type I consist of glycine and serine rich domains located on the N-terminal of serine-threonine kinase domains. The type II receptors are constitutively active and upon ligand binding phosphorylate the GS domain of Type I receptors (Huse et al., 1999). In type I receptors the kinase domain protrudes out L45 loop between kinase subdomains IV and V which interact with receptor-regulated SMADs (R-SMADs) (Huse et al., 1999). In addition to the ligand-mediated sequential assembly of receptors known as BISC (BMP induced signaling complex), the receptors can be activated via a second mode

termed as PFC (pre-formed complex) wherein the ligands can bind to pre-formed complexes (Nohe et al., 2001).

Apart from type I and type II receptors certain co-receptors have been identified that regulate signalling activity of certain ligands. For example Endoglin is expressed in endothelial cells and facilitates binding of TGFβ1-3, activin-A and BMP2/7 (Barbara et al., 1999). Additionally, RGMs are known to use BMPR II and ActRII for BMP2/4 mediated signalling (Xia et al., 2007).

The activation of BMP-induced SMAD pathways may be compartmentalized within the cell by membrane microdomains. For example, type I receptors BMPR Ia and BMPR Ib are enriched in cholesterol rich membrane domains and confined lateral mobility which is independent of ligand activation, whereas BMPR II is more mobile in the plasma membrane (Guzman et al., 2012).

1.3.4. Canonical BMP/SMAD signalling

SMADs are major transducers of the BMP signalling pathway which are phosphorylated by Type II receptor kinases after activation by Type I receptor kinase (Heldin et al., 1997). SMADs have a highly conserved MH1 and MH2 domain in the N- and C-terminal respectively which are held together by a linker. The MH1 domain is responsible for binding to DNA, DNA binding proteins and nuclear translocation, whereas the MH2 domain plays a role in interaction with receptors, other SMADs and transcriptional activation (Shi et al., 1998; Wu et al., 2000). R-SMADs form a complex with co-SMADs and translocate to the nucleus where they interact with transcription factors, transcription activators and repressors, while they are negatively regulated by inhibitors-SMADs (Shi et al., 1997).

R-SMADs can be divided into two classes – SMAD 2 and 3 which are responsible for transducing TGF-β/activin/nodal signals, whereas ii) Smad1, 5 and 8 transduce BMP pathway signals. Phosphorylation of R-SMAD by BMP type I receptors creates a binding site for co-SMAD 4. Heterotrimer comprising of two R-SMAD molecules and one SMAD4 molecule form transcriptionally active complexes and and accumulate in the nucleaus whereby co-operation with SMAD-interacting DNA-binding transcription factors can lead to transcriptional regulation of target genes in the nucleus (Chacko et al., 2004, Qin et al., 2001). Inhibitory SMADs –

SMAD 6 and SMAD 7 serve as negative feedback-loop mechanisms (Afrakhte et al., 1998). SMAD 7 represses both TGF-β and BMP signaling whereas SMAD6 preferentially inhibits the BMP pathway (Stopa et al., 2000).

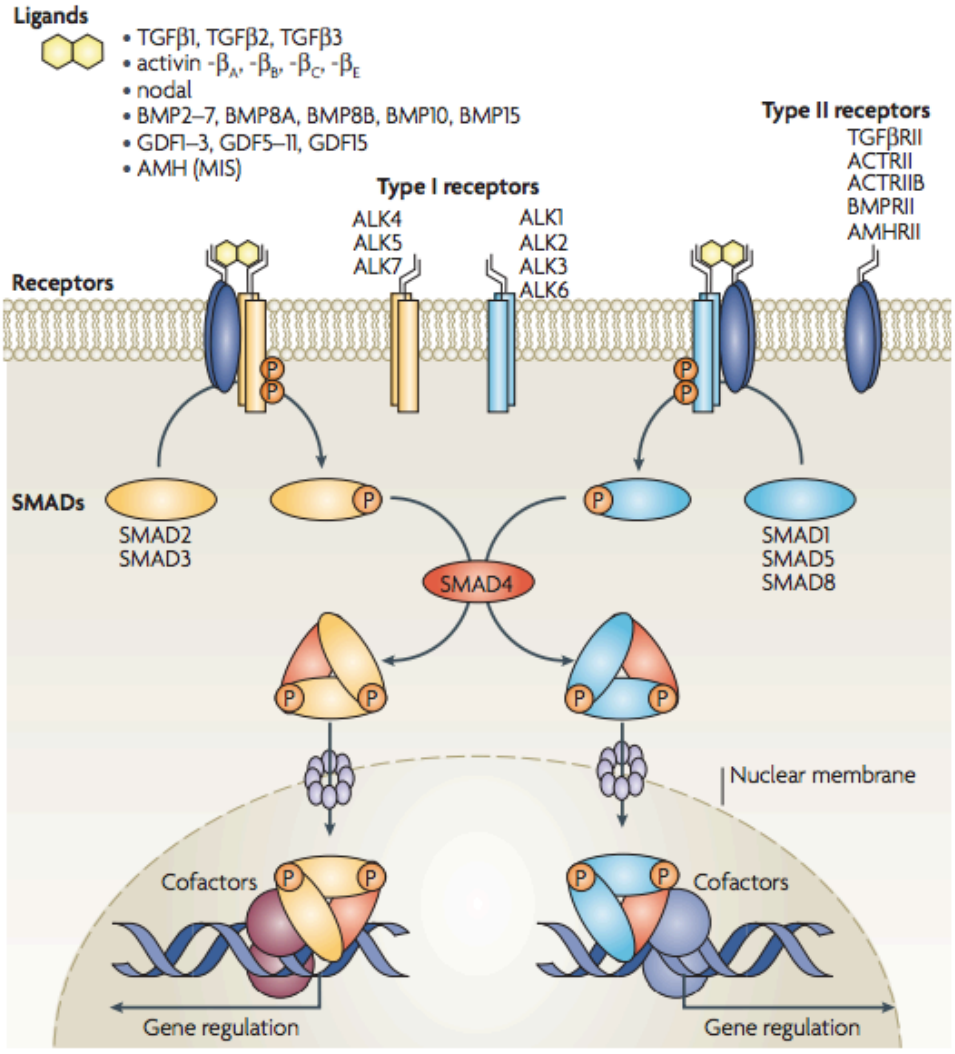

Figure 1.4: Schematic representation of BMP super family SMAD signalling
BMP, activin and TGFβ ligands can bind to Type I receptors which recruits Type II receptors. Serine-threonine kinase of Type II receptors can phosphorylate SMADs (1/5/8 or 2/3) which translocate to the nucleus with co-SMAD4 and transcriptionally regulate genes. From Schmierer and Hill, 2007.

Inhibitory SMADs can inhibit signaling by either interfering with R-SMAD/type I receptor interactions, or R-SMAD-SMAD4 interactions, or through transcriptional regulation in the nucleus. SMAD6 can bind to BMP receptors type I, preferentially Alk3 and Alk6, and inhibit phosphorylation of SMAD1/5/8 (Imamura et al., 1997; Goto et al., 2007). SMAD6 can also bind to SMAD1 thereby preventing formation of SMAD1-4 complex (Hata et al., 1998). Additionally, SMAD6 can also recruits the E3 ubiquitin ligase Smurf1 to the signaling receptor complex and inducing

degradation of type I receptors and of Smad1/5/8 via the ubiquitin-proteasome pathway (Murakami et al., 2003). Lastly, SMAD6 interacts with histone deacetylases 1 and 3 (HDAC1 and 3) leading to condensed transcriptionally inactive chromatin thereby inhibiting transcription (Bai and Cao, 2002).

R-SMAD1/5/8 are known to preferentially bind to BMP response elements (BRE) which are GC-rich sequences found in BMP target genes (Zawel et al., 1998). Numerous BMP/SMAD target genes have been identified in various cells. For example, Runx2 and Osterix are involved in osteogenic differentiation in mesenchymal progenitors (Hayashi et al., 2008). Another important BMP/SMAD target are the ID family of genes, these are basic helix-loop-helix transcription factors associate with muscle transcription factors like MyoD and myogenin and activate transcription of genes containing E-box sequences in their promoters (Miyazono et al., 2002). Recent advances in ChIP technology and next generation sequencing could help to identify new target genes of BMP/SMAD signalling.

1.4. BMP signalling during myogenesis

BMPs have largely been studied for their ability to induce osteogenesis. However, research in recent years has highlighted the role of BMPs in skeletal muscle development. In spite of the growing evidence of BMP signalling in myogenesis, research in this field has been rather limited. Hereby, the current state of research in BMP signalling in muscle development is described.

1.4.1. BMP signalling in somitic myogenesis

In vertebrates, limb muscles derive from the precursor cells in the lateral compartment of early somites (Ordahl and Le Douarin, 1992). During somatic myogenesis, Noggin and BMP4 are expressed in the dermomyotome and the lateral plate respectively. Here, Noggin antagonizes the lateralizing effect of BMP4 thereby allowing medial somite patterning (Hirsinger et al., 1997; Pourquie et al., 1996). In the dermomyotome, however, BMP signalling must be inhibited to allow the onset of myogenesis. Work in *Xenopus* embryos has shown that BMPs determine the location of the early formation of the skeletal muscle, and myogenesis is inhibited by excess or absence of this signal. Ventral regions of the embryo express BMP2, BMP4 and BMP7, while the BMP antagonists Noggin, Chordin and Follistatin are expressed in the dorsal regions. The expression of MyoD and Myf5 is dependent on the intricate balance of BMP signals. (Dosch et al., 1997; Harland, 1994; Re'em-Kalma et al., 1995). BMPs and the antagonist Noggin, together control the timing and precise location of somatic myogenesis. Explant experiments in chick somites have demonstrated that Noggin is expressed in the dermomyotome, where it anatagonizes BMP levels thereby MyoD and Myf5 expression is initiated in Pax3 expressing cells to give rise to the myotome in the medial somite (Reshef et al., 1998). Local application of BMP4 to the chick somites leads to Pax3 expression thereby enhancing MyoD expression and leading to excess muscle growth (Amthor et al., 1999). In Axolotl, BMPs regulate the formation of the dermomyotome, here upregulation or inhibition of BMP signals directly affected the expression of Pax7 (Epperlein et al., 2007). In developing zebrafish embryos, BMP2b and BMP4 are expressed in the dermomyotome and overexpression of BMP2b delays differentiation while the inhibition of BMP signals does not affect differentiation indicating that BMPs are not essential for

differentiation (Patterson et al., 2010). Studies in Noggin knockout mice have shown that Noggin is not essential for the formation of the early Pax3 expressing cell pool, but is however essential for the induction and survival of myotome derivatives in the trunk (McMahon et al., 1998) Altogether, BMPs and the antagonist gradients play a crucial role in regulating early somitic myogenesis by controlling expression of early myogenic genes and thereby allowing differentiation (Figure 1.5).

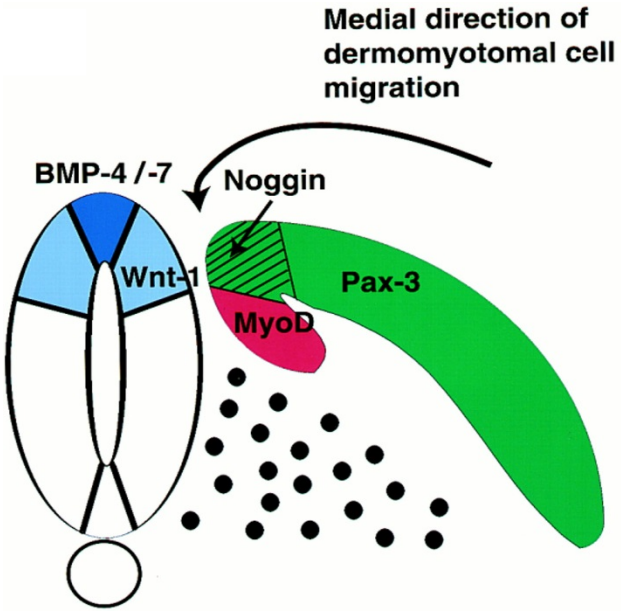

Figure 1.5: Gene expression domains in the dermomyotome
The somitic expression domains of Pax3 in the dermomyotome, Noggin in the dorsomedial lip, MyoD within the myotome, and BMP4 and BMP7 in the neural tube. From Reshef et al., 1998.

1.4.2. BMP signalling in embryonic myogenesis

During early embryogenesis limb precursors migrate into the limb bud as undifferentiated precursor cells and concentrate as two separate clusters of cells in the dorsal and a ventral mesenchyme (Wachtler, 1986). In chick embryos, BMP signals from the ectoderm maintain Pax3 expression and provide pro-proliferative signals. In contrast, removal of the ectoderm depletes the myogenic cells of BMPs thereby inducing the expression of MyoD and leading to muscle growth. These BMP signals are regulated by Noggin emanating from the neural tube as well as the central core of the limb bud. (Amthor et al., 1999; Amthor et al., 1998). BMP2 stimulation of chicken micromass cultures showed osteogenic induction in otherwise myogenic cells, indicating that BMP signals in the limb bud can eliminate

myogenic cells to regulate positioning of both muscle and skeleton (Duprez et al., 1996). In Noggin knockout mice, expression of early myogenic markers Pax3, MyoD and Myog is not affected indicated that Noggin is not required for early patterning of the muscles. However, expression of terminal myogenic differentiation marker myosin heavy chain which labels myocytes and myofibers was reduced in these mutants thereby highlighting a role for Noggin in the myogenic differentiation process (Tylzanowski et al., 2006). Altogether, this indicates that dose-response of BMP signals in the embryonic limb bud co-ordinate muscle growth via proliferation and positioning of muscles through apoptosis. Whereas, Noggin mediated inhibition of BMP signals induces the differentiation process.

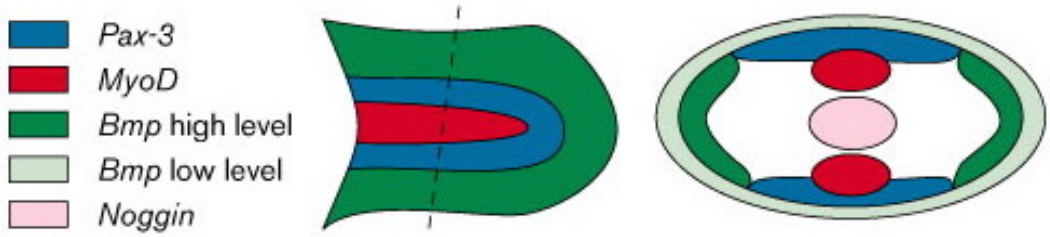

Figure 1.6: Expression domains in the embryonic limb bud
BMPs from the ectoderm (light green) and the anterior and posterior mesenchyme (light green) keep the Pax3 expressing cells in the dorsal and ventral mesenchyme in an undifferentiated state. Noggin expression from the central core of the limb bud induces MyoD expression in a subset of cells. From Amthor et al., 1998.

1.4.3. BMP signalling in fetal myogenesis

The role of BMP signalling in fetal myogenesis has not been extensively investigated. Work in chick has shown that BMP signalling regulates fetal muscle growth. Ectopic activation of BMP signals in the chick limbs leads to increased number of muscle progenitor cells and myofibers, while Noggin-mediated inhibition of BMP signalling leads to reduction in muscle progenitors and myofibers. Furthermore, activation of pSMAD in a subset of proliferating fetal progenitors at the tips of the muscles results in directional growth of the muscle (Wang et al., 2010). A recent study in Noggin knockout mice shows that enhanced pSMAD in these fetuses leads to reduced numbers and differentiation of myogenic progenitors and furthermore less myofibers. Thereby, highlighting a role for Noggin in maintaining proliferation and differentiation of muscle progenitors (Costamagna et al., 2016).

1.4.4. BMP signalling in postnatal myogenesis

BMPs regulate adult muscle satellite cells (SCs) as well as postnatal muscle growth. BMP pathway components including BMP ligands, pSMAD1/5/8 and BMP antagonist Noggin are expressed in juvenile and adult muscle SCs (Stantzou et al., 2017). *In vitro* studies have shown that stimulation of SCs with exogenous BMP4 induces proliferation, while blockage of BMP signalling with Noggin, soluble BMPR1-A fragment, or si-RNAs for SMAD4 and SMAD5 induces precocious differentiation. Furthermore, inhibition of the BMP pathway reduces the expression of Id genes, thereby indicating the mechanism by which the BMP pathway inhibits differentiation (Ono et al., 2011). Similarly, BMP7 was shown to inhibit differentiation of satellite cells and expand the SC pool (Friedrichs et al., 2011).

In postnatal mice, inhibition of BMP signalling by overexpression of Noggin or inhibitory SMAD6 or SC-specific knockout of Alk3 reduced SC proliferation and ultimately leading to retarded muscle growth (Stantzou et al., 2017). This shows that BMP signalling regulates postnatal muscle growth by generation and maintenance of the SC pool via canonical SMAD signalling. Furthermore, inhibition of BMP signalling using SMAD4 mutant mice, resulted in muscle atrophy and strongly exacerbates atrophy-phenotype of denervation and fasting. In contrast, increasing BMP signalling using soluble Alk3 counteracts the hypertrophy phenotype of Myostatin-deficient mice (Sartori et al., 2013). This highlights the role of BMPs in adult muscle growth, maintenance and homeostasis.

In regenerating muscles, upregulation of BMP signalling components controls de novo muscle formation. In activated satellite cells, pSMAD1/5/8 is expressed while inhibition of BMP signalling by injecting dorsomorphin or soluble BMPR1-A inhibits the regeneration process (Ono et al., 2011). Likewise, injection of recombinant Noggin protein into the muscle following injury reduced pSMAD1/5/8 and Id gene expression. Whereas, Id-mutant mice showed number of Pax7+ cells are reduced during regeneration (Clever et al., 2010). This indicates that BMP controls SC proliferation by maintaining Id gene expression.

1.5. Extracellular matrix in myogenesis

Skeletal myogenesis is a highly co-ordinated process that depends on the interplay between cell-autonomous and extrinsic factors. Although there is vast knowledge about the intrinsic signalling pathways that govern myogenesis, considerably less is known about the role of extracellular matrix (ECM) in initiation and progression of myogenesis.

1.5.1. Composition of the ECM

The ECM provides support to the cells, promotes cell aggregation as supporting short- and long-range migration that shapes the developing tissue. The extracellular matrix is a dynamic entity that is modified, degraded and reassembled during development and homeostasis (Daley et al., 2008). The ECM can sequester and present growth factors to the cells thereby influencing cellular processes (Selleck, 2000). The ECM is composed of a macromolecular network of glycoproteins and polysaccharides. There are two major types of ECM - the interstitial and pericellular matrix. The interstitial matrix secreted by the connective tissue and consists of collagens, fibronectin and tenascin together with proteoglycans and glycosaminoglycans. The pericellular matrix on the other hand comprises the basement membrane and is composed of laminins, collagen type IV, perlecan and nidogen (Frantz et al., 2010).

1.5.2. ECM receptors

The skeletal muscle cells bind to the ECM via three main receptors- dystroglycan, integrins and sydecans. Dystroglycan confers stability to the myofibers by binding to laminin 211, while mutations in dystrophin leads to muscular dystrophy (Moore and Winder, 2010). Integrins are heterodimeric proteins that contain extracellular, cytoplasmic and transmembrane domains are involved in regulating numerous signalling pathway. Integrins can bind to the actin cytoskeleton thereby acting as mechanotransducers to the cell (Schwartz, 2001). In the muscle, β1 integrins are majorly responsible for cell migration and differentiation while α4 integrins play a key role in myoblast fusion (Mayer, 2003). Integrin linked kinase (ILK) can inhibit GSK3β or activate Akt thereby modulating activity of Rho GTPases and affect muscle cell motility via PI3K signalling (Hiepen et al., 2014; Wickstrom et al., 2010).

Integrins can also cluster and activate signalling receptors in the absence of growth factors (Walker and Assoian, 2005). Altogether, integrins can modulate proliferation, differentiation and migration of various cell types. Lastly, sydecans (sydecan 1-4) are membrane proteoglycans that can interact with integrins and modulate adult muscle growth and regeneration (Cornelison et al., 2004).

1.5.3. Role of ECM during muscle formation

The ECM is involvement starts early on during somitogenesis, a fibronectin matrix is formed between the somites and the somite is surrounded by a basement membrane matrix consisting of laminin and collagen IV which persists through the formation of the dermomyotome (Koshida et al., 2005). In the somites, the fibronectin matrix is essential to maintain N-cadherin junctions to induce apical polarization of the cells thereby maintaining epithelial identity of the dermomyotome (Martins et al., 2009). The dermomyotome interacts with the basement membrane composed of laminin 111 and 511 via $\alpha 6\beta 1$ integrin to prevent precocious myogenesis in the dermomyotome (Bajanca et al., 2006 ; Bajanca et al., 2004). The hypaxial dermomyotomal lip gives rise to muscle progenitor cells that delaminate and migrate to give rise to distinct muscles of the limb, diaphragm, tongue etc. (Buckingham et al., 2003). Here, dissociation of adherens junctions is caused by Met signalling which downregulates expression of E-cadherins and activates expression of MMP2 and MMP9 that degrades collagen IV of the basement membrane (Desiderio et al., 2007). During delamination expression of $\alpha 6$ subunit of the $\alpha 6\beta 1$-laminin receptor is reduced while laminin and collagen IV-rich basement membrane is degraded (Bajance and Thorsteinsdóttir et al., 2002 ; Relaix e al., 2006). The ECM encountered by migrating muscle progenitors has been poorly characterized. Although it is speculated that fibronectin could play a crucial role as injection of an antibody against $\alpha 5\beta 1$, the cell binding domain of fibronectin, in chick limb bud prevents migration of muscle progenitor cells (Brand-Saberi et al., 1993). Hyaluron is also thought support migration of muscle progenitors into the limb bud either by harbouring growth actors or by creating hydrated spaces that support migration (Krenn et al., 1991). In agreement with this, limb regeneration on axolotls involves downregulation of laminin and collagens while fibronectin, hyualuronic acid and tenascin-C are

upregulated thereby providing a matrix that supports myoblast migration (Calve et al., 2010). However, whether Tenascin-C supports myoblast migration is yet to be determined. After dissociation of the dermomyotome, cell-fusion events in the myotome result in bi-nucleate and mono-nucleate cells (Venters et al., 1999). During this phase loss of laminin receptors $\alpha6\beta1$ and $\alpha7\beta1$is observed and laminin-rich basement disappears, while a fibronectin and tenascin-rich matrix remains present between the muscle masses (Cachaço et al., 2005). At this stage connective tissue cells surround the muscle cells and are known to secrete ECM that supports muscle splitting and patterning (Kardon et al., 2003 ; Mathew et al., 2011). A recent study has shown that expression of the zinc finger transcription factor, Osr1, expression in the muscle connective tissue cells supports muscle patterning by regulating expression of ECM genes like collagen VI, lumican and decorin which supports ECM assembly and cell-ECM interactions (Vallecillo-Garcia et al., 2017). In addition to Osr1, other factors including Osr2, Egr1, Klf2 and Klf4 were shown to regulate ECM signatures in connective tissue cells (Orgeur et al., 2018). Lastly, formation of multinucleate myotubes during primary and secondary myogenesis requires the expression of $\beta1$ integrin to mediate cell-ECM interactions (Hirsh et al., 1998 ; Cachaço et al., 2003) however it is still unclear which ECM components are involved in this interaction. Laminin binding $\alpha6\beta1$ and $\alpha7\beta1$ integrins appear on myotubes following myoblast fusion and co-relates with Laminin-211-rich basement membrane that surrounds the myotubes (Cachaço et al., 2005). This step also co-incides with expression of fibronectin suggesting a possible role for cell-fibronectin interactions to support cell alignment and fusion (Cachaço et al., 2005 ; Snow et al., 2008).

The ECM is a crucial regulator of the myogenic process and several gaps continue to exist regarding cell-ECM interactions that maintain muscle progenitors in a stem cell state in their niche and how proliferation and differentiation of these cells is affected by cell-ECM interactions. Furthermore, the role of connective tissue ECM in shaping muscles still needs to be addressed in detail.

1.5.4. ECM in postnatal muscle

Collagen is the major structural protein of adult skeletal muscles and accounts for upto 10% of the dry weight of the muscle (Dransfield, 1977). The basement

membrane of muscle is composed primarily of collagen IV, however collagen VI, XV and XVIII are also known to be present (Sanes, 1982). Collagen XV and XVIII are classified as multiplexins and are heparin sulphate proteoglycans which can bind to growth factors as well as link the basement membrane to other glycoproteins (Eklund et al., 2001). Collagen I is the major component of the perimysium whereas collagen III makes up the endomysium and epimysium (Light and Champion, 1984). Proteoglycans are abundant in the muscle tissue and mostly exist as small leucine rich proteoglycans (SLRPs) consisting of a core protein attached to glycosaminoglycans (GAG). The most prevalent GAG chains are chondroitin sulphate and dermatan sulphate as seen in decorin and biglycan. The proteoglycans with heparin sulphate makes up 30% of the muscle proteoglycans and are known to bind a multitude of growth factors, these include collagen XVIII, agrin and perlecan (Brandan et al., 1987). The structure and organization of the matrix is maintained by interactions between collagens and proteoglycans. Decorin, the major proteoglycan in the perimysium, binds collagen I and is known to regulate collagen fibrillogenesis (Pringle et al., 1990). Biglycan is structurally

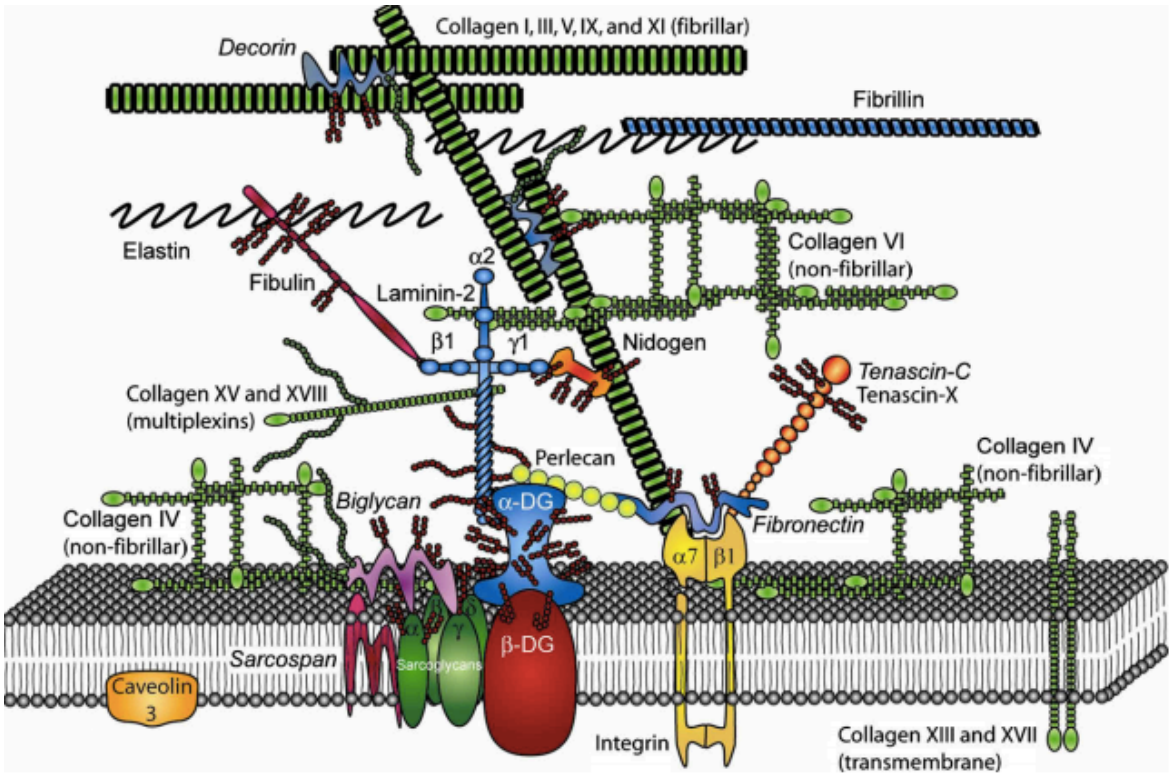

Figure 1.7: Schematic representation of the ECM in skeletal muscle
The ECM of skeletal muscle is a supramolecular network composed of transmembrane protein complexes such as dystroglycan and integrins that associates the sarcolemma with the basal lamina. This association is formed by linking non-fibrillar components such as collagen VI to densly packed fibrillar collagens such as collagen I. From Voermans et al., 2008.

similar to decorin and also binds to collagen I, and lack of biglycan leads to a mild muscular dystrophy phenotype in mice (Mercado et al., 2006). Glycoproteins function as linkers between collagen IV in the basement membrane and the sarcolemma. Laminins can bind to integrins and α-dystroglycan at the sarcolemma whereas integrins may also be bound to fibronectin (Ervasti et al., 1993). Laminins can also bind directly to collagen IV, whereas they can be indirectly bound to fibronectin or nidogen. Together with the branched structure of collagen IV, these glyproteins form the fundamental unit of the basement membrane (Grounds et al., 2005). Matricellular proteins such as osteopontin, thrombospondin and tenascin-C are secreted into the extracellular space however they do not play a structural role. Osteopontin is secreted by inflammatory cells or myoblasts during muscle regeneration (Uaesoontrachoon et al., 2008). Little is known about the function of thrombospondin however it is linked with preventing excessive capillary formation (Malek et al., 2009). Tenascin-C is localized to the neuromuscular and myotendinous junction and binds to perlecan and agrin (Chiquet, 1984). These glycoproteins play a key role in cellular signaling and organization of the ECM.

A delicate balance is maintained for ECM secretion and degradation, the turnover of the ECM is essential for cell migration, myotube formation and reorganization of the matrix during regeneration. Matrix metalloproteases (MMPs) are the key enzymes responsible for remodelling the ECM and are generally lowly expressed in otherwise uninjured skeletal muscles. Secreted MMPs include MMP2 and MMP9 which can degrade collagen IV, fibronectin, proteoglycans and laminin whereas MMP1 and MMP13 degrade collagen I and collagen XIII respectively (Gillies et al., 2007). In addition to secreted MMPs, membrane bound MMP1 can activate MMP2 thereby regulating proteolytic activity at the cell surface. The activity of MMPs can be controlled by tissue inhibitors of matrix metalloproteases (TIMPs) which can either bind to inactivate MMPs or can activate MMPs themselves (Ohuchi et al., 1997). Therefore, the ECM is tightly regulated in its synthesis, degradation and remodeling.

1.6. Aims of the study

Muscle development is a highly co-ordinated process involving tightly regulated migration, proliferation and differentiation of muscle progenitor cells. These processes are synchronised by a multitude of signalling molecules. BMP signalling has been implicated in the regulation of embryonic and fetal myogenesis in chick, and adult muscle growth and homeostasis in mice. (Amthor et al., 1999; Amthor et al., 2002; Friedrichs et al., 2011; Ono et al., 2011; Sartori et al., 2013; Stantzou et al., 2017). Noggin, a BMP antagonist, is crucial for blocking BMP signalling and thereby allowing differentiation of the myogenic stem cells (Friedrichs et al., 2011; Ono et al., 2011). However, the interplay between BMP and its antagonist Noggin precisely during mammalian fetal myogenesis is still poorly understood.

This study, therefore, specifically aims to understand:

How does BMP/Noggin signalling regulate myogenesis during mouse muscle development?

To achieve this, the BMP/Noggin axis will be challenged using a systemic combination of *in vivo* and *in vitro* systems to answer the following questions:

1. What is the role of BMP signalling in mammalian **prenatal muscle development**? For this purpose, a Noggin KO mouse model will be used.
2. How do BMP and Noggin influence the **cellular myogenic program**? For this purpose, CRISPR/Cas9 gene edited C2C12 myoblast cell line and primary myogenic cells will be used.
3. What is the role of the **muscle microenvironment** in directing the BMP/Noggin signalling axis during development? This will be addressed using the mouse model in conjugation with a cell system involving use of different stiffness substrates in conjunction with BMPs.

In addition, a side project will be undertaken to focus specifically on interdigital cell death in Nog KO mice (See Appendix A). Previous work conducted in the Stricker group revealed that Nog KO mice display cutaneous syndactyly. Discerning the mechanism that leads to the phenotype will further contribute towards gaining a better understanding of BMP/Noggin interplay in embryonic development.

Altogether, this research will bridge the current knowledge gap regarding the molecular mechanisms that govern mammalian fetal myogenesis and would contribute to get a better understanding of the intricate BMP/Noggin dynamics that regulates myogenesis. In the long run, the knowledge gained from this study could be used gain new insights into muscle regeneration and muscle disease-related biology.

2. MATERIALS

2.1. Mouse lines

Mouse lines used in this work were maintained at the animal facility of the Max Planck Institute for Molecular Genetics under the supervision of Dr. Ludgar Hartmann. All mouse lines were maintained on a C57BL6 background. The following mouse lines are used:

Noggin$^{+/LacZ}$ mice (Brunet et al., 1998) is provided by Dr. Przemko Tylzanowski. A transgene carrying beta-galactosidase is inserted under the control of the Noggin promoter.

Lbx1Cre mice (Vasyutina et al., 2007)is provided by Prof. Carmen Birchmeyer. A transgene carrying the Cre recombinase gene is inserted under control of the Lbx1 promotor.

Myf5Cre mice (Tallquist et al., 2000) is provided by Prof. Carmen Birchmeyer. A transgene carrying the Cre recombinase gene is inserted under the control of the Myf5 promotor.

ACTA1Cre mice (Miniou et al., 1999) is provided by Prof. Carmen Birchmeyer. A transgene carrying the Cre recombinase gene is inserted under the control of the ACTA1 promoter.

R26mTmG mice (Muzumdar et al., 2007) is provided by Prof. Andreas Kispert. A conditional fluorescence reporter mouse that constitutively express a conditional td-Tomato transgene (mT) that converts to the expression of EGFP (mG) following Cre recombination.

In addition to this, a Noggin/mTmG/Cre compound mouse line was generated by breeding Noggin/mTmG mice with Noggin/Cre mice. This was done for each of the three Cre mouse lines- Lbx1, Myf5 and ACTA1.

2.2. Cell lines

Table 1: Cell lines

Cell line	Cell type	Source
C2C12	Myoblast	Cell bank of Stefan Mundlos
C2C12-BRE	Myoblast	Cell bank of Petra Knaus with MTA from Peter ten Dijke

2.3. Chemicals

Analytical grade chemicals were obtained from Merck (Darmstadt), Roth (Karlsruhe) or Sigma-Aldrich (Hamburg, Seelze, Schnelldorf and Steinheim), unless stated otherwise.

2.4. Buffers and solutions

Standard buffers and solutions were prepared according to 'Molecular Cloning: A Laboratory Manual' by J.F. Sambrook and D.W. Russell (2000), and 'Molecular Cloning: A Laboratory Manual' by M.R. Green, J. Sambrook (2012).

2.5. Reagent Kits

Table 2: Reagent kits

Kit	Supplier
BigDye Terminator v3.1 Sequencing Kit	Applied Biosystems
GOTaq qPCR Master Mix	Promega
In situ cell death detection kit	Roche
MinElute PCR Purification Kit	Qiagen
Nucleobond PC100	Macherey-Nagel
NucleoSpin Gel and PCR Clean-up	Macherey-Nagel
NucleoSpin Plasmid	Macherey-Nagel
RNeasy Micro Kit	Qiagen
RNeasy Mini Kit	Qiagen
SYBR Green qPCR Master Mix	Life Technologies
TaqMan Reverse Transcription Reagents	Roche/Applied Biosystems

2.6. Non-standard cell culture dishes

Table 3: Cell culture dishes

Dish	Supplier	Modification
µ-Dish 35 mm, high ESS	Ibidi	uncoated, 15 kPa
µ-Dish 35 mm, high ESS	Ibidi	uncoated, 28 kPa

2.7. Plasmid

Table 4: Plasmid

Plasmid	Provider
pSpCas9(BB)-2A-Puro (PX459)	Zhang lab

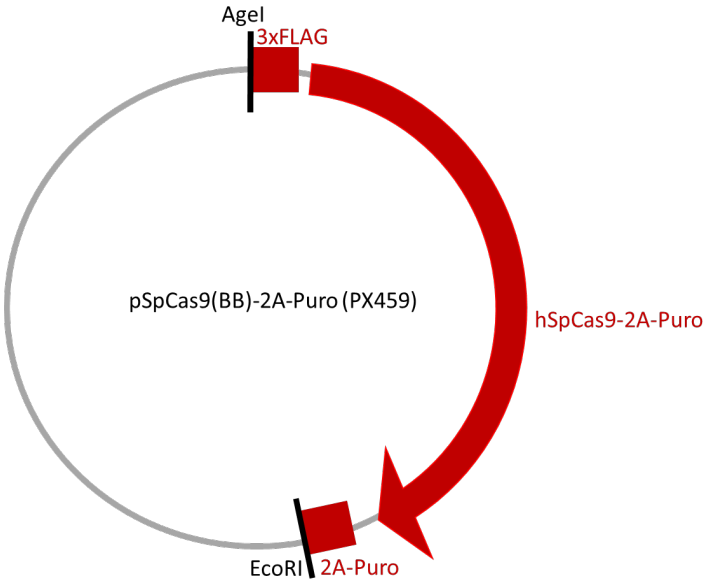

Figure 2.1: Simplified depiction of PX459 plasmid

2.8. Primers

Table 5: Genotyping primers

Gene	Primer sequence (5' -> 3')
Noggin-WTfw	GAGCAGCGAGCGCAGCAGCG
Noggin-WTrev	AAGGGCGATCGGTGCGGGCC
Noggin-KOrev	GCATGGAGCGCTGCCCCAGC
mTmG-WTfw	CTCTGCTGCCTCCTGGCTTCT
mTmG-WTrev	CGAGGCGGATCACAAGCAATA
mTmG-KOrev	TCAATGGGCGGGGGTCGTT
Cre-fw	GAGTGATGAGGTTCGCAAGA
Cre-rev	CTACACCAGAGACGGAAATC

Table 6: RT-qPCR primers

Gene	Primer orientation	Sequence
Acvr2a	F	AGCCCACTTCAAATCCTGTT
	R	TTCCCCTTGCTTTCACTTCT
Acvr2b	F	CGACTTTGTGGCTGTGAAGA
	R	TGCAACAAGTTTTCGTGCTT
Acvr1	F	TCTCTGAGCATCAACGATGG
	R	GAGAGCAACTCCAAGGATGC
Acvrl1	F	CAGACACCCACCATCCCTAA
	R	CTTTGGGCTTCTCTGGATTG
Alpl	F	AACCCAGACACAAGCATTCC
	R	GAGAGCGAAGGGTCAGTCAG
Bmp2	F	GTACCGCAGGCACTCAGG
	R	AAGTTCCTCCACGGCTTCTT
Bmp4	F	CCGGATTACATGAGGGATCT
	R	CCAGATGTTCTTCGTGATGG
Bmp6	F	GTGTTCCTTCCCACTCAACG
	R	AATGGCAACCACAAGCTCTC
Bmp7	F	CTACATGAACGCCACCAACC
	R	AGGACAGAGATGGCGTTGAG
Bmpr1a	F	TGAGACAGCAGGACCAGTCA
	R	GATTCTGCCCTTGAACATGAGA
Bmpr1b	F	AGGCCTTGCTTATCTCTGTGA
	R	TCCAGGAGGAATGCTGAAGT
Bmpr2	F	TGCTTTGGCATCAGTTTCTG
	R	GCAGCTTCAGGTTATCCAGGT
Bglap	F	GGCCCTGAGTCTGACAAAGC
	R	GGCTGCTGGCTTCTAAGTGT
Chrd	F	TCTCAAGACTTGCCCCAAAC
	R	TAATTCTGCATCCCCTCTGC
Fst	F	ACCTGAGAAAGGCCACCTG

	R	GACACAGCTCATCGCAGAGA
Gapdh	F	AACTTTGGCATTGTGGAAGG
	R	CAGTCTTCTGGGTGGCAGTG
Gdf6	F	TGCCAGCTTTTTCCAGTCTT
	R	AGGAGTGTGCGAGAGATCGT
Gdf5	F	CTGTCCGATGCTGACAGAAA
	R	CGTACCTCTGCTTCCTGACC
Grem1	F	CATACACTGTGGGAGCGTTG
	R	CTGGACTCAAGCACCTCCTC
Id1	F	CTTCAGGAGGCAAGAGGAAA
	R	CAAACCCTCTACCCACTGGA
Id2	F	GAAATCCTGCAGCACGTCAT
	R	CATTCGACATAAGCTCAGAAGGGA
Id3	F	CCAAGGACAAGAGGAGCTTT
	R	TGAAGAGGGCTGGGTTAAGA
MyoD	F	CGACACCGCCTACTACAGTGA
	R	AGATGCGCTCCACTATGCTG
Myf5	F	TGAGGGAACAGGTGGAGAAC
	R	CTGTTCTTTCGGGACCAGAC
Myog	F	CTACAGGCCTTGCTCAGCTC
	R	AGATTGTGGGCGTCTGTAGG
Msx1	F	CTCCGCAAACACAAGACGAAC
	R	CACATGGGCCGTGTAGAGTC
Msx2	F	ATCCCAGCTTCTAGCCTTGGA
	R	GACAGGTACTGTTTCTGGCGG
Noggin	F	ATGCCCCATCCCTTAAAATC ,
	R	CGCAGAAGTAGGCTTGTTCC
Pax7	F	CACTACCCGGACATCTACACC
	R	CGGCAGAAGGTGGTTGAA
Pcna	F	GGGCGTGAACCTCACCAGCA
	R	CGTGCAAATTCACCCGACGGC
Runx2	F	TAAGAAGAGCCAGGCAGGTG
	R	TAGTGCATTCGTGGGTTGG
Sox9	F	GTGGCAAGTATTGGTCAA
	R	GAACAGACTCACATCTCT
Spp1	F	CCATCTCAGAAGCAGAATCTCCTT
	R	GGTCATGGCTTTCATTGGAATT

2.9. Antibodies

Table 7: Primary antibodies

Antibody	Supplier and Clone	Host	Dilution
Myosin heavy chain	Merck (05-716)	mouse	1:500
cleaved Caspase-3	Cell signalling (5A1E)	rabbit	1:500
Pax7	DSHB (supernatant)	mouse	1:50
MyoD	Provided*	guinea pig	1:1000
BrdU	Abcam (Ab1893)	sheep	1:50
Ki67	Abcam (Ab833)	rabbit	1:500
phospho-histone3	Milipore (06-570)	rabbit	1:100
Cyclin D1	Santa Cruz (72-13G)	rabbit	1:100
Msx1/2	DSHB (4G1-c)	mouse	1:100
phosphoSMAD1/5/8	Milipore (AB3848)	rabbit	1:500
Desmin	R&D Systems (AF3844)	goat	1:100
PECAM-1	DSHB (2H8)	hamster	1:250
Fibronectin	Milipore (F0791)	mouse	1:500
Laminin	Abcam (Ab11575)	rabbit	1:500
HABP	Merck (385911)	bovine	1:500
MF-20	DSHB (supernatant)	mouse	1:100

*Provided by Carmen Birchmeier

Table 8: Secondary antibodies

Antibody	Supplier	Species
Alexa Fluor 488,568,680	Invitrogen	anti-rabbit
Alexa Fluor 488,568,680	Invitrogen	anti-mouse
Alexa Fluor488,594	Invitrogen	anti-goat
Alexa Fluor 568	Invitrogen	anti-hamster
Alexa Fluor 488- Strepavidin	Thermofischer	-

Table 9: Conjugated antibodies

Antibody	Conjugate	Supplier	Host
CD45	APC	BD Bioscience	mouse
CD31	APC	BD Bioscience	mouse
TER-119	APC	BD Bioscience	mouse
Ly-6A/E (Sca-1)	APC/Cy7	BD Bioscience	mouse
Intergrin a-7	PerCP	R&D Systems	mouse

2.10. Enzymes

Table 10: Enzymes

Enzyme	Supplier
Collagenase A	Sigma Aldrich
Proteinase K	Boehringer Ingelheim
Reverse Transcriptase Superscript II	Thermo Fisher Scientific
Taq polymerase	Produced in the group of Stefan Mundlos
DNase I	Qiagen
RNaseA	Sigma Aldrich
Plasmin	Enzyme research laboratories

2.11. Recombinant growth factors and inhibitors

Table 11: Growth factors and antagonist

Name	Supplier	Molecular weight
Recombinant BMP2	Provided by Petra Knaus (originally sourced from Walter Sebald)	25.8 kDa
Recombinant BMP4/BMP7	R&D Systems	29.1 kDa
Noggin	Gift from Aris Economides	28 kDa

Table 12: Inhibitors

Name	Supplier	Comment
LDN-193189	Provided by Petra Knaus (originally sourced from Paul Yu)	BMP type I receptor kinase inhibitor
PPACK	Sigma Aldrich	Plasmin inhibitor

2.12. Substrate coatings

Table 13: Substrate coatings

Name	Supplier	Source
Tenascin-C	Milipore	Human glioma cell line (U251)
Laminin	Sigma Aldrich	Engelbreth-Holm-Swarm murine sarcoma basement membrane
Gelatine	Sigma Aldrich	Porcine skin

2.13. Technical devices

Table 14: Technical devices

Device	Model	Manufacturer
Automated Cell Counter	Luna	Logosbio
Camera Axiocam	MRc5	Zeiss
Camera AxioCam	MRm	Zeiss
Cell culture hood	MSC-ADVANTAGE	Unity Lab
Centrifuge	5424	Eppendorf
Confocal laser scanning microscope	LSM 700	Zeiss
Cooling centrifuge	5417R	Eppendorf
Cryotome	H560	Microm
FACS	Aria II SORP	BD Bioscience
Fluorescence microscope	DMi8	Leica
Gel documentation system	Fusion FX Spectra	Vilber
Heating plate	HI1220	Lecia
Light source	KL1500 LCD	Leica
Micro centrifuge	5415D	Eppendorf
Microscope	LSM700	Zeiss
Microscope	IX50	Olympus
Microtiter plate centrifuge	5416	Eppendorf
Microplate reader	Sunrise	Tecan
Microwave	DO2329	DOMO
Nandrop	2000	Thermo Scientific
pH meter	HI2211	HANNA instruments
Photometer	NanoDrop 2000	Thermo Scientific
Plate reader	Spectra Max 250	Molecular Devices
Power supply	EPS301	Amersham Bioscience
Protein electrophoresis equipment	Mini	Bio-Rad
Protein transfer system	Mini Trans-Blot	Bio-Rad
Real-time Thermocycler	ABIPrism 7900 HT	Applied Biosystems
Rotor	JLA16.250	Beckman-Coulter
Shaker	DRS-12	neoLab
Stereomicroscope	MZ12	Leica
Table Top centrifuge	5414D	Eppendorf
Thermocycler	GeneAmp PCR System 2700, 2720 and 9700	Applied Biosystems

Thermomixer	Thermomixer compact 5350	Eppendorf
Tissuelyser	LT	Qiagen
Vortex	Microspin FV-2400	Lab4you
Water bath	MD	Julabo

2.14. Internet resources

Table 15: Internet resources

Name	Weblink
UCSC Genome Browser	http://genome.ucsc.edu/
NCBI	http://www.ncbi.nlm.nih.gov/
Ensembl Genome Browser	http://www.ensembl.org/index.html
Eurexpress	http://www.eurexpress.org/ee/
The human protein atlas	https://www.proteinatlas.org/
Primer3	http://primer3.ut.ee/
Reverse complement	https://www.bioinformatics.org/sms/rev_comp.html
Guide design resources	https://zlab.bio/guide-design-resources
PANTHER	pantherdb.org
Gene Ontology	geneontology.org

2.15. Software

Table 16: Software

Software	Application
Axiovision (Zeiss)	Microscopy imaging and processing
CorelDraw X7 (Corel)	Figure preparation
EndNote X7 (Thomas Reuters)	Bibliography
FACSDIVA (BS Bioscience)	FACS analysis
Image J (NIH)	Evaluation of microscopy images
Las X (Leica)	Microscopy imaging and processing
Prism 8 (GraphPad)	Statistical analysis
SDS v2.4 (Applied Biosystems)	RT-qPCR measurements and analysis
Zen Black edition (Zeiss)	Microscopy imaging and processing
Zen Blue edition (Zeiss)	Microscopy imaging and processing

3. METHODS

3.1. Molecular Biology Methods

Standard molecular biological procedures were conducted according to 'Molecular Cloning: A Laboratory Manual' by J.F. Sambrook and D.W. Russell (2000), and 'Molecular Cloning: A Laboratory Manual' by M.R. Green, J. Sambrook (2012).

3.1.1. DNA isolation

3.1.1.1 Plasmid DNA isolation

Isolation of plasmid DNA was performed with Nucleospin Plasmid kit (Macherey-Nagel) according to the manufacturer's instructions.

3.1.1.2 Genomic DNA isolation

Tissue biopsies were used to analyse the genotypes of animals. Genomic DNA was isolated in two different way: DNA precipitation method and QuickExtract method.

- DNA precipitation method

Animal tissue was lysed in 300µl Tissue-lysis buffer (17 mM Tris;pH 7.5, 17 mM EDTA, 170 mM NaCl, 0.85 % SDS) together with 0.2 µg/ml proteinase-K at 55 °C for 1 to 12 hours on a thermomixer at 500rpm. Insoluble fractions were removed by centrifuging the lysate at full speed at room temperature for 10 min. Supernatant was transferred to a new Eppendorf tube and precipitated with 350 µl Isopropanol. DNA pellet was obtained after centrifugation at room temperature at full speed for 10 min. The supernatant was removed and the DNA pellet was washed thrice with 500 µl 70% Ethanol. The DNA pellet was air dried for 10 min, dissolved in in 100 µl of ddH2O and stored at -20° C.

- QuickExtract™ method

Animal biopsies were digested at 68° C for 20 min in 50 µl QuickExtract™ followed by inactivation at 98° C for 2 min. Samples were cooled on ice.

3.1.2. RNA isolation

3.1.2.1 RNA extraction from tissues

Tissue was dissected, frozen in liquid nitrogen and stored at -80˚C until use. 500 µl of Trizol was added to the frozen tissue together with a steel ball in a 2 ml Eppendorf tube. The tissue was lysed using a tissue lyser for 3x30 sec at maximum speed. 100 µl of chloroform was added and the tube was pulse vortexed for 15 sec following which it was centrifuged at 10000 rpm for 15 min at 4˚C. The supernatant was collected on ice and mixed with 1 volume of 70% ethanol. The mix was loaded onto a RNeasy spin column, and the RNeasy Mini kit or RNeasy Micro kit, incase of small amounts of tissue, (Qiagen) was used according to the manufacturer's instructions. The RNA was eluted in 30 µl of RNase free water and stored at -80˚C.

3.1.2.2 RNA extraction from cells

RNA was isolated from either cells in culture or from cells in suspension i.e. in case of cells obtained from the FACS. Fore cells in culture, the cell culture media was aspirated and the cells were washed 3x with PBS. In case of cells in suspension, the cells were centrifuged at 1200 rpm for 3x5 mins with PBS. Following which cell lysis solution was added (RLT buffer + 10 µl/ml β- mercaptoethanol) and RNA isolation was performed using RNeasy Mini or Micro kit (Qiagen). The RNA was eluted in 30 µl of RNase free water and stored at -80˚C.

3.1.3. cDNA synthesis

The harvested RNA was used to transcribe cDNA for RT-qPCR using Taqman reverse transcription system (Life Technologies) and SuperScript III (Thermo Fischer Scientific). 1 µg of RNA (dissolved in 40.5 µl RNAse-free water) was transcribed per reaction using reaction mix and PCR cycle in Table 17 and 18.

Table 17: cDNA synthesis master mix

Reagent	Amount
RNA	40.50 µl
10x buffer	10 µl
25 mM MgCl2	22 µl
dNTPs	20 µl
Oligo dTs	5 µl
Reverse transcriptase	2.5 µl
Total volume	100 µl

Table 18: cDNA synthesis PCR cycles

Temperature	Time
25˚C	10 min
48˚C	30 min
95˚C	5 min
4˚C	∞

3.1.4. Real-time quantitative PCR

The expression levels of genes was assessed using Real-time quantitative PCR (RT-qPCR) with SYBR Green (Promega), a fluorescent dye, that binds to double stranded DNA during amplification and thus the measure of fluorescence is proportional to the initial amount of cDNA. The reaction was performed on a 384-well plate using ABIPrism 7900 HT thermocycler. Primers were designed using the Prime 3 online tool, and the sequence was verified by primer BLAST tool on NCBI. Primers were designed to have a Tm of 60˚C and GC content not higher than 60%, with the average product size of 150 bp. The RT-qPCR reaction was set up in a 12 µl volume with the following components: 6 µl of 2x SYBR mix, 2 µl primer pairs (2.5 µM each) and 4µl (1:10 dilution) cDNA. A standard curve was prepared from serial dilutions (1:5) of cDNA from a mixed tissue/cell pool and the values of the test samples were determined. Each sample was used in triplicate, and a water control was used for every target gene. The relative values for each target gene was normalized to a housekeeping gene (eg. *GAPDH*). Data analysis was performed using SDS 2.1 (Applied Biosystems) and the data was presented as the mean and standard deviation of three biological/clonal replicates. The RT-qPCR primers used are listed in Table 6.

3.1.5. Synthesis of digoxigenin labelled RNA probes

3.1.5.1 PCR amplification and sequencing

A pTA-GFP plasmid was used to clone the transcripts which contain T7 or T3 and SP6 binding positions at both ends of the inserted element. A sequencing PCR with T7 or T3 and SP6 primers sequence was done to determine the orientation of the transcript. The plasmid sequence was amplified using a PCR reaction (Table 19 and 20). The PCR product was purified using the NucleoSpin gel and PCR purification kit (Macherey Nagel).

Table 19: Plasmid sequence amplification PCR master mix

Reagent	Amount
Plasmid (100 ng)	X µl
5x buffer	10 µl
T7 primer	4 µl
SP6/T3 primer	4 µl
Taq polymerase	2 µl
ddH20	Up to 100 µl

Table 20: Plasmid sequence amplification PCR cycles

Temperature	Time	Cycles
94° C	5 min	
94° C	1 min	35 cycles
55° C	1 min	
72° C	1 min	
72° C	7 min	
4° C	∞	

3.1.5.2 Transcription and DIG-labelling of the RNA probes

The purified PCR product was used to transcribe RNA and simultaneous digoxigenin-labelling (DIG) of the RNA. The reagents mentioned in Table 21 were mixed on ice and incubated at 37° C for 2 hours. Then 2 µl of DNAse I was added at 37° C for 15 min to allow degradation of the DNA. The degradation was stopped with 2 µl of 0.2 M EDTA (pH 8.0). The volume was adjusted to 100 µl with DEPC-water, and 300 µl ethanol (cold, 100 %) and 10 µl of 4 M LiCL (DEPC) are added and incubated overnight at – 80° C. The tube was centrifuged at 13000 rpm at 4° C for 20 minutes. The pellet was washed with 75 % ethanol (in DEPC-water) and

resuspended in 100 µl DEPC-water. The probe was run on a 1% agarose gel to check purity and the rest was stored at – 80° C until needed.

Table 21: Transcription and DIG-labelling PCR master mix

Reagent	Amount
PCR product (100-200 ng)	x µl
DIG RNA labeling mix, 10x	2 µl
Transcriptionbuffer, 10x	2 µl
RNAse Inhibitor	1 µl
T7 RNA Polymerase (2 U/µl)	2 µl
RNAse-free water	upto 18 µl

3.1.6. Sanger sequencing

For Sanger sequencing a PCR was performed with 100ng DNA as a template and BigDye V3.1 kit (Applied Biosystems), according to manufacturer's instructions. If the GC content of the DNA template was higher than 65%, 1.5% DMSO was added to the PCR reaction mix. PCR mix and cycles are listed in Table 22 and 23. The product was cleaned with ethanol precipitation and sent for sequencing to the sequencing facility. Sequencing was carried out by Mohsen Karbasiyan (Charité Universitätsmedizin berlin) on an ABI3700 capillary sequencer.

Table 22: Sanger sequencing PCR master mix

Reagent	Amount
DNA (100 ng)	1-2.5 µl
5x BigDye buffer	0.75 µl
BigDye v3.1	0.5 µl
Primer F or R (10pmol/µl)	0.5 µl
ddH2O	Upto 5 µl

Table 23: Sanger sequencing PCR cycles

Temperature	Time	Cycles
96° C	1 min	
96° C	30 sec	25 cycles
50° C	30 sec	
60° C	4 min	
4° C	∞	

3.1.7. Genotyping PCR

The animal facility provided small tissue biopsies which were used to isolate DNA tot hen identify the genotype of the animals.

3.1.7.1 Noggin genotyping PCR

For genotyping Noggin mice the PCR was product run on a 1.5% agarose gel with an expected product size of 230bp for WT and 170 bp for mutant.

Table 24: Noggin genotyping PCR master mix

Reagent	Amount
H_2O	14,0 µl
10 x buffer	2,5 µl
dNTP's	2,0 µl
WT/KO-P	2,0 µl
WT-P	1,0 µl
KO-P	1,0 µl
Taq-Pol	0,5 µl
Total Mix	23,0 µl

Table 25: Noggin genotyping PCR cycles

Temperature	Time	Cycles
95 °C	5 min	
95 °C	30 sec	32 cycles
72 °C	1 min	
72 °C	3 min	
72 °C	7 min	
4 °C	∞	

3.1.7.2 R26mTmG genotyping PCR

For genotyping R26mTmG mice the PCR product was run on a 1.5% agarose gel with an expected product size of 330bp for WT and 250 bp for mutant.

Table 26: RmTmG genotyping master mix

Reagent	Amount
H_2O	12,0 µl
10 x buffer	2,5 µl
dNTP's	2,0 µl
Mg++	2,0 µl
Mut_R	1,0 µl
WT_R	1,0 µl
WT_F	2 µl

Taq-Pol	0,5 µl
Total mix	23,0 µl

Table 27: RmTmG genotyping PCR cycles

Temperature	Time	Cycles
95 °C	5'	
95 °C	1'	35 cycles
66 °C	1'	
72 °C	1'	
72 °C	7'	
4 °C	∞	

3.1.7.3 General Cre genotyping PCR

For genotyping Cre mice the PCR product was run on a 1.5% agarose gel with an expected product size of 700bp for hemizygous mice.

Table 28: Cre genotyping master mix

Reagent	Amount
H_2O	16,0 µl
10 x buffer	2,5 µl
dNTP's	2,0 µl
P-for	1,0 µl
P-rev	1,0 µl
Taq-Pol	0,5 µl
Total mix	23,0 µl

Table 29: Cre genotyping PCR cycles

Temperature	Time	Cycles
95 °C	5'	
95 °C	30"	35 cycles
55 °C	30"	
72 °C	1'	
72 °C	10'	
4 °C	∞	

3.2. Microbiological Methods

3.2.1. Cultivation and cryopreservation of *E. coli* strains

Bacteria were cultivated at 37℃ in LB media or LB agar plates supplemented with the antibiotic Puromycin (2 µg/ml) or Ampicillin (100 µg/ml) for selection of plasmid of interest. The bacteria were cryopreserved in LB medium containing 30% glycerol and stored at -80℃.

3.2.2. Transformation of *E. coli* strains

Bacteria were thawed on ice and mixed with 50-100ng DNA, incubated on ice for 30 mins and heat shocked for 35 secs at 42℃. Thereafter, the bacteria were incubated in LB media on the shaker at 37℃ for 1 h and subsequently plated on LB agar plates at 37℃ overnight. Individual clones were picked and plasmid was isolated.

3.3. Histological Methods

3.3.1. Mouse lines maintenance and permissions

This study was approved by the institutional animal welfare board of the Max Planck Institute for Molecular Genetics and the Landesamt für Gesundheit und Soziales Berlin (LAGeSo). Mice were maintained in an enclosed, pathogen-free facility; mice were sacrificed by cervical dislocation. Experiments were performed in accordance with European Union regulations with permission from the Landesamt für Gesundheit und Soziales (LAGeSo) Berlin under licenses ZH120 and G0346/13.

3.3.2. Preparation of mouse tissue

Adult mice were sacrificed by cervical dislocation. Juvenile mice younger than 14 days old were sacrificed by decapitation. Embryos isolated from pregnant females were decapitated and collected in fresh PBS.

3.3.3. Brdu incorporation and cell proliferation analysis

To determine the proliferation rate of cells in the the interdigital mesenchyme, 5-bromo-2'-deoxy-uridine (BrdU, Roche) was intra-peritoneally injected into the pregnant females (50 mg kg-1) at the desired embryonic stage and the embryos were collected 1h later. After paraffin embedding, immunohistological analysis was performed on the tissue sections. The labeled transcript in proliferating cells could be detected with anti-BrdU antibody (described below). The proliferation rate was determined by counting the positive cells versus DAPI positive cells.

3.3.4. Fixation of tissue

The collected embryos and muscle tissue were fixed in a solution of 4%-Paraformaldehyde (PFA) in PBS overnight at 4˚C. The tissue was washed three times in PBS for 15 min each.

3.3.5. Cryoembedding and sectioning

For cryoembedding, the limbs from the fixed embryos were dissected. The limbs were dehydrated in 15% sucrose in PBS solution overnight followed by 30% sucrose in PBS for 2 hours. Following dehydration, the limbs were immersed and oriented in metal chambers filled with Tissue-Tek OCTTM compound (Sakura Finitek). The metal chambers were chilled on a dry ice-ethanol bath.

The embedded tissue blocks were sectioned into 10 µm thin sections using HM 560M Cryo-Star (Thermo scientific). The slides were warmed at 37˚C for 30 min before storing the sections at -80˚C.

3.3.6. Whole-mount in-situ hybridisation

For whole-mount in-situ hybridisation (WISH), embryos of the stages E11.5-E13.5 were collected in PBS/DEPC and fixed overnight in 4% PFA/PBS. The embryos were washed in PBST (Tween 0.1%) for 2x15 min and dehydrated using a methanol series: 2x15 min 50% methanol and 100% methanol for 15 min. The embryos were stored at -20 °C until use. For hybridization, the embryos were incubated in a descending methanol series, washed twice with PBST and bleached in 6% hydrogen peroxide in PBST for 1 h at 4 °C. The embryos were treated with proteinase K for the following durations-E11.5 for 3 min, E13.5 for 8 min and E14.5

for 12 min. After thorough washing with PBST and PBST/glycine (2 mg / ml), the embryos were fixed for 20 min in 4% PFA/0.2% glutaraldehyde and washed several times in PBST. After prehybridization at 65 °C in hybridization buffer (1ml of 1M Tris (pH 7.5), 12ml of 5M NaCl, 200µl of 0.5M EDTA, 1.25ml of 20% SDS, 25ml of 40% Dextran sulfate, 2ml of Denhardt's reagent, 2 ml of tRNA, 50 ml of formamide in 100 ml with DEPC-water) for at least 3 h, the embryos were incubated overnight with the desired probe at 65 °C. For hybridization, the probes were diluted in hybridization buffer at a final concentration of 0.25 µg/ml, denatured at 80 °C for 5min, and then added the embryos. The unbound probes were removed the following day after washing with fresh hybridization buffer for 2x30 min at 65 °C. After the embryos had cooled to RT, RNaseA digestion was performed 37 °C. For this the mixture was washed several times with formamide buffer at 65 °C, initially with 1: 1 diluted with RNase wash buffer (5ml NaCl (5M), 500µl Tris (pH 7.5, 1M), 500µl 10% Tween20, make up to 50ml with H2O) and later diluted with (1: 1) MABT (100 ml of maleic acid (1M, pH 7.5), 30 ml of NaCl (5M), 10 ml of 10% Tween20, to 200 ml with H2O) followed by two wash steps with MABT. For saturation of nonspecific RNAs, the preparations were incubated for 1 h in 10% BBR (Boehringer Blocking Reagent) in MABT and then incubated overnight at 4 °C with anti-DIG-Fab antibody (1:5000) in 1% BBR / MABT on a shaker. Unbound antibody was removed the following day by washing with PBST/tetramisole (500mg/1l) 8x30 min on a shaker at RT. To detect the antibody signal, embryos were washed 3x20 min in ALP buffer and then stained with BM Purple. The embryos were incubated at RT shielded from light until the desired staining was obtained. To preserve the signals, the embryos were washed 3x10 min with ALP buffer and fixed in 4% PFA/PBS/ 0.2% glutaraldehyde. The embryos were imaged using the binocular microscope (Leica MZ 12).

3.3.7. Immunohistochemistry

Immunostaining was performed on tissue sections. The slides were warmed on a warming plate at 37 ℃ for 1 h prior to start of the procedure. Heat-mediated antigen retrieval was performed for specific antibodies to improve the antigen accessibility. For this, slides were chilled in methanol at -20℃ for 5 mins. A 1mM solution of EDTA was heated in a water bath to 95℃ and slides were immersed for 15 mins. Slides were washed three times with PBS and blocked with 5% Bovine serum

albumin (BSA) solution for 1h at RT. Primary antibody was diluted at the appropriate concentration in 5% BSA solution and applied onto the slides overnight at 4℃. Slides were washed three times with PBX (1xPBS, 0.1% Triton X-100). Secondary antibodies conjugated to fluorophores were diluted at 1:00 together with 1 mg/ml diamidino-2-phenylindole (DAPI) in 5% BSA solution and applied onto tissue sections for 1h at RT. Slides were washed in PBX and mounted in Fluoromount-G (Southern Biotech), which allows long term storage of slides.

3.3.8. X-gal staining

Embryos were washed in PBS and fixed in fixing solution (0.2% glutaraldehyde, 2mM MgCl2, 5mM EDTA) at 4 °C for 30 min, followed by 3x5 min wash in wash buffer (2mM MgCl2, 0.01% sodium deoxycholate, 0.02% NonidentP40 in PBS). The embryos were stained in staining solution (1mg/ml X-Gal, 5mM K3Fe(CN)6, 5mM K4Fe(CN)6, 2mM MgCl2, in PBS) at 37 °C shielded from light until the desired staining was obtained. The stained embryos were fixed for 30 min in 2% PFA / 0.2% Glutaraldehyde fixed in PBS and imaged using a binocular microscope (Leica MZ 12).

3.3.9. Haematoxylin and eosin staining

Haematoxylin and eosin (H&E) staining was performed on slides with 10 μm tissue sections. The slides were washed with dH20 and dipped in haematoxylin staining solution for 3 minutes. Slides were washed under flowing tap water. Slides were then dipped in eosin staining solution, freshly acidified with 1:200 acetic acid, for 3 minutes. Slides were briefly rinsed in distilled water and dehydrated using 70 % (v/v), 90% and 100% ethanol for 5 minutes each. For clarification the slides were dipped in Ultraclear 2x for 5 minutes, and mounted with Entellan (Sigma-Aldrich).

3.4. Biochemical methods

3.4.1. Plasmin-mediated cleavage of BMPs

BMP2 or BMP4/7 were mixed with plasmin in equimolar concentrations in upto 30 μl of plasmin buffer (50 mM Tris, 150 mM NaCl; pH7.4). The solution was mixed gently by pipetting. The mixture was incubated at 37 °C for 4 hours. PPACK was

added in 1:4 (Plasmin:PPACK) molar excess to inactivate plasmin. The mixture was used immediately for cell stimulation.

3.4.2. SDS-PAGE

A 15% SDS PAGE gel was prepared and run according to 'Molecular Cloning: A Laboratory Manual' by J.F. Sambrook and D.W. Russell (2000). Untreated or plasmin-treated BMP2 or BMP4/7 was loaded at 0.5-5 ng concentration in each well. The gel was then used for silver staining to visualize the BMP cleavage.

3.4.3. Silver staining

The SDS gel was incubated in fixing solution (40% ethanol, 10% acetic acid, 50% dH2O) for 1 hour and washed overnight in dH2O. The gel was rinsed in sodium thiosulphate solution (0.02%) for 1 min and then washed in dH2O 3x for 20 sec. Gel was incubated in silver nitrate solution (0.2 g AgNO3, 200 ml H2O, 0.02% formaldehyde) until sufficient staining was achieved, followed by dH2O wash for 20 sec. The staining was terminated by dipping the gel in acetic acid.

3.5. Cell Biology Methods

3.5.1. Extraction of cells for FACs sorting

FACS sorting was performed from either muscle of adult mice, or from embryonic limb tissue. Tissue was dissected and placed in 500 µl pre-warmed growth media (DMEM (4,5 g glucose, 20% FCS (Biochrome), 1% L-glutamine and 1% penicillin/streptavidin (Gibco)). Tissue was minced using a microscissors and transferred to 2 ml Eppendorf tubes. Digestion was performed by adding 10 mg/ml of Collagenase IV (Collagenase NB 4G proved grade 17465, SERVA). The tubes were put on a thermomixer at 37° C for 1 hr at 650 rpm. The digested tissue was passed through a 20-gauge needle at least ten times to allow separation into single cells. The single cells were filtered out using a 70 µm strainer and suspended in sorting buffer (HBSS with 1% Gentamycin and 2 mM EDTA).

FACS procedure was performed to either isolate mGFP labelled cells from reporter mice or isolation of satellite cells (SC). For SC isolation antibodies against CD45, CD31 and Ter-119 were used to negatively select out hematopoetic lineage cells.

Thereafter, α-integrin high, SCa1 low cells were collected after sorting in a tube coated with SC growth media (DMEM (4.5 g glucose, 20% FCS (Biochrome), 10% horse serum, 1% L-glutamine and 1% penicillin/streptavidin (Gibco)). The cells were either used for RNA isolation or seeded on culture dishes coated with 0.1% gelatine in growth media. FACS sorting was performed using FACS Aria II.

3.5.2. Isolation of myoblasts from juvenile mice

Muscles were dissected from juvenile mice and placed in growth media placed in 500 µl pre-warmed growth media (DMEM (4.5 g glucose, 20% FCS (Biochrome), 1% L-glutamine and 1% penicillin/streptavidin (Gibco)). Tissue was minced using a microscissors and transferred to 2 ml Eppendorf tubes. Digestion was performed by adding 10 mg/ml of Collagenase IV (Collagenase NB 4G proved grade 17465, SERVA). The tubes were put on a thermomixer at 37° C for 1 hr at 650 rpm. The digested tissue was passed through a 20-gauge needle at least ten times to allow separation into single cells. The single cells were filtered out using a 70 µm strainer and suspended in growth media. Cell suspension was added to a cell culture dish for 2 h, this allowed adhesion of fibroblasts while the myoblasts remained in suspension. The myoblasts were collected and seeded on cell culture dishes coated with 0.1 % gelatine in growth media. Differentiation was induced by switching to differentiation media (DMEM (4.5 g glucose, 2% FCS (Biochrome), 1% L-glutamine and 1% penicillin/streptavidin (Gibco)) for 5 days.

3.5.3. Scratch wound healing assay

C2C12 cells were seeded in 12-well plates at a density of $0.1x10^6$ in 10% FCS/DMEM. After 24 hours the confluent monolayer was scratched in the middle fo the well using a pipette tip and the wound was imaged. After 16 hours, the wound was imaged again and percentage of wound closure was determined using Image J.

3.5.4. Alkaline Phosphatase assay

C2C12 cells were seeded at a density of 1×10^4 cells/96-well plates in growth media (high-glucose DMEM, 10% FCS and 2 mM L-glutamine in 10% CO_2). After 24 h, stimulation with recombinant BMP2 was performed in media with reduced FCS

(high-glucose DMEM, 2% FCS and 2 mM L-glutamine in 10% CO_2) for 3 days. ALP activity was measured lysing cells in ALP-buffer1 (0.1 M glycine, pH 9.6, 1% Nonidet P-40, 1 mM $MgCl_2$ and 1 mM $ZnCl_2$). After the addition of ALP substrate in ALP-buffer2 (5 mM *p*-nitrophenyl phosphate (*p*-NPP), 0.1 M glycine (pH 9.6), 1 mM MgCl2 and 1 mM ZnCl2), and subsequent termination of the reaction by adding 0.25 volumes 2 M NaOH ALP activity was calculated by the released amount of *p*-NP from the substrate *p*-NPP, which was determined spectrophotometrically at 405 nm.

3.5.5. C2C12-BRE luciferase assay

A C2C12-BRE cell line was used for this assay. Cells were seeded in a 96 well at a density of 1000 cells per well. The next day, cells were starved in serum-free medium for 3 h and stimulated with BMP2 or BMP4/7 (or plasmin treated BMPs) for 6 hours. Cell lysis was performed using passive lysis buffer (Promega) and measurement of luciferase activity was carried out according to manufacturer's instructions using Tecan system.

To ascertain the effect of plasmin, BMP4/7 and Noggin, various combinations of these were incubated together at 37 °C before cell stimulation for 6 hours. Details in Table 30.

Table 30: Plasmin treatment of BMP4/7 and Noggin

Combination	Procedure
BMP4/7 + plasmin	Equimolar concentrations, pre-mixed for 30 min followed by addition of 4x molar PPACK for 30 min.
Noggin + plasmin	Equimolar concentrations, pre-mixed for 30 min followed by addition of 4x molar PPACK for 30 min.
(BMP4/7 + plasmin)+ Noggin	Equimolar concentrations, pre-mixed for 30 min followed by addition of 4x molar PPACK for 30 min. Then addition of equimolar concentration of Noggin for 30 min.
(BMP4/7 + Noggin) + plasmin	Equimolar concentrations, pre-mixed for 30 mins. Addition of equimolar concentration of plasmin, followed by 4x molar PPACK for 30 min.

3.5.6. BMP stimulation of myotubes

For this assay, either coverslips or Ibidi-μ dishes were coated with 0.1% gelatine solution for 20 minutes at 37 °C, and the solution was aspirated. The plates were allowed to air dry in the cell culture hood for 5 minutes.

C2C12 or primary myoblast derived myotubes were differentiated on gelatine coated dishes for 3 days. The cells were starved under serum-free DMEM for 4 hours, and stimulated with 15nM BMP4/7 or super BMP4/7 in 2% FCS/DMEM for 24 hours. Following this cells were fixed and immunostaining was performed against phospho-histone3.

In order to test the effect of ECM on myotubes an additional step was performed. The myotubes were coated with either recombinant TnC (2 μg/cm^2; Millipore) or Laminin (2 μg/cm; Sigma Aldrich) in serum-free DMEM. After 1 hour the media was aspirated and plates were gently rinsed with PBS to remove excess ECM.

3.6. Image Processing

Raw data acquired from fluorescence or bright field microscopy was post-processed and linear adjustments were made for colour and contrast using either AxioVision, Zeiss or LAS-X software. Line scans were performed in ImageJ, and an intensity plot was generated. For scratch wound healing assay, Image J was used to determine the area of wound closure.

3.7. Statistical Analysis

Statistical analysis was performed using GraphPad PRISM software. Comparative analysis between two groups was performed using two-tailed student's t-test. Comparative analysis of multiple groups was performed using two-way analysis of variance (ANOVA) with post-hoc Bonferroni correction. Statistical significance was determined as follows- * $p<0.05$, ** $p<0.001$, ***$p<0.0001$.

4. RESULTS

The role of BMP signalling has been implicated in chick fetal myogenesis and mouse adult muscle stem cells. However, the molecular mechanisms governing fetal myogenesis in mammals remain poorly understood. This study therefore encompasses a combination of *in vivo* and *in vitro* analysis to addresses BMP/Noggin dynamics in mouse muscle development.

4.1. Noggin is essential for fetal myogenesis

4.1.1. Noggin is expressed in embryonic and fetal muscles

To determine the expression of *Noggin* during development, limb muscles were isolated from embryonic, fetal and postnatal stages from embryonic day 13.5 (E13.5) to postnatal day 54 (P54) and a RT-qPCR was performed. It was seen that *Noggin* is expressed in muscle tissue starting from late embryonic stages i.e. E13.5, wherein the expression went up sharply during fetal stages and peaked at E16.5 (Figure 4.1). Furthermore, a steady decline of *Noggin* mRNA was observed in the muscles of postnatal animals which is in line with published data (Stantzou et al., 2017).

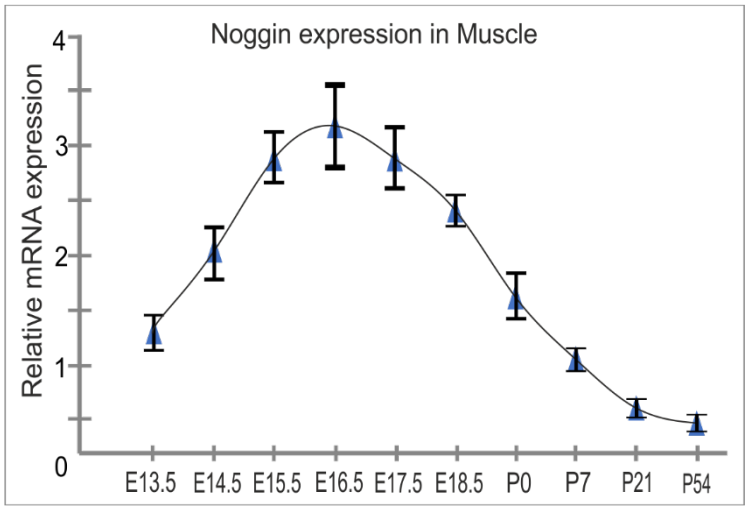

Figure 4.1: *Noggin* is expressed in muscles during development
The expression of *Noggin* was assessed by RT-qPCR in muscles isolated from limbs of embryonic, fetal and postnatal mice. *Noggin* mRNA is detected in embryonic muscles starting at E13.5, with the expression strongly peaking by E16.5. In postnatal animals *Noggin* expression goes down significantly. Points depict fold change (normalised to GAPDH). Error bars represent S.E.M. from three biological replicates. E and P refer to embryonic day and postnatal day respectively.

To visualize the expression of NOGGIN protein in the muscles an indirect approach using a Noggin$^{+/lacz}$ reporter mouse model was used. Here, a lacZ gene encoding β-galactosidase is expressed under the Noggin promoter. When the tissue sections are treated with X-gal (5-bromo-4-chloro-3-indolyl-β-D-galactopyranoside), a hydrolysis reaction generates 5-bromo-4-choloro-3-hydroxyindol, which dimerizes to give rise to a blue precipitate (5,5'-dibromo-4,4'-dicholoro-indigo) visualized here. Cross-sections of forelimbs from E14.5, E16.5 and P0 animals were stained with X-gal. Strong blue staining was observed in the developing cartilage, which is in line with the reported expression of *Noggin* (Brunet et al., 1998). In addition to the cartilage, the limb muscles also showed expression of *Noggin*. This was evident at E14.5, and was strongly enhanced at E16.5, while

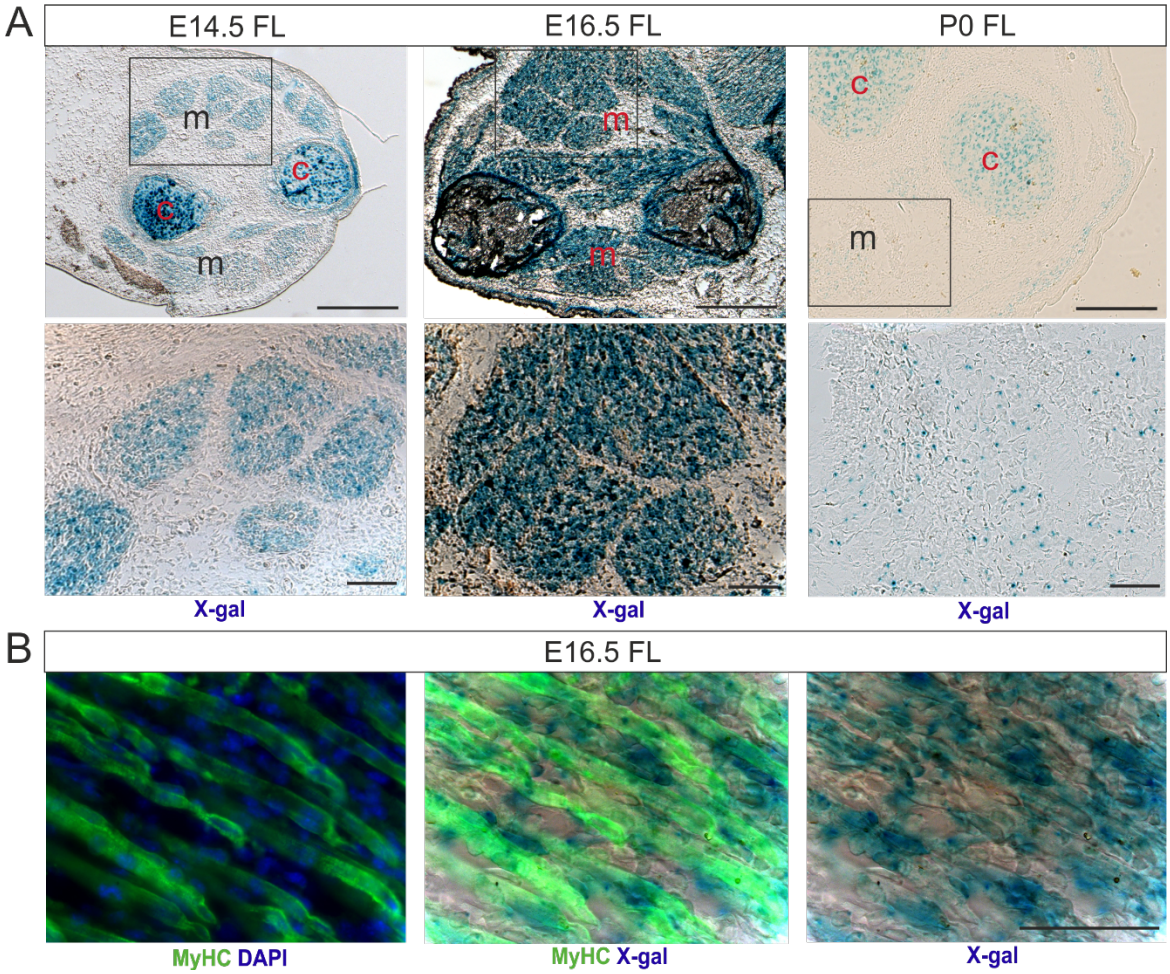

Figure 4.2: *Noggin* is expressed in embryonic and fetal muscles
Cross sections of dissected forelimbs from Noggin$^{+/lacz}$ reporter mice stained for X-gal show blue staining in the muscles (m) and cartilage (c) of E14.5 and E16.5 fetuses. At P0 only a weak blue signal is detected in muscles and cartilage. Insets show blue staining in the muscles (A). Co-staining of X-gal and MyHC at E16.5 shows expression of NOGGIN in muscle fibers as well as in interstitial regions (B). Scale bar 300µm, 100µm (inset) (A), 30µm (B). E and P refer to embryonic day and postnatal day respectively.

the expression of *Noggin* sharply diminished in the muscles by P0. (Figure 4.2A). This is in line with the expression of Noggin mRNA depicted earlier. To confirm the expression of NOGGIN in muscles, a sequential co-staining was performed together with Myosin heavy chain (MyHC), which labels the myofibers (Ribaric and Cebasek, 2013). Blue signals could be observed in MyHC+ regions i.e. within the myofibers but also in the interstitial cells which could include myogenic precursor cells and myoblasts (Figure 4.2.B). The expression of *Noggin* could however not be localized to specific cells as a) x-gal staining strongly quenches florescence in single cells, b) the antibody against β-galactosidase did not successfully stain embryonic tissue. Taken together, this was the first line of evidence showing the expression of *Noggin* mRNA and protein in mouse limb muscles during development and suggests a central contribution of Noggin in impeding BMP signals during late embryonic to late fetal stages of muscle development.

4.1.2. Loss of Noggin does not affect early myogenesis

As the expression of *Noggin* was observed in developing limb muscles, a Noggin$^{-/-}$ (Nog KO) mouse model (Brunet et al., 1998; McMahon et al., 1998; Tylzanowski et al., 2006) was used to determine the consequences of Noggin ablation on myogenesis. These animals have been shown to have a severe skeletal phenotype which includes hyperplasia of the cartilage elements thereby leading to enlarged skeletal elements and joint fusions in the limbs, ribs and vertebrae. In addition to this, the embryos show defects in the growth and patterning of the neural tubes and somites, and the neural tube fails to close. (Brunet et al., 1998; McMahon et al., 1998; Tylzanowski et al., 2006). The accumulation of these defects leads to late fetal and peri-natal lethality, therefore the analysis of this mouse model in this study is limited to pre-natal stages. Previously published work has shown that these mice have phenotypic defects in the muscles, however this has not been extensively investigated (Costamagna et al., 2016; McMahon et al., 1998; Tylzanowski et al., 2006). To investigate the expression of early myogenic markers during embryogenesis, whole-mount in-situ hybridisation (WISH) was performed. Here *Pax3* was used to mark muscle precursors that migrate into the early limb bud (Bober et al., 1994), *MyoD* identified committed myoblasts (Montarras et al., 1989) and Myogenin (*Myog*) marked differentiating myoblasts (Wright et al., 1989) At E11.5, *Pax3* staining was observed in the limb bud and no differences were

noted in the pattern or intensity of the staining between WT and Nog KO, indicating correct migration of the early muscle precursor cells (Figure 4.3A). At E12.5 and E13.5 staining for *MyoD* and *Myog* in the forelimbs did not reveal any notable differences between WT and Nog KO. The early muscle masses were correctly patterned and no changes in muscle sizes could be observed, thereby indicting

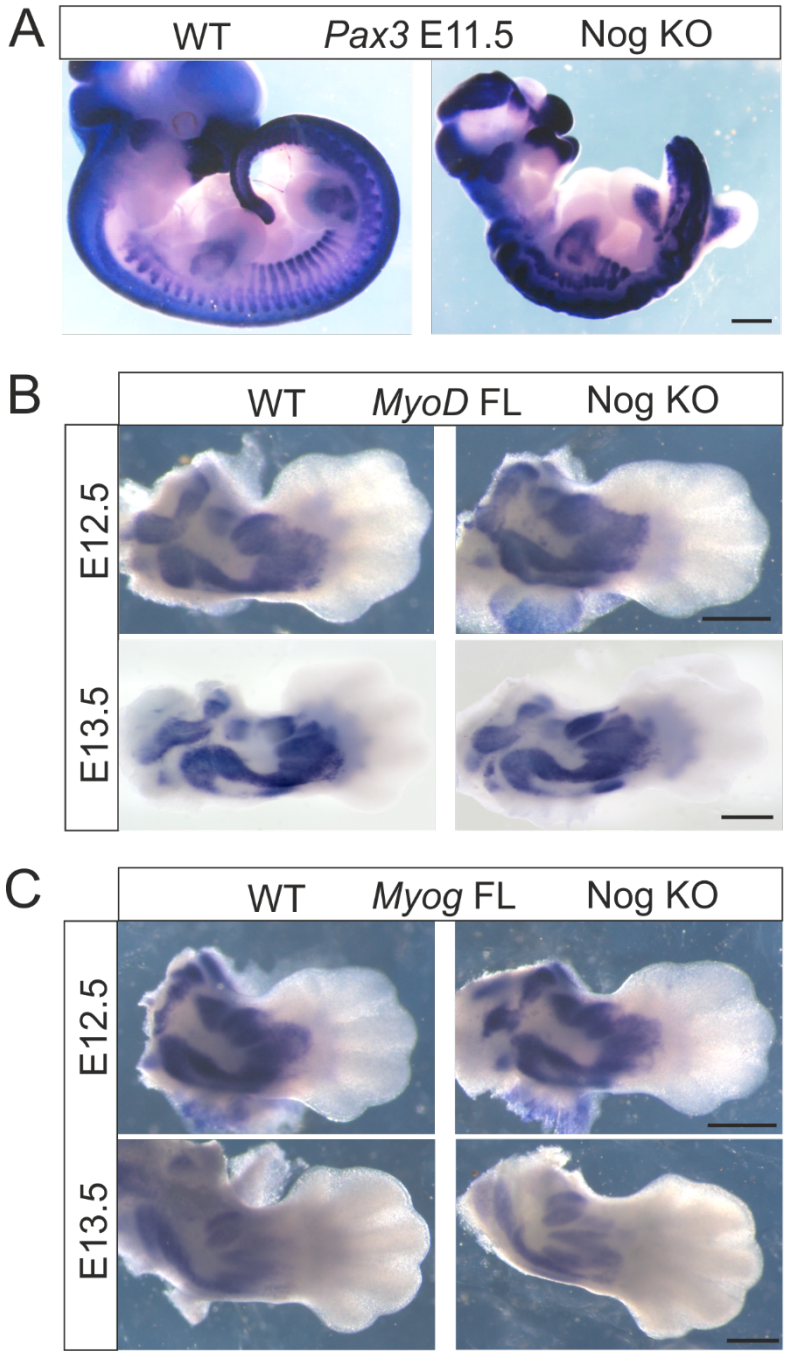

Figure 4.3: Myogenic markers remain unaffected in embryonic stages
WISH reveals mRNA expression of *Pax3* in whole embryos at E11.5 (A), *MyoD* in dissected limbs at E11.5 and E12.5 (B) and *Myog* in dissected limbs at E12.5 and E13.5 (C). No visible differences in the expression of these myogenic markers were noted between WT and Nog KO embryos. The early migration, patterning and sizes of muscles remain unaffected by Nog KO. Scale bar 50µm (A) and 100 µm (B,C).

lack of any defects in early stage cell differentiation (Figure 4.3B,C). This altogether shows that the early process of myogenesis is not affected in Nog KO embryos.

4.1.3. Noggin knockout leads to loss in muscles during fetal development

Next, myogenesis was investigated in the later stages of development. Limbs were dissected from stages E14.5, E15.5 and E16.5 and cross-sections were derived from the forelimbs as shown in Figure 4.4A. Immunostaining for Myosin heavy chain (MyHC) was performed, which labelled all the muscle fibers (Figure 4.4B). At E14.5 no visible differences between the patterning and size of the muscle masses were observed and the skeletal elements (cartilage and bone) were comparable between WT and Nog KO fetuses. However, from E15.5 through E16.5 a major loss in muscles, in particular myofibers, was observed and there was a failure in formation and growth of new muscle anlagen. Concomitantly, this was accompanied by rapid expansion of the skeletal elements which has been described before (Brunet et al., 1998). Of note, loss in muscle observed in these fetal stages, coincides with high expression of Noggin in the muscles at this stage thereby emphasising the significant role of Noggin during fetal myogenesis. Since majority of the major muscles are lost by E16.5, while at E14.5 the phenotype has not yet peaked, the intermediate stage E15.5 was chosen as the major investigation stage for further analysis.

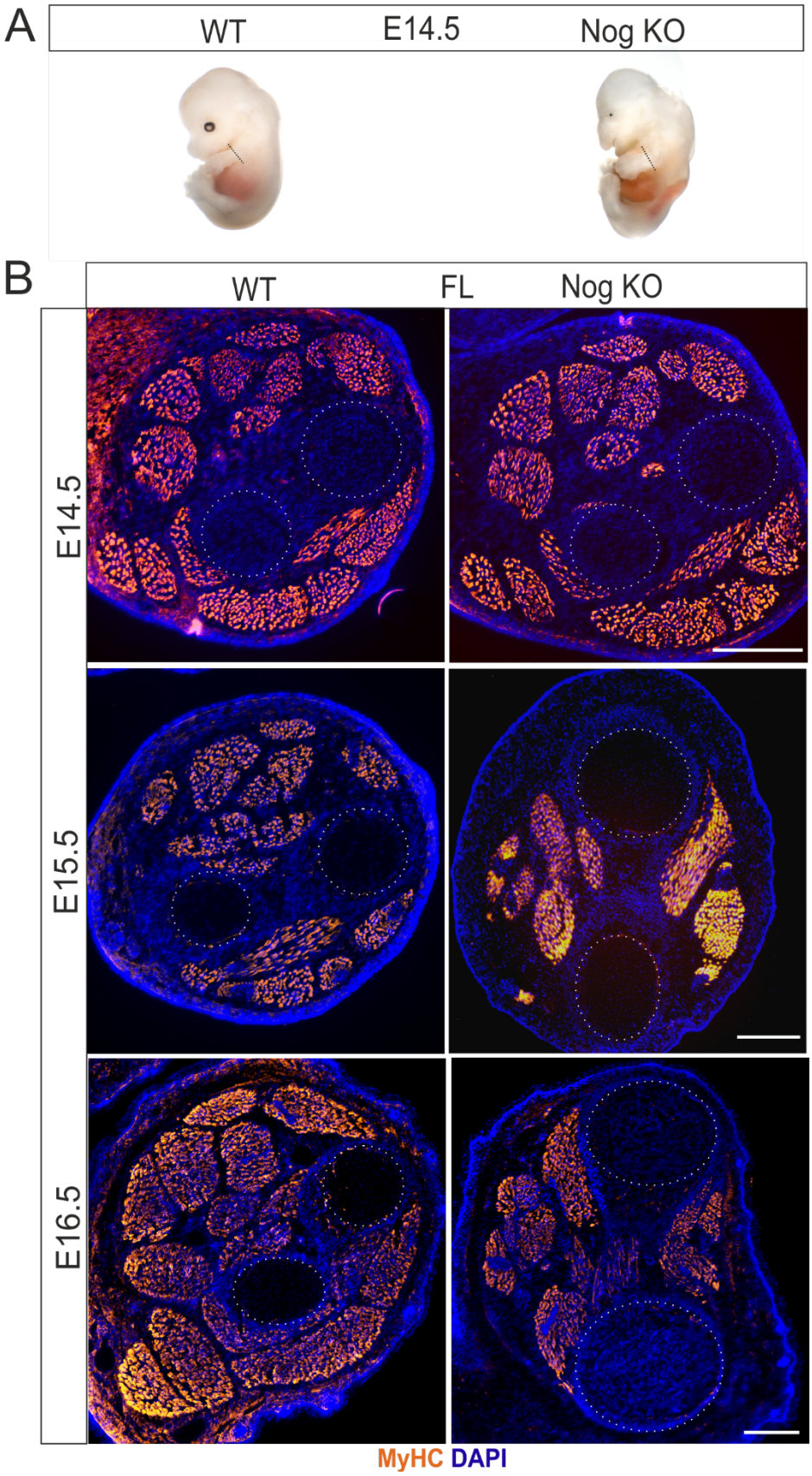

Figure 4.4: Comparative analysis of limb muscle during development
Cross-sections of WT and Nog KO forelimbs obtained as shown in A. Immunostaining against Myosin heavy chain (MyHC) reveals no changes in muscle patterning at E14.5, while from E15.5 to E16.5 extensive muscle loss together with expansion of the skeletal elements (white dotted line) is observed. Scale bar 100µm.

4.1.4. Lack of Noggin perturbs proliferation, differentiation and fusion of myogenic cells

Noggin and BMPs were shown to balance proliferation and differentiation of myogenic cells in the chicken fetus as well as in postnatal myogenesis and in mouse adult SCs (Friedrichs et al., 2011; Ono et al., 2011; Stantzou et al., 2017; Wang et al., 2010). Therefore, to understand the causes of impaired muscle growth, the fetuses were assessed for proliferation, differentiation and fusion defects in the myogenic cells. To study proliferation of muscle precursor cells and myoblasts, pregnant female mice were injected with BrdU and the fetuses were analysed 4 hours after injection. This allowed incorporation of BrdU in the DNA of proliferating cells and could be visualized by immunostaining. Co-staining of BrdU with Pax7 (labels muscle progenitors) revealed an increase in proliferation of the muscle precursor cells (Figure 4.5A) and a reduction in proliferation of MyoD expressing myoblasts in Nog KO fetuses relative to WT fetuses (Figure 4.5B). This is in line with published *in vitro* data which shows that BMPs have a positive effect

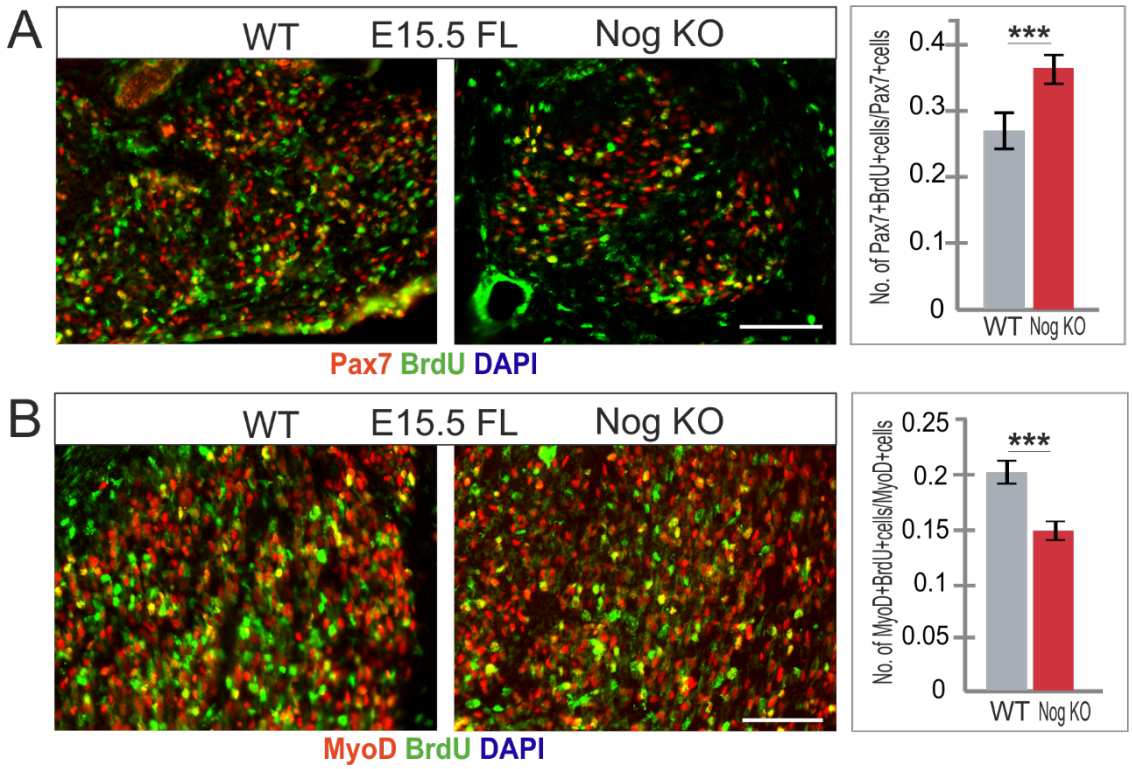

Figure 4.5: Altered proliferation of myogenic cells in Nog KO fetuses
E15.5 fetuses analysed 4 hours after BrdU injection show increase in the proliferation rate of Pax7+ muscle precursor cells, whereas a reduction in proliferation of MyoD+ myoblasts. Bar graphs depict relative ratios. Error bars represent S.E.M. from three biological replicates. Statistical analysis was done using two-tailed Student's t-test; ***p<0.0001. Scale bar 20µm.

on proliferation, while Noggin negatively effects proliferation of adult muscle stem cells (Friedrichs et al., 2011; Ono et al., 2011).

As these results strongly indicated alterations in the proliferation rate of muscle precursor cells and myoblasts were observed, a cell count was done for the various myogenic cell populations. For this, immunostaining was performed against Pax7, MyoD and MyHC at E14.5, E15.5 and E16.5 (Figure 4.6). In comparison to WT, Nog KO fetuses showed an increase in the number of muscle precursor (Pax7+/MyoD-) cells and reduction in (Pax7-/MyoD+) cells when compared to the number of myofibers. This could be explained by the aforementioned increase in proliferation rate of Pax7 expressing cells and reduction in proliferation of MyoD expressing cells observed in Nog KO fetuses. Also, a comparative decrease in the

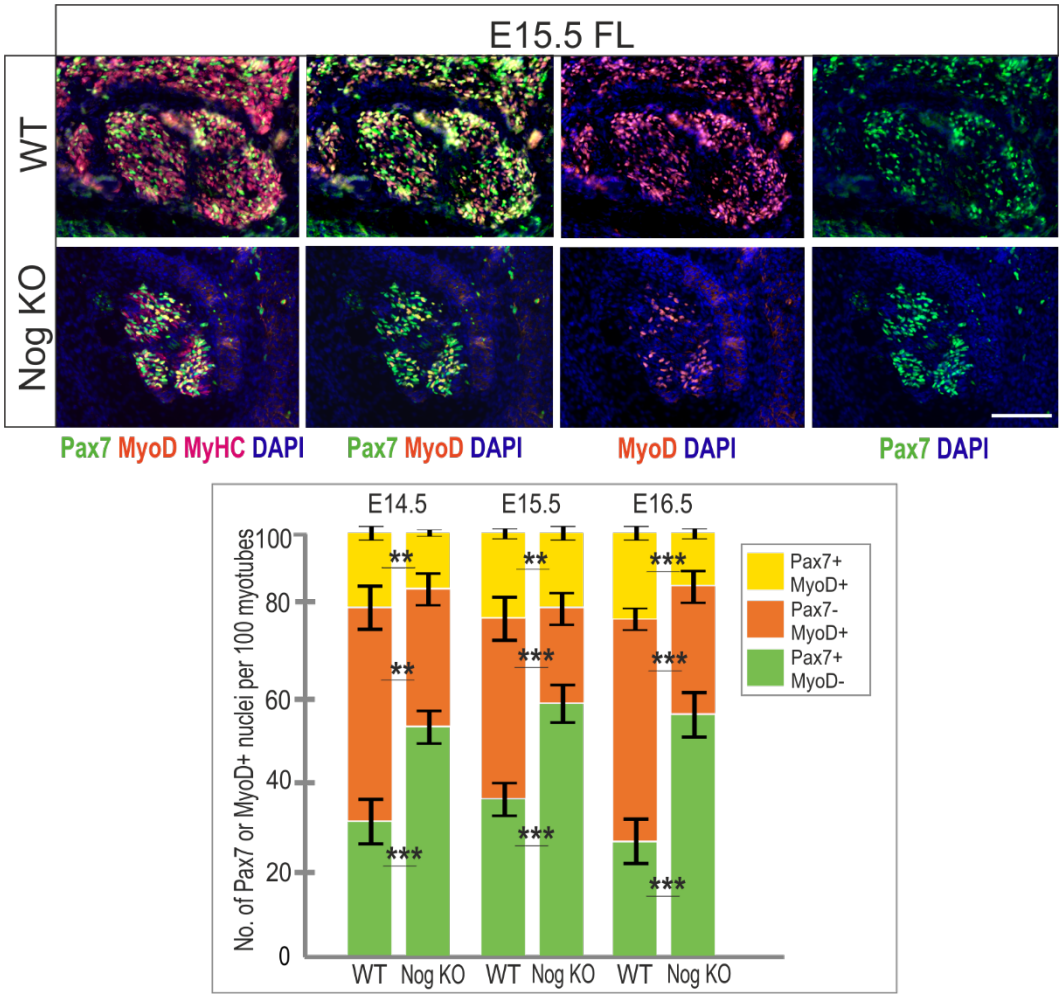

Figure 4.6: Impaired differentiation of Nog KO muscle precursor cells
Immunostaining for Pax7, MyoD and MyHC in muscle forelimbs showing representative image at E15.5. Increase in Pax7+/MyoD- cells, while decrease in Pax7+/MyoD+ and Pax7-/MyoD+ cells during E14.5, E15.5 and E16.5 was observed. Bar graphs depict relative ratios. Error bars represent S.E.M. from three biological replicates. Statistical analysis was done using two-tailed Student's t-test; ** $p<0.001$;***$p<0.0001$. Scale bar 20µm.

number of Pax7+/MyoD+ cells was seen in the Nog KO fetuses, hinting at impaired differentiation. This trend was consistently observed among the three embryonic stages analysed. Taken together, this cell count analysis revealed a differentiation defect of muscle precursor cells, whereby fewer cells differentiated from precursor state to myoblasts and could explain the lack of newer/lesser myofiber formation in the later fetal stages.

Differentiated myoblasts fuse together to give rise to multinucleate myofibers. Thereby, the fusion potential of the myogenic cells was assessed. For this, pregnant female mice were injected with BrdU at E14.5 or E15.5 and the embryos were analysed 24 hours following injection. This allowed BrdU incorporation in proliferating myoblasts, thereby allowing them to be traced until the process of fusion into myofibers. Immunostaining analysis of BrdU+ myonuclei revealed a reduction in the number of myoblasts that fused to from myofibers from E14.5 until E16.5 in Nog KO fetuses (Figure 4.7). This could be explained by a smaller myoblast pool, and/or reduction in fusion capacities of the existing myoblasts.

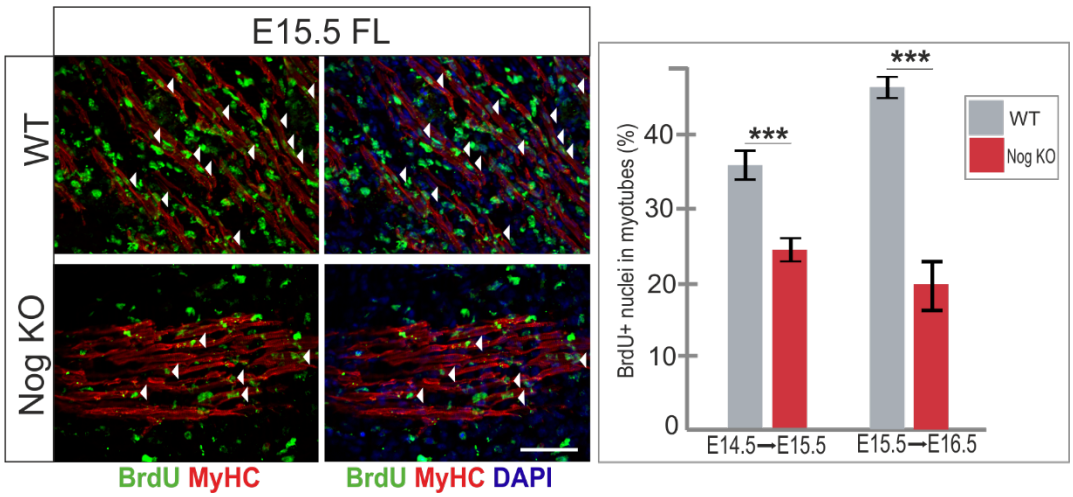

Figure 4.7: Reduced fusion of myoblasts into myofibers in Nog KO fetuses
Immunostaining for BrdU and MyHC following 24 hours of BrdU injection showing representative images of E15.5 forelimb muscles. Reduction in the number of BrdU+ myonuclei (white arrowheads) representing fused myoblasts is shown from E14.5-E15.5 and E15.5-E16.5. Bar graphs depict relative ratios. Error bars represent S.E.M. from three biological replicates. Statistical analysis was done using two-tailed Student's t-test; ***p<0.0001. Scale bar 20µm.

In conclusion, the results presented so far demonstrate the expression of Noggin in developing muscles while shedding light on the effects of Noggin deletion in mice. I found that loss of muscle mass and lack of new muscle formation which can be explained in part by altered proliferation, reduced differentiation and fusion of myogenic cells. This highlights the relevance of Noggin in fetal myogenesis. To gain a depper understanding into the molecular aspects of Noggin deletion an *in vitro* system was established in the following section to study proliferation and differentiation of the cells.

4.2. Noggin deletion in myoblast cell line affects myogenic and osteogenic differentiation

4.2.1. Confirmation of Noggin deletion in C2C12 cells

To further dissect the role of Noggin in myogenic proliferation and differentiation, a C2C12 myoblast cell line was used. This represents a commonly known myoblastic cell-line system used to study the process of myogenesis and BMP-induced osteogenesis.

CRISPR/Cas9 genome editing was used to delete the Noggin gene in this cell line. Noggin is a one-exon 700bp gene and guide RNAs were designed to flank and cut on either end of the exon sequence (Figure 4.8A). Guide RNAs chosen for the analysis has a quality score of over 90, to eliminate the possibility of off-target effects. Genomic PCR was performed with primers designed to target either side of the Noggin gene with an expected product size of 1.5kb. The deletion of the gene was confirmed by showing a reduction in the obtained PCR product from 1.5kb to 700bp at the Noggin locus (Figure 4.8B). Further confirmation of the deletion of the gene was obtained by RT-qPCR showing absence of Noggin mRNA in the C2C12 cells (Figure 4.8C). The modified cell line is mentioned here on as Nog KO cells.

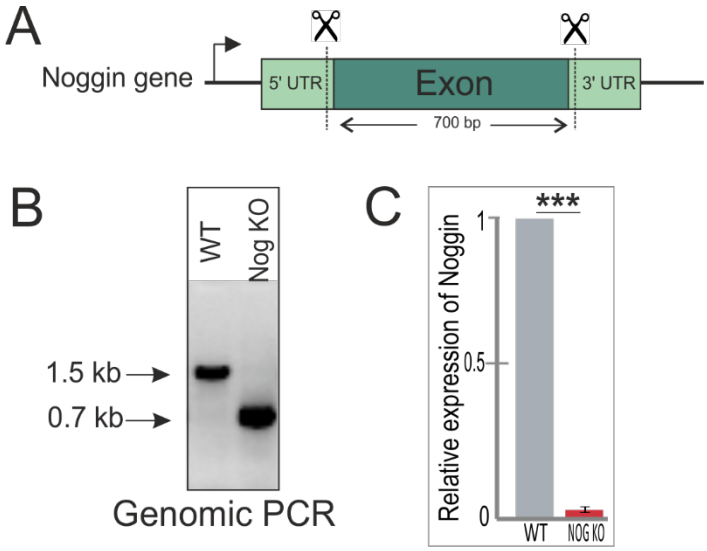

Figure 4.8: Noggin deletion in C2C12 cells
Graphic showing the Noggin gene locus and the target excision sites for the guide RNAs (A). Confirmation of Noggin deletion by genomic PCR showing a shorter PCR product (B) and RT-qPCR showing lack of Noggin mRNA produced by the cells (C).

4.2.2. Nog KO cells display reduced myogenesis

The C2C12 cells were first used to assess their myogenic capacity upon Noggin deletion. The cells were cultured in proliferation media for 24 hours and immunostained for Ki67, a reliable proliferation marker (Scholzen and Gerdes, 2000). A higher proliferation rate could be observed in the Nog KO cells which could be explained by increased BMP signalling in these cells (Figure 4.9A,C). Antibody staining used to label Pax7 and MyoD positive cells revealed an increase in Pax7 expressing cells and a reduction in MyoD expressing cells in the Nog KO cells (Figure 4.9B,D). This was further confirmed by performing a RT-qPCR which showed an increase in muscle precursor marker *Pax7* while a reduction in differentiating muscle cell genes including *MyoD*, *Myf5* and *Myog* (Figure 4.9E). These *in vitro* data on Noggin KO myoblasts are in line with the observations made in the Nog KO embryos that imply intrinsic defects in proliferation and early stages of the differentiation process.

Myogenic differentiation was analysed by exchange of the proliferation to a differentiation inducing environment for six days either with of without LDN-193189, a small molecule BMP inhibitor that competes with ATP binding to the BMP receptor kinase (Boergermann et al., 2010; Cuny et al., 2008). After this, immunostaining was perfromed using MyHC to label the myotubes (Figure 4.10A). The differentiation index was obtained by calculating the percentage of nuclei in MyHC expressing cells, and a significant reduction in the index was observed in Nog KO cells in comparison to WT cells and could be partly rescued by treatment with LDN-193189 (Figure 4.10B). Furthermore, the fusion index was assessed by counting the percentage of MyHC expressing cells. Nog KO cells showed an increase in mono- and bi-nucleated MyHC expressing cells while the number of multi-nucleated MyHC expressing cells was reduced. Treatment with LDN-193189 increased the fusion index, wherein more multinucleated MyHC expressing cells were visible (Figure 4.10C). This implied reduction in myogenic differentiation capacity of the Nog KO cells relative to WT cells, which could be partially rescued by using the pan BMtype-I receptor inhibitor LDN-193189 .

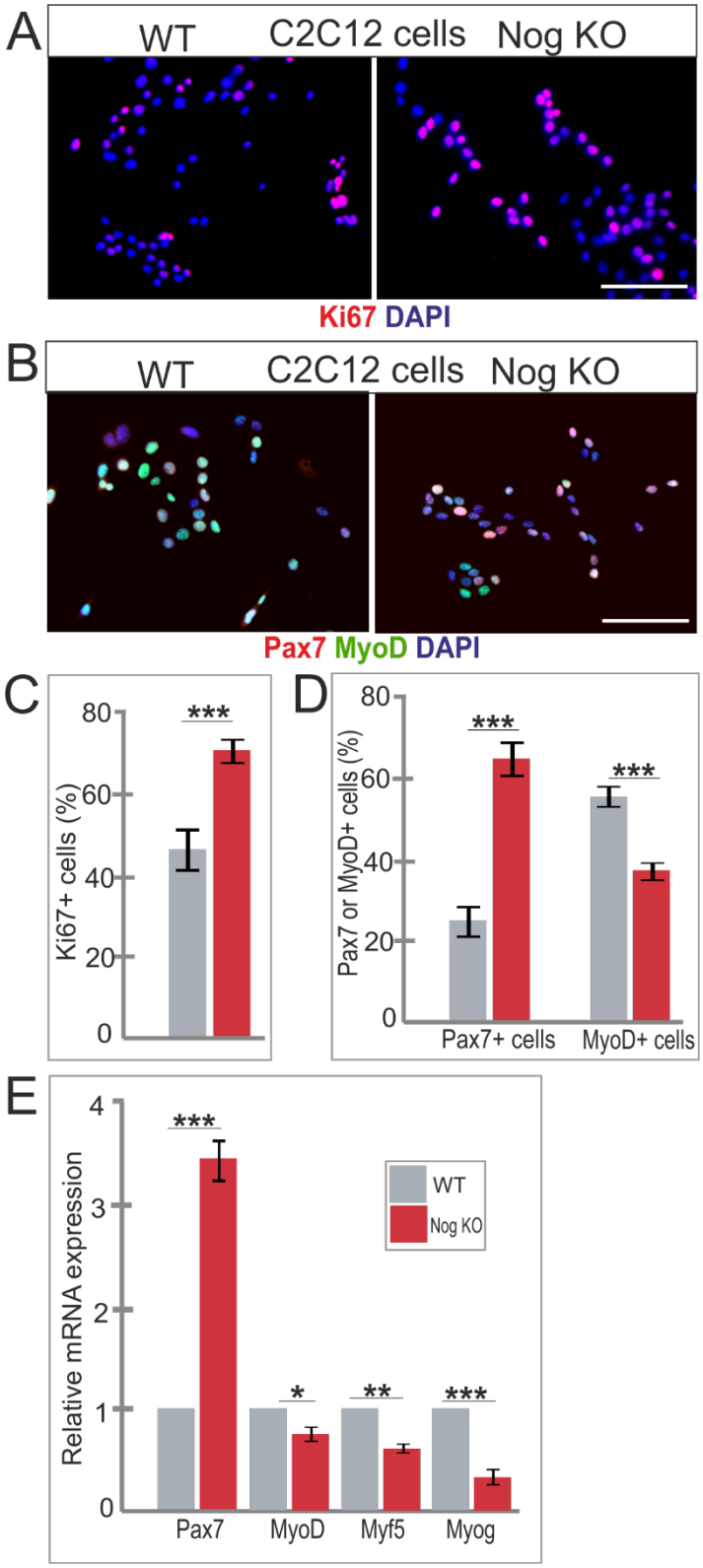

Figure 4.9: Increased proliferation and reduced myogenic markers in Nog KO C2C12 cell line

Immunostaining for Ki67 showing reduced proliferation rates (A), and increase in Pax7+ cells and reduction in MyoD+ cells (B). RT-qPCR showing increased in Pax7 and reduction in myogenic markers i.e. MyoD, Myf5 and Myog. Bar graphs depict relative ratios. Error bars represent S.E.M. from three clonal replicates. Statistical analysis was done using two-tailed Student's t-test; * $p<0.05$, ** $p<0.001$, ***$p<0.0001$. Scale bar 300µm.

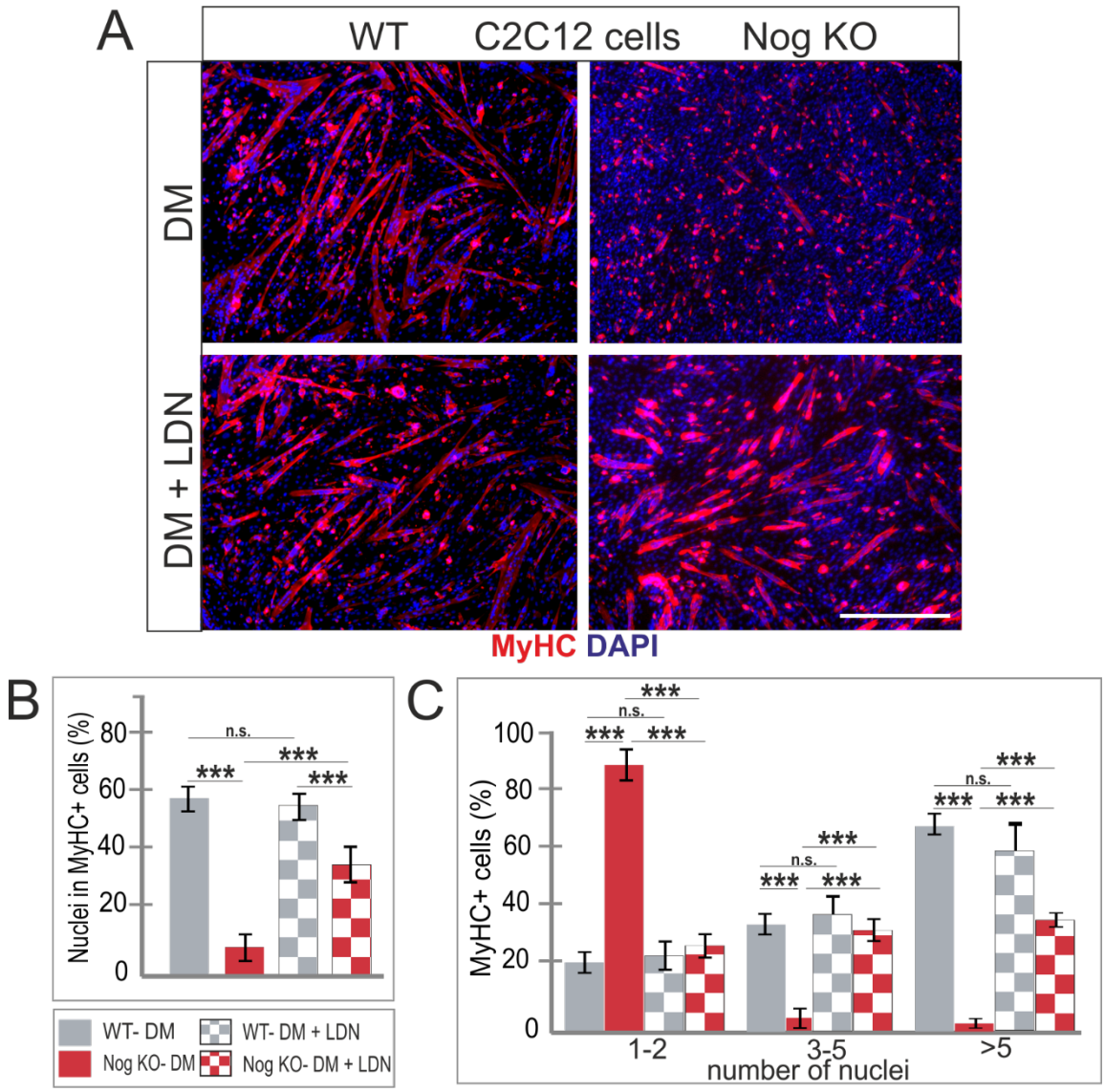

Figure 4.10: Myogenic differentiaion is impaired in Nog KO cells
Immunostaining for MyHC shows reduced myotube formation in Nog KO cells relative to WT cells after six days in differentiation media (DM) with partial rescue using LDN (A). A reduced differentiation index (B) and fusion index (C) were observed in Nog KO cells with a partial rescue by treatment with BMP-inhibitor LDN. Bar graphs depict relative ratios. Error bars represent S.E.M. from three clonal replicates. Statistical analysis was done using two-way ANOVA with Bonferroni correction; n.s. not significant, ***p<0.0001. Scale bar 400µm.

4.2.3. Nog KO cells show increased migration

Upon BMP stimulation an increase in wound healing of C2C12 cells have been previously shown (Hiepen et al., 2014), therefore I assessed whether Noggin deletion would change migration rate of C2C12 cells. A scratch wound healing assay was performed to asses for any changes in migration rate of the C2C12 cells. Here, a confluent well of C2C12 cells was scratched in the middle of the well using a pipette tip. Images were taken immediately after wounding, and then again after a period of 16 hours to assess the migration rate of the cells. The size of the wound was measured at time point 0 hours and then compared to time point 16 hours. A slight but statistically significant increase in the wound closure rate was noted in the Nog KO cells (Figure 4.11). Thereby, demonstrating higher migration rate following Noggin deletion.

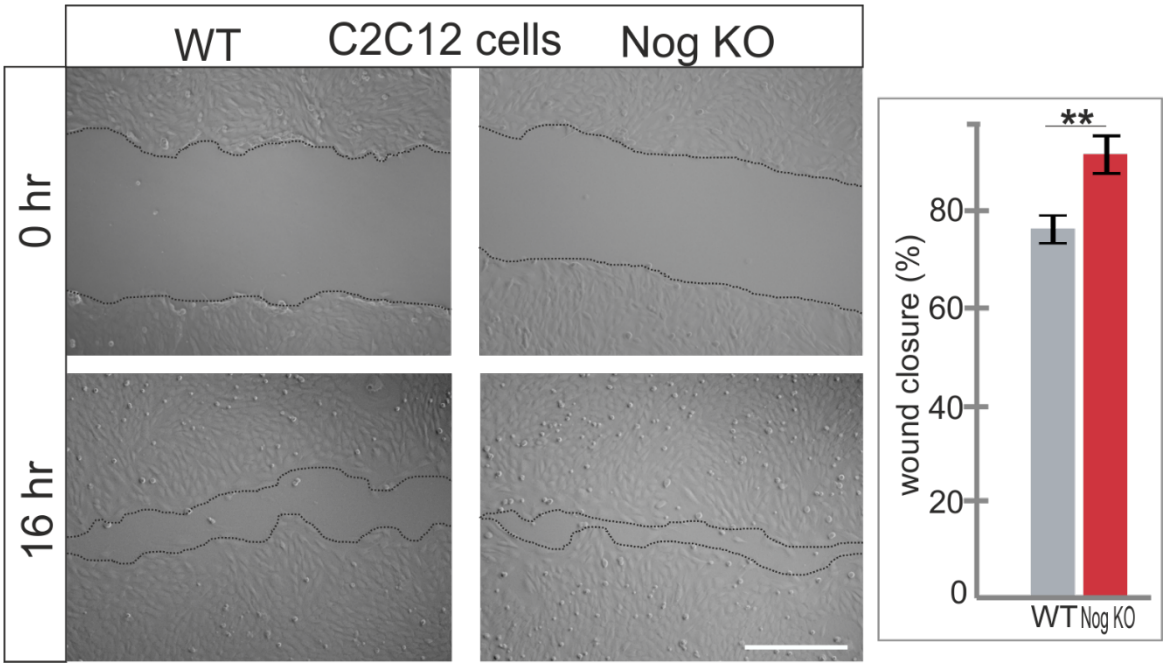

Figure 4.11: Increased migration rate in Nog KO cells
Scratch wound healing assay performed over 16 hours shows increased wound closure rate in Nog KO cells compared to WT cells. Error bars represent S.E.M. from three clonal replicates. Statistical analysis was done using two-tailed Student's t-test; ** $p<0.001$. Scale bar 400µm.

4.2.4. Osteogenic differentiation is enhanced in Nog KO cells

C2C12 cells have been shown to differentiate towards an osteogenic lineage upon BMP stimulation (Katagiri et al., 1994). To assess the osteogenic capacity of these cells, the cells were stimulated with 30 nM BMP2 for 6 days. As expected, Nog KO cells showed an in increase in alkaline phosphatase staining and activity (Figure 4.12A,B), a marker to assess osteogenic differentiation at a stage where the cells are irreversibly committed (Siller and Whyte, 2018). RT-qPCR showed an increase in osteogenic markers- alkaline phosphatase (*Alpl*), *Runx2*, Osteopontin (*Spp1*) and Osteoclacin (*Bglap*) (Figure 4.12C). This thereby indicates that deletion of Noggin supports an expected promotion of BMP-induced osteogenic commitment and differentiation versus myogenic tendencies of C2C12 cells.

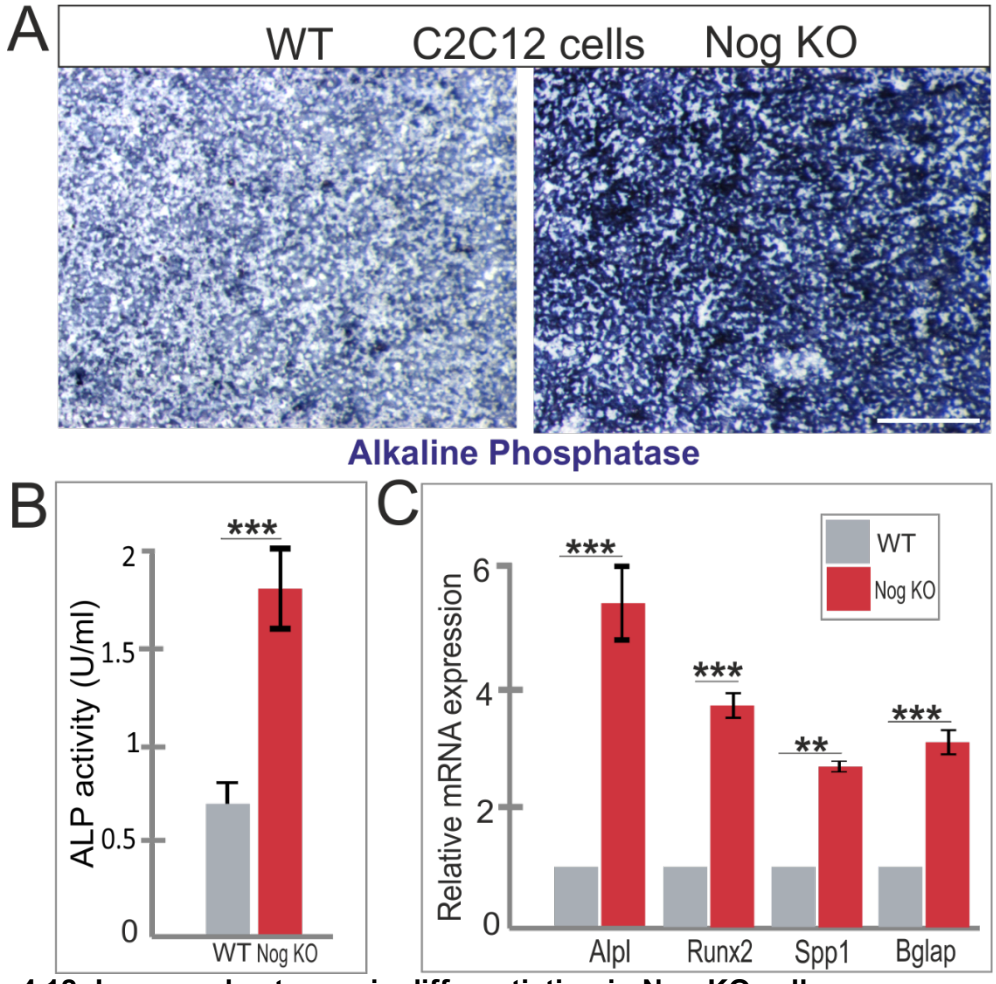

Figure 4.12: Increased osteogenic differentiation in Nog KO cells
C2C12 cells stimulated with BMP2 for 6 days stained for alkaline phosphatase (A) and assayed for ALP activity (B) show enhanced osteogenesis. RT-qPCR showing increase in osteogenic markers- *Alpl, Runx2, Spp1* and *Bglap*. Bar graphs depict relative ratios. Error bars represent S.E.M. from three clonal replicates. Statistical analysis was done using two-tailed Student's t-test; ** $p<0.001$, ***$p<0.0001$. Scale bar 400µm.

Altogether, the analysis of the genetically engineered Noggin deficient C2C12 cells confirms a role for Noggin in promoting myogenic differentiation. A lack thereof resulted in increased proliferation, reduction in differentiation and increased migration of cells. The proliferation and myogenic differentiation defect of Nog KO cells confirming the conclusions from the Nog KO fetuses. Nog KO cells showed increased potential for non-myogenic (in this case osteogenic) differentiation. Therefore, in the next section I questioned whether deletion of Noggin could switch the fate of myogenic cells *in vivo* to osteogenic lineage.

4.3. Loss of Noggin results in cell-fate switch of the myogenic lineage

In Section 4.1, Nog KO fetuses were shown to have impaired proliferation, differentiation and fusion of myogenic cells. Nevertheless, this developmental defect cannot explain the striking loss in muscle mass seen in Figure 4.4. Interestingly, the analysis of C2C12 cells in Section 4.2 revealed a propensity in Nog KO cells for osteogenic over myogenic differentiation. However, progenitors that switch cell fate between myogenic and osteogenic lineages have not been reported *in vivo* before. Previous studies in amphibians and mammalian cells have shown that muscle fibers have the ability to de-differentiate and fragment into mononucleated cells (Kumar et al., 2004; Odelberg et al., 2000; Wagner et al., 2017; Wang et al., 2015; Yilmaz et al., 2015). However, this phenomenon has never been observed in a mammalian *in vivo* model. I thereby hypothesized that the loss of muscles in Nog KO fetuses could be attributed, at least in part, to muscle de-differentiation. Therefore, in this section Nog KO fetuses were assessed for signs of de-differentiation and/or trans-differentiation.

4.3.1. Nog KO fetuses display hallmarks of de-differentiation

Nog KO fetuses were chosen to be analysed at E15.5, which is the intermediate stage where maximum loss of muscle occurs. The muscle fibers as well as the muscle progenitor cells were closely examined for signs of de-differentiation. Focussed observation of the muscles following immunostaining revealed MyHC expressing mono- and bi-nucleated cells emerging out of the muscle anlagen in the Nog KO muscles (Figure 4.13A). These cells appeared very uncharacteristic for normal MyHC expressing cells, and were often followed by large MyHC expressing cellular tails. This could be interpreted as delaminating/detaching migrating cell populations derived from the myofiber. In contrast to these atypical structural aspects, the WT muscles appear homogenous and structurally intact, and do not display any signs of muscle fragmentation. Furthermore, immunostaining detecting Pax7 and MyoD at E15.5 showed single Pax7 expressing or MyoD expressing cells present outside the muscle areas in the Nog KO limbs. These cells could either be remnants of the lost muscle or could be speculated to be fragments derived from myofibers that delaminate from the

muscle region. On the other hand, in the WT limbs the immunostained muscle cells were restricted to the muscle masses and no stray cells could be observed (Figure 4.13B). Altogether this strongly hints at muscle fragmentation in Nog KO fetuses.

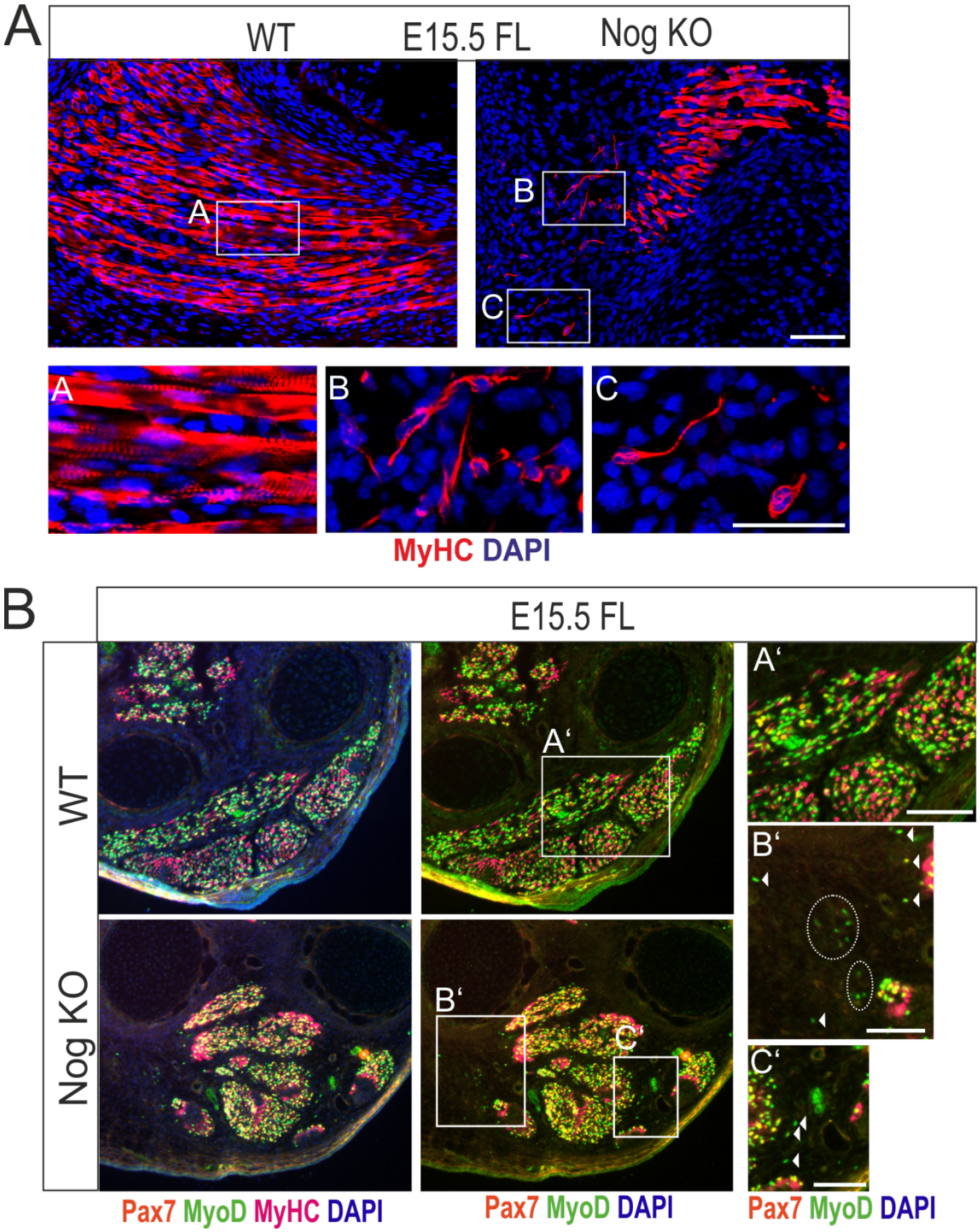

Figure 4.13: Fragmentation of muscle leads to muscle loss in Nog KO fetuses
Immunostaining for MyHC showing delamination and fragmentation of myofibers at E15.5 in Nog KO fetuses. Insets show well-structured myofibers in WT, while mononucleate and binucleate MyHC+ cells are seen in the vicinity of Nog KO muscles (A). Pax7 and MyoD+ cells (muscle precursors and myoblasts) seen outside the muscle regions in Nog KO fetuses at E15.5. Scale bar 50µm, 30µm (inset) (A), 100µm, 50µm(inset) (B).

Previous work carried out in amphibians has shown that de-differentiation of myofibers is preceded by cell cycle re-entry of otherwise post-mitotic nuclei in myofibers (Sandoval-Guzman et al., 2014; Wang et al., 2015). To check for cell cycle re-entry in the Nog KO fetuses, immunostaining was performed against three different cell cycle markers. In the WT muscles, nuclei positive for phosho-histone 3 (Figure 4.14A), cyclin D1 (Figure 4.14B) and Ki67 (Figure 4.14C) were observed in proliferating interstitial cells which are interspersed between the myofibers. Interestingly, in addition to interstitial cells, myonuclei positive for each of the cell cycle markers were observed in Nog KO muscle. This data therefore confirmed the occurrence of cell cycle re-entry in the myofibers of Nog KO fetuses.

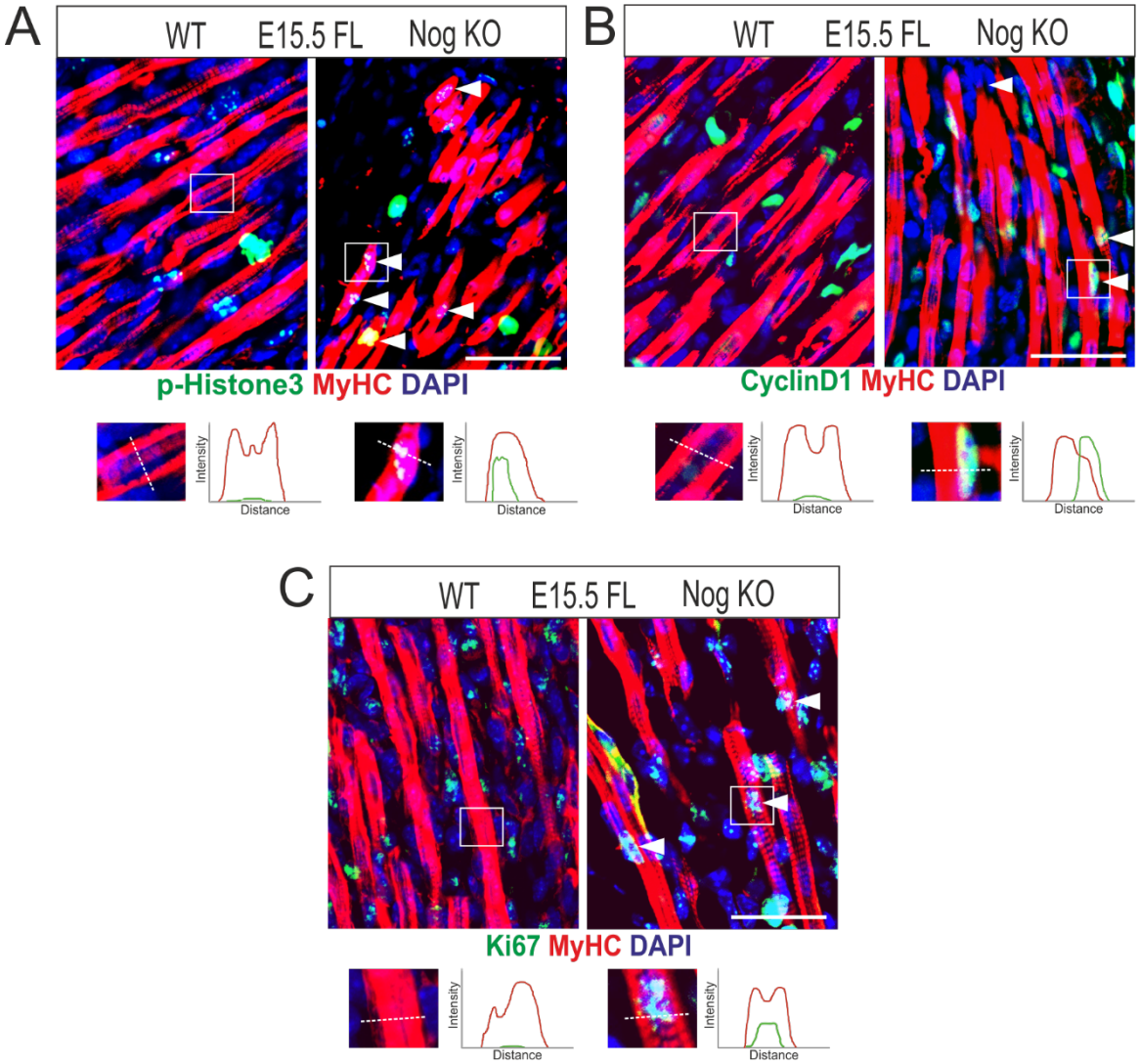

Figure 4.14: Cell cycle re-entry in Nog KO fetuses
Immunostaining at E15.5 in forelimb muscles showing myonuclei positive for phospho-histone3 (A), Cyclin D1 (B) and Ki67 (C) in Nog KO fetuses (arrow heads) while this is absent in WT muscles. Intensity plots show expression of the respective cell cycle marker together with MyHC from the line of division (white dots) shown in insets. Scale bar 50µm.

Cleaved caspase 3 (cc3), an early apoptotic marker, has previously been shown to be essential for myotube cell cycle re-entry in amphibians. Following limb amputation, myonuclei enter early stages of the apoptotic pathway but do not undergo cell death. This was shown to be a critical step for cell cycle induction in myotubes (Wang et al., 2015). To assess whether cc3 plays a key role in mammalian de-differentiation, immunostaining against cc3 was performed at E15.5 and compared to TUNEL, a late marker for apoptosis (Figure 4.15).. Nog KO embryos showed an increase in cc3+ as well as TUNEL+ myonuclei in comparison to the WT embryos. Strikingly, there were fewer TUNEL+ cells

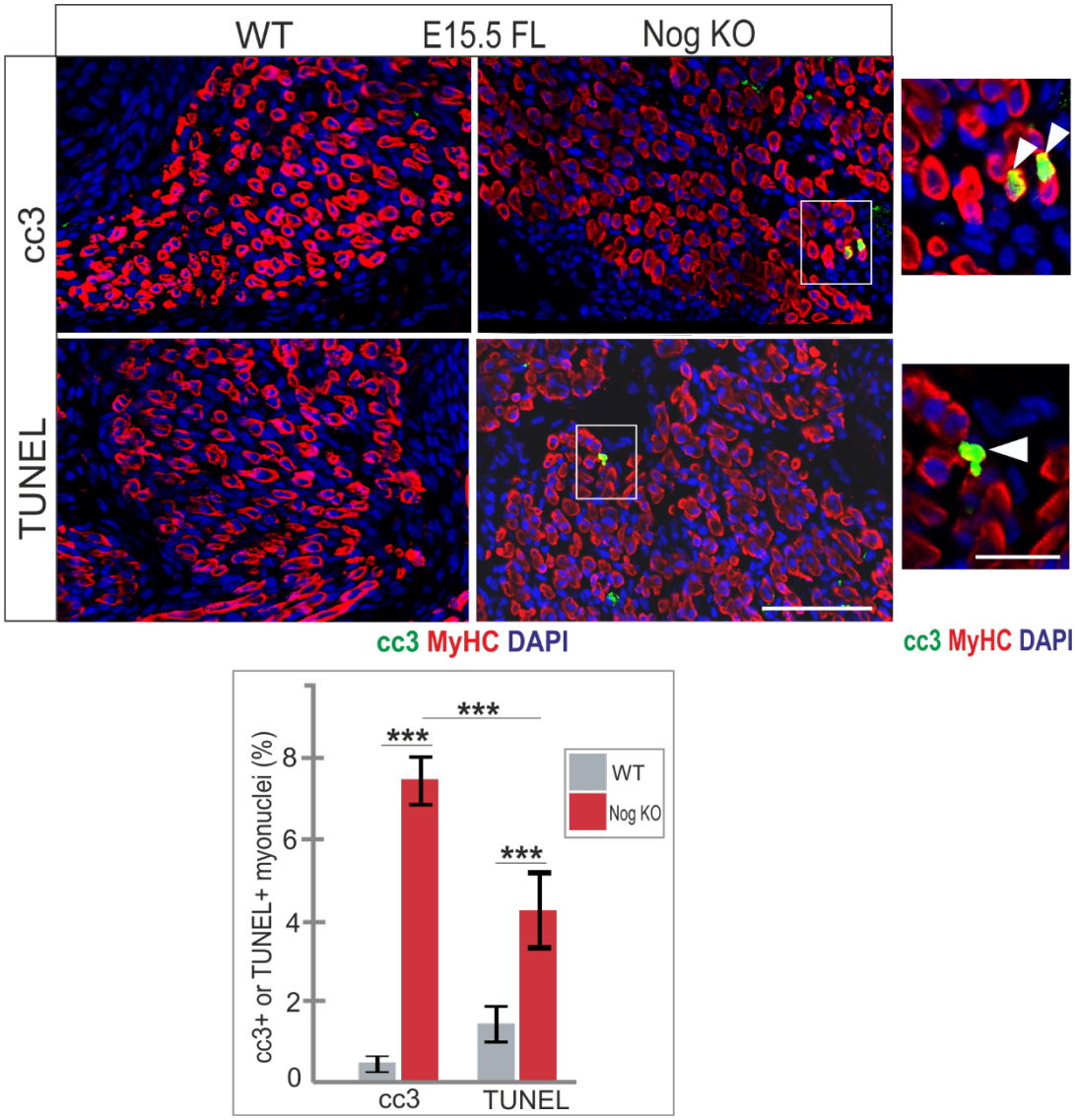

Figure 4.15 Cell death pathway is activated in myonuclei of Nog Ko fetuses
Immunostaining for cc3 and TUNEL reveals increased cc3+ and TUNEL+ myonuclei in Nog KO fetuses, while fewer TUNEL+ myonuclei in comparison to cc3+ myonuclei indicating activation but not execution of cell death pathway. N = 3 biological replicates. Statistical analysis was done using two-tailed Student's t-test; ***p<0.0001. Scale bar 100µm, inset 50µm.

compared to cc3+ cells indicating that cells enter the apoptotic process yet only a fraction of them execute the cell death program. This result provided another line of evidence for the occurrence of de-differentiation in Nog KO myofibers.

4.3.2. Committed myogenic progenitors display a lineage switch

Several key hallmarks of de-differentiation were observed in the Nog KO fetuses, hence the fate of myogenic cells was traced by generating mouse models that genetically label and trace the myogenic cells. To achieve this, a complex mating strategy generated dual-fluorescent mTmG-reporter animals driven by a muscle-specific-Cre, in combination with the Noggin allele. Schematic diagram describes the excision of the red florescent (mTomato) gene in cells with active expression of the muscle-specific-Cre recombinase (Figure 4.16A).. Using this genetic strategy, mouse strains were generated whereby myogenic cells coming from the muscle lineage are labelled in green by expressing mGFP, while non-muscle lineage cells are in red. This distinction can be clearly observed in the longitudinal section of the WT forelimb at E18.5 (Figure 4.16B).

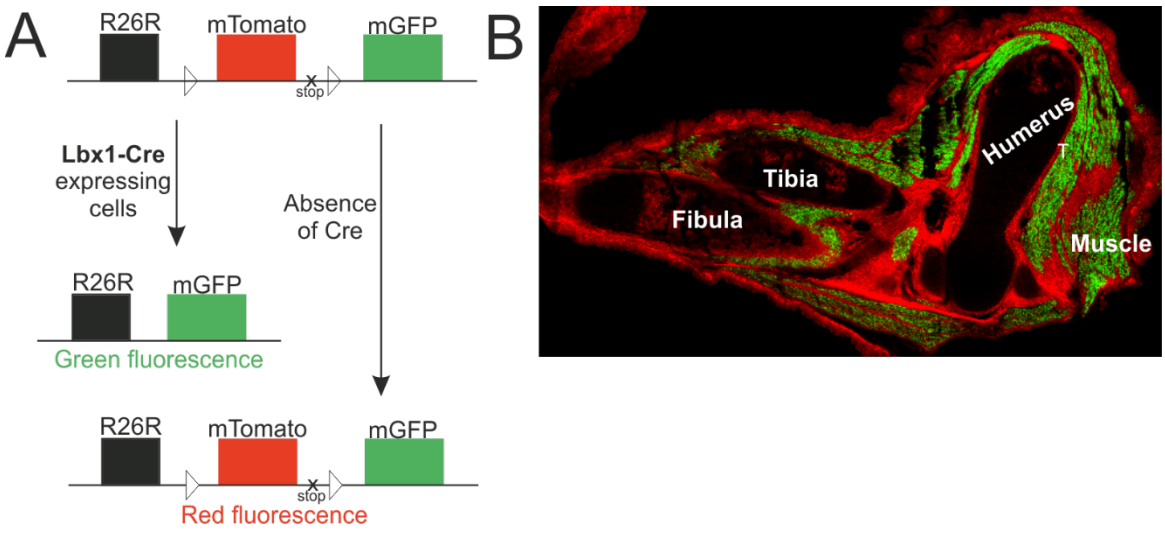

Figure 4.16: Trans-differentiation of Lbx1 lineage cells in Nog KO fetuses
Graphical representation of mTmG-Cre reporter system (A). Lineage analysis showing mGFP+ cells in cartilage, bone and dermis of E18.5 Nog KO fetuses while the WT is devoid of green cells. This reveals a fate switch of Lbx1 lineage cells. Scale bar 50µm.

To label the myogenic populations mTmG-Lxb1Cre and mTmG-Myf5Cre reporter mouse lines were used. Lbx1 is a marker for all early muscle precursor cells of the limb bud (Vasyutina and Birchmeier, 2006) while Myf5 labels the committed myoblasts (Montarras et al., 1991) . Remarkably, in Nog KO fetuses analysed at E18.5, limb sections showed mGFP+ cells interspersed in the cartilage, in the bone, as well as in the layers of the dermis. This was clearly observed in Nog KO embryos from both mTmG-Lbx1Cre and mTmG-Myf5Cre reporter mouse lines. In the WT limbs, however, no mGFP+ cells were observed outside of the muscles (Figure 4.17). These observations, demonstrate conversion of the cells from myogenic lineage, including committed progenitors, to other mesoderm-derived tissues. This approach however could not distinguish between lineage conversion of mononucleate muscle cells and myofibers and thereby a myofiber-specific-Cre

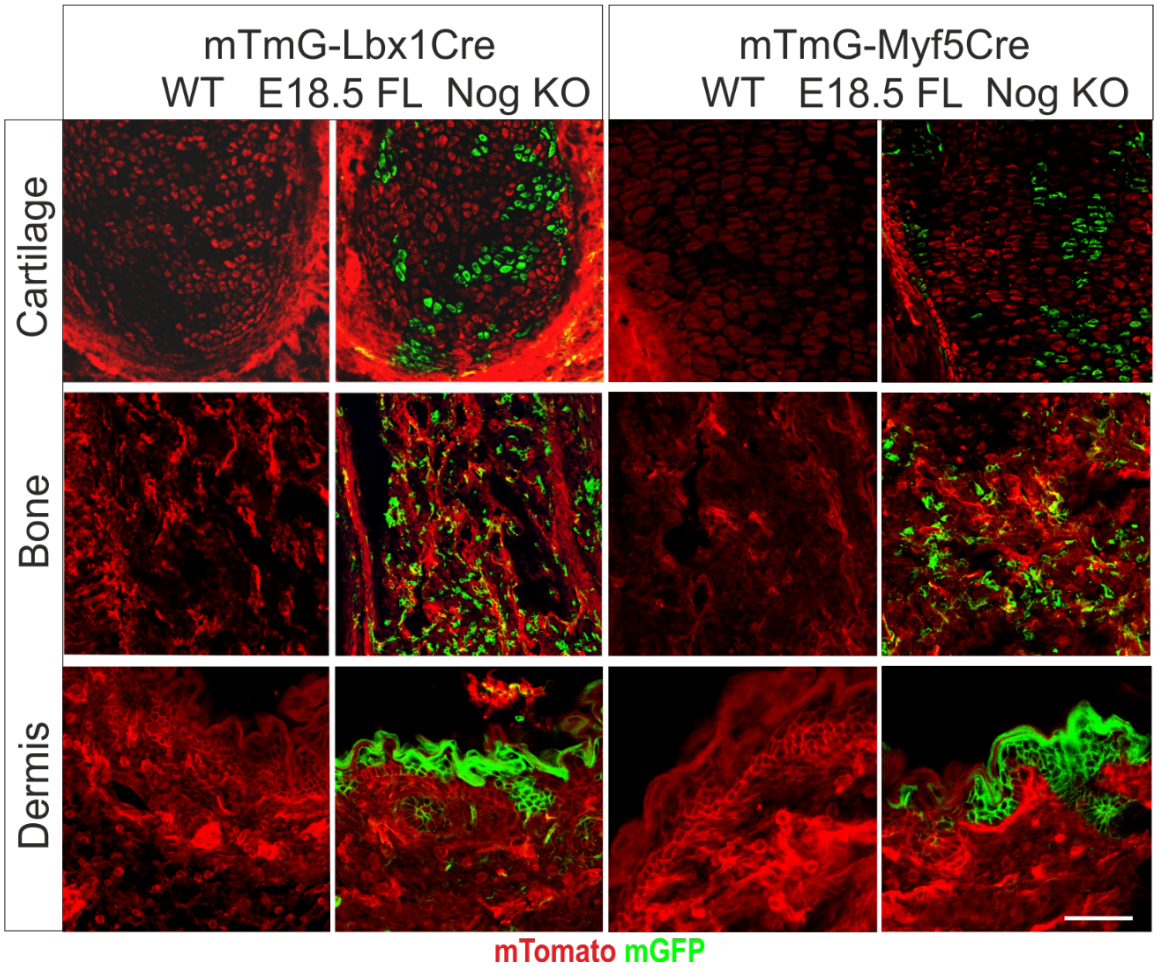

Figure 4.17: Trans-differentiation of Myf5 lineage cells in Nog KO fetuses
Lineage analysis from Nog KO fetuses from mTmG-Lbx1Cre and mTmG-Myf5Cre reporter mice showing presence of mGFP+ cells in cartilage, bone and dermis of E18.5 fetuses. Note that the WT tissues are devoid of green cells. Thus, revealing a fate switch of Lbx1 lineage and Myf5 lineage cells. Scale bar 50µm.

reporter mouse line was generated.

4.3.3. Terminally differentiated myofibers transdifferentiate to other lineages

To determine the fate of terminally differentiated myofibers, an ACTA1Cre (Miniou et al., 1999) reporter mouse line was used. Nog KO fetuses from the mTmG-ACTA1Cre reporter mouse line were analysed at E18.5. These fetuses showed presence of ACTA1 lineage-derived cells (mGFP+) in cartilage, in bone, as well as in the layers of the dermis surrounding the hair follicles (Figure 4.18). While in the WT these tissues remained devoid of mGFP+ cells. This exciting finding strongly indicates trans-differentiation of post-mitotic myofibers in Nog KO fetuses. Notably, this is the first evidence of myofiber trans-differentiation in a mammalian *in vivo* system.

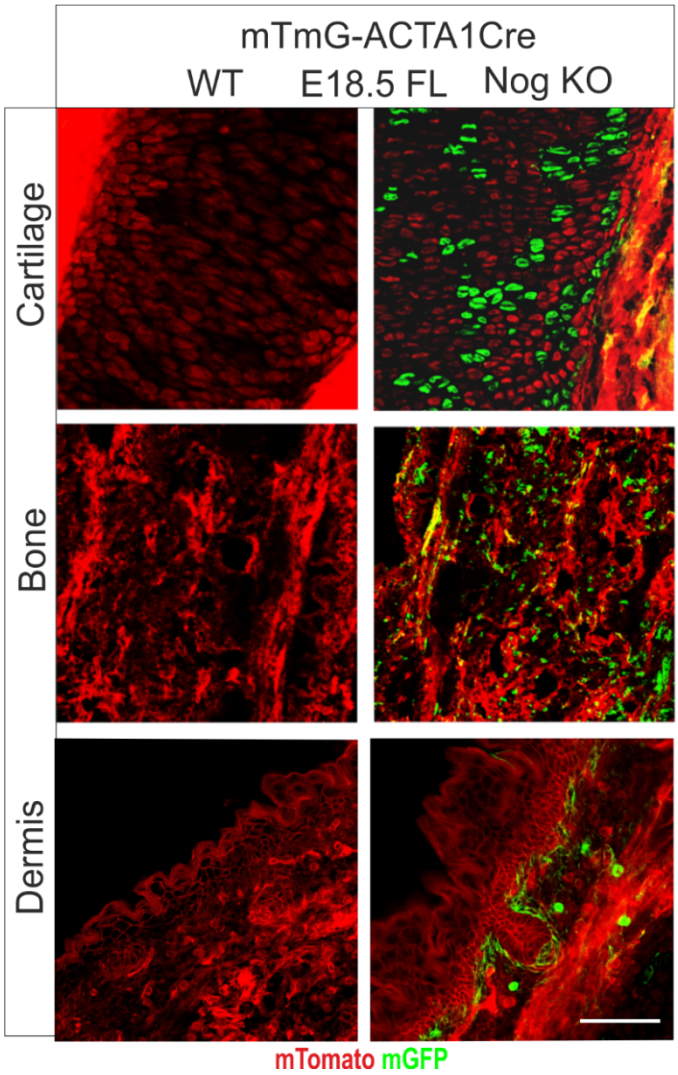

Figure 4.18: Transdifferentiated cells express chodro- and osteogenic markers
Schematic showing isolation of mGFP+ cells from E18.5 forelimbs (A). Semi-quantitative PCR shows expression of myog and low expression of Sox9 in cells isolated from muscle and connective tissue, while Sox9 and Runx2 expression is seen in cells from the skeleton.

To further analyse the transdifferentiated cells, limbs were dissected from Nog KO embryos from the mTmG-ACTA1Cre reporter mouse line at E18.5 and the muscle and connective tissue was separated from the bone and cartilage. FACS analysis was used to isolate mGFP+ cells from both the tissue compartments (Figure 4.19A). Myoblasts isolated from WT fetuses were used as controls. cDNA was then transcribed from the isolated RNA and semi-quantitative PCR was performed (Figure 4.19B). WT myoblasts showed expression of the myogenic marker *Myog* and lacked the expression of osteochondrogenic markers *Sox9* and *Runx2*. mGFP+ cells obtained from Nog KO muscle and connective tissue showed expression of *Myog* and low expression of cartilage marker *Sox9*. The low expression chondrogenic genes at this stage indicates the beginning of lineage

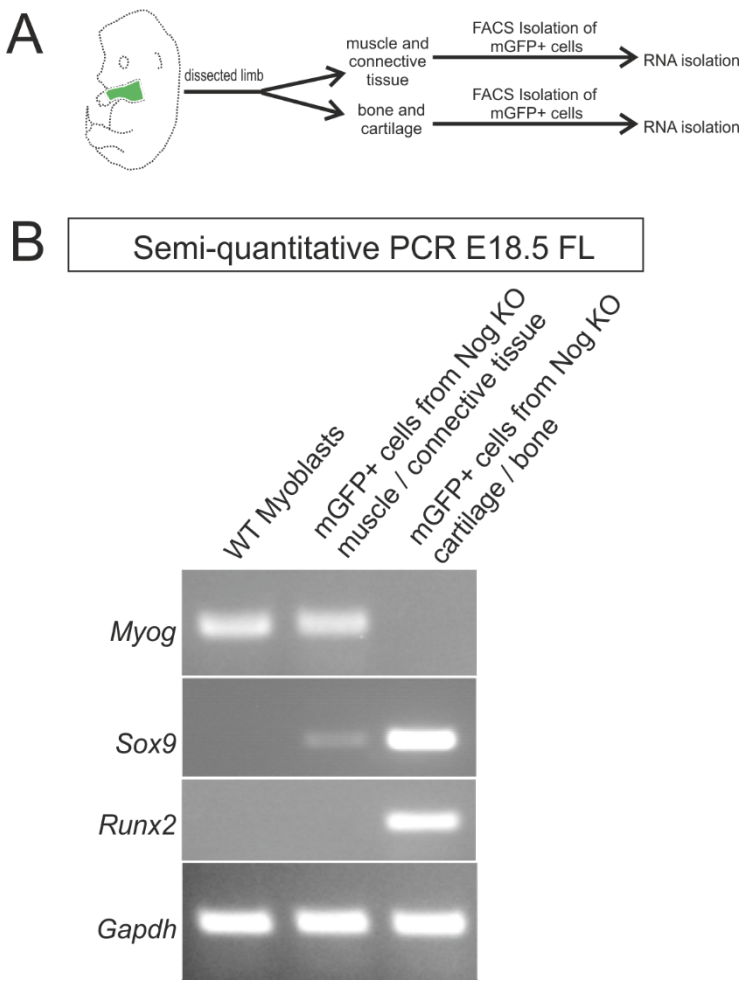

Figure 4.19: Transdifferentitation of myofibers in Nog KO fetuses
Lineage analysis showing mGFP+ cells in cartilage, bone and dermis of E18.5 Nog KO mTmG-ACTA1Cre reporter fetuses while the WT is devoid of green cells. Thus, revealing fate switch of ACTA1 lineage cells. Scale bar 50µm.

conversion. Furthermore, mGFP+ cells derived from Nog KO bone and the cartilage tissue were positive for the chondrogenic marker *Sox9* and osteogenic marker *Runx2*, while being negative for Myog. This thereby confirms the identity switch of the myogenic lineage cells towards the chondrogenic and osteogenic lineages.

4.3.4. Lineage switch could be driven by Msx1

To investigate the early stages of the lineage switching process, Nog KO embryos from the mTmG-ACTA1Cre reporter line were analysed at E14.5. Cross-sections of the forelimbs revealed presence of mononucleate mGFP+ cells in the vicinity of the muscle area (Figure 4.20A). It is highly probable that the mononucleate cells are derived from early stages of myofiber fragmentation. These mGFP+ cells were FACS isolated and cytospun (Figure 4.20B). Immunostaining for Msx1/2 revealed

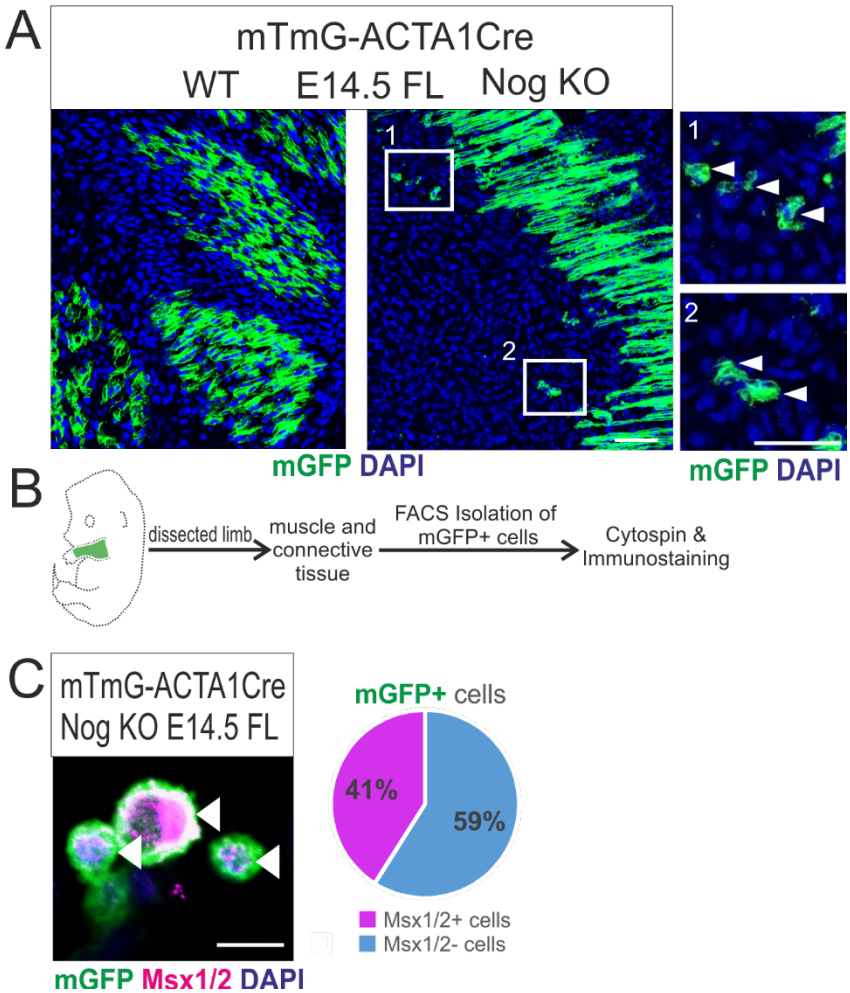

Figure 4.20: Lineage switch is driven by Msx1
mTmG-ACTA1Cre fetuses show mononucleate mGFP+ cells in the vicitnity of the muscle anlagen in the Nog KO background (A). mGFP+ cells were isolated using FACS and cytospun (B). Immunostaining for Msx1/2 shows 41% positive cells (C). Scale bar 50µm

that 41% of these cells are positive for Msx1/2 (Figure 4.20C). Interestingly, Msx1 and Msx2, which are downstream targets of BMPs, have been implicated in fragmentation of C2C12 derived myotubes as well as amphibian myofibers (Kumar et al., 2004; Odelberg et al., 2000; Yilmaz et al., 2015).

This section revealed the occurrence of various hallmarks of de-differentiation in the Nog KO fetuses including fragmentation of the myofiber, cell cycle re-entry and presence of cc3+ myonuclei. Genetic lineage tracing of the myogenic cells using Lbx1Cre and Myf5Cre, and that of the myofibers using ACTA1Cre demonstrated trans-differentiation of the myogenic lineage towards cartilage, bone and dermis. Initial indications show the involvement of BMP-downstream Msx genes in the de-differentiation process. Therefore, in the next section I investigated the role of BMP signalling in influencing the de-differentiation process.

4.4. Dysregulated BMP signalling affects myotube integrity

4.4.1. Nog KO fetuses show enhanced BMP signalling

Noggin is a bonafide BMP antagonist (Smith and Harland, 1992), therefore it is essential to determine whether the deletion of Noggin enhances BMP signalling in Nog KO embryo muscles. To test this, pSMAD1/5/8, was used as a measure of active BMP signalling. Binding of the BMPs to the high affinity receptor type I, leads to formation of complex with Type II receptors activating serine threonine kinase leading of phosphorylation and diffusion of R-SMADs (including the SMAD1/5/8 complex) to the nucleus (Massague et al., 2005). Previous work performed in chick has shown that the tips of the developing myofibers are active centres for BMP signalling while the rest of the myofiber is devoid of myonuclear pSMAD1/5/8 (Wang et al., 2010). In line with this, pSMAD1/5/8 immunostaining performed on E15.5 limb cross-sections in WT mice showed active centres for BMP signalling in the tips of the muscle fibers, while in the Nog KO pSMAD1/5/8+ myonuclei could be observed along the whole length of the myofiber (Figure 4.21A). Furthermore, myoblasts were isolated from E15.5 embryos and immunostained for pSMAD1/5/8 either in culture or fresh after isolation. In both cases, a significantly higher number of pSMAD1/5/8+ nuclei were seen in myoblasts derived from Nog KO fetuses (Figure 4.21B,C). Thereby, it can be concluded that deletion of Noggin results in enhanced BMP signalling in the myofibers as well as in the myoblasts.

To further analyse the consequences of Noggin deletion on BMP signalling, myoblasts were isolated from E15.5 fetuses and RT-qPCR was performed for the BMP pathway members and Nog KO cells were compared to WT cells. Upregulation of mRNA of BMP ligands- *Bmp2*, *Bmp4* and *Bmp7* was observed while an increase in the BMP antagonist- *Gremlin1* was seen. No major changes in the expression of Type 1 receptors was observed, while Type 2 receptors *Acvr2a* and *Acvr2b* were upregulated. Also, direct BMP/SMAD target genes *Id1* and *Id3* were upregulated (Figure 4.22A). To understand the expression dynamics of myotubes, the isolated myoblasts were cultured in differentiation media to allow myotube formation. RT-qPCR analysis from the myotubes revealed increase in BMP ligands *Bmp4* and *Bmp7*, and in Gdf ligands *Gdf5* and *Gdf6*. Also, an increase

in BMP Type 1 receptors and Type 2 receptors was observed. A high induction of *Id1*, *Id2* as well as *Id3* was observed (Figure 4.22B). Thereby, it can be concluded that both myoblasts as well as myotubes show enhanced BMP signalling as evident from dysregulation of the BMP pathway components and increased expression of *Id* genes.

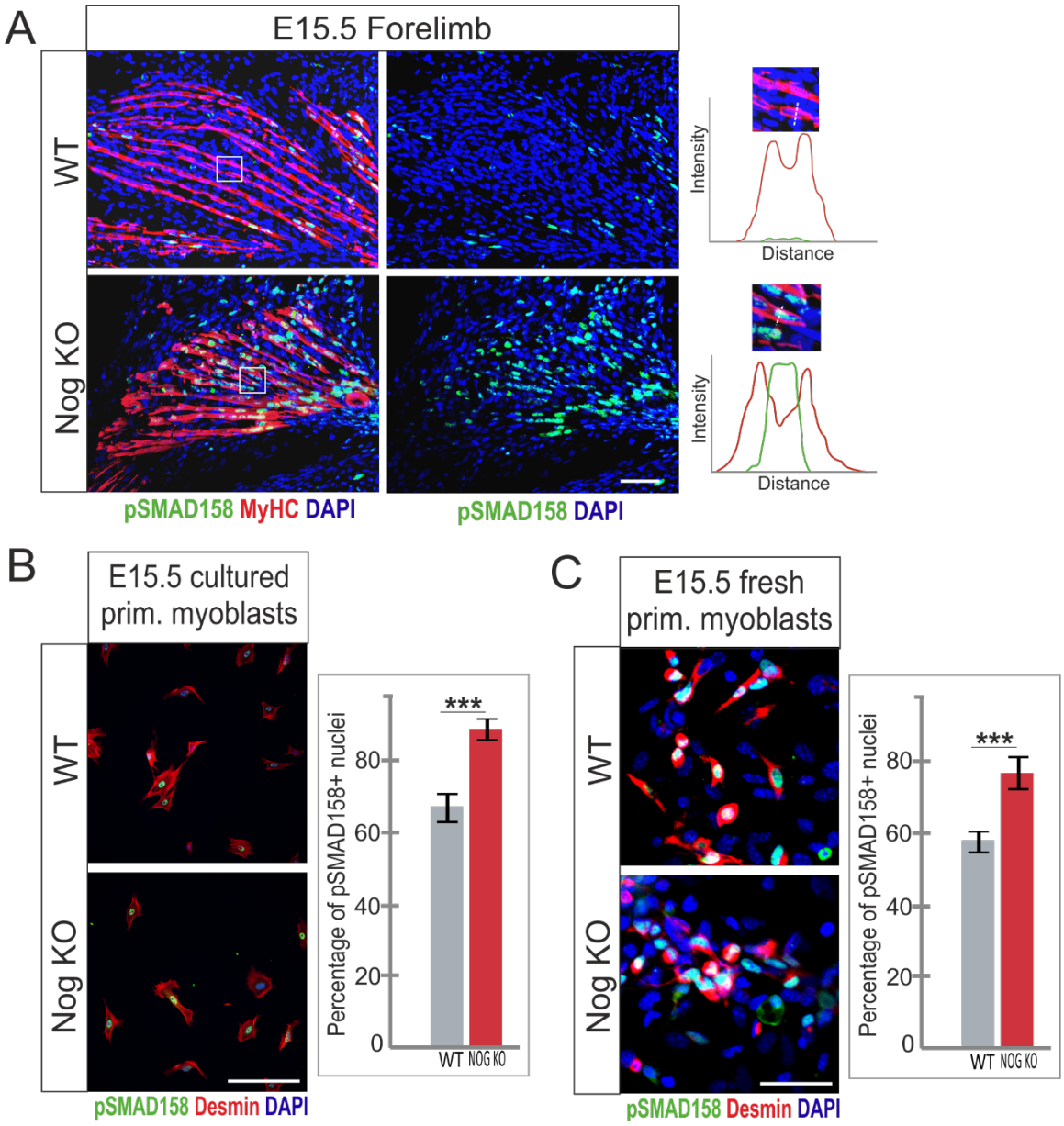

Figure 4.21: Nog KO muscles show enhanced BMP signalling
Immunostaining for pSMAD1/5/8 at E15.5 shows positive myonuclei at the tips of the myofibers in WT fetuses whereas positive myonuclei are seen along the whole length of the Nog KO myofibers. Intensity plots show expression of pSMAD1/5/8 together with MyHC (A). Immunostaining for pSMAD1/5/8 in myoblasts isolated from E15.5 fetuses, quantification reveals increase in pSMAD1/5/8+ myoblasts from Nog KO fetuses (B). Bar graphs depict relative ratios. Error bars represent S.E.M. from three biological replicates. Statistical analysis was done using two-tailed Student's t-test; ***p<0.0001. Scale bar 50µm.

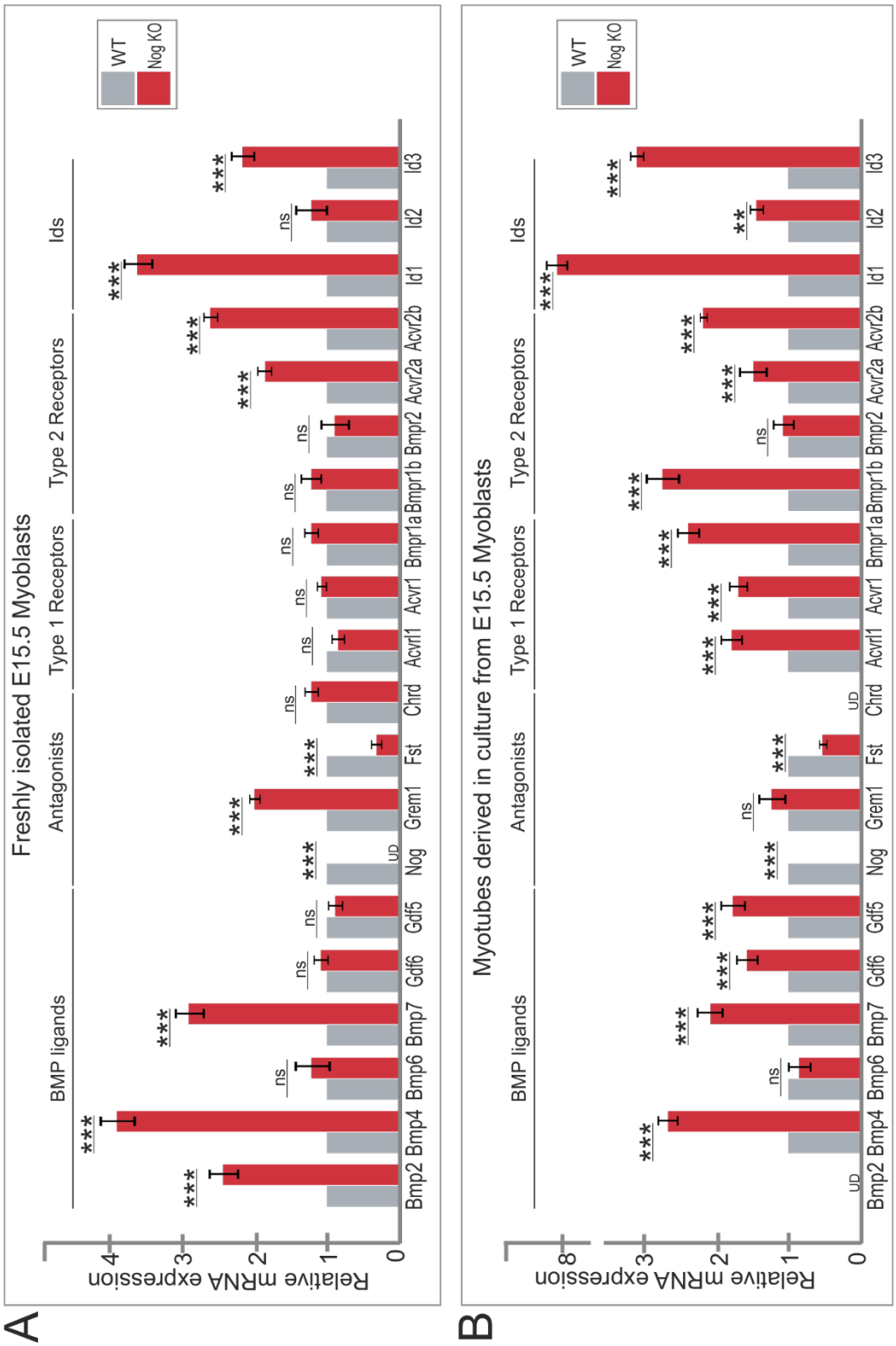

Figure 4.22: Altered expression of BMP pathway components in Nog
RT-qPCR from freshly isolated E15.5 WT vs. Nog KO myoblasts (A) and from myotubes derived from cultured myoblasts (B) Bar graphs depict relative ratios. Error bars represent S.E.M. from three biological replicates. Statistical analysis was done using two-tailed Student's t-test; n.s. not significant, **p<0.001, ***p<0.0001.

4.4.2. Increased vascular permeability could lead to increased BMP activity in Nog KO fetuses

The vasculature plays a key role in proper muscle development. Blood vessels have been shown to form in regions of future muscle splitting, and are crucial for separation of individual muscles during the developmental process (Tozer et al., 2007). BMPs are known as critical regulators of vessel development and maintenance in the embryo and in turn play a role in maturation and homeostasis of blood vessels (Garcia de Vinuesa et al., 2016; Lowery and de Caestecker, 2010). Therefore, the vasculature was analysed in fetal limbs to assess for any changes in vasculature morphology. A co-staining was performed for MyHC and PECAM-1 (CD-31) on cross-sections of E15.5 limbs. In the WT fetuses, PECAM-1 staining delineated well-structured vessels with a clear demarcation of the vessel borders. In Nog KO mice, the vessels appeared much larger and the network was more extensive. Within the muscles masses large vascular networks were observed. Furthermore, close observation of the vessels revealed atypical PECAM-1 staining in the vessels, and diffused staining of PECAM-1 outside the vessel regions. This is highly indicative of vascular hyperpermeability (Figure 4.23A). To further assess the muscle histology, a haemotoxylin and eosin staining was performed (Figure 4.23B). Strikingly, clusters of red blood cells were observed interspersed within the muscles in the Nog KO fetuses. Whereas, in the WT muscles no blood cells were observed. This further indicates that Nog KO fetuses indeed have increased vascular permeability.

In a recent study it was shown that plasmin and thrombin in blood plasma cleave BMPs at their N-terminal thereby rendering them more potent than the uncleaved BMPs (Wagner et al., 2017). This was seen in amphibians, and it is speculated that following limb amputation the vessels leak plasmin and thrombin onto the muscle tissue thereby acting on the tissue resident BMPs and increasing their biological activity.

Taken together, it is highly possible that enhanced BMP signalling observed in the Nog KO fetuses is, at least in part, a consequence of hyper-permeable vasculature derived serum-proteases that accentuate the activity of the BMPs present in the muscle tissue.

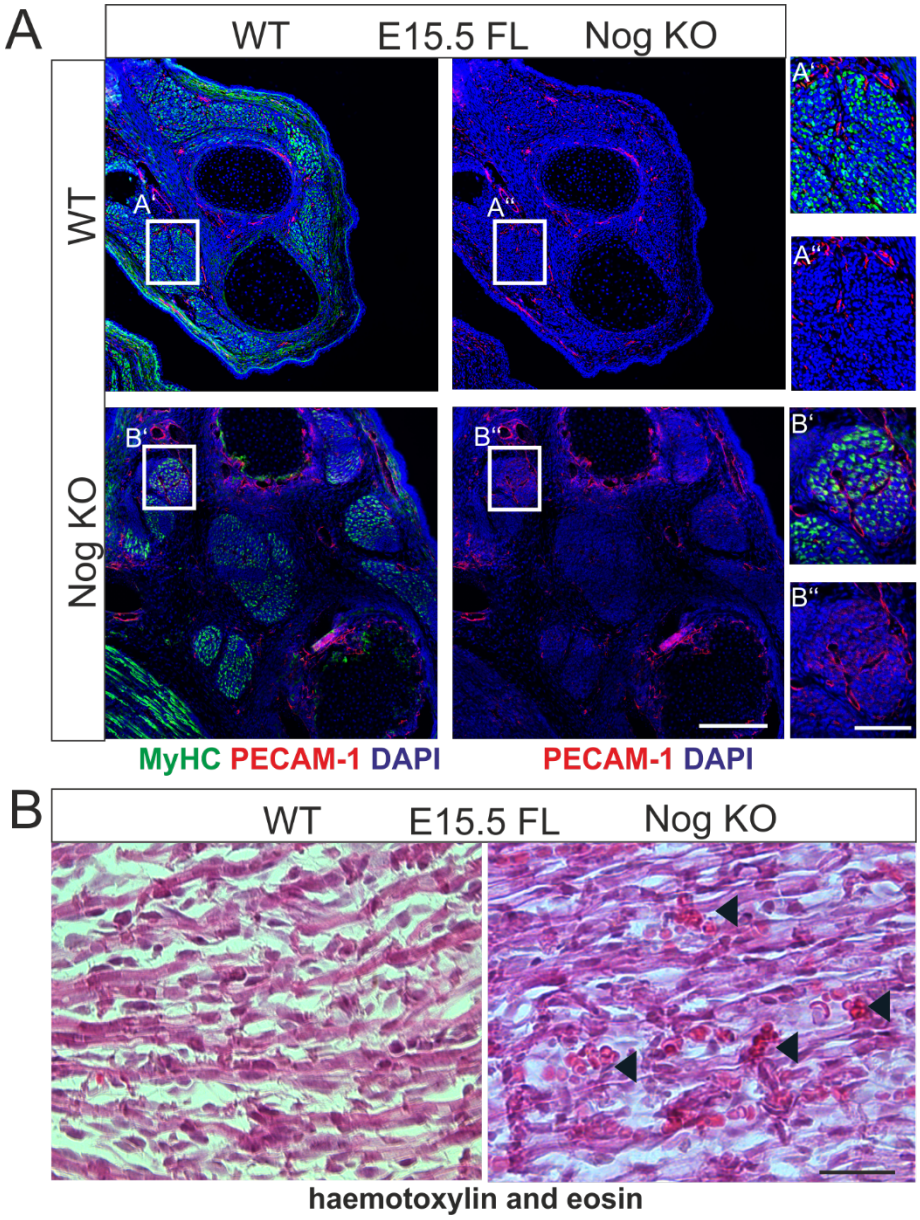

Figure 4.23: Increased vascular permeability in Nog KO fetuses
Cross-sections of E15.5 limbs stained for MyHC and PECAM marking the muscles and vasculature respectively. In the Nog KO limbs PECAM staining is not as demarcated as in the WT, but rather diffused staining is observed around the vessels (A). Haemotoxylin and eosin staining showing clusters of red blood cells in the muscles of the Nog KO fetuses at E15.5 (black arrowheads), while these are absent in the WT (B). Scale bar 100µm, 50 µm (inset)

4.4.3. Proteolytic cleavage of BMP2 and BMP4/7

Recent publication has shown that proteolytic cleavage of the N-terminal of BMPs renders them highly potent (Wagner et al., 2017). Therefore, I tested whether the cleavage of BMPs could be reproduced. For this purpose, BMP2 and BMP4/7 heterodimers were used. Plasmin cleavage sites on BMP 4 and BMP 7 protein sequences are marked with red arrows (Figure 4.24A). Recombinant BMP2 as well as BMP4/7 heterodimer were treated with equimolar plasmin concentration for 30min. Confirmation of cleavage was obtained by separation of the proteins on a SDS gel and visualization by silver staining whereby a reduction in size was

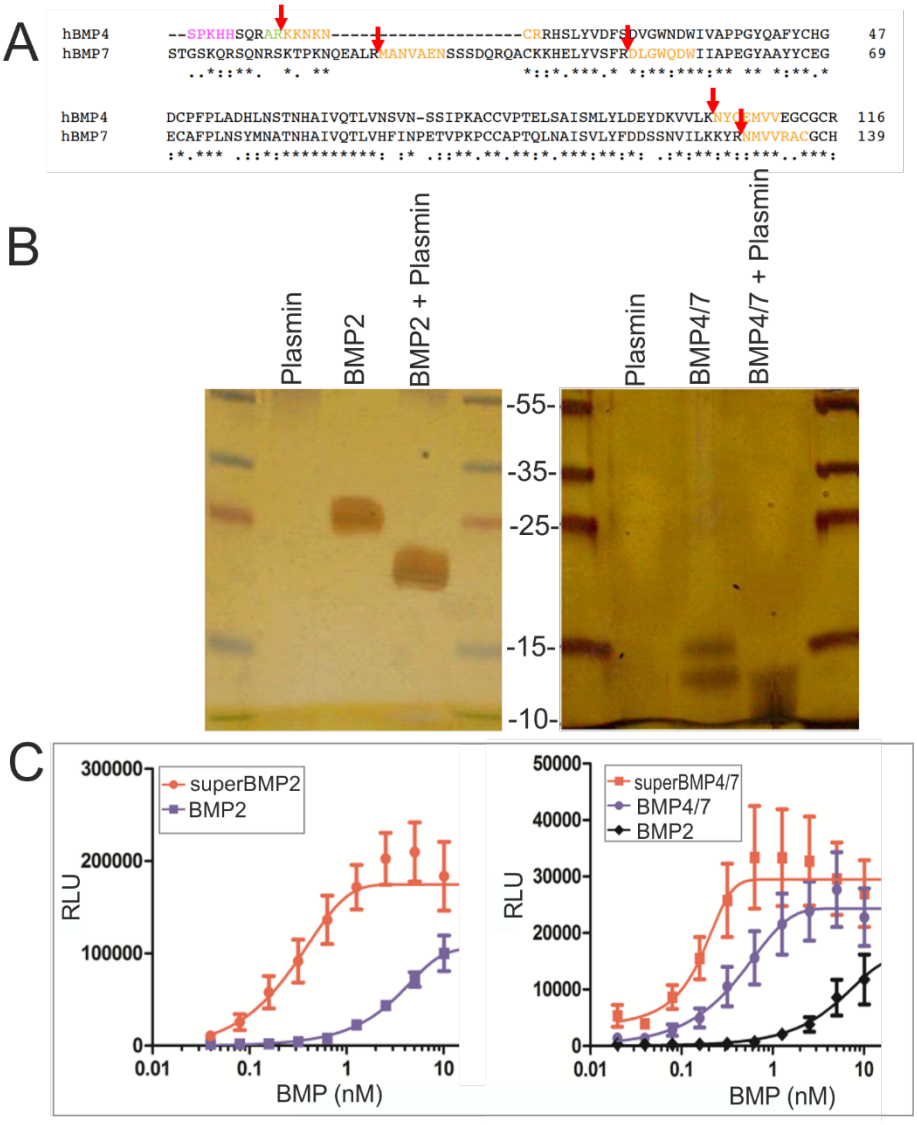

Figure 4.24: Cleavage of BMPs and their potency
Sequence of BMP4 and BMP7 showing plasmin cleavage sites marked with red arrows; modified from Wagner et al., 2017 (A). Silver staining showing cleavage of BMP2 and BMP4/7 as evident by reduction in molecular weight (B). Increased potency of superBMPs in comparison to the uncleaved version as evident by C2C12-BRE luciferase assay after 6 hours of BMP stimulation. Performed by Charles Haggerty.

observed for both cleaved BMP2 and BMP4/7 (Figure 4.24B). The cleaved BMPs are hereby termed as 'super BMPs'. Activity of the super BMPs was tested by stimulating C2C12-BRE luciferase cells (Herrera and Inman, 2009) which have a luciferase gene under the control of a BMP response element of the ID gene. The luciferase gene is activated upon binding of SMAD1/5/8 to the repetitive sequence of the ID-promoter and the luciferase activity is therefore a direct measure of BMP signalling. The cells were stimulated with BMP2 and BMP4/7 (uncleaved and super) for 6 hours and the luciferase activity was measured. Interestingly, super BMP2 as well as super BMP4/7 showed an increase in luciferase activity thereby confirming higher potency in comparison to the uncleaved version (Figure 4.23C).

To further understand the dynamics of plasmin cleavage C2C12 BRE-luciferase assay was performed and cells were stimulated for 6 hours with BMP4/7, plasmin, noggin or combinations of these (Figure 4.25). Untreated cells showed basal levels of luciferase activity. Interestingly, stimulation with plasmin increased BMP activity indicating the cleavage of BMPs contained in the serum. BMP4/7 stimulation increased luciferase activity, while plasmin treated BMP4/7 (superBMP4/7)

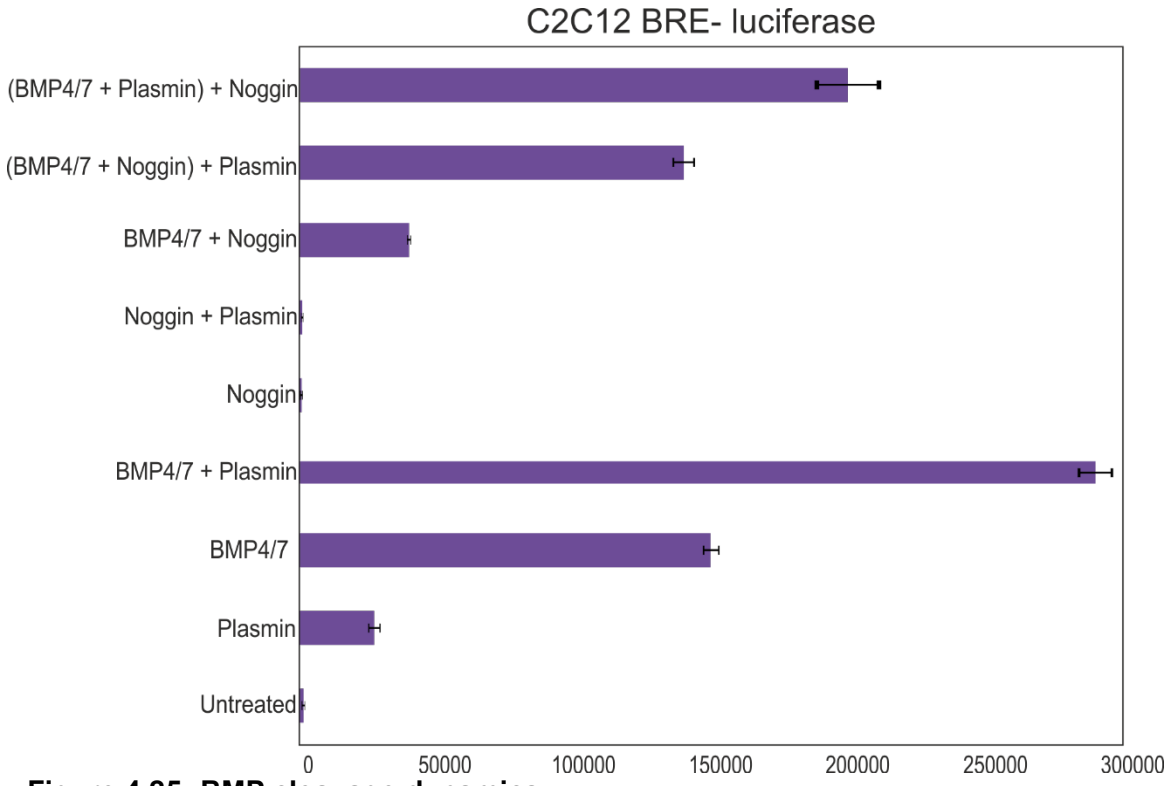

Figure 4.25: BMP cleavage dynamics
C2C12 BRE luciferase cell line was used to assay BMP signalling levels in response to BMP (1nM), Noggin (3nM), plasmin (1nM) and combinations of them. The cells were stimulated for 6 hours.

enhanced this even further. As expected, Noggin and plasmin treated Noggin did not influence the luciferase activity. BMP4/7-Noggin dimers were formed by mixing the two for 30 minutes in solution. The dimers themselves weakly increased luciferase activity while plasmin treated dimers enhanced the luciferase signal. This indicates that BMPs in complex with Noggin can be cleaved by plasmin. Lastly, plasmin treated BMP4/7 was complexed with Noggin and an increase in luciferase levels were observed, this indicated that super BMP4/7 is sensitive to Noggin.

4.4.4. BMPs induce cell cycle re-entry in C2C12 cell and primary cell derived myotubes

Section 4.4.1. showed BMP 4 and BMP 7 as the main BMPs upregulated in Nog KO myoblast derived myotubes. Also, Wagner et al. 2017 demonstrated BMP4/7 heterodimer to be the most potent BMP dimer in inducing cell cycle re-entry in Newt myotubes. Therefore, BMP4/7 was chosen as the key BMP molecule for further analysis. C2C12 cells were differentiated into myotubes and stimulated with BMP4/7 under serum reduced conditions. Cell cycle re-entry, as evident from Ki67 staining, was observed in C2C12 cells with as low as 5nM superBMP4/7, which steadily went up with increasing concentrations of BMP4/7. This observation was more prominent with super BMP4/7 in comparison to its uncleaved counterpart (Figure 4.26A&B). Although 20nM BMP4/7 showed highest rate of cell cycle re-entry, the rate of apoptosis was significantly increased at this concentration. Therefore, 15nM was chosen as the working concentration for further experiments.

Next, the influence of BMP stimulation on myotubes derived from primary cells was assessed. For this myoblasts were isolated from juvenile mice and satellite cells were obtained from adult animals. The cells were differentiated for 72 hours and stimulated with 15nM BMP4/7 for 4 hours or 24 hours (Figure 4.27A). Cell cycle-re-entry was measured by counting myonuclei that are positive for phosho-histone3. A striking increase in cell cycle re-entry was observed in myotubes where super BMP4/7 outperformed the uncleaved BMP4/7. Untreated myotubes showed no cell cycle re-entry (Figure 4.27B&C). Next, I tested whether BMP stimulation for 24 hours versus a 2 hour BMP pulse would yield any differences in cell cycle re-entry. Notably, no significant differences were observed between the two treatments (Figure 4.27D). Therefore, for the rest of the study a 24 hour BMP

stimulation treatment was used as a norm in order to avoid media changes and disturbing the cells after stimulation.

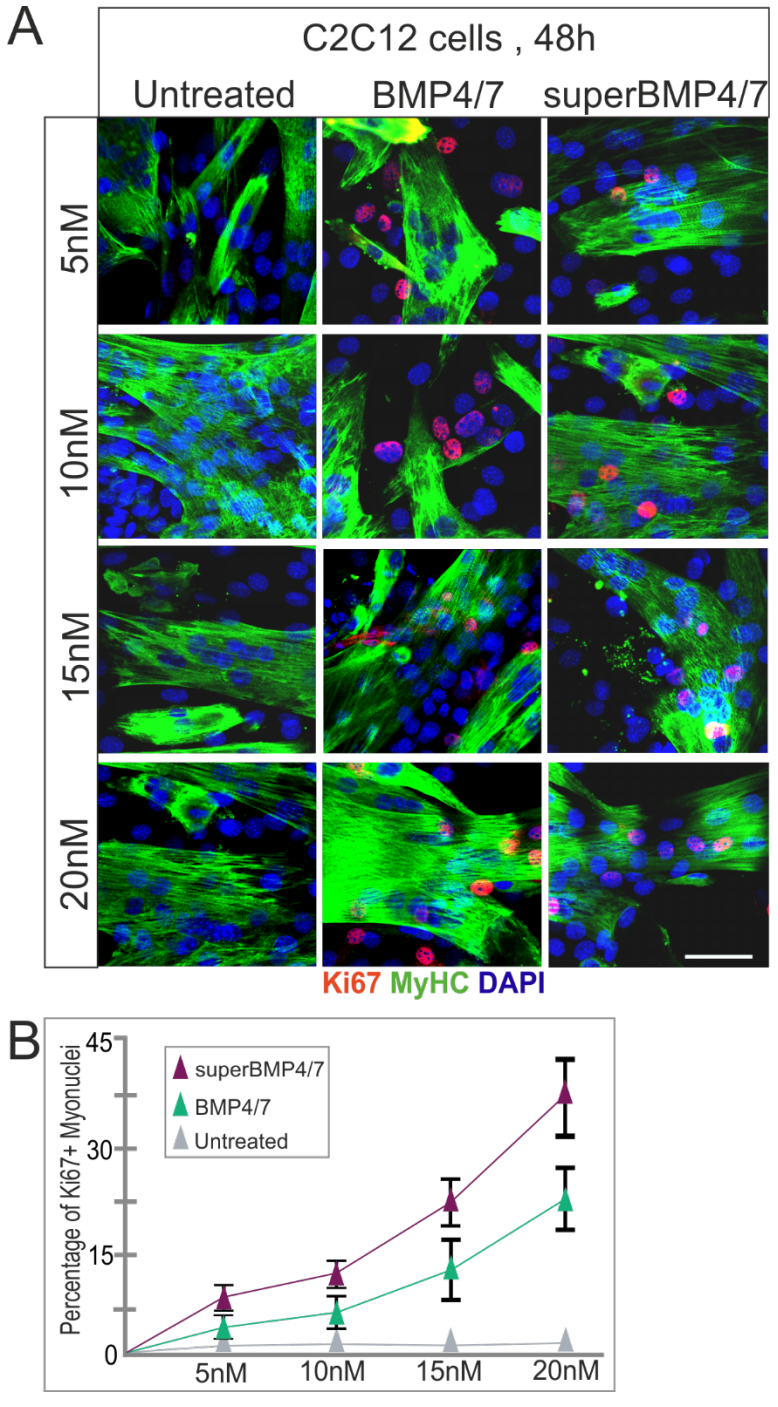

Figure 4.26: Cell cycle re-entry in C2C12 myotubes
C2C12 myoblast derived myotubes were stimulated with increasing concentrations of BMP4/7 and super BMP4/7. Immunostaining shows Ki67+ myonuclei (A) and quantification reveals a concentration dependent increase in cell cycle re-entry which is further enhanced by super BMP4/7 stimulation. Scale bar 50µm.

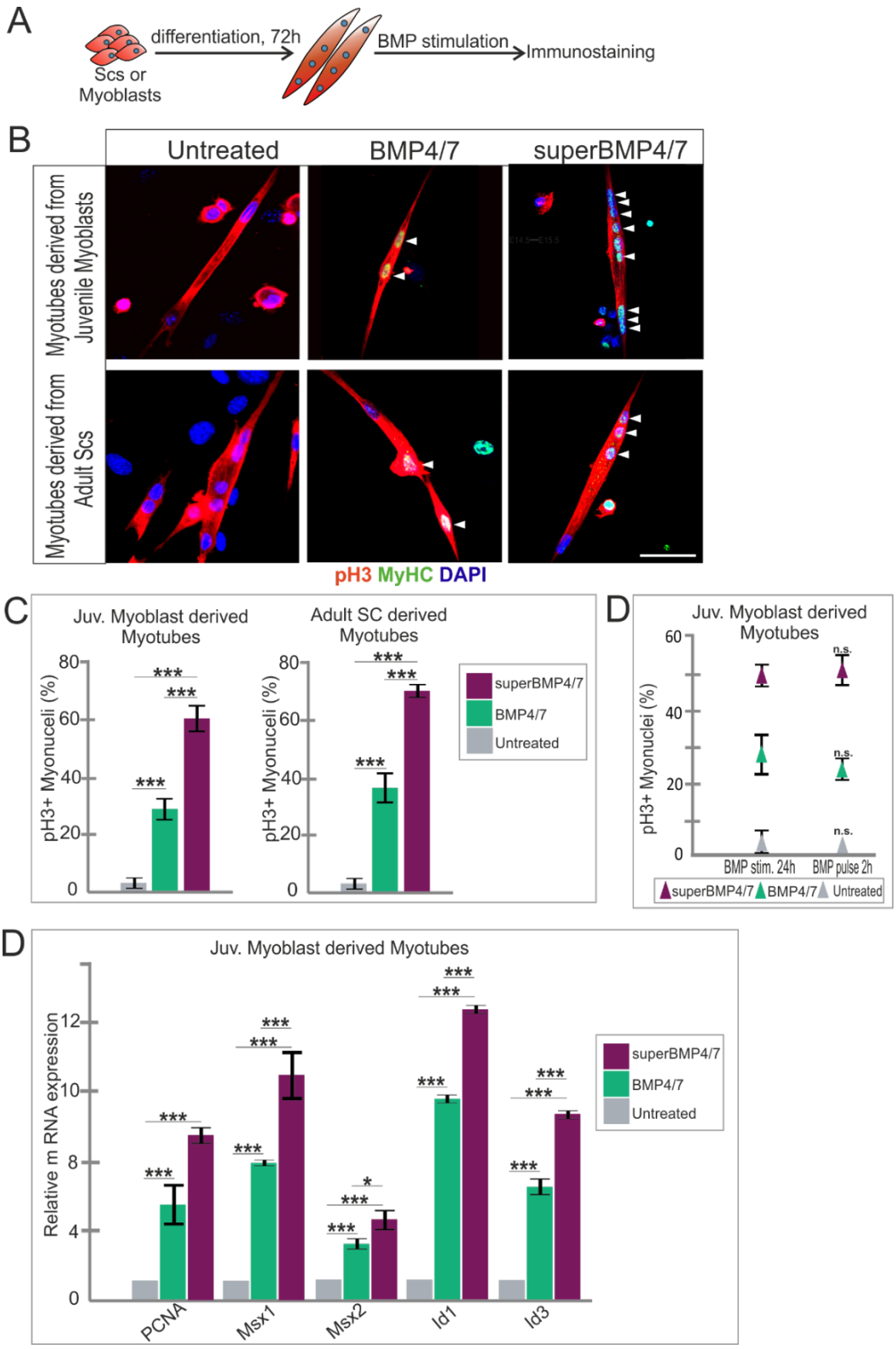

Figure 4.27: Cell cycle re-entry in primary cell derived myotubes
Schematic showing treatment of myotubes with BMP4/7 (A). Immunostaining showing phosho-histone 3 positive myonuclei in myotubes derived from juvenile myoblasts as well as adult satellite cells (B). Quantification shown in (C). No significant changes in 24 hour BMP4/7 stimulation versus 2 hour BMP4/7 pulse (D). Bar graphs depict relative ratios. Error bars represent S.E.M. from three biological replicates. Statistical analysis was done using two-way ANOVA with Bonferroni correction; n.s. not significant, ***p<0.0001. Scale bar 50µm.

To test whether the BMP-induced cell cycle re-entry process is sensitive to inhibition by Noggin, Noggin was added to BMP4/7 and super BMP4/7 to form a complex and then cells were stimulated with this pre-formed complex. At 5nM Noggin concentration a significant reduction in cell cycle re-entry was noted, which was further reduced by increasing the concentration of Noggin to 15nM (Figure 4.28A). Conversely, the impact of Noggin deletion in myotubes was assessed by obtaining myoblasts derived myotubes *in vitro* from $Nog^{fl/fl}$/ACTA1Cre^{+} animals i.e. conditional deletion of Noggin in the differentiated myotubes. Noggin mRNA levels were greatly reduced in $Nog^{fl/fl}$/ACTA1Cre^{+} myotubes, thereby confirming lack of

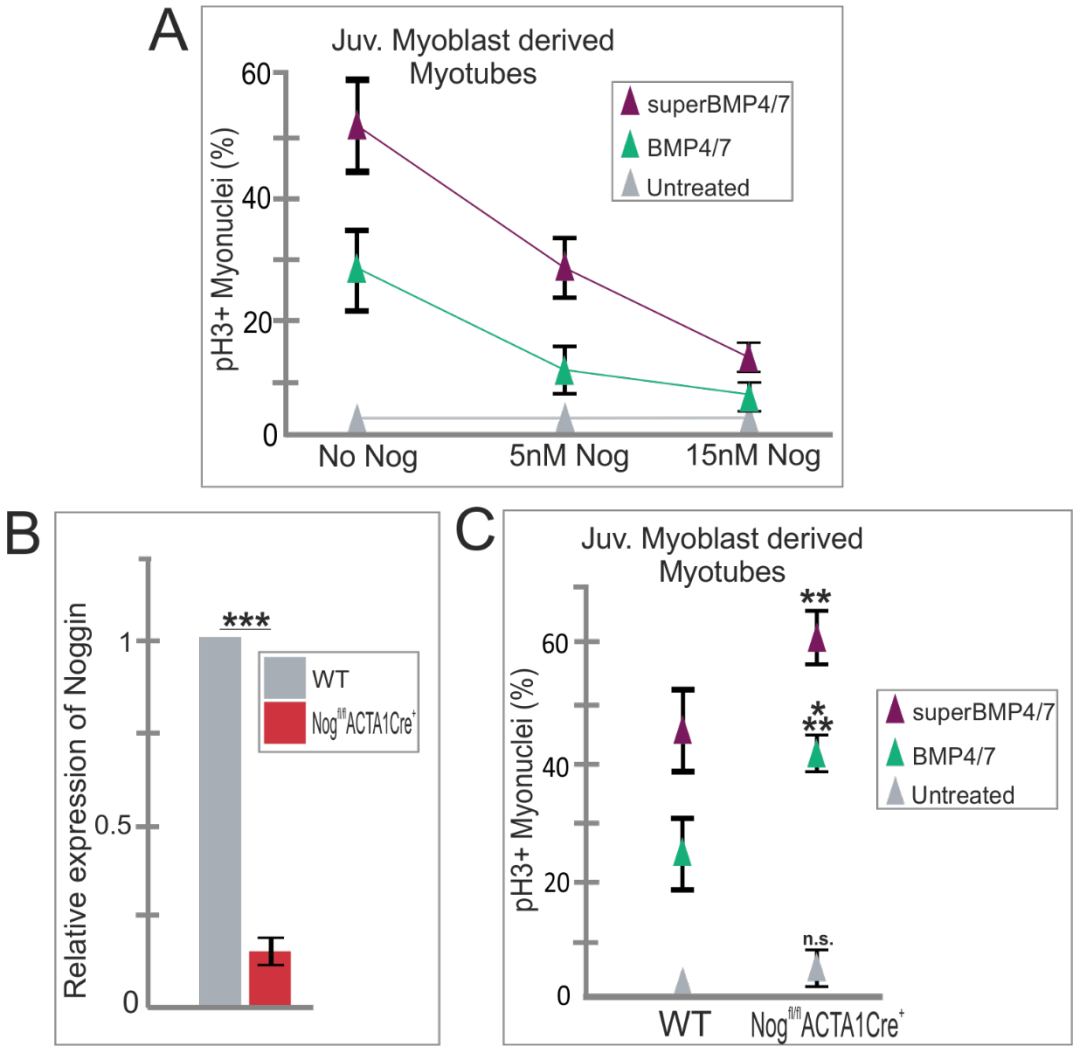

Figure 4.28: Cell cycle re-entry is Noggin sensitive
Quantification showing increasing concentrations of Noggin are effective in reducing cell cycle re-entry in primary myotubes (A). Myotubes derived from $Nog^{fl/fl}$/ACTA1Cre^{+} myoblasts lack Noggin mRNA (B) and show increased cell cycle re-entry upon stimulation with BMP 4/7 (C)). Bar graphs depict relative ratios. Error bars represent S.E.M. from three biological replicates. Statistical analysis was done using two-tailed Student's t-test; n.s. not significant, **p<0.001, ***p<0.0001.

Noggin in the myotubes (Figure 4.28B). BMP4/7 stimulation of the myotubes showed an increase in cell cycle re-entry thereby demonstrating that the cell cycle re-entry process is Noggin sensitive (Figure 4.28C).

4.4.5. BMP incduced myonuclear cell cycle re-entry is Msx1 dependent

Ectopic Msx1 has been shown to induce fragmentation of C2C12 derived myotubes (Kumar et al., 2004; Odelberg et al., 2000). Also, Section 4.3.4. showed Msx1/2 expression in mononucleated cells derived from the ACTA1 lineage after fragmentation. I therefore assessed the effect of Msx1 knockdown on BMP-stimulated primary myotubes. Primary myoblasts were treated with short-hairpin Msx1 vector (shMsx1) and allowed to differentiate before stimulating with 15nM BMP4/7 for 24 hours Figure 4.29A). RT-qPCR analysis showed induction of *Msx1* and to a lesser extent *Msx2* after BMP4/7 stimulation which is further enhanced by super BMP4/7 stimulation. Treatment with shMsx1 shows approximately 50% reduction in mRNA levels of *Msx1*, and importantly *Msx2* does not show compensatory upregulation (Figure 4.29B). When shMsx1 treated myotubes were stimulated with BMP4/7, a significant reduction in cell cycle re-entry was observed for BMP4/7 and more so for super BMP4/7 (Figure 4.29C). This indicated that BMP-induced cell cycle re-entry is dependent on BMP/SMAD target Msx1.

To conclude, this section demonstrated that Nog KO fetuses show enhanced BMP signalling in the myoblasts as well as in the myotubes. This is evident on the mRNA as well as protein level. This could be a consequence of hyperpermeable vasculature in the muscles. It was demonstrated that BMP4/7 can be cleaved with plasmin to generate a highly potent molecule which can induce a high rate of cell cycle re-entry in primary myotubes. Leaky blood vessels in Nog KO fetuses could be a source of plasmin/thrombin that can act of muscle endogenous BMPS thereby further enchancing BMP signalling in the tissues. This process is sensitive to Noggin and is dependent on Msx1. As paracrine signalling is greatly affected by the surrounding microniche, in the next section I analysed whether this microenvironment could influence the de-differentiation process.

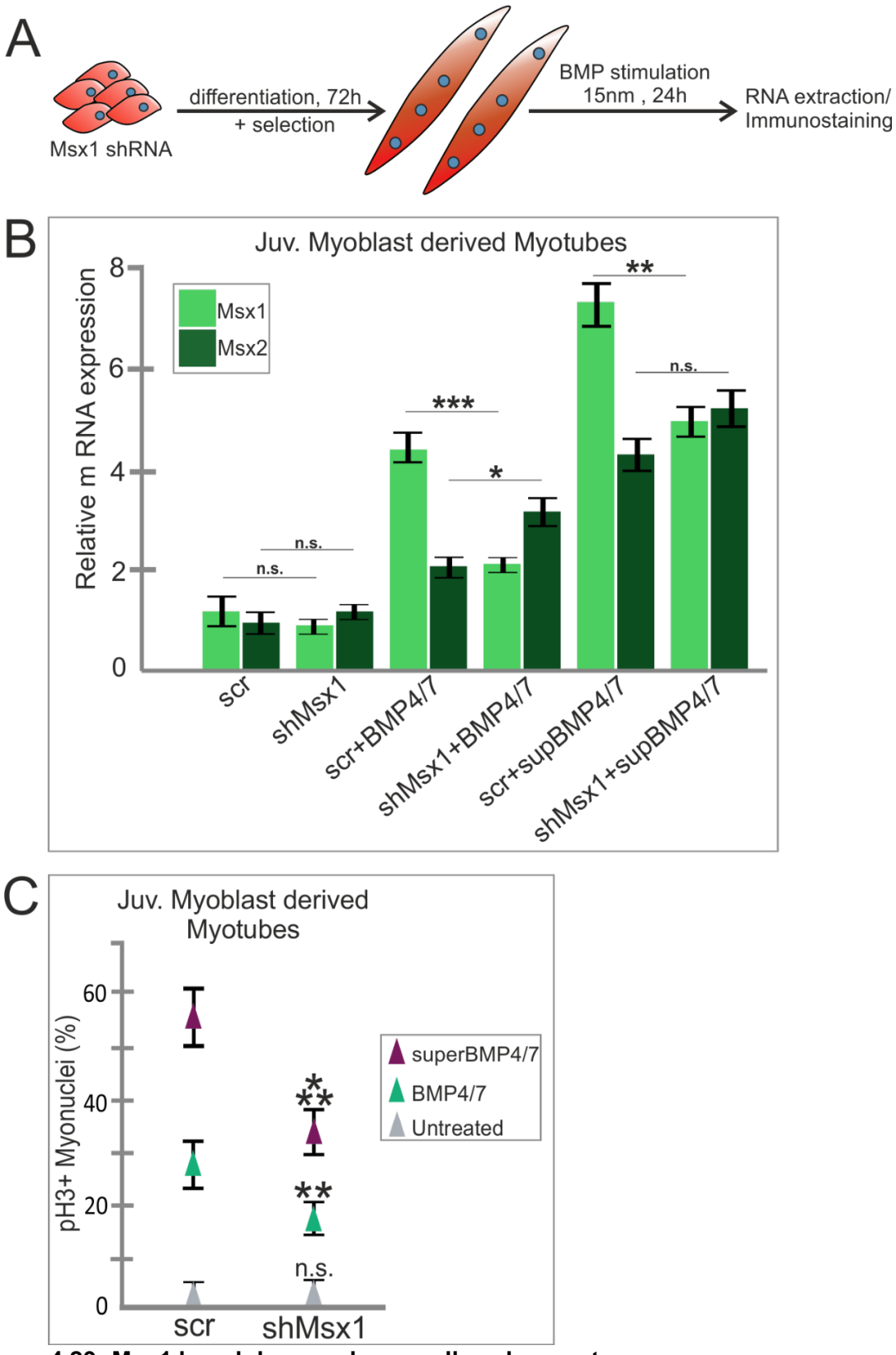

Figure 4.29: Msx1 knockdown reduces cell cycle re-entry
Schematic representation showing the experimental setup (A), RT-qPCR showing induction of *Msx1* and *Msx2* upon BMP4/7 stimulation as well as efficiency of the *Msx1* knockdown (B). Quantification of cell cycle re-entry shows knockdown of *Msx1* also reduces cell cycle re-entry in primary myotubes (C). Bar graphs depict relative ratios. Error bars represent S.E.M. from three biological replicates. Statistical analysis was done using two-tailed Student's t-test; n.s. not significant, *p<0.05, **p<0.001, ***p<0.0001.

4.5. Altered ECM composition and mechanics leads to myonuclear cell cycle re-entry

4.5.1. Differential expression of key ECM genes

To understand the phenotypic consequences of Noggin deletion in fetuses, a genome-wide transcriptomic analysis was performed from muscle and connective tissue dissected from the fetal limbs. Following RNA-sequencing, a gene ontology (GO) analysis was performed whereby differentially expressed genes were assigned GO terms. Among the differentially expressed genes, the GO term 'extracellular matrix organization' was highly prominent. Other GO terms included striated muscle cell differentiation, connective tissue development, muscle cell development, cartilage development which indicate a strong influence on various tissues following Noggin deletion (Figure 4.30A) . Further analysis of the ECM components showed up-regulation of ECM genes like *Col6a4* and *Col8a2*, while a reduction in muscle ECM components like fibronectin (*Fn1*), hyaluronic acid synthesizing enzymes (*Has1* and *Has2*) and tenascin-XB (Tnxb) (Figure 4.30B). Furthermore, a number of ECM modifying genes were de-regulated including Matrix metalloproteinase genes as *Mmp9, Mmp11 and Mmp24*, Hepsin (*Hpn*) and chymase (*Cma1*) which is highly indicative of ECM remodelling (Figure 4.30C). Lastly, BMP/SMAD target genes *Ids* and *Msx1* were upregulated further confirming increased BMP signalling (Figure 4.30D).

The muscles of E15.5 fetuses was then analysed to determine how the global de-regulation of the ECM altered the expression of muscle ECM genes. Immunostaining for laminin, a major myofiber basal lamina component, showed well-structured basal lamina surrounding the myofiber in the WT. However, in Nog KO embryos the laminin staining was discontinuous and highly reduced (Figure 4.31A). Next, fibronectin which is actively expressed in the developing muscle (de Almeida et al., 2016), was highly down regulated in the Nog KO embryos with low expression between the myofibers. While it is actively expressed in the interstitial regions and surrounding myofiber in the WT muscles (Figure 4.31B). Hyaluron-binding protein (HABP) which is expressed in myoblasts (Hunt et al., 2013) was observed in WT fetuses in the muscle interstitium, while the expression as virtually absent in the Nog KO muscles (Figure 4.31C).

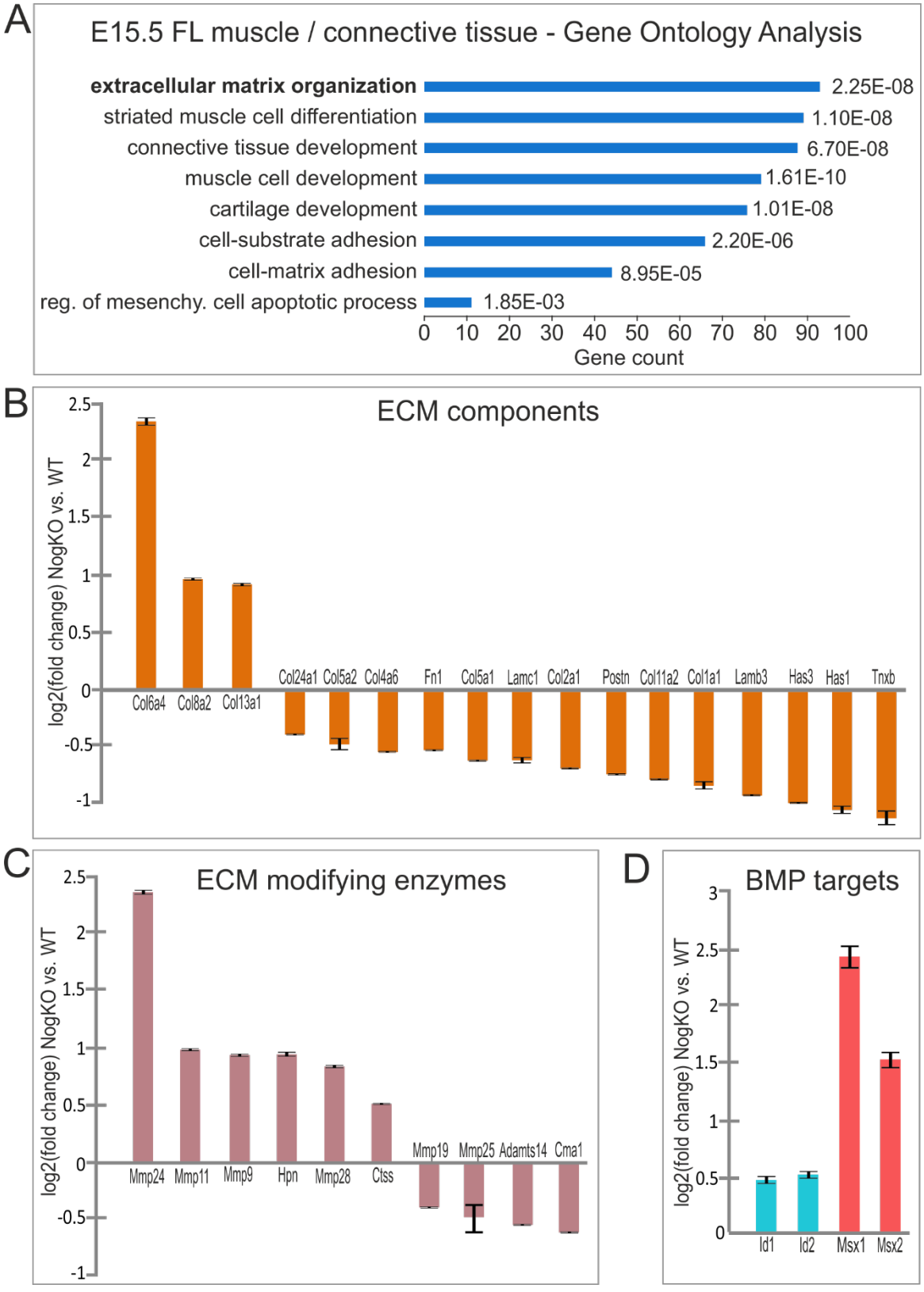

Figure 4.30: Gene oantology analysis shows indicates ECM remodelling in Nog mutants

RNA-sequencing was performed from muscle and connective tissue of E15.5 fetuses, gene antology analysis shows top GO terms with highest number of gene counts noted in GO term extracellular matrix organization. P-values are shown adjacent to the bars (A). De-regulated ECM components (B), ECM modifyijg enzymes (C) and BMP targets (D) are shown as a representation of log2 (foldchange) in the Nog KO relative to WT fetuses. Error bars represent S.E.M. from two biological replicates.

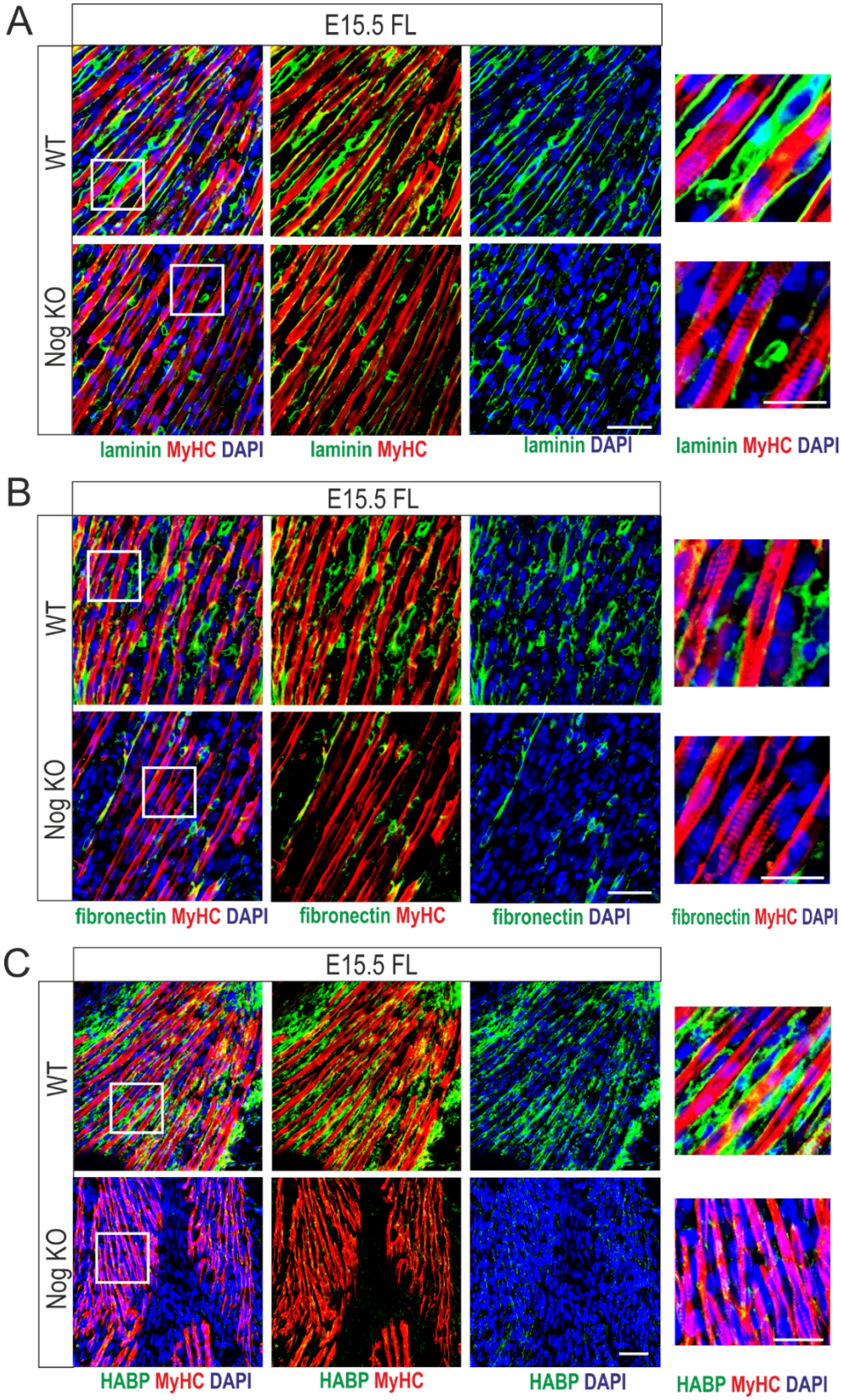

Figure 4.31: Marked reduction of muscle ECM proteins in Nog KO fetuses
Longitudinal sections of E15.5 forelimbs immunostained for muscle ECM genes. Relative to WT, Nog KO myofibers show discontinuity and reduction in basal lamina (laminin) (A). Nog KO muscles show a reduction in interstitial fibronectin, which is present in interstitial regions in the WT (B). HABP is seen in interstitium of WT muscles and is virtually absent in Nog KO muscles (C). Scale bar 50μm.

4.5.2. Laminin has a protective role against myonuclear cell cycle re-entry

The basal lamina of the muscle is a supramolecular structure comprising of collagens and laminins (Hohenester and Yurchenco, 2013) that serves to protect the myofiber and offers a specialized niche for the muscle stem cells. In the Nog KO embryos, a progressive loss of the basal lamina marked by laminin was noted. Therefore, the effect of laminin under conditions that induce cell cycle re-entry was assessed. For this, myoblasts were differentiated on gelatine coated dishes. The myotubes were then coated with recombinant laminin (rec. laminin) and stimulated with BMP4/7 for 24 hours (Figure 4.32A). Myonuclear cell cycle-rentry was assessed by immunostaining for pH3 and performing a count for pH3+ myonuclei. A marked reduction in cell cycle re-entry was noted in rec. laminin treated myotubes after BMP4/7 as well as superBMP4/7 stimulation (Figure 4.32B). Thereby, this suggests that laminin offers a protective function and stability to

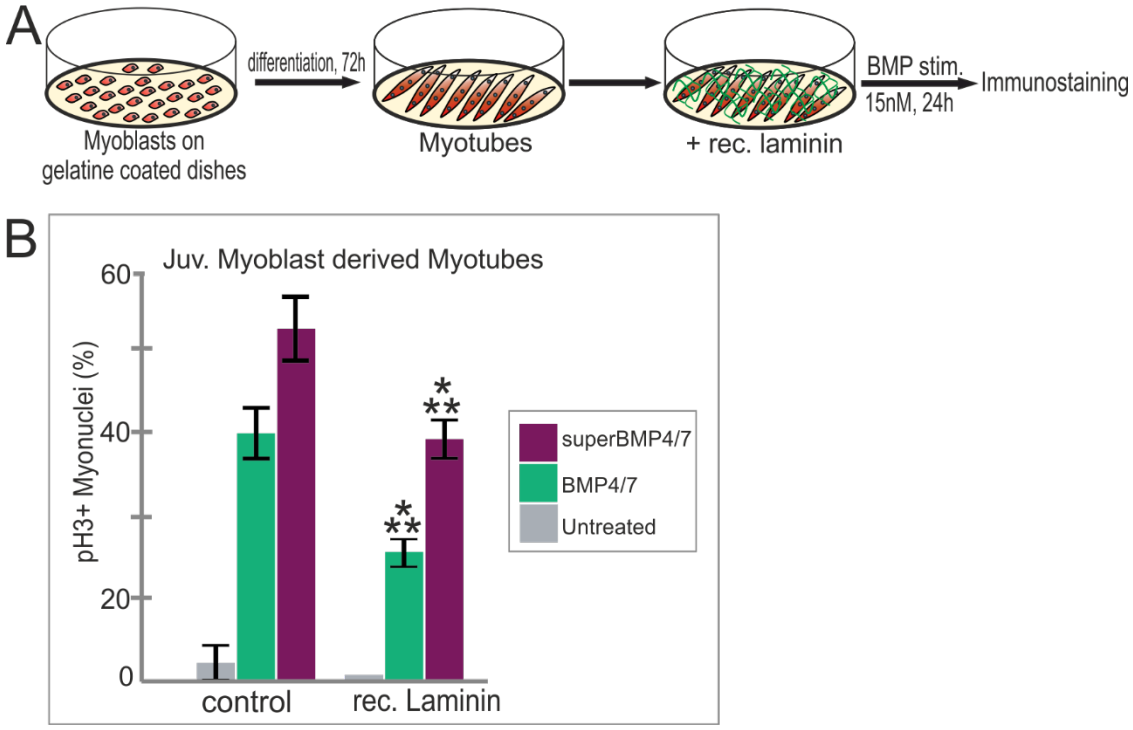

Figure 4.32: Laminin reduces BMP-induced cell cycle re-entry in myotubes
Schematic representation of the methodology shows myoblasts were differentiated on gelatine coated dishes and the myotubes were coated with rec. laminin and stimulated with 15nM BMP4/7 for 24 hours and immunostained for pH3 (A). Count for pH3 shows reduction of cell cycle re-entry in laminin treated myotubes following BMP4/7 and super BMP4/7 stimulation (B). Bar graphs depict relative ratios. Error bars represent S.E.M. from three biological replicates. Statistical analysis was done using two-tailed Student's t-test; ***p<0.0001. Note: statistical analysis shows comparison between laminin treated and untreated conditions.

differentiated myotubes and the absence of which makes the myotubes more vulnerable to BMP-induced cell cycle re-entry.

4.5.3. Tenascin-C supports cell cycle re-entry in myotubes

Tenascin-C (TnC) is an extracellular matrix protein which is highly expressed in dense connective tissue like the tendons during development (Midwood et al., 2016). Studies in amphibians have shown that TnC plays a significant role in inducing myotube fragmentation. Therefore, the spatiotemporal expression of TnC was assessed in E14.5 and E15.5 fetuses by immunostaining for TnC. At E14.5, the WT and Nog KO tissue showed expression of TnC only in the tendons (Figure 4.33A). At E15.5, the WT forelimb tissue also showed TnC staining in the tendons of the muscle. However in the Nog KO tissues, in addition to the tendons, ectopic

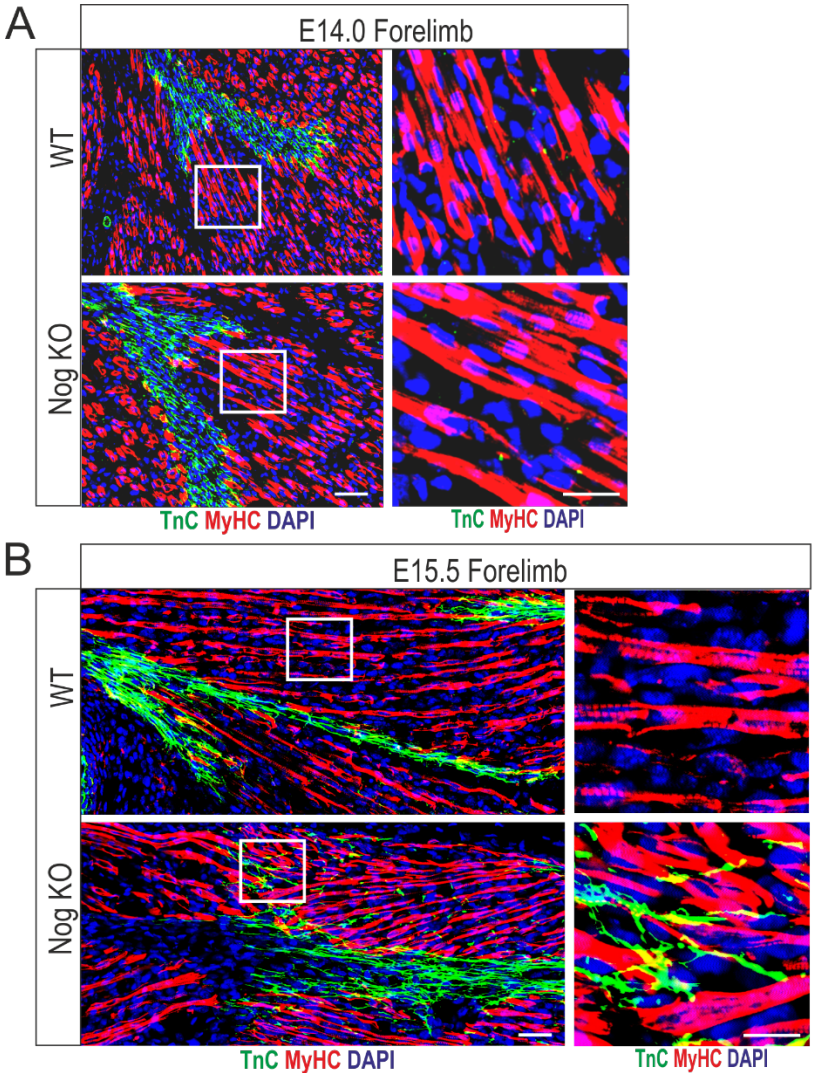

Figure 4.33: TnC is ectopically expressed in Nog KO muscles
Immunostaining for TnC at E14.5 (A) and E15.5 (B) forelimbs shows expression of TnC in the tendons in WT and Nog KO fetuses. Additionally, Nog KO fetuses show ectopic expression of TnC at E15.5 in the muscles. Scale bar 50µm.

TnC expression was observed in the muscle tissue (Figure 4.33B). Here, TnC was seen interspersed between the myofibers therefore hinting at the involvement of TnC in the myofiber de-differentiation process.

To further determine the effect of TnC on myotube de-differentiation, myoblasts were seeded on gelatine coated dishes and differentiated on myotubes and treated with recombinant Tenascin-C of varying concentrations (rec. TnC). Following 15nM BMP4/7 stimulation for 24 hours, cell cycle re-entry was assessed by immunostaining against pH3 (Figure 4.34A). A count for pH3+ myonuclei showed that 0.1µg of TnC had a positive influence on cell cycle re-entry in comparison to the conditions lacking TnC. While lower and higher concentrations showed either no significant changes, or reduced cell cycle re-entry (Figure 4.34B). A test was conducted to determine whether a TnC-BMP pre-mix would induce a stronger effect. TnC and BMP were pre-mixed for 30minutes and compared to BMP stimulation after TnC coating. No significant changes were observed, therefore in the following sections BMP stimulation was conducted after TnC coating (Figure 4.34C). To further understand the effect of TnC, primary and C2C12 myotubes were stimulated with superBMP4/7 for 24 hours either with or without 0.1µg TnC and a RT-qPCR was performed. An upregulation in cell cycle marker *PCNA* and BMP/SMAD targets *Id1*, *Msx1* and *Msx2* was observed. This indicated that TnC is competent in inducing cell cycle re-entry as well as enhanced BMP signalling in myotubes and can induce *Msx* genes which are essential for the de-differentiation process as shown above

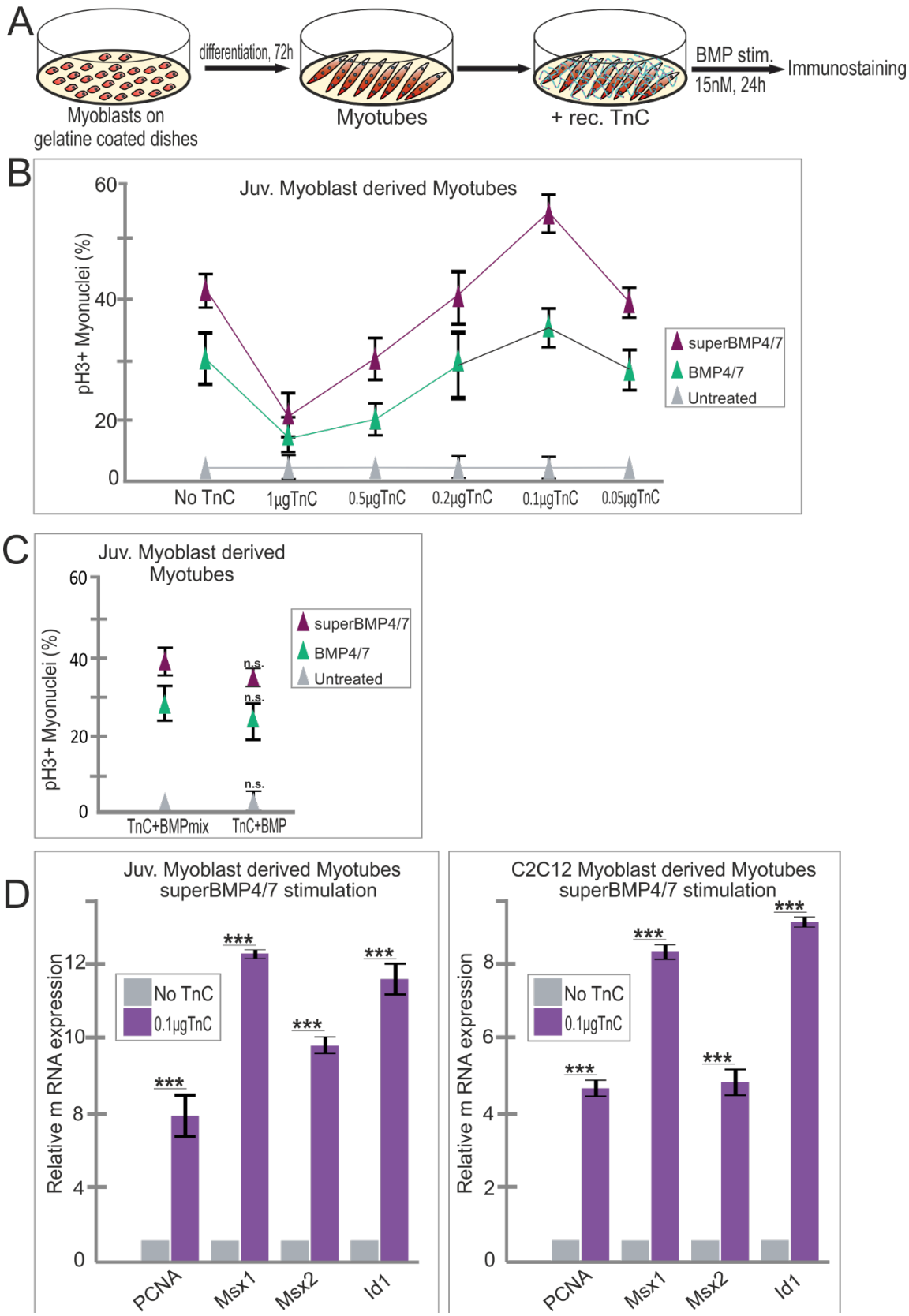

Figure 4.34: TnC supports myotube de-differentiation
Scheme showing the methodology. Myotubes were immunostained against pH3 (A). TnC titration curve to determine the optimal TnC concentration that induced myonuclear cell cycle re-entry (B). No significant changes in cell cycle re-entry were noted when TnC and BMP were pre-mixed for 30 mins before treatment (TnC+BMPmix) versus BMP stimulation after TnC coating (TnC+BMP) (C). *Continued on next page.*

Figure 4.34: TnC supports myotube de-differentiation (Contd.)
RT-qPCR after superBMP4/7 treatment of primary and C2C12 myotubes treated with and without TnC show upregulation of cell cycle marker PCNA and BMP downstream targets (D) Graphs depict relative ratios. Error bars represent S.E.M. from three biological replicates. Statistical analysis was done using two-tailed Student's t-test; n.s. not significant, ***p<0.0001.

4.5.4. Tissue and substrate stiffness play pivotal role in promoting myonuclear cell cycle re-entry

Tenascin is a mecho-regulated ECM component and it is possible that ECM remodelling in the Nog KO tissues including expression of ectopic TnC alters the tissue stiffness. This was tested by performing atomic force microscopy (AFM) on 10µm longitudinal sections derived from E15.5 forelimb tissue (Figure 4.35A). Topography scan was performed to distinguish the myofibers from the extre-myofiber areas (Figure 4.35B). Analysis of the WT and Nog KO showed a reduction in Young's modulus in Nog KO tissue in the myofiber as well as extra-myofiber regions (Figure 4.35C). AFM measurements were also performed from E14.0 embryos, as the muscles at this stage appear normal and no ectopic expression of TnC is observed. In line with these observations, no significant changes in the Young's modulus are observed at E14.0 (Figure 4.35D). This strongly indicated that the alteration in tissue stiffness noted at E15.5 are a result of the ECM remodelling and possibly attributed to ectopic TnC expression in muscles.

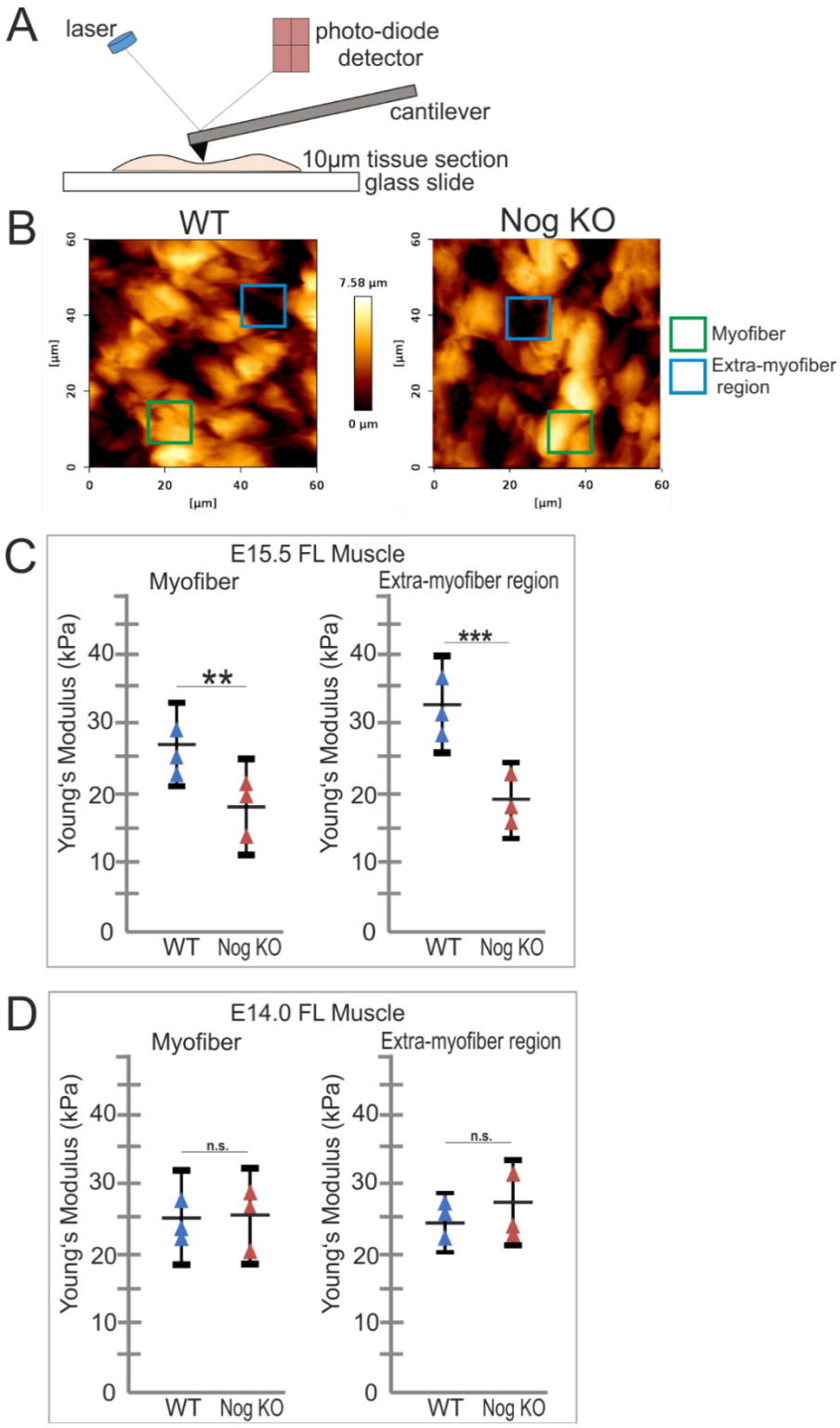

Figure 4.35: Nog KO fetuses show alterations in muscle tissue stiffness
Scheme showing Young's modulus measurements using AFM on 10µM longitudinal sections from fetal forelimbs (A). Topography scan from muscles allows distinction between myofiber and extra-myofiber regions (B). Analysis of E15.5 fetuses shows significant reduction in Young's modulus of myofiber and extra-myofiber regions (C). Young's modulus at E14.0 remains unchanged in both regions in WT and Nog KO fetuses. Graphs depict absolute values. Error bars represent S.E.M. from three biological replicates. Statistical analysis was done using two-tailed Student's t-test; n.s. not significant, **p<0.001, ***p<0.0001

Studies in amphibians have shown that TnC in conjugation with the right substrate stiffness is very effective in inducing myotube cell cycle re-entry (Calve and Simon, 2012). As Nog KO fetuses showed reduction in muscle tissue stiffness, the effect of TnC and substrate stiffness were tested in combination. Myoblasts were coated on gelatine coated glass dishes or on commercially available µ-dish of 28kPa and 15kPa stiffness. Myoblasts were differentiated into myotubes, and stimulated with BMP4/7 either in the presence or absence of TnC (Figure 4.36A). Immunostaining against pH3 was conducted to perform a count for pH3+ myonuclei as a marker for cell cycle re-entry. It was observed that 15kPa induced the highest rate cell cycle re-entry followed by 28kPa and glass. This was noted for BMP4/7 and superBMP4/7 treated myotubes. The same was observed when myotubes were stimulated with BMPs in conjugation with TnC treatment. Notably under rec. TnC treatment conditions, substrate stiffness of 15kPa induces very high rates of cell cycle re-entry when stimulated with superBMP4/7 (Figure 4.36B). It can be concluded from the AFM results as well as the *in vitro* data that a 'soft' substrate stiffness supports myonuclear cell cycle re-entry.

In summary, this section demonstrates that Nog KO fetuses show reduction in key muscle ECM proteins and ectopic TnC in muscles which alters the mechanical properties of the tissue. Myotubes *in vitro* are sensitive to cell cycle re-entry under 'soft' substrate conditions in combination with TnC. The modulations in ECM as well as tissue stiffness, alters the microenvironment of the muscle and plays a key role in supporting the process of muscle de-differentiation.

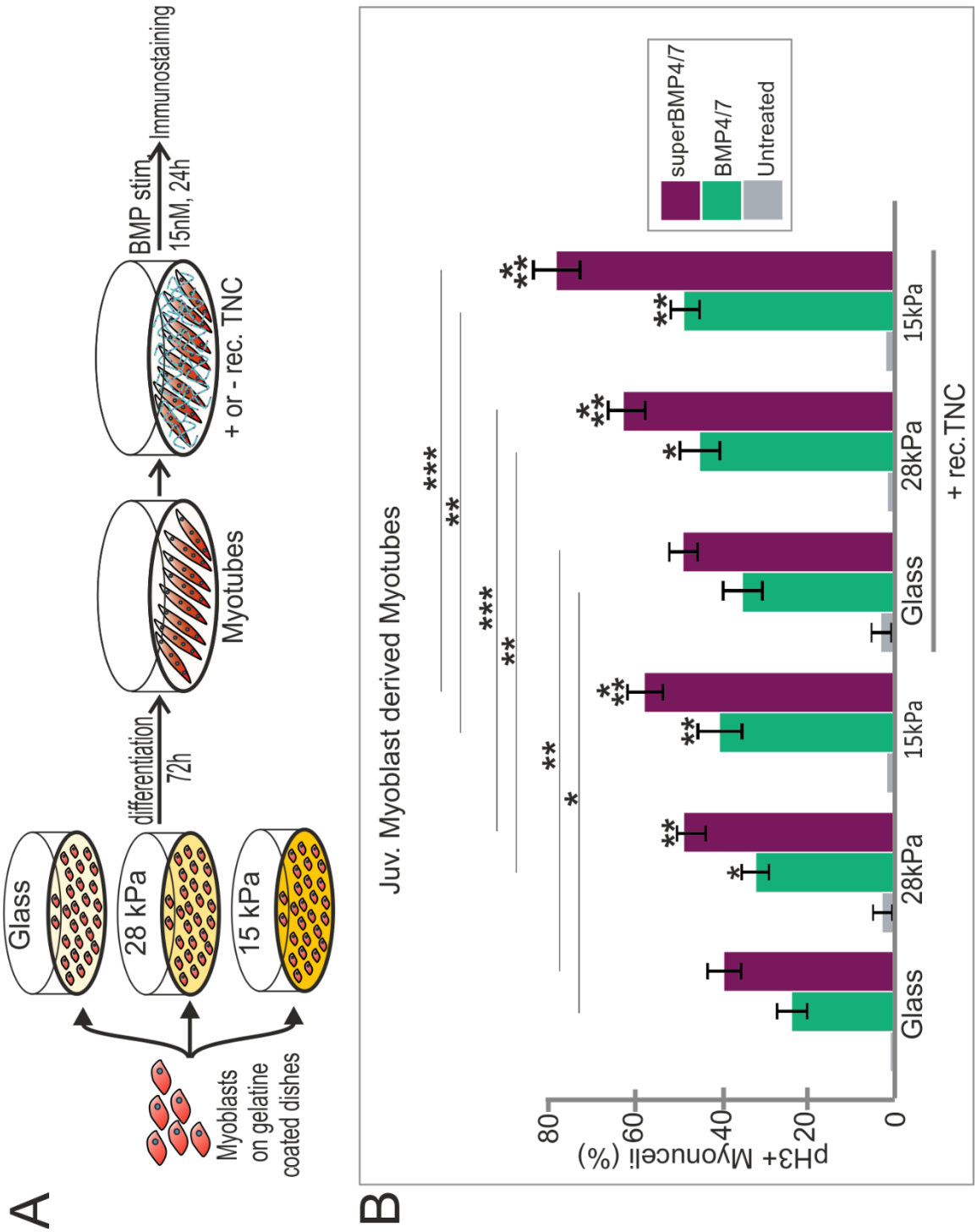

Figure 4.36: Substrate stiffness in combination with TnC potentiates monuclear cell cycle re-entry

Scheme shows myoblasts were seeded on gelatine coated glass or 28kPa or 15kPa µ-dishes and differentiated into myotubes. These were stimulated with 15nM BMP4/7 for 24 hours in the absence or presence of TnC coating (A). Immunostaining for pH3 was used to count pH3+ myonuclei. 15kPa induced highest level of cell cycle re-entry in comparison to glass and 28kPa. 15kPa in combination with TnC after superBMP4/7 stimulation induced the highest rate of cell cycle re-entry (B). Graphs depict relative ratios. Error bars represent S.E.M. from three biological replicates. Statistical analysis was done using two-tailed Student's t-test; *p<0.01, **p<0.001, ***p<0.0001. Note: asterisk on the bars show statistical analysis between the different BMP treatments conditions on the same substrate.

4.6. Summary of results

This study aimed to investigate the role of BMPs and the antagonist Noggin in mouse fetal myogenesis using Nog KO mouse model, C2C12 myoblasts and primary mouse cells. The following are the key findings of this study:

1. Noggin is necessary for fetal but not embryonic myogenesis. Lack of Noggin results in proliferation, differentiation and fusion deviations in the Nog KO fetuses. These defects contribute towards defects and deficits in formation of new myofibers. During fetal stages Nog KO animals progressively lose myofibers thereby leading to reduced muscle mass.
2. Noggin deletion in C2C12 cells recapitulates increased proliferation of myoblasts and reduced differentiation into myotubes. These defects could be partially rescued using a BMP signalling inhibitor (LDN-193189). The Nog KO cells showed increased migration and furthermore, higher degree of osteogenic differentiation in comparison to WT cells.
3. Nog KO fetuses show hallmarks of de-differentiation including muscle fragmentation, myonuclear cell cycle re-entry and cleaved-caspase 3. *In vivo* genetic lineage tracing shows trans-differentiation of muscle cells and myofibers to other mesenchymal lineages which is possibly driven by Msx1.
4. Nog KO fetuses show enhanced BMP signalling and permeability of blood vessels in the muscles. It is plausible that blood plasma derived plasmin can cleave and render them super potent (superBMPs). BMPs, especially superBMP4/7, can induce cell cycle re-entry in C2C12 and primary cell derived myotubes and this process is dependent on Msx1.
5. ECM genes are highly deregulated in the Nog KO fetuses and loss of muscle ECM along with ectopic Tenascin-C (TnC) is observed. This leads to reduced muscle stiffness. *In vitro* experiments on C2C12 cells and primary cells show that myonuclear cell cycle re-entry can be influenced by TnC and substrate stiffness.

In conclusion, this study highlights the role of BMP/Noggin balance in altering the biomechanical niche and further maintaining muscle cell plasticity during myogenesis.

5. DISCUSSION

Research in the last two decades has elucidated the importance of BMP signalling during muscle growth and homeostasis. BMPs and the antagonist Noggin regulate chick embryonic and fetal myogenesis (Amthor et al., 1999; Amthor et al., 2002; Reshef et al., 1998; Wang et al., 2010), as well as proliferation and differentiation of mouse adult satellite cells (SCs) (Friedrichs et al., 2011; Ono et al., 2011). Furthermore, BMPs facilitate the formation of the muscle stem cells pool in juvenile mice and regulate satellite cell (SC) dependent myofiber growth (Stantzou et al., 2017). BMPs also play a key role in maintaining muscle mass during adult homeostasis (Sartori et al., 2013). However, despite these key advancements there remain many open questions in this field regarding BMP/Noggin interplay during mouse fetal development as well as its role in regulating the muscle microenvironment. It is essential to fill in these knowledge gaps in order to gain a deeper perspective on muscle disease pathology and to promote muscle regeneration.

Therefore, in this study the role of BMPs in regulating developmental myogenesis was determined by a combination of *in vivo* and *in vitro* systems that allow investigation of myogenesis under exacerbated BMP signalling conditions. A special focus of this study was to determine the effect of BMP signalling on not only the muscle progenitor cells but also the myotubes themselves. Furthermore, this study provides a novel insight into the role of BMP/Noggin in modulating the biomechanical niche of muscles. Altogether, this study reveals that disrupting the BMP/Noggin balance can strongly affect fetal myogenesis by perturbing myofiber integrity as a consequence of altered ECM and mechanical properties of the tissue. Thereby, revealing a novel role of BMPs in maintaining myotube plasticity.

5.1. BMP/Noggin regulates fetal myogenesis

Studies, primarily done in chicken, show that BMPs regulate proliferation and prevent precocious differentiation of muscle progenitors during early embryogenesis (Amthor et al., 1999; Pourquie et al., 1996). Whereas in fetal chick limbs BMP expression in muscle progenitors at the tips of the muscles allows recruit of new progenitors to the muscle fibers and maintains the satellite cell pool (Wang et al., 2010). However not much is known about the role of BMP signalling in fetal myogenesis in mice. Therefore, this section addresses the role of BMP/Noggin in mouse embryonic and fetal myogenesis.

5.1.1. Noggin expression in muscles

Although studies have demonstrated the role of Noggin during chick fetal development in muscles, its expression have not been shown in muscles before (Amthor et al., 1999; Wang et al., 2010). In this study RT-qPCR was performed from dissected limbs muscles and a $Noggin^{lacZ/+}$ reporter mouse was used to show for the first time that Noggin is expressed in embryonic and fetal muscle interstitial cells and myofibers (See Section 4.1.1). Furthermore, a sharp decline in Noggin expression was noted in the postnatal stages, and expression was limited to interstitial cells which is in line with published data (Stantzou et al., 2017). However, it is difficult to state with certainty that Noggin is indeed expressed in myofibers, as the signal detected in the myofibers could be a remnant of the fusing myocyte. This technical limitation could be overcome by using a Noggin-GFP reporter mouse line or by in-situ hybridisation on tissue sections. In conclusion, this study shows the expression of Noggin for the first time in developing muscles.

5.1.2. Proliferation, differentiation and fusion defects

BMPs and Noggin regulate proliferation and differentiation of chicken fetal progenitors and mouse adult SCs (Friedrichs et al., 2011; Ono et al., 2011; Wang et al., 2010). In this study, a Noggin knockout mouse model (Nog KO) was used to investigate the role of Noggin in myogenesis. These mutants shows severe skeletal and neural tube defects and thus pre-natal lethality (Brunet et al., 1998; McMahon et al., 1998). Hence, the analysis was limited to only to embryonic and fetal stages.

In addition, a CRISPR/Cas9-mediated Noggin deletion C2C12 cell (Nog KO cells) line was generated to further confirm the phenotype observed in the mouse line. This cell line confirmed the deletion of Noggin on a DNA and mRNA level.

Embryonic analysis of the Nog KO mice using WISH revealed that deletion of Noggin did not affect the early establishment of the Pax3+ muscle progenitor pool at E11.5. This in line with previous study that shows that Pax3 expression is unaffected in early Noggin embryos (Tylzanowski et al., 2006). Additionally, the differentiation of the progenitors was apparently not impaired as the mice showed no muscle patterning or size defects in comparison to the WT embryos at E12.5 and E13.5 (See Section 4.1.2). The normal muscle development in the Nog KO embryos could be explained by the fact that embryonic and fetal myoblasts show intrinsic differences in gene expression. Embryonic myoblasts are insensititve to BMPs while fetal progenitors require abrogation of BMP signalling to differentiate (Biressi et al., 2007).

Analysis of fetal stages showed that Nog KO mice progressively loss muscle mass as fetal development proceeded (See Section 4.1.3). SMAD6-mediated abrogation of BMP signalling in adult mice causes severe muscle atrophy, while injecting constitutively active BMP receptor Alk3 into the muscle lead to muscle hypertrophy (Sartori et al., 2013). Additionally, injecting recombinant Noggin protein into the muscles leads to decreased satellite cells pool and thereby less muscle mass (Sartori et al., 2013; Stantzou et al., 2017). This altogether indicates that the disruption of the fine balance of BMP signalling, leading to either increase or decrease in BMP signalling negatively affects muscle mass. However, it is not yet clear whether under such atrophy conditions the myofibers undergo apoptosis or undergo a cell fate change.

During fetal stages Nog KO mice display intrinsic defects in proliferation and differentiation of myogenic cells (See Section 4.1.4). These mice show increased numbers and proliferation of Pax7 muscle progenitors which is in line with the role of BMPs in supporting proliferation of chick fetal progenitors and adult satellite cells (Friedrichs et al., 2011; Ono et al., 2011; Stantzou et al., 2017; Wang et al., 2010). Furthermore, reduced differentiation of Pax7+ cells was noted in Nog KO mice thereby resulting in reduced number of MyoD+ myoblasts. Noggin-mediated BMP abrogation is necessary to allow differentiation of fetal progenitors and adult SCs

(Friedrichs et al., 2011; Ono et al., 2011; Wang et al., 2010). The inhibitory effect of BMP signalling on the myogenic program is a result of the sequestration of the E-proteins by the direct BMP target Id genes. This leads to blockage of MRF-mediated activation of the myogenic program, which is dependent on the binding of the MRFs to these E-proteins (Clever et al., 2010). Therefore, differentiation defects in Nog KO mice could be explained by lack of such pro-differentiation signals.

Nog KO C2C12 cells line further validated these findings (See Section 4.2.2), wherein it could be shown that these cells show high proliferation and increase in *Pax7* gene expression. While a reduction in myotube formation and myogenic genes including *Myf5* and *MyoD* was observed. The differentiation defect could be partially rescued using a BMP pathway inhibitor, LDN-193189 -193189. Thereby, indicating that this defect is in fact due to enhanced BMP signalling.

During the course of this investigation a muscle phenotype analysis of the Nog KO mice was published (Costamagna et al., 2016). In this study it was shown that loss of Noggin did not affect proliferation in late fetal stage E18.5, which is in contrast to my data. This data set in this study was generated by counting the number of Ki67+ cells in the muscle regions, however no co-staining for myogenic cells was performed. They also show that Nog KO fetuses have less Pax7+ cells, however the number of Pax7 cells was not normalized to the number of myofibers. This is essential because Nog KO mice displace differences in number and density of myofibers. Furthermore, this discrepancy can be explained by the fact that my investigation was done at E15.5 and E16.5, while this study was performed from E16.5-E18.5. However, this study confirms the differentiation defect wherein myoblasts isolated from Nog KO fetuses show reduced differentiation.

Lastly, a reduction in the number of fusing myoblasts was noted in the Nog KO mice. It cannot be ascertained whether this is due to an intrinsic fusion defect of the myoblasts or because of reduced initial pool of the myoblasts. However, in the Nog KO C2C12 cells, a reduction in fusion index was observed. Till date, there is no evidence showing a direct regulation of myoblast fusion by either BMP or Noggin. To assess this a ‘salt-and-pepper’ analysis could be done to determine whether Noggin from the myotube or in the myoblasts plays a role in myoblast

fusion. Here, one population of cells would be labelled with a GFP while the other with RFP thereby allowing one to follow and trace the cells into myotubes.

In summary, this section demonstrated that Noggin is essential during fetal myogenesis to maintain correct balance of proliferation, differentiation and fusion of myogenic cells. The lack of Noggin results in increased number of muscle progenitors, while a reduction in the number of myoblasts as well as myofibers. Furthermore, an interesting observation was the loss of myofibers in fetal stages thereby indicating the importance of upholding the balance of BMP signalling to maintain muscle mass.

5.1.3. Migration of myogenic cells

A scratch wound healing assay was performed to assess migration of C2C12 cells (See Section 4.2.3). A slight but significant increase in migration was observed in Nog KO C2C12 cells. BMPs has been shown to promote migration of human aortic vascular smooth muscle cells and various cancer cells (Jiramongkolchai et al., 2016; Willette et al., 1999). In mesenchymal cells BMP2 via a PI3K axis is known to regulate cell polarity and directional cell migration (Hiepen et al., 2014). Although the muscle cells, in particular the stem cells, are responsive to autocrine and paracrine BMP signals, the role of BMPs in directional migration of muscle cells has not yet been established. Likewise, the biological significance of increased migration observed in Nog KO cells is debatable. Transwell chemotaxis assays could determine the effect, if any, of different BMPs on directional migration of fetal progenitors and adult SCs.

Conclusion: Altogether, it can be concluded that Noggin is expressed in muscles and is essential to support fetal myogenesis. The lack of which leads to proliferation and differentiation defects, leading to increased numbers of muscle progenitor cells, reduced myofiber formation and furthermore loss of muscle mass. Reduced myofiber formation could be explained by high BMP signals that prevents cells from entering the differentiation program, however this cannot explain the loss of muscles and will be addressed in the upcoming section.

5.2. Loss of Noggin leads to cell fate switch in the myogenic lineage

The loss of muscle mass observed in the Nog KO mice cannot solely be explained by differentiation and fusion defects. Therefore, I questioned the possibility of cell-fate switch of the myogenic lineage. Interestingly, myoblasts derived from Noggin knockout mice were shown to have increased adipogenic differentiation compared to control myoblasts *in vitro*, indicating that high BMP signalling leads to increased adipogenic responsiveness in these cells (Costamagna et al., 2016). Additionally, BMPs have shown to block myogenic differentiation and induce osteogenic differentiation of C2C12 cells (Katagiri et al., 1994). BMP2 stimulation of Nog KO C2C12 cells increases their osteogenic potential in comparison to WT cells (See Section 4.2.4). Taken together this indicates that exacerbated BMP signalling conditions in the Nog KO fetuses could indeed lead to cell fate change of the myogenic cells. Therefore, this section addresses cell fate switch in myogenic cells and myofibers.

5.2.1. Hallmarks of muscle de-differentiation

Previous studies in amphibians and C2C12-derived myotubes cells have shown that muscle fibers have the capacity to de-differentiate and fragment (Kumar et al., 2004; Ono et al., 2011; Wagner et al., 2017; Wang et al., 2015; Yilmaz et al., 2015). Recently, it was shown that de-differentiation in amphibians is in fact induced by BMPs (Wagner et al., 2017). Furthermore, de-differentiation of muscles was observed in drosophila larval alary muscles as a part of the normal developmental program (Schaub et al., 2015). However, de-differentiation has not been observed in a mammalian animal model before. Analysis of Nog KO fetuses at E15.5 interestingly revealed hallmarks of de-differentiation in the muscles (See Section 4.3.1).

Close examination of the muscles showed signs of muscle fragmentation and stray muscle progenitors were observed in the vicinity of the muscles. This gave the first line of evidence that the loss of muscles in Nog KO fetuses could indeed be attributed to muscle fragmentation.

Cell cycle re-entry in myotubes is classically seen as a sign of de-differentiation in amphibians (Tanaka et al., 1997) Myonuclei in the Nog KO fetuses were positive for cell cycle markers- Ki67, Cyclin D1 and phosphor-histone3 (pH3). Ki67 marks every stage of the cell cycle while being absent in non-dividing cells (Gerdes et al., 1984), while Cyclin D1 marks G1 and G2 phase, and pH3 marks the M phase of the cell cycle (Crosio et al., 2002; Yang et al., 2006). This indicates that myonuclei entering the cell cycle go through each of these distinct cell cycle phases. G2/M transition could be further validated by staining for mitotic machinery that regulate this phase of the cell cycle i.e. phospho-cyclin B1 or phospho-cdk1/cdc2. BrdU labelling of the myonuclei could be performed in the future to confirm the transition into S-phase of the cell cycle. Futhermore, the possibility of endoreplication or endomitosis in the myofibers cannot be ruled out. This could lead to increase in the number of gene copies thereby resulting in increased protein synthesis of, for example, cell cycle genes. In *Arabidopsis*, endoreplication is an essential mechanism for maintaining the cell identity of the trichome cells and determining the final cell-fate (Bramsiepe et al., 2010).

Under normal physiological conditions, myonuclei are postmitotic and cannot divide and replicate (Shenkman et al., 2010). In myocytes after myogenin has been expressed, cell cycle arrest is mediated by p21 and p57 by downregulating the activity of Cyclin-Dependent Protein Kinase (Cdk) and maintainence of retinoblastoma (Rb) in an (hyperphosphorylated) activate state (Zhang et al., 1999). Studies in mammalian myotubes and C2C12 cells have shown that *in vitro* suppression of Rb and Arf, a tumor suppressor, leads to cell cycle re-entry in postmitotic myocytes and myotubes (Wang et al., 2015). Interestingly, BMP2 was shown to reduce Rb levels in breast and prostate cancer cells (Huang et al., 2017; Tomari et al., 2005), therefore it is possible that high BMP signalling in the myotubes leads to partial suppression of Rb and thereby cell cycle re-entry.

To determine whether myotubes in the Nog KO mice are lost due to apoptosis a staining for cleaved caspase 3 (cc3) and TUNEL was performed and in Nog KO fetuses higher numbers of cc3+ and TUNEL+ myonuclei were observed in comparison to the wildtype fetus. However, the number of cc3+ myonuclei exceeded those of TUNEL+ cells. This hinted at initiation of a cell death response, but not full execution of it. Interestingly, myotube fragmentation in amphibians

proceeds via a programmed cell death (PCD) response via cc3 (Wang et al., 2015). This indicates that cells that enter PCD could possibly be susceptible to cell fate change. It is still unclear how cc3 mechanistically induces cell cycle re-entry in myotubes. BMPs were shown to activate caspases in pulmonary artery smooth muscle cells and embryonal carcinoma cells (Fujita et al., 1999; Lagna et al., 2006), thereby demonstrating that BMPs can directly target caspases. Interestingly, cc3 was shown to have a pro-proliferative and anti-apoptotic role in sebaceous glands. Here, cc3 activates proliferation in a YAP1-dependent manner (Yosefzon et al., 2018). High YAP1 levels in myoblasts were shown to induce the expression of cell cycle genes including cyclins, cyclin-related kinases, cell cycle checkpoint-regulating genes (Judson et al., 2012). Furthermore, inhibition of Hippo signalling in planarians lead to nuclearization of Yki (YAP1 ortholog) which was shown to promote de-differentiation of postmitotic cells (de Sousa et al., 2018). Moreover, in liver and intestine hippo pathway inactivation induces cell de-differentiation thereby highlighting a role for YAP1 in restricting plasticity of cells (de Sousa et al., 2018; Gregorieff et al., 2015; Yimlamai et al., 2014).

In summary, it can be hypothesized that BMPs-mediated activation of caspase 3 can further activate YAP1, and YAP1 targets the cell cycle genes to then allow cell cycle re-entry in myotubes. YAP1 was shown to be a regulator of cell plasticity in other cell types, as stated above, thereby making it an interesting target to test in the future. Further studies need to be done to validate this, and could give an interesting molecular insight into the mechanisms of de-differentiation.

5.2.2. Trans-differentiation of myogenic cells

To determine the fate of myogenic cells, a genetic lineage tracing was performed using R26mTmG reporter mice with Lbx1Cre, Myf5Cre and ACTA1Cre (See Sections 4.3.2 and 4.3.3). The three different Cre mice allowed tracing of muscle precursor cells (Lbx1), myoblasts (Myf5) and terminally differentiated myofibers (ACTA1). Notably, it cannot be stated with certainty whether ACTA1 also labels post mitotic myocytes in addition to differentiated myofibers. Strikingly, lineage switch was observed for myogenic cells from all three Cre backgrounds in the Nog KO mice. Here myogenic cells switched to other mesoderm lineages including osteogenic, chondrogenic and connective tissue cells. Semi-quantitative PCR

showed the expression of chondro-osteogenic markers *Runx2* and *Sox9* and absence of myogenic marker *Myog* in transdifferentiated cells derived from the Nog KO fetal limb skeletal elements. Also, low levels of *Sox9* was seen in Nog KO myoblasts indicating the start of the lineage switch. Overall, this demonstrates that myogenic cells, as well as myotubes can switch their fate into other tissue lineages.

Plasticity of myogenic cells into other mesenchymal lineages has been demonstrated before. Treatment of C2C12 myoblasts with reversine, a potent inhibitor of the mitotic kinase Mps1, switches them to a multipotent state whereby they can differentiate into adipogenic and osteogenic lineages (Chen et al., 2004). C2C12 myoblasts can also be primed for osteogenic differentiation by BMP2 stimulation (Katagiri et al., 1994). *In vitro* studies show that adult SCs can be differentiated into osteogenic cells by BMP4 and BMP7 stimulation and into adipocytes by BMP4 stimulation (Asakura et al., 2001). Moreover, non-mesenchymal lineage switch was shown for adult human myoblasts by stimulation with ciliary neurotrophic factor (CNTF), a growth factor which is upregulated upon muscle denervation. CNTF stimulation could switch myoblasts into neurons, glial cells, smooth muscle cells, and adipocytes (Chen et al., 2005).

Plasticity of myogenic cells especially during development has been speculated upon but has not yet been demonstrated *in vivo*. Whereas, plasticity of myotubes is still debated upon and has not been observed in a mammalian animal model. Therefore, this study shows that under pathological BMP conditions during mouse fetal development, myogenic cells and myotube plasticity can be challenged. This finding defies the dogma which states that myotubes are in an irreversible terminal state of differentiation.

5.2.3. Msx1 induced trans-differentiation

To understand the early trans-differentiation events, Nog KO fetuses from mTmG-ACTA1Cre reporter line were analysed at E14.5 and mononucleate cells derived from the ACTA1 lineage were observed in the vicinity of the muscle (See Section 4.3.4). It is likely that these cells represent the initial wave of muscle fragmentation, and will probably trans-differentiate as they are re-localized within the limb. These mononucleate cells were isolated via FACS and immunostained for Msx1/2. Interesting a high percentage of cells were positive for Msx1/2 expression. Msx

genes have been implicated in de-differentiation and plasticity of a multitude of cell types discussed below.

Msx1 acts downstream of BMP/SMAD signalling, and BMPs were shown to induce cell cycle re-entry in amphibian myotubes (Wagner et al., 2017). *Msx1* expression was observed in fragmenting amphibian myotubes in culture and the process could be significantly reduced by *Msx1* knockdown (Kumar et al., 2004). Ectopic expression of *Msx1* in C2C12 myotubes was shown to induce fragmentation and reduction of muscle proteins MyoD, myogenin, MRF4, and cell cycle regulator p21 (Odelberg et al., 2000). Similarly, ectopic expression of *Msx2* in cultured mouse myotubes reduced expression of myogenic genes *MyoD* and *Mrf4* while inducing cellularization and cell cycle re-entry (Yilmaz et al., 2015). In jellyfish, Msx1 induces trans-differentiation of striated muscles into smooth muscle cells and neuronal progenitors in an ECM-dependent manner (Galle et al., 2005) Furthermore, regeneration of *Xenopus* spinal cord and muscle in the tail was shown to be a result of Msx1-dependent BMP signalling (Beck et al., 2003). Msx1 has also been implicated in digit tip regeneration in fetal and neonatal mice, while it is absent during wound healing (Han et al., 2003; Reginelli et al., 1995). Interestingly, YAP1 knockout in the endothelial lineage (Tie2) leads to reduction in the expression of *Msx1* and *Msx2* and affects endothelial to mesenchymal transition of the atrioventricular cushion (Zhang et al., 2014).

Lastly, Msx1 was shown to associate with the polycomb complex to repress myogenic differentiation genes via H3K27me3 repressive mark in myoblasts (Wang et al., 2011). Polycomb complex has been shown to be essential for maintaining cell-fate and identity during development by switching off differentiation genes in embryonic stem cells, while repressing pluripotency genes in differentiated cells (Schuettengruber and Cavalli, 2009). It would be interesting to assess for changes in polycomb-mediated active or repressive histone marks (like H3K27me3 or H3K4me2/3) for pluripotency genes and muscle differentiation genes in the Nog KO fetal myofibers. This would further confirm the occurrence of de-differentiation of the myofibers.

Conclusion: Loss of Noggin leads to fragmentation and trans-differentiation of Noggin into other lineages. This process is likely driven by BMP-targeted Msx1 upregulation. Furthermore, it can be speculated that upregulation of Msx genes leads to downregulation of muscle-specific genes (via polycomb complex) and cell cycle inhibitors like p21 thereby allowing cell fate switch of myotubes.

5.3. Enhanced BMP signalling and cell cycle re-entry in myotubes

Myofiber fragmentation and trans-differentiation events observed in the Nog KO fetus muscles are likely driven by *Msx* genes which are a direct-downstream target of BMP/SMAD signalling. Recent study done in Amphibians has implicated BMP signalling as a key regulator of cell cycle re-entry in myotubes during amphibian limb regeneration (Wagner et al., 2017). Therefore, I questioned whether the cell fate switch observed in Nog KO mouse muscles could indeed be a phenotypic consequence of enhanced BMP signalling. This section addresses BMP signalling pathway in the Nog KO mice and the consequences of exogenous BMP signalling on myotubes.

5.3.1. Myoblasts and myotubes show increased BMP/SMAD signalling

Noggin, is a major antagonist of the BMP signalling pathway and was shown to be expressed in embryonic and fetal muscles (See Section 4.1.1). Global deletion of Noggin thereby lead to increased BMP/SMAD signalling in the muscles as evident in Section 4.4.1.

Myoblasts isolated from Nog KO fetuses showed a significantly higher percentage of nuclear pSMAD1/5/8 in comparison to the WT. Similarly, on mRNA level increased BMP signalling was evident in Nog KO mouse derived myoblasts in comparison to WT myoblasts. Increased expression of BMP ligands BMP2, BMP4 and BMP7 was noted. BMP 4 and BMP7 have been shown to promote proliferation and maintain Pax7 expression in adult muscle SCs, while Noggin supports differentiation (Friedrichs et al., 2011; Ono et al., 2011). This inhibition of differentiation is mediated by Id genes which bind to E-proteins thereby preventing them from forming active complexes with myogenic regulatory factors (Benezra et al., 1990; Jen et al., 1992). In line with this, an increase in the expression of Id1 and Id3 was observed. This could explain the increased proliferation rate and reduced differentiation observed in Nog KO fetal mucles (See Section 4.1.4). Although no changes in the expression of BMP-type 1 receptors was detected, an increase in BMP-type 2 receptors Acvr2a and Acvr2b was observed. Myostatin is

known to signal via Acvr2a and Acvr2b, to limit muscle growth (Lee et al., 2005; Sartori et al., 2013) thereby this could be additionally contributing to reduced muscle mass in Nog KO fetuses.

BMP signalling at the tips of the myofibers plays a key role in the recruitment of myoblasts to the developing myofibers (Wang et al., 2010). As expected in the WT muscles at E15.5, active BMP signalling was observed only at the tips of the myofibers while in the Nog KO muscles pSMAD1/5/8+ myonuclei were present along the whole length of the myofiber. Thereby, indicating ectopic regions of active BMP signalling in Nog KO myofibers. Myotubes derived from Nog KO myoblasts at also showed increased levels of BMP signalling components on mRNA level in comparison to the WT myotubes. BMP ligands BMP4 and BMP7 were upregulated in the myotubes, which were recently shown to have a high potency in inducing cell cycle re-entry in amphibian myotubes (Wagner et al., 2017). While a significant upregulation of *Id* genes was noted which could contribute to reduction in myogenic markers in the myotubes. Additionally, increase in expression of BMP-type 1 receptors was noted thereby suggesting that increased SMAD signalling in the myotubes occurs via these receptors.

As BMPs were implicated to be key players in amphibian myotube cell cycle re-entry (Wagner et al., 2017), it is plausible that enhanced BMP signalling observed in the Nog KO embryos is responsible for the muscle fragmentation and trans-differentiation phenotype.

5.3.2. Proteolytic cleavage and increased potency of BMPs

In Amphibian myotubes, myonuclear cell cycle re-entry was shown to be induced by serum exposure and could be potentiated by plasmin and thrombin treatment (Tanaka et al., 1997). These cell cycle inducing factors were recently identified as BMPs, mainly BMP4 and BMP7. BMP4 was shown to be cleaved by plasmin at the heparin binding N-terminal at R10, thereby potentiating its activity (Wagner et al., 2017). It is speculated that following amphibian limb amputation the damaged vasculature leaks plasma containing plasmin and thrombin onto the surrounding tissue thereby cleaving tissue resident BMPs and potentiating their activity. BMPs have been implicated in inducing hyperpermeability of endothelial cells via BMP6 dependent interaction of VE-cadherin with BMPR1 and BMPRII (Benn et al., 2016).

Additionally, loss of BMPRII in endothelial cells alters the biomechanical niche leading to a gain in TGF-β signalling favouring endothelial-mesenchymal transition (Hiepen et al., 2019). Altogether, it is likely that increased vascular permeability observed in Noggin KO mice is a result of dysregulated BMP signalling (See Section 4.4.2). Furthermore, enhanced BMP signalling observed in Nog KO fetuses could indeed be a result of proteolytic cleavage and increased activity of muscle resident BMP4 and BMP7. Blood plasma contains high levels of BMP9/10 heterodimers (Tillet et al., 2018) and it is possible that vascular permeability in Nog KO foetuses leads to leakage of plasmin-cleaved BMP9/10 onto the muscle. However, it is unlikely this contributes to the muscle phenotype in Nog KO mice as both BMP9 and BMP10 are insensitive to Noggin inhibition (Seemann et al., 2009).

Cleavage of the N-terminal of BMP2 and BMP4/7 could be demonstrated and superBMP2 and superBMP4/7 were shown to be more potent than their uncleaved versions in inducing a BMP response in C2C12 BRE-luciferase cells (See Section 4.4.3). Increased BMP response induced by superBMPs could be explained by a study published by Ohkawara et. al, 2002. BMP2 and BMP4 have unique core of amino acid sequence in their N-terminal that is highly conserved among species and the N-terminal in BMP4 plays a crucial role in restricting it to the neural ectoderm in developing embryos, likely by binding to heparin residues in the extracellular matrix. However, this sequence is lacking in TGF-β and activins which are highly diffusible growth factors. It is interesting to note that, BMP4 mutants lacking amino acids in the N-terminal do not show any changes in biological activity, including binding affinity to BMP receptors or antagonists Noggin and chordin however they show long range diffusion abilities in comparison to wildtype BMP4 (Ohkawara et al., 2002). Thereby, it is plausible that cleavage of N-terminal in BMP2 and BMP4 increases their biological activity in C2C12 BRE-luciferase cells by making them more diffusible across the cells. Moreover, to assess the similarities and differences on a genetic level, a RNA-sequencing analysis could be performed on muscle cells stimulated with uncleaved BMPs in comparison to super BMPs.

Furthermore, stimulation of C2C12 BRE-luciferase cells with plasmin, BMP4/7, noggin and combinations of these gave a new insight into the cleavage dynamics (See Section 4.4.3). SuperBMP4/7 (plasmin cleaved BMP4/7) was more potent

than uncleaved BMP4/7, however plasmin alone could induce luciferase activity indicating that serum contains factors, likely BMPs, whose activity can be potentiated by plasmin. Treatment of cells with Noggin or plasmin in combination with Noggin did not reveal differences in comparison to untreated cells indicating that BMP activity of the serum is sensitive to Noggin inhibition. Furthermore, plasmin treated BMP4/7-Noggin complex showed higher luciferase activity in comparison to BMP4/7-Noggin complex thereby showing that BMP4/7 can be cleaved by plasmin even when it is complexed with Noggin. When Noggin forms a complex with BMP7, it blocks the binding epitopes of BMP type I and type II receptors while the N-terminal of BMP7 is on the exterior of the complex (Groppe et al., 2003) and can hence be targeted for cleavage by plasmin. Lastly, stimulation of C2C12 BRE-luciferase cells with superBMP4/7 complexed with Noggin showed lower luciferase activity in comparison to only superBMP4/7 indicating Noggin sensitivity of superBMP4/7. A more comprehensive analysis should be performed by visualising the various complexes on a SDS gel and furthermore performing mass-spectrometry analysis.

5.3.3. BMPs induce Msx1-dependent cell cycle re-entry in myotubes

Myotubes derived from Nog KO fetuses showed an increase in expression of BMP ligands, predominantly BMP4 and BMP7, in comparison to wildtype fetuses. BMP4/7 heterodimers were shown to be more potent than homodimers BMP4/4, BMP7/7 and BMP2/2 in inducing cell cycle re-entry in amphibian myotubes (Wagner et al., 2017). Therefore, I chose BMP4/7 for *in vitro* experiments and it was seen that BMP4/7 induces cell cycle re-entry in C2C12 and primary mouse myotubes (See Section 4.4.4). SuperBMP4/7 showed higher capacity to induce myonuclear cell-cycle re-entry relative to uncleaved BMP4/7, which could be observed even at low concentrations and this activity could be combated with Noggin. Furthermore, deletion of Noggin in myotubes using Noggin$^{flox/flox}$ACTA1Cre animals, reduced cell cycle re-entry indicating that myotube-derived Noggin is essential to preserve myotube integrity. In amphibian myotubes following amputation, rate of cell cycle re-entry was reduced upon induction of dominant negative BMP receptors, Alk2, Alk3 and Alk6 in myogenic

cells, while the cell cycle re-entry could be promoted by injection of BMP4 and to a greater extent by plasmin-cleaved BMP4 injection into the limb. In cultured amphibian myotubes, BMP-induced cell cycle re-entry could be counteracted by abrogation of BMP signalling using recombinant Noggin (Wagner et al., 2017). Altogether, this confirms a role for protease activity as an upstream regulator of BMP-driven induction of the cell cycle during limb regeneration. Limb regeneration is preceded by formation of a specialized structure celled the blastema. In the fish, *Poecilia latipinna*, BMPs acts via PI3K/AKT on the blastema cells to balance of cell proliferation, migration and apoptosis (Patel et al., 2019). Furthermore, blastema formation during tail regeneration in Amphioxus was shown to be regulated by BMP2 and BMP4, while abrogation of BMP signalling using morpholino for *Bmp2* and *Bmp4* prevented blastema formation (Liang et al., 2019). This thereby highlights the critical role of BMPs in the early process of regeneration.

Stimulation of primary mouse myotubes with BMP4/7 induced expression of *Id1* and *Id3* genes (See Section 4.4.4) indicating that BMPs act via *Id* genes. Ids lead to blockage of MRF-mediated activation of the myogenic program, and is dependent on the binding of the MRFs to these E-proteins (Clever et al., 2010). Furthermore, an upregulation of BMP target genes *Msx1* and to a lower extent *Msx2* was observed in BMP4/7 stimulated myotubes. Whereas, shRNA mediated knockdown of *Msx1* lead to reduction in cell cycle induction (See Section 4.4.5). As previously discussed, Msx genes are known to induce cell cycle in C2C12 and amphibian myotubes (Kumar et al., 2004; Odelberg et al., 2000; Yilmaz et al., 2015) Msx1 likely exerts this effect by upregulation of cyclin D1 and cdk4 thereby keeping cells in the cell cycle (Hu et al., 2001).

Conclusion: Altogether it can be shown that deletion of Noggin in fetuses leads to enhanced BMP signalling, in particular ectopic pSMAD1/5/8 signals and upregulation of BMP4 and BMP7. Increased vascular permeability in Nog KO fetuses leads to leakage of plasma-derived plasmin which acts on the muscle resident BMPs thereby potentiating their activity. Plasmin cleaved BMPs (superBMPs) induce high rates of cell cycle re-entry in mouse myotubes which is mediated via *Id* and *Msx* genes. This demonstrates that, as in the case of amphibians, BMPs are key players in mammalian cell cycle re-entry.

5.4. Extracellular matrix and myotube integrity

The extracellular matrix (ECM) constitutes 1-10% of the skeletal muscle mass and is responsible for providing structural integrity and support to the muscle. Apart from providing structural support, the ECM adheres to the cells providing a channel of molecular communication and mechanical transduction (Kjaer, 2004). The ECM plays a critical role in modulating the bioavailability and diffusion of signalling molecules like BMPs (Umulis et al., 2009). Although it is likely that BMPs themselves exert an effect on the biochemical properties of the ECM, this has not been investigated under conditions of dysregulated BMP signalling in the muscle. In the study presented here, the muscle ECM was investigated under an enhanced BMP signalling scenario and its influence on myotube integrity was determined.

5.4.1. ECM remodelling in Nog KO fetuses

Transcriptomic analysis of muscle and connective tissue was performed from E15.5 fetuses. As the individual muscles cannot be dissected at this fetal stage, the muscle and connective tissue were collected together. During the dissection procedure, the skin, the skeletal elements and the autopod were removed and the remaining tissue (assumed to be primarily muscle and connective tissue) was used for analysis. It is important to note that at this developmental stage the loss in muscle mass has already started, thereby creating a differential tissue bias between the WT and Nog KO fetuses. In order to visualize subtle differences between WT and Nog KO, the log2-fold change value was set to 0.3 and p-value to <0.1. Despite this, the data set could not identify major differences in various signalling pathways. This limitation could be overcome by performing laser-microdissection of muscle from tissue sections which could then be used for transcriptomics.

Transcriptome and gene ontology analysis revealed large-scale ECM remodelling events in the Nog KO fetuses (See Section 4.5.1). Several muscle specific genes like *Fn1*, *Has1*, *Has3* and *Col4a6* were downregulated. Fibronectin (encoded by *Fn1*) is important for alignment for myoblasts for fusion, migration and for myofiber organization (Roman et al., 2018; Snow et al., 2008). Downregulation of fibronectin, observed on a transcript as well as protein level, in Nog KO mice could

be responsible for reduction in myoblast fusion and therefore less myofiber formation. Likewise, a downregulation in hyaluronic acid synthesizing genes (*Has1* and *Has 3*) and HA protein via immunostaining was observed, which could further negatively affect myoblast fusion and migration (Calve et al., 2012). Col4a6 is a constituent of the basement membrane of the myofiber, its downregulation in the Nog KO mice likely affects stability of the basal lamina (Poschl et al., 2004).

An up-regulation of a number of ECM remodelling genes encoding MMPs (eg. *Mmp 24*, and *Mmp9*) was noted. Highest upregulation was seen in *Mmp24*, which is known to cleave N-cadherin, a cell adhesion mediating transmembrane protein (Porlan et al., 2014). N-cadherin is expressed on the surface of myoblasts and the absence of which leads to defects in myoblast fusion and myotube formation (Goichberg and Geiger, 1998). This could provide an explanation for reduced formation of new myotubes in the fetal stages. Next, an upregulation of *Mmp9* was seen in Nog KO muscles. *Mmp9* is up-regulated under muscle pathological conditions, for example in dystrophin-deficient *mdx* mice and following muscle injury and results in degradation of the basal membrane of the muscle (Li et al., 2009; Roach et al., 2002). Therefore, increase in *Mmp9* in Nog KO could be responsible, at least in part, for basal lamina degradation. In addition to this, upregulation of *Hpn* (encoding hepsin) was observed. Hepsin is an activator of pro-MMPs and was shown to release collagen from cartilage explant cultures (Wilkinson et al., 2017). This could in effect explain the loss of collagens (Col4a6) observed in the Nog KO fetuses.

Overall, the transcriptomic analysis and muscle immunostaining reveals that deletion of Noggin results in loss of basal lamina as well as muscle interstitial ECM during mouse fetal development. This ECM remodelling is facilitated by matrix modulating genes like the *Mmp*s. The global ECM dysregulation may affect differentiation and fusion of myogenic cells, and downregulation of the basal lamina components possibly affects myofiber integrity. To determine the overall functional consequence of these ECM alterations *in vitro* setups were used.

5.4.2. Laminin protects myotubes from fragmentation

Laminin the key component of the basement membrane of the muscles and is responsible for cell adhesion, proliferation, migration and survival of muscle cells

(Holmberg and Durbeej, 2013). Loss of laminin in muscles leads to pathological muscular dystrophy leading to reduction in mass strength and mass (Meier and Southard, 1970; Sunada et al., 1995; Xu et al., 1994). While systemic treatment of merosin-deficient congenital muscular dystrophy mice with Laminin-111 improved reduce muscle pathology and aids in muscle regeneration (Rooney et al., 2012; Van Ry et al., 2014). Thereby, suggested a key role of laminins in preserving muscle mass. A discontinuous basal lamina (marked by antibody against laminin) is observed in the Nog KO muscles (See Section 4.5.1) at E15.5. This indicates that the muscle loss observed in these fetuses could be a consequence of disintegration of the basal lamina.

In order to further test this, primary myoblast-derived myotubes were coated with recombinant laminin (rec. laminin). Cell cycle re-entry was assessed (antibody against phospho-histone3) and a comparison was drawn between myotubes coated with or without rec. laminin after BMP4/7 and superBMP4/7 stimulation. A striking reduction in cell cycle re-entry was observed when myotubes were coated with laminin. This was in line with studies from Newts where laminin substrate coating does not support myotube fragmentation (Calve and Simon, 2012).

Therefore, it can be concluded that the loss of the basal lamina, possibly by dysregulated *Mmp* expression, rendered myofibers in Nog KO embryos vulnerable to enhanced BMP signalling which in turn led to myofiber fragmentation and de- or trans-differentiation.

5.4.3. Tenascin supports muscle de-differentiation

Tenascin-C (TnC) is an extracellular matrix protein that is present in myotendinous and myofascial junctions where it is controlled by mechanical stresses induced by the tendon, while it is absent from normal skeletal muscle (Jarvinen et al., 2003). TnC is also expressed as a part of the transitional ECM that directs muscle de-differentiation in amphibian limbs following amputation (Calve et al., 2010). In Nog KO embryos at E15.5, ectopic TnC was seen in the muscle interstitium in addition to the myotendinious junctions, while at E14.5 TnC expression was only restricted to the myotendinous junctions (See Section 4.5.3). This data conflicts with a study where transcriptomic analysis and immunostaining showed expression of TnC in fetal muscle stem cells (Tierney e al., 2016). The transcriptomics analysis was

performed at a later fetal stage of E16.5 in comparison to my analysis, whereas the specificity of TnC antibody depicted in the immunofluorescence images can be questioned. Thereby, explaining the discrepancy observed between the two studies.

To test the functional consequences of ectopic TnC in the muscles, *in vitro* experiments were performed. Here, myotubes were coated with recombinant TnC (rec. TnC) rather than differentiating myotubes on TnC coated dishes. This was done as TnC does not support fusion of myoblasts thereby resulting in a lack of myotube formation (Calve and Simon, 2012). When titration of TnC concentrations was done and BMP induced myotube cell cycle re-entry was assessed (using antibody against pH3), it was seen than TnC in high and low concentrations did not support cell cycle re-entry indicating a threshold that balances cell interaction with TnC. However, when used at 0.1µg/ml concentration an increase in cell cycle re-entry was observed in myotubes in comparison to untreated cells, in conjugation with upregulation of *PCNA*, *Msx* and *Id* genes. Thereby, supporting studies done in Amphibans where TnC was shown to promote myotube fragmentation (Calve and Simon, 2012). Cell cycle re-entry was significantly increased upon superBMP4/7 stimulation in comparison to BMP4/7. One might speculate that this could be a result of increased bioavailability of superBMP4/7 as it lacks the N-terminal that binds to heparin (Wagner et al., 2017). However, ELISA performed on TnC with different BMP ligands, either with or without heparin, showed that TnC can bind to BMP2 but not to BMP4 and BMP7 (De Laporte et al., 2013). This indicates that the increased potency of superBMP4/7 in inducing cell cycle re-entry is not a result of its increased bioavailability (at least in the context of TnC). However, this ELISA experiment was performed with TnC fragments and therefore needs to be reviewed with caution as this might not be reflective of binding dynamics of native TnC in tissues.

It has been shown that TnC can bind to a multitude of growth factors via its heparin binding domain including TGF-β, FGFs, VEGF PDGF, and even BMP2 (De Laporte et al., 2013). This sequestration of growth factors could consequently be responsible for cancer pathophysiology of TnC. For example TnC expression in breast cancer cells was shown to promote survival and outgrowth of the metastatic cells by increasing the expression of stem cell signalling components (Oskarsson

et al., 2011). The pro-dedifferentiation properties of TnC shown in my work, could possibly be attributed to the fact that TnC can present various pro-pluripotency signalling molecules or even BMPs to the myotubes which further sensitize them towards de-differentiation.

TnC has been termed as a de-adhesive ECM component that reduces cell adhesion by loss of actin-stress fibers and focal-adhesion molecules like vinculin and alpha-actin (Murphy-Ullrich, 2001). As strong adhesion is characteristic of differentiated cells, it is likely that ectopic TnC reduces the adhesion of myotubes thereby rendering them more vulnerable to BMP-induced cell cycle re-entry. Furthermore, as strong cell adhesion promotes cell survival, it is likely that programmed cell death response seen in the muscle fibers of Nog KO mice could in part be a consequence of ectopic TnC.

Lastly, it is important to note that TnC is an ECM component that is upregulated during amphibian limb regeneration (Calve et al., 2010) as well as early stages of mouse muscle regeneration (See Section 8.2). It is interesting to question what distinguishes TnC from other muscle ECM genes like collagen IV, collagen VI or laminin in its ability to support myofiber de-differentiation. One possibility is the integrin-binding profile of TnC which could selectively support myotube de-differentiation. Tenascin-C interacts with α9β1 and αVβ3 to promote cell proliferation while with integrin α7β1 and α9β1 to influence the differentiation of mesenchymal stem cells into the neuronal lineage (Tucker and Chiquet-Ehrismann, 2015). Of these only α7β1 is known to be expressed in muscles, and loss of which results in muscular dystrophy (Pegoraro et al., 2002). Interestingly, studies have shown that co-operation between integrins and BMPRs in an ECM-dependent manner can augment BMP signalling levels. For example binding of BMP2 to collagen IV recruits BMPRs into a complex with integrins to thereby promoting BMP signalling (Sawala et al., 2015). Similarly, fibronectin bound to BMP2 can regulate interaction between BMPR and αVβ3 thereby leading to increased stability and phosphorylation of SMAD (Fourel et al., 2016). As TnC can also interact with αVβ3, it is plausible that ectopic expression of TnC in muscles in combination with increased concentration of BMP ligands can facilitate integrin-mediated SMAD signalling thereby rendering the myotubes vulnerable to BMP-dependent cell cycle re-entry and fragmentation. Although it is unclear whether

ectopic expression of TnC in Nog KO muscles alters the integrin expression profile of myotubes, this could be tested in the future by performing a meta-analysis of integrins that are expressed in myotubes upon BMP stimulation.

Overall, it was demonstrated that TnC significantly influences myotube integrity. Ectopic TnC expression seen in Nog KO muscles together with BMP-induced cell cycle re-entry on TnC coated myotubes establishes that TnC supports de-differentiation of mouse myotubes. Although, the molecular mechanism governing TnC-aided myotube fragmentation is yet to be explored, it can be speculated that TnC/integrin interaction further potentiates BMP signalling thereby rendering myotubes vulnerable to de-differentiation.

5.4.4. ECM remodelling and BMP signalling

ECM is a dynamic and instructive regulator of BMP signalling by either presenting, sequestering or allowing diffusion of signalling molecules. BMPs can bind to the various ECM matrix components via their N-terminal domain, in particular proteoglycans, which are rich in heparin binding domains. Binding of BMPs to ECM components inhibits their diffusion into the extracellular space resulting in increased pericellular BMP levels leading to enhanced autocrine BMP signalling (Ruppert et al., 1996; Sedlmeier and Sleeman, 2017).

Changes in the composition of the ECM can therefore regulate the bioavailability of the BMPs. This has been shown in osteoblasts where fibrillin-1 and fibrillin-2 deposit and store TGF-β and BMPs thereby regulating their concentration and gradual release to the cells (Nistala et al., 2010). Furthermore, it was shown that upon binding to fibrillin, BMP7 undergoes conformational changes that promotes latency and prevents binding of the BMP molecule to its receptor (Wohl et al., 2016). ECM remodelling, including degradation of muscle specific ECMs like fibronection, laminin and Col4a6 in conjunction with ectopic TnC is seen in the Nog KO fetuses. Although BMPs are known to bind with varying degree to laminin and collagens (Paralkar et al., 1992), it is unclear whether degradation of these ECM components could directly contribute to alterations in BMP signalling levels in the surrounding muscle tissue. Likewise, it cannot be ascertained whether ectopic expression of TnC can alter BMP signalling in the muscles. Altogether, it is not known which BMPs are bound to specific ECM components, and if degradation of

these ECMs releases matrix bound BMPs into the extracellular space and furthermore the consequence of this on BMP signalling levels in the surrounding tissue. It is essential to answer these questions to predictively model the direct co-relation between presence of specific ECM components and BMP signalling consequences.

BMP signalling can modulate ECM production in a number of cell types including osteoblasts, adipocytes and endothelial cells (Hiepen et al., 2019; Schreiber et al., 2017; Xiao et al., 2002). Additionally, inhibition of BMP signaling using LDN-193189 leads to altered ECM remodelling via reduced expression of *Mmp2* and *Mmp9* during blastema formation in *Poecilia latipinna* (Patel et al., 2019). The ECM in developing muscles is thought to be synthesized majorly by the muscle connective tissue fibroblasts (Chapman et al., 2016). However, it is not known whether enhanced BMP signalling, as seen in the Nog KO mice, could affect ECM secretion by these fibroblast cells. A comprehensive transcriptomic analysis on BMP stimulated fibroblasts would be essential to determine the consequences of BMP signalling on muscle ECM production.

Altogether, the BMP and muscle biology field lacks answers to key fundamental questions about ECM-BMP binding and release, and BMP-mediated ECM secretion of cells. This will be essential to understand the overall bi-directional consequences of ECM and BMPs under dysregulated BMP conditions as seen in Nog KO fetuses.

Conclusion: Altogether, this study shows that enhanced BMP signalling in Nog KO fetuses leads to ECM remodelling including loss of muscle ECM genes and ectopic expression of TnC. Together with *in vitro* data it can be shown that TnC supports myonuclear cell cycle re-entry while laminin has a protective role on the myotubes. A mechanistic insight into the biochemical signatures that make TnC conducive to de-differentiation, for example integrin-binding, together with the consequences of altered ECM on BMP signaling needs to be explored.

5.5. Mechanical influences on the myotube

Classical molecular biology studies in the past have largely focussed on dissecting signalling pathways and gene regulatory systems during development and regeneration of the organism. However, in the last decade research has highlighted the importance of mechanicals forces in directing molecular signals and cellular processes during organogenesis. The developing musculoskeletal system is strongly influenced by mechanical forces exerted by the tendons in conjunction with those of contracting muscles (Lemke and Schnorrer, 2017). These forces can be transmitted across cells via mechanotransduction molecules into the ECM and reciprocally biochemical feedback from the ECM-bound molecules can be sensed by the cells (Mammoto and Ingber, 2010). In the study presented here, the mechanical properties of the muscle tissue was assessed and its consequence on myotube integrity was determined.

5.5.1. ECM remodelling affects muscle tissue stiffness

Interaction of cells with the local ECM allows them to receive exogenous mechanical forces, and the stiffness of this ECM is a direct effector of the cell behaviour. In turn, cells can deposit, remove or alter the ECM to allow normal cell and tissue homeostasis (Humphrey et al., 2014).

In this study, the Nog KO fetuses show a shift in the composition of the ECM at E15.5 wherein the muscle tissues show reduced classical muscle ECM components like laminin, fibronectin, hyaluronic acid and various collagens. This is accompanied by accumulation of the TnC in the interstitial spaces. Remodelling of the ECM in these fetuses resulted in reduced stiffness of the myotubes as well of the extra-myofiber regions i.e. the interstitial space present between the muscle fibers (See Section 4.5.4). The reduction in the stiffness of the muscle tissue however cannot be mainly attributed to the loss, gain or switch of any one ECM component. The decrease in muscle collagens (eg. Col6a4) and laminin, which constitute the majority of the myofiber basement membrane, could however play a significant role in reducing the stiffness of the myofibers. The muscle ECM composition directly influences muscle contractility, which in turn affects further ECM production (Kim et al., 2019). It is therefore possible that Nog KO fetuses

show reduced muscle contractility, as a result of decreased collagen and laminin, which could in turn lead to further alterations in ECM composition and thereby reducing the tissue stiffness. Notably, at E14.5 Noggin fetuses do not show ectopic TnC expression, the muscle morphology appears normal and the stiffness of the muscle tissue is comparable to that of the WT.

5.5.2. Stiffness affects myotube integrity

Biomechanical changes in the microenvironment of cells direct cell behaviour and influences the fate of stem cells during the developmental process. During development mechanical forces guide patterning and organogenesis while in adults the interaction of stem cells with their biomechanical niche maintains their stemness and potency (Vining and Mooney, 2017). *In vitro* studies have shown that adult muscle stem cells cultivated on PEG-scaffolds that mimic the muscle tissue stiffness show a high rate of self-renewal and a high regenerative capacity upon transplantation (Gilbert et al., 2010). Similarly, substrate stiffness has been shown to affect TGF-β mediated apoptosis versus EMT decision in tumor cells (Leight et al., 2012).

I therefore questioned whether the terminal-state of differentiated myotubes could be influenced by tuning the substrate stiffness. Intriguingly, myotubes cultivated on ‘soft’ substrate of 15kPa showed a high rate of cell cycle re-entry upon superBMP4/7 stimulation. This effect could be further increased by coating the myotubes with TnC (See Section 4.5.4). This data is in line with what has previously been shown in Amphibians, wherein fragmentation of myotubes could be induced by a combination of soft substrate (15kPa) and TnC substrate coating (Calve and Simon, 2012). It would be interesting to perform live-cell imaging to assess whether in addition to cell cycle re-entry, myotube fragmentation could also be induced under this setting.

Changes in BMP signalling as a result of alterations in ECM are known to induce mechano-transduction in various cell types. Mechanical loading of human fetal osteoblasts upon BMP2 stimulation leads to phosphorylation of SMAD1/5/8 and expression of BMP target genes (Kopf et al., 2012). Upon shear stress induction in endothelial cells, the interaction between BMPRIB and αvβ3 integrin mediate canonical SMAD signalling via Shc/Fak/Erk pathway (Kopf et al., 2012; Zhou et al.,

2013). Therefore, mechanical properties of the ECM regulate BMP signalling wherein stabilization of BMPR/integrin complexes occurs under higher degrees of stiffness. This highlights the role of integrins and BMP signalling in regulating cellular responses to mechanical aspects of the ECM. It is therefore essential to determine changes in integrin expression in the Nog KO fetuses that could lead to altered mechanosensing by the myogenic cells. Another potential mechanistic candidate could be Yes-associated protein 1 (YAP1), a mechanotansducer, that can bind to SMAD1 and enhances BMP-mediated transcriptional activity (Alarcón et al., 2009). In addition, YAP1 is involved in cell fate decisions and serves as a stemness factor in progenitor cells, can regulate cell cycle and furthermore organ size and development (Fischer et al., 2016). In muscle cells, mechanical overloading leads to activation of YAP1 and overexpression of YAP1 leads to muscular hypertrophy (Goodman et al., 2015). The localization and transcriptional response of YAP1 in superBMP4/7 stimulated myotubes together with TnC and 15kPa substrate stiffness should be assessed.

Conclusion: It could be demonstrated that the biomechanical niche in the Nog KO mouse muscles was altered as a result of ECM remodelling, and this further provided an environment conducive for muscle fragmentation and trans-differentiation. Reduction of substrate stiffness *in vitro* below the endogenous muscle stiffness further proved to be supportive of myonucelar cell cycle re-entry.

5.6. Conclusion and open questions

This study reveals a novel role for BMP/Noggin signalling in fetal myogenesis. I show for the first time that Noggin is expressed in mouse muscles during development. Deletion of Noggin leads to an increased muscle precursor pool while a reduction in myoblast differentiation and myofiber formation during fetal development. This is in line with *in vitro* studies which show that BMPs balance proliferation and differentiation of adult muscle SCs (Friedrichs et al., 2011; Ono et al., 2011). Furthermore, lack of Noggin leads to myotube fragmentation, cell cycle re-entry and activation of capase3 in the myonuclei which are the key hallmarks of de-differentiation in amphibians (Tanaka et al., 1997; Wagner et al., 2017; Wang et al., 2015). Myotube cell cycle re-entry is induced by enhanced BMP signalling as demonstrated for amphibian myotubes (Wagner et al., 2017). Increased BMP/SMAD signalling in Nog KO animals could be a consequence of vascular hyperpermeability which is a potential source of serum proteases that cleave muscle tissue resident BMPs into super BMPs. Enhanced BMP signalling in the myotubes drives *Msx1* expression which is known to induce myotube fragmentation in amphibians and C2C12 cells (Kumar et al., 2004; Odelberg et al., 2000). It is likely that Msx1 exerts this effect by suppressing myogenic differentiation genes and cell cycle inhibitor genes as seen in amphibians (Odelberg et al., 2000). Alterations in BMP signalling leads to ECM remodelling where loss in muscle gene expression is concomitant with ectopic expression of TnC which then reduces the stiffness of the muscle tissue. It is unclear whether these biomechanical changes in the muscle tissue can further influence BMP signalling. One possible scenario could be TnC-mediated integrin/BMPR complex formation that can potentiate BMP/SMAD signalling. Second possibility is YAP1, which is a key regulator of mechanotransduction and has also been shown to modulate BMP signalling and cell plasticity thereby making it a useful molecular target for future investigation. Furthermore, *in vitro* it could be demonstrated that exogenous BMP signalling via superBMP4/7 and downstream target Msx1, together with TnC and soft substrate stiffness can potentiate cell cycle re-entry in mouse myotubes. Lastly, genetic lineage tracing in Nog KO fetuses demonstrated trans-differentiation of muscle precursor cells, myoblasts and myotubes into other

mesoderm-derived lineages. Thereby, providing the first evidence of muscle fragmentation and trans-differentiation in a mammalian animal model. However, it is still unclear whether myotubes have the potential to de-differentiate back into myoblasts or muscle progenitor cells in Nog KO fetuses. Altogether, this study sheds light on a novel role of paracrine BMP signalling and the biomechanical niche in influencing mammalian muscle cell plasticity.

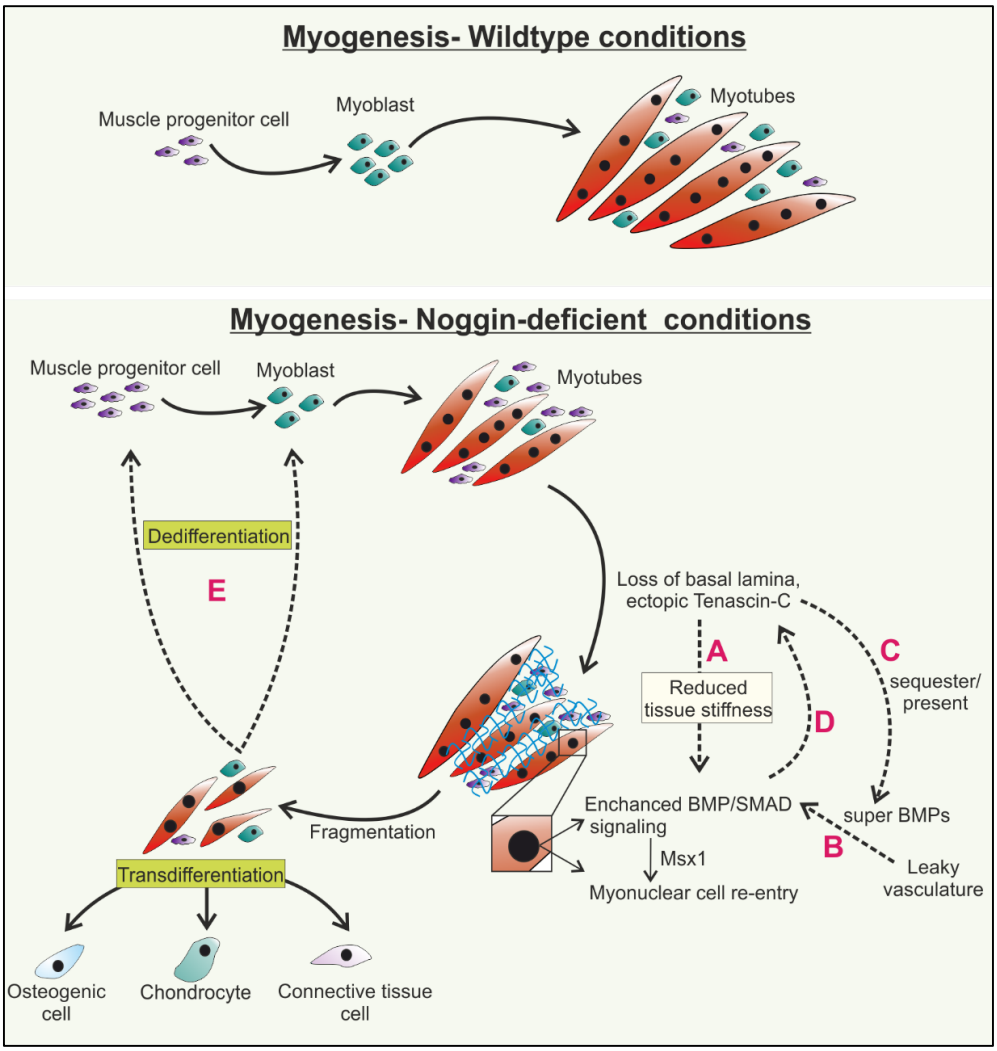

Figure 5.1: Scheme summarizing findings and the open questions
Top panel shows wildtype conditions where muscle progenitor cells differentiate into myoblasts which then fuse together to form myotubes. Botton panel shows myogeneiss under lack of Noggin. Noggin deletion leads to increase in muscle progenitor cells and reduced differentiation into myoblasts and myotubes. ECM remodelling in the muscles leads to ectopic Tenascin-C and reduced muscle tissue stiffness, the consequences of which on BMP signalling in the muscle tissue are unclear (A). Leaky vasculature possibly leads to cleavage of muscle tissue resident BMPs (superBMPs) thereby potentiating their activity (B). It is unclear how TnC affects sequestration and presentation of BMPs (C) and whether enhanced BMP/SMAD signalling can in turn influence TnC production (D). Altogether, this leads to Msx1-induced myonuclear cell cycle re-entry, myofiber fragmentation and trans-differentiation of muscle cells into osteogenic, chondrogenic and connective tissue cells. It is yet to be determined whether fragmented muscles could de-differentiate back into muscle precursor cells and myoblasts (E).

6. FUTURE PERSPECTIVE

This study elucidates a novel role for BMP/Noggin signalling in compromising mammalian myotube integrity. Artificially increasing BMP signalling conditions in myotubes leads to cell cycle re-entry and fragmentation. Such increased BMP stimuli could be likely occurring *in vivo* during a pathological event in the muscle such as muscle damage followed by acute inflammation or haemorrhages. Although myotube de-differentiation is a well-known phenomenon in amphibian biology, the same has never been observed before in a mammalian organism. This study furthermore highlights a novel dynamic between paracrine signalling and the biomechanical niche of the tissue in creating a permissive environment for de-differentiation and trans-differentiation of myotubes. The molecular mechanisms governing this phenomenon in mammals, as well as in amphibians, have not yet been discovered. Thereby, the future work undertaken in this field should aim to elucidate the intracellular molecular signals that modulate the process of de-differentiation in mature muscle cells.

The Nog KO mouse model can further be investigated to understand the underlying **molecular mechanisms** of de- and trans-differentiation. Single-cell RNA sequencing can be performed from cells that are in the process of trans-differentiation. This data set could be used to generate a trajectory showing the transcription profile of myogenic cells, the transitory population and lastly the fate of the transdifferentiated cells. This transcriptomic data could be used to identify novel signalling factors that play a crucial role in this process. Current collaborations with the sequencing facility at the Max-Delbrück centre in Berlin are underway to achieve this goal.

To gain a mechanistic insight into the interactions between **BMP signalling and ECM** composition and stiffness, the artificial *in vitro* system using biomimetic alginate matrices used here could be further employed. These matrices can be tuned to varying stiffness and could also be used to incorporate cells thereby creating a three-dimensional niche. To further discern the role of the ECM, the matrices could incorporate de-differentiation permissive ECM like Tenascin-C. This system could be tuned further to in-corporate and slow-release BMPs to the cells in synergy with altering substrate stiffness. A genome-wide transcriptomic analysis

of the cells could reveal molecular and epigenetic targets that allow transcription of otherwise repressed genes in the differentiated myogenic cells. This sophisticated *in vitro* system could be beneficial to gain important insights into the dynamics between BMP, the ECM and substrate stiffness. The Stricker group is currently collaborating with Sven Geissler at Julius-Wolf Institute to generate the biomimetic matrices.

A long term goal would be to assess whether a de-differentiation process might play a role in **muscle disease** conditions. Together with our collaboration partner, Helge Amthor at UVSQ, France this phenomenon could be investigated under a verified muscle atrophy model of muscle denervation. Muscle denervation is accompanied by muscle atrophy as well as fatty infiltration in the muscle, and, importantly, of transiently increased BMP signalling. Thereby, lineage tracing of myofibers following denervation could determine the contribution of muscle fragmentation to this process.

Beyond this, future lineage tracing analysis should focus on identifying additional tissues that can originate from de-differentiated muscle. As my analysis shows that osteogenic, chrodrogenic and connective tissues are built up by de-differentiated muscle. Thus, current dogmas in the plasticity of muscle tissue have to be revisited and a stronger emphasis should be given to the pleiotropic character of muscle tissue in disease contexts such as muscle atrophy conditions and Fibrodysplasia ossificans progressive (FOP).

The knowledge derived from the above mentioned investigations would be used to gain new perspective on muscle biology and could in the long run be used to a) prevent muscle fragmentation under atrophy conditions, or b) induce muscle fragmentation to foster muscle regeneration.

7. REFERENCES

Amthor, H., Christ, B., Patel, K., 1999. A molecular mechanism enabling continuous embryonic muscle growth - a balance between proliferation and differentiation. Development 126, 1041-1053.

Amthor, H., Christ, B., Rashid-Doubell, F., Kemp, C.F., Lang, E., Patel, K., 2002. Follistatin regulates bone morphogenetic protein-7 (BMP-7) activity to stimulate embryonic muscle growth. Dev Biol 243, 115-127.

Amthor, H., Christ, B., Weil, M., Patel, K., 1998. The importance of timing differentiation during limb muscle development. Curr Biol 8, 642-652.

Asakura, A., Komaki, M., Rudnicki, M., 2001. Muscle satellite cells are multipotential stem cells that exhibit myogenic, osteogenic, and adipogenic differentiation. Differentiation 68, 245-253.

Bajanca, F., Luz, M., Raymond, K., Martins, G.G., Sonnenberg, A., Tajbakhsh, S., Buckingham, M., Thorsteinsdottir, S., 2006. Integrin alpha6beta1-laminin interactions regulate early myotome formation in the mouse embryo. Development 133, 1635-1644.

Beck, C.W., Christen, B., Slack, J.M., 2003. Molecular pathways needed for regeneration of spinal cord and muscle in a vertebrate. Dev Cell 5, 429-439.

Benezra, R., Davis, R.L., Lockshon, D., Turner, D.L., Weintraub, H., 1990. The protein Id: a negative regulator of helix-loop-helix DNA binding proteins. Cell 61, 49-59.

Benn, A., Bredow, C., Casanova, I., Vukicevic, S., Knaus, P., 2016. VE-cadherin facilitates BMP-induced endothelial cell permeability and signalling. J Cell Sci 129, 206-218.

Biressi, S., Tagliafico, E., Lamorte, G., Monteverde, S., Tenedini, E., Roncaglia, E., Ferrari, S., Cusella-De Angelis, M.G., Tajbakhsh, S., Cossu, G., 2007. Intrinsic phenotypic diversity of embryonic and fetal myoblasts is revealed by genome-wide gene expression analysis on purified cells. Dev Biol 304, 633-651.

Bober, E., Franz, T., Arnold, H.H., Gruss, P., Tremblay, P., 1994. Pax-3 is required for the development of limb muscles: a possible role for the migration of dermomyotomal muscle progenitor cells. Development 120, 603-612.

Boergermann, J.H., Kopf, J., Yu, P.B., Knaus, P., 2010. Dorsomorphin and LDN-193189 inhibit BMP-mediated Smad, p38 and Akt signalling in C2C12 cells. Int J Biochem Cell Biol 42, 1802-1807.

Bragdon, B., Moseychuk, O., Saldanha, S., King, D., Julian, J., Nohe, A., 2011. Bone morphogenetic proteins: a critical review. Cell Signal 23, 609-620.

Bramsiepe, J., Wester, K., Weinl, C., Roodbarkelari, F., Kasili, R., Larkin, J.C., Hulskamp, M., Schnittger, A., 2010. Endoreplication controls cell fate maintenance. PLoS Genet 6, e1000996.

Brown, M.A., Zhao, Q., Baker, K.A., Naik, C., Chen, C., Pukac, L., Singh, M., Tsareva, T., Parice, Y., Mahoney, A., Roschke, V., Sanyal, I., Choe, S., 2005. Crystal structure of BMP-9 and functional interactions with pro-region and receptors. J Biol Chem 280, 25111-25118.

Brunet, L.J., McMahon, J.A., McMahon, A.P., Harland, R.M., 1998. Noggin, Cartilage Morphogenesis, and Joint Formation in the Mammalian Skeleton. Science 280, 1455-1457.

Calve, S., Isaac, J., Gumucio, J.P., Mendias, C.L., 2012. Hyaluronic acid, HAS1, and HAS2 are significantly upregulated during muscle hypertrophy. Am J Physiol Cell Physiol 303, C577-588.

Calve, S., Odelberg, S.J., Simon, H.G., 2010. A transitional extracellular matrix instructs cell behavior during muscle regeneration. Dev Biol 344, 259-271.

Calve, S., Simon, H.G., 2012. Biochemical and mechanical environment cooperatively regulate skeletal muscle regeneration. Faseb j 26, 2538-2545.

Carosio, S., Berardinelli, M.G., Aucello, M., Musaro, A., 2011. Impact of ageing on muscle cell regeneration. Ageing Res Rev 10, 35-42.

Chapman, M.A., Meza, R., Lieber, R.L., 2016. Skeletal muscle fibroblasts in health and disease. Differentiation 92, 108-115.

Chen, S., Zhang, Q., Wu, X., Schultz, P.G., Ding, S., 2004. Dedifferentiation of lineage-committed cells by a small molecule. J Am Chem Soc 126, 410-411.

Chen, X., Mao, Z., Liu, S., Liu, H., Wang, X., Wu, H., Wu, Y., Zhao, T., Fan, W., Li, Y., Yew, D.T., Kindler, P.M., Li, L., He, Q., Qian, L., Fan, M., 2005. Dedifferentiation of adult human myoblasts induced by ciliary neurotrophic factor in vitro. Mol Biol Cell 16, 3140-3151.

Clever, J.L., Sakai, Y., Wang, R.A., Schneider, D.B., 2010. Inefficient skeletal muscle repair in inhibitor of differentiation knockout mice suggests a crucial role for BMP signalling during adult muscle regeneration. Am J Physiol Cell Physiol 298, C1087-1099.

Cornelison, D.D., Wilcox-Adelman, S.A., Goetinck, P.F., Rauvala, H., Rapraeger, A.C., Olwin, B.B., 2004. Essential and separable roles for Syndecan-3 and Syndecan-4 in skeletal muscle development and regeneration. Genes Dev 18, 2231-2236.

Costamagna, D., Mommaerts, H., Sampaolesi, M., Tylzanowski, P., 2016. Noggin inactivation affects the number and differentiation potential of muscle progenitor cells in vivo. Sci Rep 6, 31949.

Crosio, C., Fimia, G.M., Loury, R., Kimura, M., Okano, Y., Zhou, H., Sen, S., Allis, C.D., Sassone-Corsi, P., 2002. Mitotic phosphorylation of histone H3: spatio-temporal regulation by mammalian Aurora kinases. Mol Cell Biol 22, 874-885.

Cuny, G.D., Yu, P.B., Laha, J.K., Xing, X., Liu, J.F., Lai, C.S., Deng, D.Y., Sachidanandan, C., Bloch, K.D., Peterson, R.T., 2008. Structure-activity relationship study of bone morphogenetic protein (BMP) signalling inhibitors. Bioorg Med Chem Lett 18, 4388-4392.

Daley, W.P., Peters, S.B., Larsen, M., 2008. Extracellular matrix dynamics in development and regenerative medicine. J Cell Sci 121, 255-264.

de Almeida, P.G., Pinheiro, G.G., Nunes, A.M., Goncalves, A.B., Thorsteinsdottir, S., 2016. Fibronectin assembly during early embryo development: A versatile communication system between cells and tissues. Dev Dyn 245, 520-535.

De Laporte, L., Rice, J.J., Tortelli, F., Hubbell, J.A., 2013. Tenascin C promiscuously binds growth factors via its fifth fibronectin type III-like domain. PLoS One 8, e62076.

de Sousa, N., Rodriguez-Esteban, G., Rojo-Laguna, J.I., Salo, E., Adell, T., 2018. Hippo signalling controls cell cycle and restricts cell plasticity in planarians. PLoS Biol 16, e2002399.

Dosch, R., Gawantka, V., Delius, H., Blumenstock, C., Niehrs, C., 1997. Bmp-4 acts as a morphogen in dorsoventral mesoderm patterning in Xenopus. Development 124, 2325-2334.

Duprez, D.M., Coltey, M., Amthor, H., Brickell, P.M., Tickle, C., 1996. Bone morphogenetic protein-2 (BMP-2) inhibits muscle development and promotes cartilage formation in chick limb bud cultures. Dev Biol 174, 448-452.

Epperlein, H.H., Vichev, K., Heidrich, F.M., Kurth, T., 2007. BMP-4 and Noggin signalling modulate dorsal fin and somite development in the axolotl trunk. Dev Dyn 236, 2464-2474.

Frantz, C., Stewart, K.M., Weaver, V.M., 2010. The extracellular matrix at a glance. J Cell Sci 123, 4195-4200.

Friedrichs, M., Wirsdoerfer, F., Flohe, S.B., Schneider, S., Wuelling, M., Vortkamp, A., 2011. BMP signalling balances proliferation and differentiation of muscle satellite cell descendants. BMC Cell Biol 12, 26.

Fujita, E., Soyama, A., Kawabata, M., Momoi, T., 1999. BMP-4 and retinoic acid synergistically induce activation of caspase-9 and cause apoptosis of P19 embryonal carcinoma cells cultured as a monolayer. Cell Death Differ 6, 1109-1116.

Galle, S., Yanze, N., Seipel, K., 2005. The homeobox gene Msx in development and transdifferentiation of jellyfish striated muscle. Int J Dev Biol 49, 961-967.

Gandhi, N.S., Mancera, R.L., 2012. Prediction of heparin binding sites in bone morphogenetic proteins (BMPs). Biochim Biophys Acta 1824, 1374-1381.

Garcia de Vinuesa, A., Abdelilah-Seyfried, S., Knaus, P., Zwijsen, A., Bailly, S., 2016. BMP signalling in vascular biology and dysfunction. Cytokine Growth Factor Rev 27, 65-79.

Gerdes, J., Lemke, H., Baisch, H., Wacker, H.H., Schwab, U., Stein, H., 1984. Cell cycle analysis of a cell proliferation-associated human nuclear antigen defined by the monoclonal antibody Ki-67. J Immunol 133, 1710-1715.

Gilbert, P.M., Havenstrite, K.L., Magnusson, K.E., Sacco, A., Leonardi, N.A., Kraft, P., Nguyen, N.K., Thrun, S., Lutolf, M.P., Blau, H.M., 2010. Substrate elasticity regulates skeletal muscle stem cell self-renewal in culture. Science 329, 1078-1081.

Goichberg, P., Geiger, B., 1998. Direct involvement of N-cadherin-mediated signalling in muscle differentiation. Mol Biol Cell 9, 3119-3131.

Gregorieff, A., Liu, Y., Inanlou, M.R., Khomchuk, Y., Wrana, J.L., 2015. YAP1-dependent reprogramming of Lgr5(+) stem cells drives intestinal regeneration and cancer. Nature 526, 715-718.

Groppe, J., Greenwald, J., Wiater, E., Rodriguez-Leon, J., Economides, A.N., Kwiatkowski, W., Baban, K., Affolter, M., Vale, W.W., Izpisua Belmonte, J.C., Choe, S., 2003. Structural basis of BMP signalling inhibition by Noggin, a novel twelve-membered cystine knot protein. J Bone Joint Surg Am 85-A Suppl 3, 52-58.

Han, M., Yang, X., Farrington, J.E., Muneoka, K., 2003. Digit regeneration is regulated by Msx1 and BMP4 in fetal mice. Development 130, 5123-5132.

Harland, R.M., 1994. The transforming growth factor beta family and induction of the vertebrate mesoderm: bone morphogenetic proteins are ventral inducers. Proc Natl Acad Sci U S A 91, 10243-10246.

Hernández-Martínez, R., Castro-Obregón, S., Covarrubias, L., 2009. Progressive interdigital cell death: regulation by the antagonistic interaction between fibroblast growth factor 8 and retinoic acid. Development 136, 3669-3678.

Herrera, B., Inman, G.J., 2009. A rapid and sensitive bioassay for the simultaneous measurement of multiple bone morphogenetic proteins. Identification and quantification of BMP4, BMP6 and BMP9 in bovine and human serum. BMC Cell Biol 10, 20.

Hiepen, C., Benn, A., Denkis, A., Lukonin, I., Weise, C., Boergermann, J.H., Knaus, P., 2014. BMP2-induced chemotaxis requires PI3K p55gamma/p110alpha-

dependent phosphatidylinositol (3,4,5)-triphosphate production and LL5beta recruitment at the cytocortex. BMC Biol 12, 43.

Hiepen, C., Jatzlau, J., Hildebrandt, S., Kampfrath, B., Goktas, M., Murgai, A., Cuellar Camacho, J.L., Haag, R., Ruppert, C., Sengle, G., Cavalcanti-Adam, E.A., Blank, K.G., Knaus, P., 2019. BMPR2 acts as a gatekeeper to protect endothelial cells from increased TGFbeta responses and altered cell mechanics. PLoS Biol 17, e3000557.

Hirsinger, E., Duprez, D., Jouve, C., Malapert, P., Cooke, J., Pourquie, O., 1997. Noggin acts downstream of Wnt and Sonic Hedgehog to antagonize BMP4 in avian somite patterning. Development 124, 4605-4614.

Hohenester, E., Yurchenco, P.D., 2013. Laminins in basement membrane assembly. Cell Adh Migr 7, 56-63.

Holmberg, J., Durbeej, M., 2013. Laminin-211 in skeletal muscle function. Cell Adh Migr 7, 111-121.

Hu, G., Lee, H., Price, S.M., Shen, M.M., Abate-Shen, C., 2001. Msx homeobox genes inhibit differentiation through upregulation of cyclin D1. Development 128, 2373-2384.

Huang, P., Chen, A., He, W., Li, Z., Zhang, G., Liu, Z., Liu, G., Liu, X., He, S., Xiao, G., Huang, F., Stenvang, J., Brunner, N., Hong, A., Wang, J., 2017. BMP-2 induces EMT and breast cancer stemness through Rb and CD44. Cell Death Discov 3, 17039.

Humphrey, J.D., Dufresne, E.R., Schwartz, M.A., 2014. Mechanotransduction and extracellular matrix homeostasis. Nat Rev Mol Cell Biol 15, 802-812.

Hunt, L.C., Gorman, C., Kintakas, C., McCulloch, D.R., Mackie, E.J., White, J.D., 2013. Hyaluronan synthesis and myogenesis: a requirement for hyaluronan synthesis during myogenic differentiation independent of pericellular matrix formation. J Biol Chem 288, 13006-13021.

Jarvinen, T.A., Jozsa, L., Kannus, P., Jarvinen, T.L., Hurme, T., Kvist, M., Pelto-Huikko, M., Kalimo, H., Jarvinen, M., 2003. Mechanical loading regulates the expression of tenascin-C in the myotendinous junction and tendon but does not induce de novo synthesis in the skeletal muscle. J Cell Sci 116, 857-866.

Jen, Y., Weintraub, H., Benezra, R., 1992. Overexpression of Id protein inhibits the muscle differentiation program: in vivo association of Id with E2A proteins. Genes Dev 6, 1466-1479.

Jiramongkolchai, P., Owens, P., Hong, C.C., 2016. Emerging roles of the bone morphogenetic protein pathway in cancer: potential therapeutic target for kinase inhibition. Biochem Soc Trans 44, 1117-1134.

Johnson, E.E., Urist, M.R., Finerman, G.A., 1988. Bone morphogenetic protein augmentation grafting of resistant femoral nonunions. A preliminary report. Clin Orthop Relat Res, 257-265.

Judson, R.N., Tremblay, A.M., Knopp, P., White, R.B., Urcia, R., De Bari, C., Zammit, P.S., Camargo, F.D., Wackerhage, H., 2012. The Hippo pathway member YAP1 plays a key role in influencing fate decisions in muscle satellite cells. J Cell Sci 125, 6009-6019.

Kaltcheva, M.M., Anderson, M.J., Harfe, B.D., Lewandoski, M., 2016. BMPs are direct triggers of interdigital programmed cell death. Developmental Biology 411, 266-276.

Katagiri, T., Yamaguchi, A., Komaki, M., Abe, E., Takahashi, N., Ikeda, T., Rosen, V., Wozney, J.M., Fujisawa-Sehara, A., Suda, T., 1994. Bone morphogenetic protein-2 converts the differentiation pathway of C2C12 myoblasts into the osteoblast lineage. J Cell Biol 127, 1755-1766.

Kim, H., Kim, M.C., Asada, H.H., 2019. Extracellular matrix remodelling induced by alternating electrical and mechanical stimulations increases the contraction of engineered skeletal muscle tissues. Sci Rep 9, 2732.

Kintner, C.R., Brockes, J.P., 1985. Monoclonal antibodies to the cells of a regenerating limb. J Embryol Exp Morphol 89, 37-55.

Kjaer, M., 2004. Role of extracellular matrix in adaptation of tendon and skeletal muscle to mechanical loading. Physiol Rev 84, 649-698.

Kopf, J., Petersen, A., Duda, G.N., Knaus, P., 2012. BMP2 and mechanical loading cooperatively regulate immediate early signalling events in the BMP pathway. BMC Biol 10, 37.

Koshida, S., Kishimoto, Y., Ustumi, H., Shimizu, T., Furutani-Seiki, M., Kondoh, H., Takada, S., 2005. Integrinalpha5-dependent fibronectin accumulation for maintenance of somite boundaries in zebrafish embryos. Dev Cell 8, 587-598.

Kumar, A., Velloso, C.P., Imokawa, Y., Brockes, J.P., 2004. The regenerative plasticity of isolated urodele myofibers and its dependence on MSX1. PLoS Biol 2, E218.

Lacraz, G., Rouleau, A.J., Couture, V., Sollrald, T., Drouin, G., Veillette, N., Grandbois, M., Grenier, G., 2015. Increased Stiffness in Aged Skeletal Muscle Impairs Muscle Progenitor Cell Proliferative Activity. PLoS One 10, e0136217.

Lagna, G., Nguyen, P.H., Ni, W., Hata, A., 2006. BMP-dependent activation of caspase-9 and caspase-8 mediates apoptosis in pulmonary artery smooth muscle cells. Am J Physiol Lung Cell Mol Physiol 291, L1059-1067.

Lee, S.J., Reed, L.A., Davies, M.V., Girgenrath, S., Goad, M.E., Tomkinson, K.N., Wright, J.F., Barker, C., Ehrmantraut, G., Holmstrom, J., Trowell, B., Gertz, B., Jiang, M.S., Sebald, S.M., Matzuk, M., Li, E., Liang, L.F., Quattlebaum, E., Stotish, R.L., Wolfman, N.M., 2005. Regulation of muscle growth by multiple ligands signalling through activin type II receptors. Proc Natl Acad Sci U S A 102, 18117-18122.

Leight, J.L., Wozniak, M.A., Chen, S., Lynch, M.L., Chen, C.S., 2012. Matrix rigidity regulates a switch between TGF-beta1-induced apoptosis and epithelial-mesenchymal transition. Mol Biol Cell 23, 781-791.

Lemke, S.B., Schnorrer, F., 2017. Mechanical forces during muscle development. Mech Dev 144, 92-101.

Li, H., Mittal, A., Makonchuk, D.Y., Bhatnagar, S., Kumar, A., 2009. Matrix metalloproteinase-9 inhibition ameliorates pathogenesis and improves skeletal muscle regeneration in muscular dystrophy. Hum Mol Genet 18, 2584-2598.

Liang, Y., Rathnayake, D., Huang, S., Pathirana, A., Xu, Q., Zhang, S., 2019. BMP signalling is required for amphioxus tail regeneration. Development 146.

Lowery, J.W., de Caestecker, M.P., 2010. BMP signalling in vascular development and disease. Cytokine Growth Factor Rev 21, 287-298.

Mammoto, T., Ingber, D.E., 2010. Mechanical control of tissue and organ development. Development 137, 1407-1420.

Martins, G.G., Rifes, P., Amandio, R., Rodrigues, G., Palmeirim, I., Thorsteinsdottir, S., 2009. Dynamic 3D cell rearrangements guided by a fibronectin matrix underlie somitogenesis. PLoS One 4, e7429.

Massague, J., Seoane, J., Wotton, D., 2005. Smad transcription factors. Genes Dev 19, 2783-2810.

Mayer, U., 2003. Integrins: redundant or important players in skeletal muscle? J Biol Chem 278, 14587-14590.

McMahon, J.A., Takada, S., Zimmerman, L.B., Fan, C.M., Harland, R.M., McMahon, A.P., 1998. Noggin-mediated antagonism of BMP signalling is required for growth and patterning of the neural tube and somite. Genes Dev 12, 1438-1452.

Meier, H., Southard, J.L., 1970. Muscular dystrophy in the mouse caused by an allele at the dy-locus. Life Sci 9, 137-144.

Midwood, K.S., Chiquet, M., Tucker, R.P., Orend, G., 2016. Tenascin-C at a glance. J Cell Sci 129, 4321-4327.

Miniou, P., Tiziano, D., Frugier, T., Roblot, N., Le Meur, M., Melki, J., 1999. Gene targeting restricted to mouse striated muscle lineage. Nucleic Acids Res 27, e27.

Miyazono, K., Kamiya, Y., Morikawa, M., 2010. Bone morphogenetic protein receptors and signal transduction. J Biochem 147, 35-51.

Montarras, D., Chelly, J., Bober, E., Arnold, H., Ott, M.O., Gros, F., Pinset, C., 1991. Developmental patterns in the expression of Myf5, MyoD, myogenin, and MRF4 during myogenesis. New Biol 3, 592-600.

Montarras, D., Pinset, C., Chelly, J., Kahn, A., Gros, F., 1989. Expression of MyoD1 coincides with terminal differentiation in determined but inducible muscle cells. Embo j 8, 2203-2207.

Moore, C.J., Winder, S.J., 2010. Dystroglycan versatility in cell adhesion: a tale of multiple motifs. Cell Commun Signal 8, 3.

Mueller, T.D., Nickel, J., 2012. Promiscuity and specificity in BMP receptor activation. FEBS Lett 586, 1846-1859.

Murphy-Ullrich, J.E., 2001. The de-adhesive activity of matricellular proteins: is intermediate cell adhesion an adaptive state? J Clin Invest 107, 785-790.

Muzumdar, M.D., Tasic, B., Miyamichi, K., Li, L., Luo, L., 2007. A global double-fluorescent Cre reporter mouse. Genesis 45, 593-605.

Nelsen, S.M., Christian, J.L., 2009. Site-specific cleavage of BMP4 by furin, PC6, and PC7. J Biol Chem 284, 27157-27166.

Nistala, H., Lee-Arteaga, S., Smaldone, S., Siciliano, G., Carta, L., Ono, R.N., Sengle, G., Arteaga-Solis, E., Levasseur, R., Ducy, P., Sakai, L.Y., Karsenty, G., Ramirez, F., 2010. Fibrillin-1 and -2 differentially modulate endogenous TGF-beta and BMP bioavailability during bone formation. J Cell Biol 190, 1107-1121.

Odelberg, S.J., Kollhoff, A., Keating, M.T., 2000. Dedifferentiation of mammalian myotubes induced by msx1. Cell 103, 1099-1109.

Ohkawara, B., Iemura, S., ten Dijke, P., Ueno, N., 2002. Action range of BMP is defined by its N-terminal basic amino acid core. Curr Biol 12, 205-209.

Ono, Y., Calhabeu, F., Morgan, J.E., Katagiri, T., Amthor, H., Zammit, P.S., 2011. BMP signalling permits population expansion by preventing premature myogenic differentiation in muscle satellite cells. Cell Death Differ 18, 222-234.

Ordahl, C.P., Le Douarin, N.M., 1992. Two myogenic lineages within the developing somite. Development 114, 339-353.

Oskarsson, T., Acharyya, S., Zhang, X.H., Vanharanta, S., Tavazoie, S.F., Morris, P.G., Downey, R.J., Manova-Todorova, K., Brogi, E., Massague, J., 2011. Breast cancer cells produce tenascin C as a metastatic niche component to colonize the lungs. Nat Med 17, 867-874.

Pajni-Underwood, S., Wilson, C.P., Elder, C., Mishina, Y., Lewandoski, M., 2007. BMP signals control limb bud interdigital programmed cell death by regulating FGF signalling. Development 134, 2359-2368.

Paralkar, V.M., Weeks, B.S., Yu, Y.M., Kleinman, H.K., Reddi, A.H., 1992. Recombinant human bone morphogenetic protein 2B stimulates PC12 cell differentiation: potentiation and binding to type IV collagen. J Cell Biol 119, 1721-1728.

Patel, S., Ranadive, I., Rajaram, S., Desai, I., Balakrishnan, S., 2019. Ablation of BMP signalling hampers the blastema formation in Poecilia latipinna by dysregulating the extracellular matrix remodeling and cell cycle turnover. Zoology (Jena) 133, 17-26.

Patterson, S.E., Bird, N.C., Devoto, S.H., 2010. BMP regulation of myogenesis in zebrafish. Dev Dyn 239, 806-817.

Pegoraro, E., Cepollaro, F., Prandini, P., Marin, A., Fanin, M., Trevisan, C.P., El-Messlemani, A.H., Tarone, G., Engvall, E., Hoffman, E.P., Angelini, C., 2002. Integrin alpha 7 beta 1 in muscular dystrophy/myopathy of unknown etiology. Am J Pathol 160, 2135-2143.

Porlan, E., Marti-Prado, B., Morante-Redolat, J.M., Consiglio, A., Delgado, A.C., Kypta, R., Lopez-Otin, C., Kirstein, M., Farinas, I., 2014. MT5-MMP regulates adult neural stem cell functional quiescence through the cleavage of N-cadherin. Nat Cell Biol 16, 629-638.

Poschl, E., Schlotzer-Schrehardt, U., Brachvogel, B., Saito, K., Ninomiya, Y., Mayer, U., 2004. Collagen IV is essential for basement membrane stability but dispensable for initiation of its assembly during early development. Development 131, 1619-1628.

Pourquie, O., Fan, C.M., Coltey, M., Hirsinger, E., Watanabe, Y., Breant, C., Francis-West, P., Brickell, P., Tessier-Lavigne, M., Le Douarin, N.M., 1996. Lateral and axial signals involved in avian somite patterning: a role for BMP4. Cell 84, 461-471.

Re'em-Kalma, Y., Lamb, T., Frank, D., 1995. Competition between noggin and bone morphogenetic protein 4 activities may regulate dorsalization during Xenopus development. Proc Natl Acad Sci U S A 92, 12141-12145.

Reddi, A.H., 2005. BMPs: from bone morphogenetic proteins to body morphogenetic proteins, Cytokine Growth Factor Rev, England, pp. 249-250.

Reginelli, A.D., Wang, Y.Q., Sassoon, D., Muneoka, K., 1995. Digit tip regeneration correlates with regions of Msx1 (Hox 7) expression in fetal and newborn mice. Development 121, 1065-1076.

Reshef, R., Maroto, M., Lassar, A.B., 1998. Regulation of dorsal somitic cell fates: BMPs and Noggin control the timing and pattern of myogenic regulator expression. Genes Dev 12, 290-303.

Ribaric, S., Cebasek, V., 2013. Simultaneous visualization of myosin heavy chain isoforms in single muscle sections. Cells Tissues Organs 197, 312-321.

Roach, D.M., Fitridge, R.A., Laws, P.E., Millard, S.H., Varelias, A., Cowled, P.A., 2002. Up-regulation of MMP-2 and MMP-9 leads to degradation of type IV collagen during skeletal muscle reperfusion injury; protection by the MMP inhibitor, doxycycline. Eur J Vasc Endovasc Surg 23, 260-269.

Roman, W., Martins, J.P., Gomes, E.R., 2018. Local Arrangement of Fibronectin by Myofibroblasts Governs Peripheral Nuclear Positioning in Muscle Cells. Dev Cell 46, 102-111.e106.

Rooney, J.E., Knapp, J.R., Hodges, B.L., Wuebbles, R.D., Burkin, D.J., 2012. Laminin-111 protein therapy reduces muscle pathology and improves viability of a mouse model of merosin-deficient congenital muscular dystrophy. Am J Pathol 180, 1593-1602.

Ruppert, R., Hoffmann, E., Sebald, W., 1996. Human bone morphogenetic protein 2 contains a heparin-binding site which modifies its biological activity. Eur J Biochem 237, 295-302.

Salas-Vidal, E., Valencia, C., Covarrubias, L., 2001. Differential tissue growth and patterns of cell death in mouse limb autopod morphogenesis. Developmental Dynamics 220, 295-306.

Sandoval-Guzman, T., Wang, H., Khattak, S., Schuez, M., Roensch, K., Nacu, E., Tazaki, A., Joven, A., Tanaka, E.M., Simon, A., 2014. Fundamental differences in dedifferentiation and stem cell recruitment during skeletal muscle regeneration in two salamander species. Cell Stem Cell 14, 174-187.

Sartori, R., Schirwis, E., Blaauw, B., Bortolanza, S., Zhao, J., Enzo, E., Stantzou, A., Mouisel, E., Toniolo, L., Ferry, A., Stricker, S., Goldberg, A.L., Dupont, S.,

Piccolo, S., Amthor, H., Sandri, M., 2013. BMP signalling controls muscle mass. Nat Genet 45, 1309-1318.

Schaub, C., Marz, J., Reim, I., Frasch, M., 2015. Org-1-dependent lineage reprogramming generates the ventral longitudinal musculature of the Drosophila heart. Curr Biol 25, 488-494.

Scholzen, T., Gerdes, J., 2000. The Ki-67 protein: from the known and the unknown. J Cell Physiol 182, 311-322.

Schreiber, I., Dorpholz, G., Ott, C.E., Kragesteen, B., Schanze, N., Lee, C.T., Kohrle, J., Mundlos, S., Ruschke, K., Knaus, P., 2017. BMPs as new insulin sensitizers: enhanced glucose uptake in mature 3T3-L1 adipocytes via PPARgamma and GLUT4 upregulation. Sci Rep 7, 17192.

Schuettengruber, B., Cavalli, G., 2009. Recruitment of polycomb group complexes and their role in the dynamic regulation of cell fate choice. Development 136, 3531-3542.

Schwartz, M.A., 2001. Integrin signalling revisited. Trends Cell Biol 11, 466-470.

Sedlmeier, G., Sleeman, J.P., 2017. Extracellular regulation of BMP signalling: welcome to the matrix. Biochem Soc Trans 45, 173-181.

Selleck, S.B., 2000. Proteoglycans and pattern formation: sugar biochemistry meets developmental genetics. Trends Genet 16, 206-212.

Sengle, G., Charbonneau, N.L., Ono, R.N., Sasaki, T., Alvarez, J., Keene, D.R., Bachinger, H.P., Sakai, L.Y., 2008a. Targeting of bone morphogenetic protein growth factor complexes to fibrillin. J Biol Chem 283, 13874-13888.

Sengle, G., Ono, R.N., Lyons, K.M., Bachinger, H.P., Sakai, L.Y., 2008b. A new model for growth factor activation: type II receptors compete with the prodomain for BMP-7. J Mol Biol 381, 1025-1039.

Shenkman, B.S., Turtikova, O.V., Nemirovskaya, T.L., Grigoriev, A.I., 2010. Skeletal muscle activity and the fate of myonuclei. Acta Naturae 2, 59-66.

Sieber, C., Kopf, J., Hiepen, C., Knaus, P., 2009. Recent advances in BMP receptor signalling. Cytokine Growth Factor Rev 20, 343-355.

Siller, A.F., Whyte, M.P., 2018. Alkaline Phosphatase: Discovery and Naming of Our Favorite Enzyme. J Bone Miner Res 33, 362-364.

Smith, W.C., Harland, R.M., 1992. Expression cloning of noggin, a new dorsalizing factor localized to the Spemann organizer in Xenopus embryos. Cell 70, 829-840.

Snow, C.J., Peterson, M.T., Khalil, A., Henry, C.A., 2008. Muscle development is disrupted in zebrafish embryos deficient for fibronectin. Dev Dyn 237, 2542-2553.

Stantzou, A., Schirwis, E., Swist, S., Alonso-Martin, S., Polydorou, I., Zarrouki, F., Mouisel, E., Beley, C., Julien, A., Le Grand, F., Garcia, L., Colnot, C., Birchmeier, C., Braun, T., Schuelke, M., Relaix, F., Amthor, H., 2017. BMP signalling regulates satellite cell-dependent postnatal muscle growth. Development 144, 2737-2747.

Sunada, Y., Bernier, S.M., Utani, A., Yamada, Y., Campbell, K.P., 1995. Identification of a novel mutant transcript of laminin alpha 2 chain gene responsible for muscular dystrophy and dysmyelination in dy2J mice. Hum Mol Genet 4, 1055-1061.

Tallquist, M.D., Klinghoffer, R.A., Heuchel, R., Mueting-Nelsen, P.F., Corrin, P.D., Heldin, C.H., Johnson, R.J., Soriano, P., 2000. Retention of PDGFR-beta function in mice in the absence of phosphatidylinositol 3'-kinase and phospholipase Cgamma signalling pathways. Genes Dev 14, 3179-3190.

Tanaka, E.M., Gann, A.A., Gates, P.B., Brockes, J.P., 1997. Newt myotubes reenter the cell cycle by phosphorylation of the retinoblastoma protein. J Cell Biol 136, 155-165.

Taylor, G.P., Anderson, R., Reginelli, A.D., Muneoka, K., 1994. FGF-2 induces regeneration of the chick limb bud. Dev Biol 163, 282-284.

Tomari, K., Kumagai, T., Shimizu, T., Takeda, K., 2005. Bone morphogenetic protein-2 induces hypophosphorylation of Rb protein and repression of E2F in androgen-treated LNCaP human prostate cancer cells. Int J Mol Med 15, 253-258.

Tozer, S., Bonnin, M.A., Relaix, F., Di Savino, S., Garcia-Villalba, P., Coumailleau, P., Duprez, D., 2007. Involvement of vessels and PDGFB in muscle splitting during chick limb development. Development 134, 2579-2591.

Tucker, R.P., Chiquet-Ehrismann, R., 2015. Tenascin-C: Its functions as an integrin ligand. Int J Biochem Cell Biol 65, 165-168.

Tylzanowski, P., Mebis, L., Luyten, F.P., 2006. The Noggin null mouse phenotype is strain dependent and haploinsufficiency leads to skeletal defects. Dev Dyn 235, 1599-1607.

Umulis, D., O'Connor, M.B., Blair, S.S., 2009. The extracellular regulation of bone morphogenetic protein signalling. Development 136, 3715-3728.

Urist, M.R., 1965. Bone: formation by autoinduction. Science 150, 893-899.

Van Ry, P.M., Minogue, P., Hodges, B.L., Burkin, D.J., 2014. Laminin-111 improves muscle repair in a mouse model of merosin-deficient congenital muscular dystrophy. Hum Mol Genet 23, 383-396.

Vasyutina, E., Birchmeier, C., 2006. The development of migrating muscle precursor cells. Anat Embryol (Berl) 211 Suppl 1, 37-41.

Vasyutina, E., Lenhard, D.C., Wende, H., Erdmann, B., Epstein, J.A., Birchmeier, C., 2007. RBP-J (Rbpsuh) is essential to maintain muscle progenitor cells and to generate satellite cells. Proc Natl Acad Sci U S A 104, 4443-4448.

Vining, K.H., Mooney, D.J., 2017. Mechanical forces direct stem cell behaviour in development and regeneration. Nat Rev Mol Cell Biol 18, 728-742.

Vortkamp, A., Lee, K., Lanske, B., Segre, G.V., Kronenberg, H.M., Tabin, C.J., 1996. Regulation of rate of cartilage differentiation by Indian hedgehog and PTH-related protein. Science 273, 613-622.

Wachtler, B.C.M.J.H.J.J.B.B.F., 1986. Myogenesis: A Problem of Cell Distribution and Cell Interactions.

Wagner, D.O., Sieber, C., Bhushan, R., Borgermann, J.H., Graf, D., Knaus, P., 2010. BMPs: from bone to body morphogenetic proteins, Sci Signal, United States, p. mr1.

Wagner, I., Wang, H., Weissert, P.M., Straube, W.L., Shevchenko, A., Gentzel, M., Brito, G., Tazaki, A., Oliveira, C., Sugiura, T., Simon, A., Drechsel, D.N., Tanaka, E.M., 2017. Serum Proteases Potentiate BMP-Induced Cell Cycle Re-entry of Dedifferentiating Muscle Cells during Newt Limb Regeneration. Dev Cell 40, 608-617.e606.

Walker, J.L., Assoian, R.K., 2005. Integrin-dependent signal transduction regulating cyclin D1 expression and G1 phase cell cycle progression. Cancer Metastasis Rev 24, 383-393.

Wang, H., Loof, S., Borg, P., Nader, G.A., Blau, H.M., Simon, A., 2015. Turning terminally differentiated skeletal muscle cells into regenerative progenitors. Nat Commun 6, 7916.

Wang, H., Noulet, F., Edom-Vovard, F., Tozer, S., Le Grand, F., Duprez, D., 2010. Bmp signalling at the tips of skeletal muscles regulates the number of fetal muscle progenitors and satellite cells during development. Dev Cell 18, 643-654.

Wang, J., Kumar, R.M., Biggs, V.J., Lee, H., Chen, Y., Kagey, M.H., Young, R.A., Abate-Shen, C., 2011. The Msx1 Homeoprotein Recruits Polycomb to the Nuclear Periphery during Development. Dev Cell 21, 575-588.

Wickstrom, S.A., Lange, A., Hess, M.W., Polleux, J., Spatz, J.P., Kruger, M., Pfaller, K., Lambacher, A., Bloch, W., Mann, M., Huber, L.A., Fassler, R., 2010. Integrin-linked kinase controls microtubule dynamics required for plasma membrane targeting of caveolae. Dev Cell 19, 574-588.

Wilkinson, D.J., Desilets, A., Lin, H., Charlton, S., Del Carmen Arques, M., Falconer, A., Bullock, C., Hsu, Y.C., Birchall, K., Hawkins, A., Thompson, P., Ferrell, W.R., Lockhart, J., Plevin, R., Zhang, Y., Blain, E., Lin, S.W., Leduc, R., Milner, J.M., Rowan, A.D., 2017. The serine proteinase hepsin is an activator of pro-matrix metalloproteinases: molecular mechanisms and implications for extracellular matrix turnover. Sci Rep 7, 16693.

Willette, R.N., Gu, J.L., Lysko, P.G., Anderson, K.M., Minehart, H., Yue, T., 1999. BMP-2 gene expression and effects on human vascular smooth muscle cells. J Vasc Res 36, 120-125.

Wohl, A.P., Troilo, H., Collins, R.F., Baldock, C., Sengle, G., 2016. Extracellular Regulation of Bone Morphogenetic Protein Activity by the Microfibril Component Fibrillin-1. J Biol Chem 291, 12732-12746.

Wozney, J.M., Rosen, V., Celeste, A.J., Mitsock, L.M., Whitters, M.J., Kriz, R.W., Hewick, R.M., Wang, E.A., 1988. Novel regulators of bone formation: molecular clones and activities. Science 242, 1528-1534.

Wright, W.E., Sassoon, D.A., Lin, V.K., 1989. Myogenin, a factor regulating myogenesis, has a domain homologous to MyoD. Cell 56, 607-617.

Xiao, G., Gopalakrishnan, R., Jiang, D., Reith, E., Benson, M.D., Franceschi, R.T., 2002. Bone morphogenetic proteins, extracellular matrix, and mitogen-activated protein kinase signalling pathways are required for osteoblast-specific gene expression and differentiation in MC3T3-E1 cells. J Bone Miner Res 17, 101-110.

Xiao, Y.T., Xiang, L.X., Shao, J.Z., 2007. Bone morphogenetic protein. Biochem Biophys Res Commun 362, 550-553.

Xu, H., Wu, X.R., Wewer, U.M., Engvall, E., 1994. Murine muscular dystrophy caused by a mutation in the laminin alpha 2 (Lama2) gene. Nat Genet 8, 297-302.

Yang, K., Hitomi, M., Stacey, D.W., 2006. Variations in cyclin D1 levels through the cell cycle determine the proliferative fate of a cell. Cell Div 1, 32.

Yilmaz, A., Engeler, R., Constantinescu, S., Kokkaliaris, K.D., Dimitrakopoulos, C., Schroeder, T., Beerenwinkel, N., Paro, R., 2015. Ectopic expression of Msx2 in mammalian myotubes recapitulates aspects of amphibian muscle dedifferentiation. Stem Cell Res 15, 542-553.

Yimlamai, D., Christodoulou, C., Galli, G.G., Yanger, K., Pepe-Mooney, B., Gurung, B., Shrestha, K., Cahan, P., Stanger, B.Z., Camargo, F.D., 2014. Hippo pathway activity influences liver cell fate. Cell 157, 1324-1338.

Yosefzon, Y., Soteriou, D., Feldman, A., Kostic, L., Koren, E., Brown, S., Ankawa, R., Sedov, E., Glaser, F., Fuchs, Y., 2018. Caspase-3 Regulates YAP1-Dependent Cell Proliferation and Organ Size. Mol Cell 70, 573-587.e574.

Zhang, H., von Gise, A., Liu, Q., Hu, T., Tian, X., He, L., Pu, W., Huang, X., Cai, C.L., Camargo, F.D., Pu, W.T., Zhou, B., 2014. YAP11 is required for endothelial to mesenchymal transition of the atrioventricular cushion. J Biol Chem 289, 18681-18692.

Zhang, P., Wong, C., Liu, D., Finegold, M., Harper, J.W., Elledge, S.J., 1999. p21(CIP1) and p57(KIP2) control muscle differentiation at the myogenin step. Genes Dev 13, 213-224.

Zhou, J., Lee, P.L., Lee, C.I., Wei, S.Y., Lim, S.H., Lin, T.E., Chien, S., Chiu, J.J., 2013. BMP receptor-integrin interaction mediates responses of vascular endothelial Smad1/5 and proliferation to disturbed flow. J Thromb Haemost 11, 741-755.

8. APPENDIX – A

During the course of this PhD two side projects were undertaken. The first project focused on analysing interdigital cell death during embryogenesis. This project provided me an avenue to integrate the knowledge I gained in BMP/Noggin signalling during the course of this PhD into a different embryonic context. The second project focuses on defining the muscle microenvironment during regeneration Here, I could further extrapolate my expertise to tissue microenvironment and apply it towards understanding muscle regeneration and ageing.

8.1. Cooperation of BMP and IHH signalling in interdigital cell fate determination

This project resulted in the publication of the manuscript (Murgai et al, 2018) available under https://doi.org/10.1371/journal.pone.0197535.

Abstract:

Abstract as written in Murgai et al, 2018 states that “The elaborate anatomy of hands and feet is shaped by coordinated formation of digits and regression of the interdigital mesenchyme (IM). A failure of this process causes persistence of interdigital webbing and consequently cutaneous syndactyly. Bone morphogenetic proteins (BMPs) are key inductive factors for interdigital cell death (ICD) in vivo. NOGGIN (NOG) is a major BMP antagonist that can interfere with BMP-induced ICD when applied exogenously, but its in vivo role in this process is unknown. We investigated the physiological role of NOG in ICD and found that Noggin null mice display cutaneous syndactyly and impaired interdigital mesenchyme specification. Failure of webbing regression was caused by lack of cell cycle exit and interdigital apoptosis. Unexpectedly, Noggin null mutants also exhibit increased Indian hedgehog (Ihh) expression within cartilage condensations that leads to aberrant extension of IHH downstream signalling into the interdigital mesenchyme. A converse phenotype with increased apoptosis and reduced cell proliferation was found in the interdigital mesenchyme of Ihh mutant embryos. Our data point

towards a novel role for NOG in balancing Ihh expression in the digits impinging on digit-interdigit cross talk. This suggests a so far unrecognized physiological role for IHH in interdigital webbing biology."

Results and conclusion:

This project was commenced in the Stricker/Mundlos lab before I started my PhD, first data had been gathered by two master students. As a part of this study, I analysed Nog- /- mutants and observed subcutaneous syndactyly at E14.5 (Figure 4.1A). I therefore assessed the mutants to determine the underlying mechanisms for this phenotype. The onset of cell death in the mouse coincides with the regression of the AER and thus the loss of *Fgf8* signals (Salas-Vidal et al., 2001) However, these mutants displayed persistent expression of Fgf8 in the AER overlying the interdigit region (Figure 8.1B). Fgfs antagonize retinoic acid which is known to be a potent cell death inducer and induces interdigital regression (Hernández-Martínez et al., 2009). RT-QPCR for *Aldh1a2*, an enzyme that catalyzes the synthesis of retinoic acid, showed reduced expression in the interdigit of Nog-/- embryos (Figure 8.1C), thus indicating reduced retinoic acid synthesis. BMPs are known potent interdigit cell death inducers (Kaltcheva et al., 2016) therefore I checked Msx genes which are downstream effectors of the BMP pathway. Quantification of *Msx1* and *Msx2* expression levels via real time RT-qPCR on mRNA extracted from microdissected hand plate interdigit tissue confirmed an overall downregulation of both genes in the interdigit region (Figure 8.1D). Altogether, this points towards decreased BMP signalling in the interdigits. Indian Hedgehog (IHH) is expressed in pre-hypertrophic chondrocytes and it regulates proliferation and differentiation of chondrocytes (Vortkamp et al., 1996). Rather surprisingly, RT-QPCR showed enhanced expression of *Ihh* in the digit and its downstream targets *Gli1* and *Ptc* in the interdigit region of Nog-/- mutants (Figure 8.1E). To define the relationship between NOGGIN/BMP and IHH signalling, I analysed Ihh-/- mutants in conjugation with Nog-/- mutants for changes in BMP signalling. RT-QPCR showed that the expression of Bmp genes was altered in Nog-/- embryos, whereby, Bmp2 and Bmp7 were downregulated, while Bmp4 expression appeared slightly increased. However, in Ihh-/- mutants, the expression of *Bmp2* and *Bmp4* also was downregulated at E13.5 while Bmp7 appeared unchanged. Among the BMP antagonists, Gremlin 1 is known to be

expressed in the interdigit during ICD exerting an anti-apoptotic effect (Pajni-Underwood et al., 2007). In both Nog-/- and Ihh-/- embryos *Grem1* did not show a compensatory upregulation (Figure 8.1F). Thus, reduction of BMPs in the

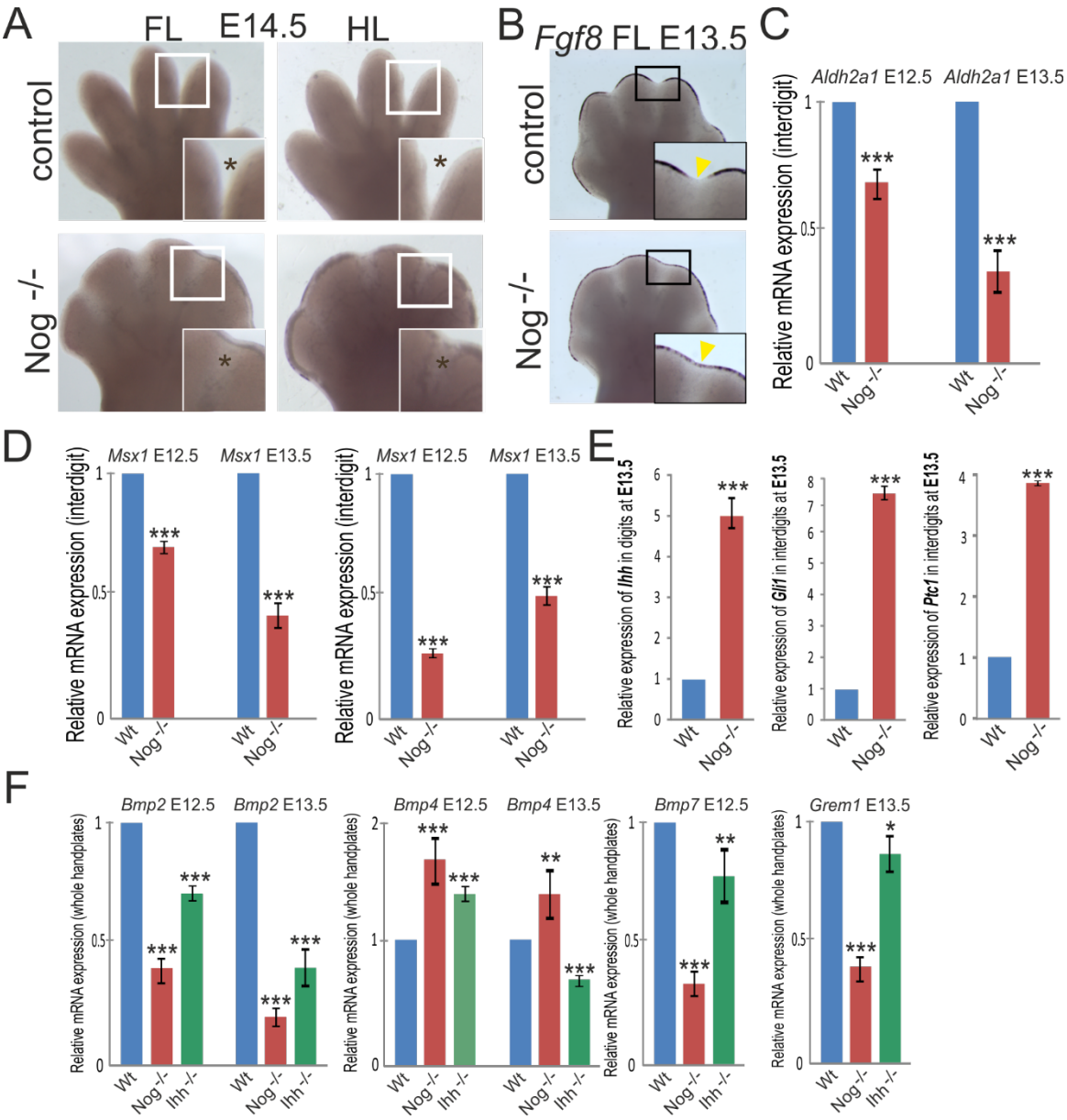

Figure 8.1 Expression of interdigit markers is impaired in Nog-/- and Ihh-/- mutants
Unstained autopods show subcutaneous syndactyly in Nog-/- mutants (interdigit region is marked with *) (A) WISH shows persistent expression of *Fgf8* in the AER overlying the interdigits (yellow arrowheads) in *Nog*$^{-/-}$ hand plates (B) RT-qPCR on mRNA extracted from microdissected interdigit tissue shows that *Nog*$^{-/-}$ interdigits exhibit impaired *Aldh1a2* expression at E12.5 and E13.5 (C) Interdigital xpression of *Msx1* and *Msx2* is reduced in Nog-/- mutants at E12.5 and E13.5 (D) E13.5 hand plates were microsurgically dissected into interdigit and digit mesenchyme. RT-qPCR confirms increased *Ihh* expression in digit condensations and increased expression of *Ptc1* and *Gli1* in interdigit mesenchyme of Nog-/- mutants (E) Expression of *Bmp2*, *Bmp4*, *Bmp7* and the BMP antagonist *Grem1* were as assessed by RT-qPCR on mRNA extracted from whole hand plates at E12.5 and E13.5 (F) Error bars represent S.E.M. T-test: * p<0.05; ** p<0.01; *** p<0.001 (n = 3)

Noggin- /- mutants could be in part responsible for reduced interdigital cell death however, this is highly unlikely as Ihh-/- mutants which also show downregulation of BMP genes, do not display cutaneous syndactyly.

To determine whether IHH is responsible for the interdigital phenotype in Nog-/- mutants, I analysed $Nog^{-/-};Ihh^{+/-}$ mutants to obtain a partial rescue of the phenotype. However, no significant difference in the expression of *Msx1*, *Msx2* and *Aldh1a2* were observed (Figure 8.2). Indicating that the loss of a single *Ihh* allele may not cause sufficient reduction of *Ihh* expression.

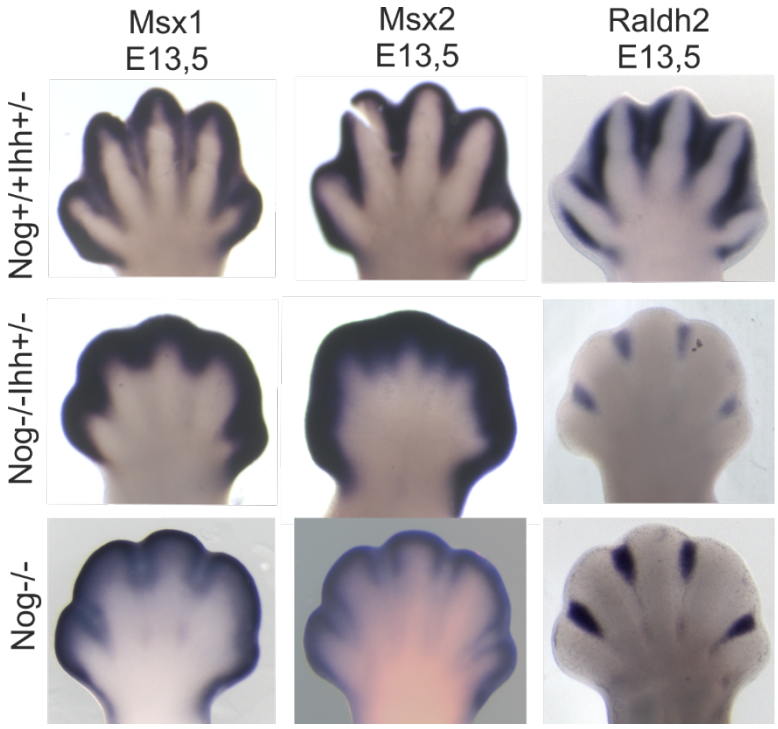

Figure 8.2 Analysis of Nog / Ihh compound mutants.
Nog+/+;Ihh+/- (control), Nog-/-;Ihh+/+ (normal Nog KO) and Nog-/-;Ihh+/- (compound mutant: Nog KO lacking one allele of Ihh) were analysed via whole-mount in-situ hybridisation for the expression of interdigit markers Msx1, Msx2 and Aldh1a2. No amelioration of the Nog KO phenotype can be seen in compound mutants.

In conclusion, this study demonstrates that syndactyly in Nog-/- mutants could be a result of ectopic IHH signalling that extends from the digit into the interdigit, as a direct or indirect consequence of Noggin deletion. Further investigations need to be done to determine the molecular interactions between BMP/NOGGIN and IHH signalling.

8.2. A Quantitative Approach to ECM Function in Aged Muscle Regeneration: Towards Predictive Modelling of Cell-Matrix Interplay

This project was funded by the Einstein-centre for Regenerative therapies (ECRT) to establish novel interdisciplinary collaborations. The work presented here was done in collaboration with Dr. Vikram Sunkara (Zuse Institute Berlin) and Georgios Kotsaris (Department of Biochemistry) at Freie Universität Berlin.

Background & Aims:

Ageing affects the regenerative abilities of skeletal muscle resulting in compromised healing associated with fibrosis, impairing mobility and affecting quality of life. Current research is largely focused on intrinsic muscle stem cell function, but local extrinsic changes are mostly neglected (Carosio et al., 2011). However, skeletal muscle repair relies on a dynamic interplay between muscle satellite cells (SCs) and the extracellular matrix (ECM) microenvironment. We have preliminary evidence for a transient developmental-like ECM during early phases of muscle regeneration (Calve et al., 2010). We believe that this creates a biomechanical three-dimensional micro-niche conducive to SC expansion, differentiation and self-renewal during regeneration, and that its derailment in aging or disease contributes to SC malfunction. However, the mechanical properties of the pro-regenerative ECM, especially during aging, has not been analysed and the influence of the bio-mechanical properties of the aged ECM on stem cell behaviour remains unclear. By combining experimental and mathematical analysis in an interdisciplinary approach, we aim to comparatively determine and quantify the dynamic spatio-temporal structure, composition and functionality of the transitory ECM in young and old mice. Iterative mathematical modeling via integration of biological data in a stepwise fashion will in the future develop a predictive landscape to achieve a new level of understanding of ageing processes prospectively transferable to muscle-degenerative disorders.

Results and conclusion:

Although muscle satellite cells (SCs) are the principal contributors to the regeneration of injured muscle, it is becoming increasingly clear that their activity

is influenced by environmental cues such as the extracellular matrix (ECM). Similar to that of amphibians, this transient early-stage ECM is rich in “developmental” components as tenascin, fibronectin and hyaluronic acid instead of classical “mature” ECM components like laminin and collagens (Calve et al., 2010). Previous studies have demonstrated that ECM remodeling during ageing leads to an increase in tissue stiffness caused by augmented collagen deposition hence leading to reduced tissue function (Lacraz et al., 2015). We hypothesize that this will also apply to the transient ECM during regeneration, likely contributing to reduced healing efficacy.

For this study a comparative analysis of young and old mice was conducted. Wherein, young mice were from 2-3 months of age and old mice were 18-20 months old. Since the presence of a transient ECM was never shown for mammalian systems, we tested and established staining protocols for our primary target ECM components- Fibronectin (FN), Hyaluronic acid (HA) and Tenascin-C (TnC). Next we used Haematoxylin-Eosin staining to depict the general tissue morphology, which could then be used to train the computer to generate an algorithm that can distinguish between the injured and uninjured area on the same

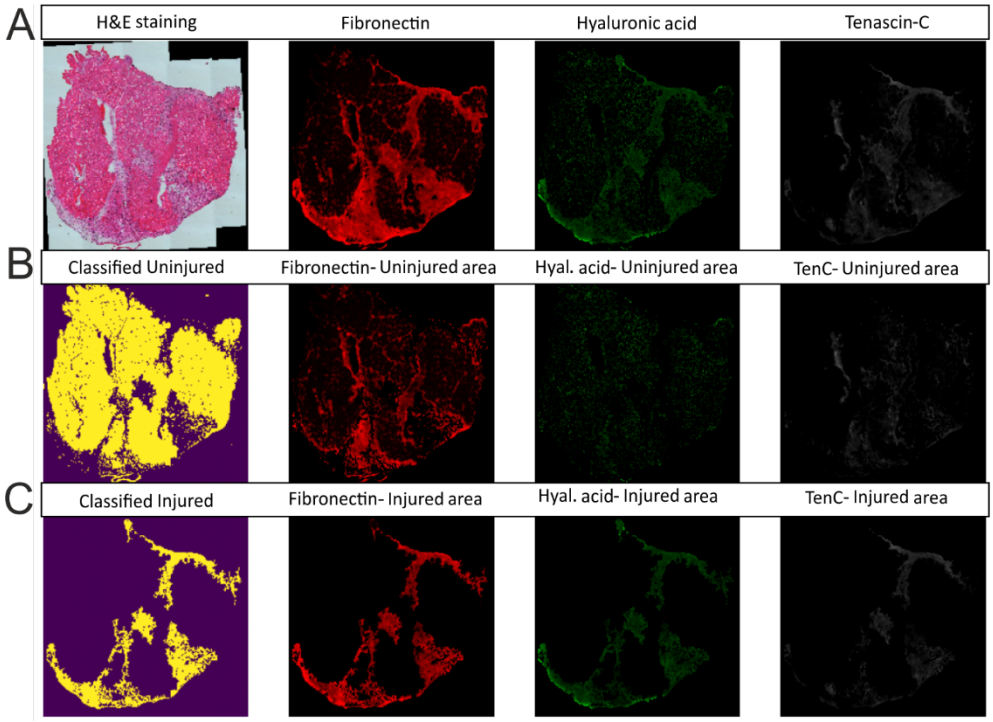

Figure 8.3 Computer-generated quantification algorithm for ECM stainings
Tissue section from an injured muscle stained with Haematoxylin-Eosin (H&E) dye together with immunofluorescence staining for fibronectin (FN), hyaluronic acid (HA) and Tenascin-C (TnC) (A) Computer generated mask showing only the uninjured areas of the tissue for each of the channels (B) Computer generated mask showing only the injured areas of the tissue for each of the channels (C)

tissue section. This computer generated segmentation mask could then be applied to the individual immunofluorescence stainings to generate two-different sets if images one containing the florescence signal in the injured region and other containing the florescence signal in the uninjured region (Figure 8.3). The computational algorithm was developed and trained by Dr. Vikram Sunkara.

The raw images generated from the computer algorithm were then subject to a florescence intensity calculating software that could now aid in generating a quantification of each of the ECM components. This revealed a previously unreported dynamic remodeling of the muscle ECM components following the early days after injury, highly reminiscent of the situation reported in lower vertebrates. In young animals, TnC seems is most abundant for 3-4 days after injury after which its level come back to normal, whereas HA and FN both increase 3-5 days after injury and probably resume normal expression at the later time point. In contrast, in old animals we observed marked differences in ECM dynamics. TnC expression is delayed and decreased, and does not go back to initial levels by day 5. Furthermore there is a strong deficiency in the expression of FN and HA. These findings were validated by performing a qPCR on whole muscle tissue samples (data not shown). An interesting observation is that ECM remodeling is not only limited to the area of injury but also the surrounding regions (Figure 8.4).

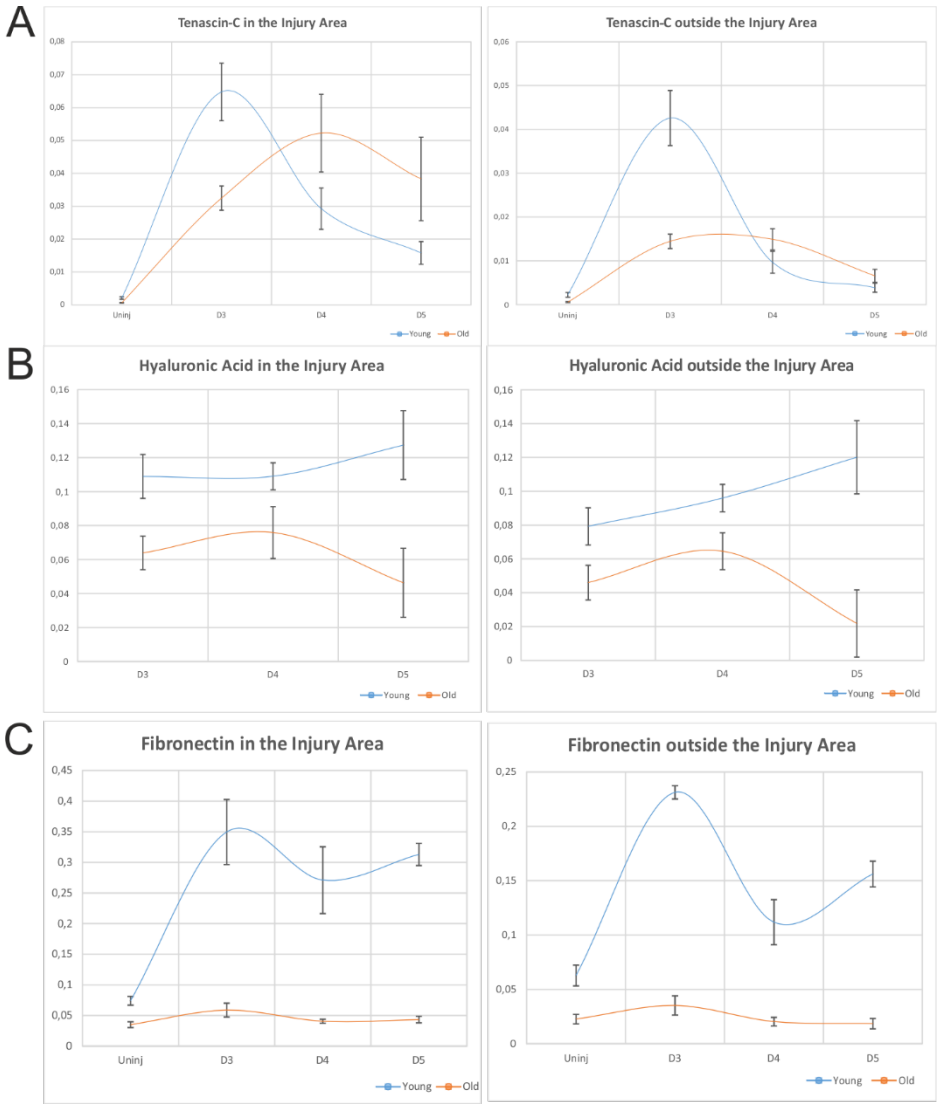

Figure 8.4 Quantification of ECM components in young and old during regeneration
Analysis done between uninjured mice and regenerating mice at day 3, 4 and 5 after injury. Comparative analysis between young and aged mice shows that TnC expression within and surrounding the injured region (A), amount of HA expressed within and surrounding the injured region (B), and amount of FN expressed within and surrounding the injured region (C)

To understand the impact of the changing ECM on tissue-mechanics, Georgios Kotsaris established and performed nanoindentation to generate reliable data from tissue sections. We observed an increase in tissue stiffness early after injury, which returned to normal levels by day 5. However in old animals, tissue stiffening after injury was increased and failed to resume the initial stiffness by day 5 (Figure 8.5). Predictively, this may alter proliferation, differentiation and migration of the resident muscle stem cells.

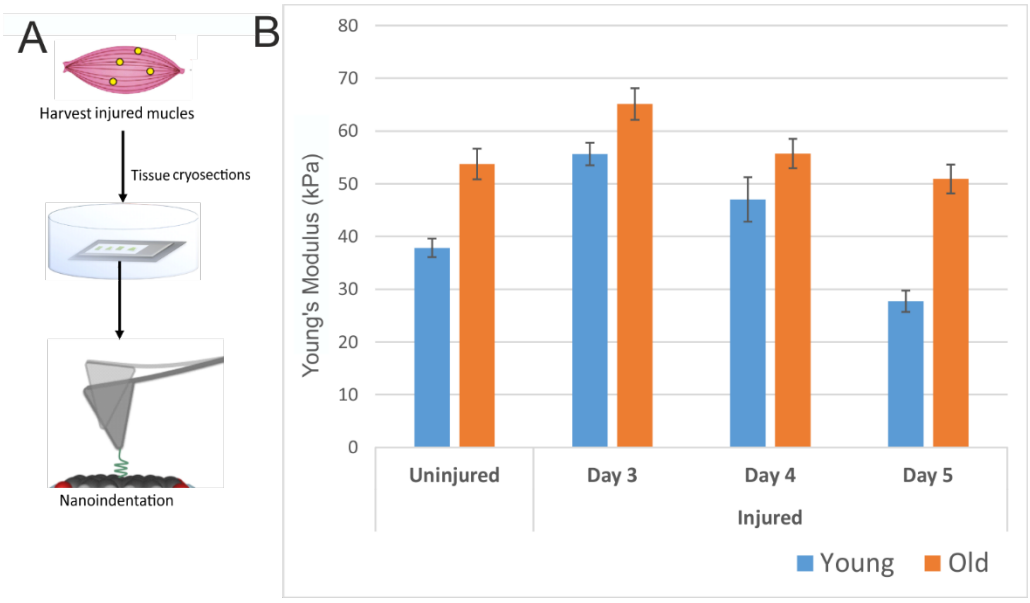

Figure 8.5 Mechanical properties of the tissue during regeneration
Scheme showing nanoindentation procedure (A). Young's modulus generated following nanoindentation of tissues shows comparative analysis between young and aged mice over the course of muscle regeneration (B)

In summary, we were able to demonstrate age-related differences in early transient ECM component expression resulting in altered tissue mechanics during muscle regeneration. Importantly, we developed a novel image quantification system to assess ECM components during muscle regeneration on tissue sections, enabling this analysis.

Outlook:

The long term goals of this study would entail a collection of experiments that can further validate and consolidate our mathematical model to generate a reliable prediction system. Mouse mutants that lack the ECM components FN, TnC and HA respectively could be sued to analyse the early stages of regeneration to study alterations in cell behaviour and mechanical properties. Furthermore, in vitro experiments could be undertaken to develop the 'ideal' ECM composition in conjugation with substrate stiffness that supports SC function. This will be an important study to generate a comprehensive mechanistic understanding of the complex regenerative processes and their derailment in age which can further be applied develop scaffolds that support regeneration and prevent scarring of the healing tissue.

9. APPENDIX - B

9.1. List of abbreviations and acronyms

Abbreviations and acronyms	
°C	degree Celsius
ACTA1	Actin Alpha 1
ACVR1/2	Activin receptor type 1/2
Alk	Activin receptor-like kinase
ALP	Alkaline phosphatase
Bglap	Osteocalin
BMP	bone morphogenetic protein
BMPR1/2	BMP receptor type 1/2
bp	base pairs
BSA	bovine serum albumin
Cc3	Cleaved caspase 3
cDNA	complementary deoxyribonucleic acid
CRISPR	Clustered Regularly Interspaced Short Palindromic Repeats
Ct	threshold cycle
C-terminus	carboxy-terminus
Cdk	Cyclin-dependent protein kinase
DAPI	4′,6-Diamidino-2-phenylindole dihydrochloride
dH20	distilled water
DMEM	Dulbecco's modified Eagle's medium
DMSO	dimethyl sulfoxide
DNA	deoxyribonucleic acid
dNTP	deoxyribonucleotide triphosphate
ECM	extraceullar matrix
EDTA	ethylenediaminetetraacetic acid
ERK	extracellular signal-regulated kinases
FACS	Fluorescence activated cell sorting
FAK	focal adhesion kinase
FBS	fetal bovine serum
FGF-2	Fibroblast growth factor 2
FOP	Fibrodysplasia ossificans progressive
g	gram
GDFs	growth and 161otential161ation factors
h	hours
HDAC	histone deacetylases
ID1-3	Inhibitor of differentiation 1-3

kDa	kilo Dalton
KO	Knockout
L	liter
Lbx1	Ladybird Homeobox 1
MAPK	mitogen-activated protein kinase
min	minutes
ml	mililiter
mM	milimolar
MMPs	matrix metalloproteases
Mrf	Myelin regulatory factor
mRNA	messenger-RNA
MSCs	mesenchymal stem cells
Msx1/2	Msh homeobox 1/2
mw	molecular weight
Myf5	Myogenic Factor 5
MyHC	Myosin heavy chain
MyoD	myoblast determination protein 1
Nog	Noggin
N-terminus	amino terminus
Pax3	Paired box 3
Pax7	Paired box 7
PBS	phosphate buffered saline
PBX	phosphate buffered saline with Triton-X
PCD	programmed cell death
PCR	Polymerase chain reaction
PECAM1	Platelet endothelial cell adhesion molecule
pH	potential Hydrogenii
RA	retinoic acid
Rb	retinoblastoma
rec.	recombinant
RNA-Seq	RNA-Sequencing
rpm	rotations per minute
RUNX2	Runt-related transcription factor 2
SC	satellite cell
SDS	sodium dodecyl sulfate
shRNA	short hairpin RNA
SMAD	Sons of mothers against decapentaplegic
Spp1	Osteopontin
TGFβ	Transforming growth factor β
TnC	Tencascin-C
WISH	whole-mount in situ hybridization
YAP1	Yes associated protein 1
µl	microliter
µM	micromolar

9.2. List of figures

9.3. List of tables

9.4. Availability of data

The RNA-sequencing data with the complete list of all differentially regulated genes is available at https://box.fu-berlin.de/s/zZf5mSojixiMPbS and can be accessed with the password murgai2020.

10. CURRICULUM VITAE

For reasons of data protection the curriculum vitae is not published in the electronic version

11. TEACHING AND SUPERVISION

11.1. Teaching

2015 – present: Practical course for BSRT **PhD students** 'Analysing Musculoskeletal Development *In vivo'*

2015 – present: Practical course for **Master's students** 'Analysing Musculoskeletal Development *In vivo*'

11.2. Supervision

2018: **Master's Internship** Caspar Hoyer (FU Berlin, Biochemistry)

2017: **Bachelor's Internship** and co-supervision of **Bachelor's thesis** Akin Sesver (FU Berlin, Biochemistry)

2017: **Master's Internship** Charles Haggerty (FU Berlin, Biochemistry)

2017: **Master's Internship** Kira Lenz (FU Berlin, Biochemistry)

2017: **Master's Internship** Mareike Rentzsch (FU Berlin, Biochemistry)

2016: Co-supervision of **Bachelor's thesis** Franziska Schwarz (FU Berlin, Biochemistry)

2016: Co-supervision of **Master's Internship** Markus Schliffka (FU Berlin, Biochemistry)

2016: Co-supervision of **Erasmus Internship** Georgios Kotsaris (MPI for Molecular Genetics)

2016: **Master's Internship** Miriam Rodi (FU Berlin, Biochemistry)

2015: **Bachelor's Internship** Manuel Cosme (FU Berlin, Biochemistry)

12. GRANTS AND SCHOLARSHIPS

12.1. Grants

ECRT (Einstein Centre for regenerative Therapies) Career Kickoff Grant "A Quantitative Approach to ECM Function in Aged Muscle Regeneration – Towards Predictive Modeling of Cell-Matrix Interplay" ; October 2019-present

ECRT Advanced Scientist- Kickbox Seed Grant "A Quantitative Approach to ECM Function in Aged Muscle Regeneration – Towards Predictive Modeling of Cell-Matrix Interplay" ; March 2018

ECRT Young Scienstist- Kickbox Seed Grant "Remodeling the Extracellular Matrix during Muscle Regeneration- A combined wet-lab-dry-lab approach" July 2017

BSRT (Berlin-Brandenburg School for Regenerative therapies) Grant for Joint Student Assistant "Mechanically mimetic hydrogel platform to elucidate the paracrine interaction between MSCs and satellite cells" ; May 2016

BSRT Grant for Joint Research Project "The role of ZAK in limb development and regeneration" ; September 2014

BSRT Grant for Joint Research Project "Mechanically mimetic hydrogel platform to elucidate the paracrine interaction between MSCs and satellite cells" ; September 2014

12th International BMP Conference Travel Grant October 2018

BSRT Travel Grant October 2018, May 2017, October 2016, June 2016

FU Berlin Advancement of Women Travel Grant July 2017, September 2014

12.2. Scholarships

BSRT Doctoral Scholarship November 2013-October 2016

13. LIST OF PUBLICATIONS

13.1. Journal Publications

Murgai A., Hiepen C., Haggerty C., Simon H.G., Börno S., Timmerman B., Lensen M., Knaus P., Stricker S., (2019) BMP signalling induces cell cycle re-entry in mammalian myotubes. *In preparation*.

Wei X., Grohmann J., Ost M., **Murgai A.**, Perez A.C., Börno S., Meierhofer D., Timmermann B., Glauben R., Siegmund B., Klaus S., Stricker S., (2019) Inactivation of Neurofibromin in muscle progenitors induces long-lasting metabolic reprogramming transmitted to mature muscle fibers. *In preparation*.

Hiepen C., Jatzlau J., Hildebrandt S., Kampfrath B., Goktas M., **Murgai A.**, Camacho J. L. C., Haag R., Ruppert C., Sengle G., Cavalcanti-Adam E.A., Blank K.G., Knaus P., (2019). BMPR2 acts as a gatekeeper to protect endothelial cells from increased TGFβ responses and altered cell mechanics. PLOS Biology, 17(12), p.e3000557

Murgai, A., Altmeyer, S., Wiegand, S., Tylzanowski, P. and Stricker, S., 2018. Cooperation of BMP and IHH signalling in interdigital cell fate determination. PloS one, 13(5), p.e0197535.

Dörpholz, G., **Murgai, A.**, Jatzlau, J., Horbelt, D., Belverdi, M.P., Heroven, C., Schreiber, I., Wendel, G., Ruschke, K., Stricker, S. and Knaus, P., 2017. IRS4, a novel modulator of BMP/Smad and Akt signalling during early muscle differentiation. Scientific reports, 7(1), p.8778.

13.2. Oral Presentations

12th International BMP Conference, Japan “Novel Insights into the Role of Noggin: Determining Cell-fate and Directing Differentiation & Fusion of Myogenic Cells” ; October 2018

Biochemistry Retreat, Freie Universität Berlin, Germany “Novel Insights into the Role of Noggin: Determining Cell-fate and Directing Differentiation & Fusion of Myogenic Cells” ; July 2017

Gordan Research Conference- Myogenesis, Italy “Novel Insights into the Role of Noggin: Determining Cell-fate and Directing Differentiation & Fusion of Myogenic Cells” ; July 2017 **Selected Young Scientist Talk**

Gordan Research Seminar- Myogenesis, Italy “Novel Insights into the Role of Noggin: Determining Cell-fate and Directing Differentiation & Fusion of Myogenic Cells” ; July 2017 **Best talk**

MyoGrad Summer School, France “Novel Insights into the Role of Noggin: Determining Cell-fate and Directing Differentiation & Fusion of Myogenic Cells” ; June 2017 **Best talk**

BSRT PhD symposium, Germany “Novel aspects of NOGGIN-BMP interplay during limb muscle development” ; December 2017

13.3. Poster Presentations

Biochemistry Retreat, Freie Universität Berlin, Germany “Novel aspects of NOGGIN-BMP interplay during limb muscle development” ; July 2018

Muscle Development, Disease and Regeneration Meeting, Germany “Novel aspects of NOGGIN-BMP interplay during limb muscle development” ; March 2018

N2 Science Communication Conference, Germany “Could we one day regrow our limbs” ; October 2017 **Best ‘Art as Science’ Presentation**

Gordan Research Conference- Myogenesis, Italy “Novel aspects of NOGGIN-BMP interplay during limb muscle development” ; June 2017

Joint Meeting of the German and French Societies of Developmental Biologists, Germany “Novel aspects of NOGGIN-BMP interplay during limb muscle development” ; March 2017 **Best Poster**

11th International BMP Conference, USA “Novel aspects of NOGGIN-BMP interplay during limb muscle development” ; October 2016

MyoGrad Summer School, France ““Novel aspects of NOGGIN-BMP interplay during limb muscle development” ; June 2016 **Best Poster**

BSRT PhD symposium, Germany “Novel aspects of NOGGIN-BMP interplay during limb muscle development” ; December 2015

Max Planck PhD student retreat, Germany “Novel aspects of NOGGIN-BMP interplay during limb muscle development” ; October 2015 **Best Poster**

Joint Meeting of the German and French Societies of Developmental Biologists, Germany “Cooperation of BMP/NOGGIN and IHH signalling in interdigital cell fate decision” ; March 2015

BSRT PhD symposium, Germany “Novel aspects of NOGGIN-BMP interplay during limb muscle development” December 2014

10th International BMP Conference, Germany “Cooperation of BMP/NOGGIN and IHH signalling in interdigital cell fate decision” September 2014